Development and refinement of integrated management strategies for Sclerotinia stem rot of soybean

by

Jaime F. Willbur

A dissertation submitted in partial fulfillment of the requirements for the degree of

Doctor of Philosophy

Plant Pathology

at the

UNIVERSITY OF WISCONSIN-MADISON

2018

Date of final oral examination: 01/29/2018

The dissertation is approved by the following members of the Final Oral Committee:

Damon L. Smith
Assistant Professor, Plant Pathology

Shawn P. Conley
Professor, Agronomy

Mehdi Kabbage
Assistant Professor, Plant Pathology

Patricia S. McManus
Professor, Plant Pathology

Amanda J. Gevens
Associate Professor, Plant Pathology

I dedicate this work to my family for their love, encouragement, and support. Especially to my parents, Carl Willbur, Bernadette Aldan, and David Paine, for their personal sacrifices and constant support over the years. And, to my beloved sister and future brother-in-law, Erin Willbur and Anthony Kazyaka, for becoming two of my best friends during this experience. Without them this work would not have been possible.

ACKNOWLEDGEMENTS

I gratefully acknowledge the contributions and support of my co-authors, collaborators, mentors, mentees, peers, friends, and family. Their guidance, advice, assistance, and encouragement over the years has culminated in many research successes and priceless personal growth throughout this experience.

To my adviser and the many wonderful members, past and present, of the Smith lab, thank you for being a part of five absolutely wonderful years of my life. I cannot thank Dr. Damon Smith enough, for his constant and excellent mentorship as an adviser, colleague, and friend which have enabled me to complete this work and prepare for my near-future career.

Also, Drs. Carol Groves and Scott Chapman, thank you for always providing the technical (and sometimes emotional) support necessary for these laboratory and field experiments. I also thank Dr. Craig Grau for providing a solid foundation and wealth of knowledge for much of this research.

To my fellow graduate student siblings, Megan McCaghey, Brian Mueller, Christina Zambrana-Echevarria, and Chris Bloomingdale, thank you for everything. We went through this together, supported and encouraged one another, and I could not have done it without you. It has been a pleasure to be a part of our lab family together.

I would also like to acknowledge all the undergraduate research assistants who made this extensive research possible. To Hannah Lucas, Maria Weber, Theresa Blackwell, and Kelsey Azzolino who contributed tireless time and effort to this work, thank you for being fantastic. Also, I thank all the students from the summer crews for their invaluable assistance in seemingly never-ending apothecial scouting and data collection.

This research was also made possible by our many amazing out-of-state collaborators. Special thanks to Drs. Martin Chilvers and Daren Mueller, and their lab team members, for their willingness to participate in and contribute to this research.

Within the Departments of Agronomy and Plant Pathology, I would like to acknowledge my committee members, Drs. Shawn Conley, Amanda Gevens, Mehdi Kabbage, and Patricia McManus, for their mentorship through my current and toward my future professional career. I would also like to acknowledge the Plant Pathology faculty, students, and staff who have contributed to the truly enriching environment of this department.

I would especially like to acknowledge my graduate student cohort-mates, Katelyn Butler, Shunping Ding, Sachin Jain, Ryan Kessens, and Michelle Marks. I am eternally grateful for their friendship, support, and encouragement.

Finally, I would like to acknowledge my parents, Carl Willbur, Bernadette Aldan, and David Paine, my sister, Erin Willbur, and future brother-in-law, Anthony Kazyaka, for all their love and support. And, for all the times they helped me collect data on weekends when they were visiting.

ABSTRACT

Sclerotinia stem rot (SSR), or white mold, is caused by *Sclerotinia sclerotiorum* and is one of the top ten yield reducing diseases of soybean worldwide. Complete commercial resistance is confounded by an incomplete understanding of resistance mechanisms and the diversity within *S. sclerotiorum* populations. Characterization of a diverse isolate collection facilitated the selection of a representative panel of isolates for use in ongoing germplasm resistance evaluations. These isolates were used to further identify candidate germplasm lines exhibiting durable SSR resistance for further integration into commercial soybean cultivars. Monitoring infection of resistant and susceptible lines further helped to understand *S. sclerotiorum* infection and potential resistance mechanisms. Chemical control is also currently incomplete and, in some cases, unnecessary as disease development requires conditions conducive for simultaneous apothecial germination, ascospore release, and soybean flowering. Multiple site-years of fungicide efficacy trials were evaluated using meta-analyses to identify effective control programs, which will assist growers in making economical management decisions. Risk assessment tools are sometimes used to more accurately predict the timing of effective fungicide applications; however, reliable tools were not available in soybean systems prior to this research. In the SSR pathosystem, dense canopies, cool temperatures, high relative humidity, and moist soil conditions have been shown to favor *S. sclerotiorum* infection and subsequent disease development. Additionally, studies have shown that apothecial development is sensitive to a narrow range of ultraviolet wavelengths (276-319 nm). Virtual weather data and detailed epidemiological studies have led to the development and validation of models for non-irrigated and irrigated fields which

predict apothecial presence based on 30-day averages of mean air temperature, relative humidity, and maximum leaf wetness. These models will be incorporated into a mobile web-based recommendation tool. Moreover, controlled environment and in-field light studies have identified a crucial range of light (295-330 nm) which are required for apothecial development and could be targeted to further improvement of SSR management. Overall, the development of germplasm with broad-spectrum resistance, the study of resistance mechanisms, multiple site-year fungicide efficacy evaluations, and an optimized spray advisory system will provide a new, fresh approach to integrated management of SSR in soybean.

Approved by:

Damon L. Smith, Advisor: 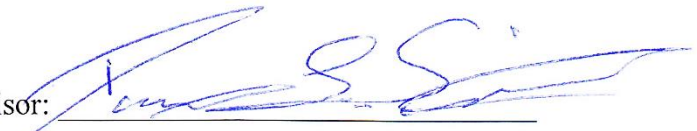

on this date: 2/2/2018

TABLE OF CONTENTS

CHAPTER 1: Literature Review

Soybean (*Glycine max* L. Merrill)

History. Soybean [*G. max* (L.) Merr.] is a globally-grown oil and protein crop. Soybean originated in Southeast Asia, was domesticated in China, and was brought to North America in 1765 (Grau and Hartman 2015; Shurtleff and Aoyagi 2010). Soybean is believed to have been derived from the weedy, wide-spread wild species, *G. soja* (L.) Sieb. & Zucc. (Cui et al. 1999). The process of domestication is thought to have occurred as early as circa 1500-1100 BCE, during the Shang Dynasty; the modern domesticate *G. max* (L.) Merr. likely originated from the eastern region of northern China during the following Zhou Dynasty (Grau and Hartman 2015). Originally as many as 20,000 landraces were available in China (ca. 1900); relatively few of the original landraces, however, were used as breeding stock in Chinese or North American soybean breeding efforts (Cui et al. 2001). By 1995, 341 ancestors (including 250 landraces) were used to develop 651 modern Chinese cultivars (Cui et al. 1999). In contrast, Gizlice et al. identified only 50 dominant ancestors which contributed to over 97% of the genes in 258 North American cultivars (1945). Furthermore, a study of 136 US cultivars (released pre-1980) found only 12 plant introductions which contributed to 88% of the germplasm (Specht and Williams 1984). While the genetic base of US cultivars is limited, the distinct genetic pool in Chinese cultivars could offer genetic improvements of US soybean.

According to a study conducted by the Keystone Alliance for Sustainable Agriculture, total soybean production has increased by 96% from 1980-2011 and yield has increased 55% in this period (WSA and WSMB 2013). Between 1924 and 2011, yield was estimated to

improve by 23.4 kg ha^{-1} yr^{-1} (Suhre et al. 2014). Almost 100 years of extensive breeding efforts have resulted in US soybean cultivars with significantly higher yield performance, approximately double that of historical cultivars (Suhre et al. 2014). It is estimated that approximately 50% of yield increase is attributable to improved genetics and the remaining 50% is from improved agronomic practices (Specht et al. 1999). Genetic yield improvements of modern soybean cultivars are due to many factors including reduced plant height, increased number of nodes per stem, increased number of pods per node, enhanced branch yield, higher energy conversion efficiency, and increased compensation capacity at lower seeding rates (Suhre et al. 2014).

Production. According to the United States Department of Agriculture Foreign Agricultural Service (USDA-FAS), soybean and other oilseed crops rank third in global crop production behind coarse grains (including maize) and wheat (2017). A 2016-17 report estimated that a little over 120 million hectares of soybeans were grown worldwide, producing approximately 351 million metric tons of soybean (USDA-FAS 2017). In the United States, soybeans are the leading agricultural export at a value of $23 billion (WSA and WSMB 2013). US soybean production continues to account for about 34% of the total international soybean production (USDA-FAS 2017; USDA-NASS 2017). Soybean is also the second largest agricultural crop grown (by acreage) in the United States, and in 2016, production reached a value of $40.9 billion USD (USDA-NASS 2017). While soybeans are grown across 31 states from the midsouth to northeast US, production is concentrated in the North Central region. This region of 12 Midwestern states accounts for 84.5% of US soybean production, totaling 98 million metric tons and earning growers a corresponding $34.2 billion

USD in 2016 (USDA-NASS 2017). Wisconsin ranks 13th in the US for soybean production, and approximately 11,000 growers cultivate a total of 1.8 million acres of soybean (WSA and WSMB 2013). Soybeans are primarily used as refined oil for cooking and biofuel production or in animal agriculture as protein for animal feed.

Common diseases. Common soybean diseases in northern regions of the United States include 16 major diseases caused by fungal or oomycete pathogens as well as bacterial, seed, seedling, viral, and nematode diseases (Grau and Hartman 2015; Wrather et al. 2003). In Wisconsin, 19 of these diseases or disease categories consistently caused yield reductions from 1999-2001; the most damaging of these diseases were soybean cyst nematode, brown stem rot, Sclerotinia stem rot, Phytophthora rot, pod and stem blight, as well as seedling and viral diseases (Wrather, Koenning, and Anderson 2003). More recently, sudden death syndrome, charcoal rot, Septoria brown spot, Fusarium wilt and root rot, and stem canker have also been identified in the top ten most destructive soybean diseases in the Northern United States (Allen et al. 2017). Soybean diseases can affect all parts of the soybean plant including the stems, leaves, roots, pods, seeds, and flowers. In Wisconsin, the growing season typically ranges from April to September. Given conducive environmental conditions and susceptible soybean cultivars, common soybean diseases may be prevalent throughout the entire growing season from planting to harvest (Jensen and Smith 2017).

Growth stages. Infection occurs during the vegetative and reproductive growth stages, which have been previously defined (Broeske et al. 2016; Fehr et al. 1971; Pedersen 2004). Germination of the soybean seed is characterized by the emergence, growth, and elongation of the radical and hypocotyl. Vegetative emergence (VE) occurs when the

cotyledons emerge through the soil surface, followed by the vegetative cotyledon (VC) stage where the unifoliate leaves have unrolled. The following vegetative stages are according to Fehr et al. and Pedersen et al. where the V*n* stage (*n* = 1, 2, …, *n*) refers to the *nth* unrolled trifoliate leaf prior to flowering (1971, 2004). Flowering begins approximately after the V5 or V6 growth stages and signals the start of the reproductive growth phase; the following reproductive phases are agreed upon by Fehr et al. Pedersen et al., and Broeske et al. and occur when 50% of the field is at each of the defined stages (1945, 2004, 2016). The R1 (beginning flowering) stage refers to the presence of one open flower at any node. The R2 stage (full flowering) is reached when open flowers are present at one of the two uppermost nodes on the main stem. When pods at one of the four uppermost nodes reach 3/16 and 3/4 inches in length, this represents the R3 (beginning pod) and R4 (full pod) stages, respectively. Once seed in the pods are 1/8 inches long at one of the four uppermost nodes, this signals the R5 growth stage (beginning seed). The seeds at the R6 (full seed) stage will be green and fill the pod cavity of pods at one of the four uppermost nodes. The soybeans will continue to maturity which begins at R7 (beginning maturity) when one pod on the main stem has matured to brown or tan. Finally, the R8 (full maturity) growth stage indicates that 95% of the pods have reached mature pod color. Soybeans may be harvested 7-10 days after the R8 growth stage has been reached (Pedersen 2004).

***Sclerotinia sclerotiorum* (Lib.) de Bary**

History and distribution. *S. sclerotiorum* (Lib.) de Bary, the soilborne causal agent of Sclerotinia stem rot (SSR), is a devastating fungal pathogen affecting more than 400 host species globally (Boland and Hall 1994). These species include important field, vegetable,

fruit, ornamental, tree, shrub, and numerous weed crops (Saharan and Mehta 2008). While virtually all dicotyledonous crops may become infected, the fungus also infects some monocotyledonous hosts, such as onion and tulip (Bolton et al. 2006). The species was initially described *Peziza sclerotiorum* by Madame M.A. Libert (1837), until Fuckel described the genus *Sclerotinia* and renamed the fungus *Sclerotinia libertiana* (1869); the genus *Whetzelinia* was also proposed by Korf and Dumont (1972), however, the now accepted *Sclerotinia sclerotiorum* binomial was eventually cited according to the International Rules of Botanical Nomenclature by de Bary (1887) and Massee (Purdy 1979; Saharan and Mehta 2008; Wakefield 1924). The distribution of *S. sclerotiorum* covers 95 countries and almost every continent, including Africa, Asia, Australia, Europe, North America, and South America (Saharan and Mehta 2008). In the United States, *S. sclerotiorum* has been reported in 44 states throughout the northern, southern, central, eastern, and western regions of the country (Saharan and Mehta 2008).

Biology. *S. sclerotiorum* belongs to the kingdom Fungi, phylum Ascomycota, class Discomycetes, order Helotiales, family Sclerotiniaceae, and genus *Sclerotinia,* which has been defined to include only species which produce tuberoid sclerotia not incorporating host tissue, developing an apothecial ectal excipulum composed of globose cells, and not producing a disseminative conidial state (Kohn 1979; Saharan and Mehta 2008). In other words, *Sclerotinia* spp. have thick, tuber-like sclerotia (survival structures) which do not contain host tissue, produce apothecia (ascocarp) containing a cup-shaped layer of asci which is situated near the outer-surface, and do not produce conidia (asexual spores). Since no asexual conidia are produced, *S. sclerotiorum* is typically identified by its hyaline, septate,

multinucleate hyphae and white to tan mycelium (Bolton et al. 2006). *S. sclerotiorum* does produce sexual ascospores through homothallic, or self-fertile, reproduction via a single *MAT* locus which contains both domains encoding the *MAT1-1* and *MAT1-2* mating type genes (Amselem et al. 2011).

The fungus persists in the soil as either mycelium or sclerotia, which are melanized survival structures composed of compact mycelia and may remain viable in the soil for up to eight years (Adams and Ayers 1979; Willetts and Wong 1980). During this time a conditioning period (at least 8 weeks at 8-16°C) is typically required prior to apothecial germination (Dillard et al. 1995; Phillips 1986). After appropriate conditioning, and given sufficient light, moisture (near saturation), and temperature (10-25°C) stimuli (Abawi and Grogan 1979; Sun and Yang 2000), either myceliogenic or carpogenic germination can occur. Myceliogenic germination produces infective hyphae (Willetts and Wong 1980). Carpogenic germination results in the production of apothecia and asci containing hyaline ascospores (sexual spores); millions of ascospores (covered in mucilage) are ejected and carried via the wind to infect susceptible plant tissue (Abawi and Grogan 1979; Bolton et al. 2006; Willetts and Wong 1980). Necrotic or senescing tissues typically serve as a nutrient source to initiate ascospore germination (Abawi and Grogan 1979). Mycelia can then penetrate the cuticle using enzymes, mechanical force, or through stomata (Bolton et al. 2006; Lumsden and Dow 1973). As infections progress, plants become reservoirs of newly formed sclerotia which become primary sources of inoculum in subsequent years.

S. sclerotiorum is generally considered a necrotrophic fungal pathogen; however, a brief biotrophic phase has been identified suggesting that a hemi-biotrophic designation may

be more appropriate (Kabbage et al. 2015). During the infection process, *S. sclerotiorum* uses a variety of pathogenicity factors, including reactive oxygen species (ROS) generators, cell-wall-degrading enzymes, oxalic acid, and possibly secreted effector proteins (Amselem et al. 2011; Bolton et al. 2006). These factors manipulate the host environment or host processes to favor fungal colonization and infection. Oxalic acid, one of the key pathogenicity factors, even suppresses host defenses (ROS burst) early in the infection process (Williams et al. 2011) which is typically a characteristic of biotrophic and hemi-biotrophic pathogens (Kabbage et al. 2015). The functions of oxalic acid are discussed in further detail later in this review. Ultimately, *S. sclerotiorum*-host interactions are much more complex than a typical necrotrophic designation implies and requires comprehensive investigation of these relationships.

Population structure. While overwintering sclerotia may myceliogenically germinate in the soil, the millions of ascospores generated from the apothecial sexual fruiting body are typically the primary source of SSR inoculum (Peltier et al. 2012; Willetts and Wong 1980). The limited dispersal of ascospores (Ben-Yephet and Bitton 1985) and homothallic life cycle of *S. sclerotiorum* (Willetts and Wong 1980) support regional clonality. Individual clones, however, may be more widely distributed by seed-borne transmission of sclerotia (Hartman et al. 1998). As a result, *S. sclerotiorum* clones are considered highly dispersive, and agricultural populations may contain a conglomeration of different clones (Anderson and Kohn 1995).

Predictably, diverse isolate populations have been documented in US soybean fields (Aldrich-Wolfe et al. 2015; Koga et al. 2014; Kull et al. 2004; Petrofeza and Nasser 2012).

These findings suggest that soybean genotypes should be selected for resistance using appropriately representative isolates. In Brazil, the importance of characterizing *S. sclerotiorum* isolate diversity has been investigated for dry bean resistance evaluations; however, little or no regional variation in aggressiveness was found and/or no interaction between isolate diversity and cultivars was observed (Koga et al. 2014; Lehner et al. 2016; Zancan et al. 2015). As such, resistance evaluations, should account for the regional variation within a pathogen population to ensure the development and release of a durable product. Pathogen diversity should, therefore, be investigated for use in representative resistance evaluations.

Isolate diversity. *S. sclerotiorum* isolate diversity has been investigated using growth characteristics, aggressiveness properties, mycelial compatibility groups (MCGs), and the production of the key pathogenicity factor oxalic acid (OA) (Koga et al. 2014; Kohn et al. 1991; Kull et al. 2004). *In vitro* mycelial compatibility is used as an indication of isolate homogeneity and may be used to detect variation within a fungal population (Kohn et al. 1990). Multiple MCGs have been detected in North America and South America (Kohn et al. 1991; Kull et al. 2004). Isolate genotype, however, is not necessarily associated with isolate aggressiveness at the regional level (Kull et al. 2004; Lehner et al. 2016).

The non-specific key pathogenicity factor, OA, largely contributes to the extraordinarily broad host range of *S. sclerotiorum* (Godoy et al. 1990; Maxwell and Lumsden 1970; Noyes and Hancock 1981). The roles of OA in *S. sclerotiorum* infection include pH-dependent regulation of cell wall degrading enzymes (Bateman and Beer 1965), stomatal regulation (Stotz and Guimaraes 2004), and suppression of host defenses (Cessna et

al. 2000; Williams et al. 2011; Kabbage et al. 2013). OA production may, therefore, more accurately describe isolate aggressiveness. Indeed, OA production by *S. sclerotiorum* isolates has been previously described, and was found to explain isolate aggressiveness in populations recovered from European red clover (Vleugels et al. 2013).

Evaluation of *S. sclerotiorum* populations in the Great Lakes region of the US, using growth characteristics, aggressiveness, and OA production, will help select isolates for resistance evaluations. Breeding programs should consider the overall diversity of *S. sclerotiorum* isolates in areas targeted for release. Isolate characterization, therefore, will improve existing breeding efforts.

Sclerotinia stem rot

Soybean. Soybean is one of the most economically important hosts impacted by SSR (Peltier et al. 2012). Sclerotinia stem rot (SSR) consistently ranks in the top ten most destructive diseases of global soybean crops (Allen et al. 2017; Wrather et al. 2010). In the United States, SSR ranked in the top ten yield reducing diseases of soybeans in 2000, 2004, 2006, and 2009, and continues to significantly contribute to soybean yield reduction (Allen et al. 2017; Koenning and Wrather 2010; Wrather and Koenning 2009). From 2010 to 2014, SSR was responsible for almost 2.8 million metric tons of yield loss in soybeans, which cost growers $1.2 billion USD according to market prices (Allen et al. 2017; USDA-NASS 2017). In 2011 in the Great Lakes region, 94% of the yield losses due to SSR occurred in this region, according to the United Soybean board; producers lost a corresponding ~$138 million according to 2011 market values (USDA-NASS 2017).

Disease cycle. *S. sclerotiorum* overwinters as sclerotia, which are dormant, soilborne survival structures that are resistant to prolonged periods of freezing and thawing (Grau and Hartman 2015). Sclerotia often require a conditioning period (at least 8 weeks at 8-16°C) prior to apothecial germination (Dillard et al. 1995; Phillips 1986). Once sclerotial conditioning is achieved, apothecia will germinate from sclerotia present in the top 2-3 centimeters of soil (Abawi and Grogan 1979); germination generally occurs after canopy closure and after sufficient soil moisture (matric potentials ≥ -5 bars) (Boland and Hall 1988a). Apothecia produce ascospores which are ejected and carried via the wind to infect nearby flowers and pods. Ascospores produced from *S. sclerotiorum* apothecia are the primary source of inoculum for infection by this fungus in soybean (Abawi and Grogan 1974; Grau and Hartman 2015; Peltier et al. 2012; Saharan and Mehta 2008). Flower colonization is followed by stem colonization and lesion development which can drastically reduce yield potential (135 – 336 kg ha^{-1} for every 10% increase in disease severity) (Grau and Hartman 2015). Typical symptoms are water-soaked tan or brown lesions and wilting; obvious signs of *S. sclerotiorum* are the presence of fluffy, white mycelia and black sclerotia on or in plant tissue (Bolton et al. 2006). Disease development is favored by cool (temperatures below 28°C) and moist conditions (continuous surface wetness for 40-112 hr) (Boland and Hall 1988a). Conducive conditions, however, must coincide with apothecial germination and soybean flowering for SSR development.

Disease assessment and yield loss. For SSR, disease incidence (DI) and disease severity (DS) ratings are often combined into a disease severity index score (DSI or DIX; we will use DIX) (Grau et al. 1982; Kim et al. 2000). The DIX score assigns a severity rating of

0 to 3 to some number of evaluated plants (e.g. 30), where 0 = no disease, 1 = disease on the secondary branches or petioles, 2 = non-girdling disease on the main stem which does not impact yield, and 3 = disease girdling the main stem which results in plant wilt or death and impacts yield (Grau et al. 1982). These severity ratings can then be combined with SSR incidence, estimated from the rated plants, by multiplying the DI by the average severity of symptomatic plants divided by 3, which results in a DIX score equivalent to other reported DSI calculations (Fall et al. 2018). While studies of the relationship between incidence and yield have been conducted (Yang et al. 1999; Danielson et al. 2004; Lehner et al. 2016; Hoffman et al. 1998; Chun et al. 1987), few studies have reported the impact of DIX on soybean yield (Fall et al. 2018) and none have been conducted across an entire growing region. Use of this severity rating, represented by the DIX score, in yield loss analysis would provide a novel model that appropriately describes the impact of SSR on modern (highly branching) soybean varieties (Suhre et al. 2014).

Meta-analytic methods. Meta-analytic methods have been devised to analyze results from multiple independent studies (Madden and Paul 2011), and further methods have been developed and implemented to analyze multiple treatments simultaneously (Madden et al. 2016; Paul et al. 2010, 2008; Machado et al. 2017). Meta-analysis can either consider the results or original observations (or individual participant data) of different studies (Madden and Paul 2011). Network, or multivariate analyses, are especially useful to synthesize results from multiple treatments, which are evaluated together, separately, or in various combinations across multiple independent studies, while accounting for between- and within-study variability (Madden et al. 2016). In other words, appropriate models are used to

account for correlations between treatments (or the covariance structure) in the same study and allow for comparisons between these treatments (Madden et al. 2016). Using these methods, moderator variable effects or study-level characteristics such as disease pressure can also be considered (Madden, Piepho, and Paul 2016). Compilation of independent SSR fungicide efficacy trial results using these methods has not been previously performed and would, therefore, provide powerful data-driven recommendations for growers when making management decisions.

Sclerotinia stem rot management

Integrated management. The integrated management of SSR utilizes a combination of cultural, chemical, and biological control practices (Peltier et al. 2012). Some practices may include, crop rotation using non-host crops (Gracia-Garza et al. 2002; Mueller et al. 2002; Rousseau et al. 2007), practicing reduced tillage (Gracia-Garza et al. 2002; Kurle et al. 2001; Mueller et al. 2002), using resistant cultivars (Grau et al. 1982; Hoffman et al. 2002; Kurle et al. 2001), modifying the soybean canopy through seeding rate and row spacing (Jaccoud-Filho et al. 2016; Kurle et al. 2001; Lee et al. 2005), and applying in-season chemical control (Mueller et al. 2004; Peltier et al. 2012; Sumida et al. 2015; Saharan and Mehta 2008). Many of these practices manipulate the host environment to be unfavorable for diseases development, for example, by increasing air flow through the canopy or reducing inoculum development in the field. The most commonly available and well-studied biological agent for SSR control is *Coniothyrium minitans* (Contans®); this parasitic fungus was shown to degrade sclerotia, the survival structure of *S. sclerotiorum* (Campbell 1947). Models predicting risk of fungal or disease development have also been useful to effectively

time fungicide applications in integrated *Sclerotinia* disease management (Clarkson et al. 2014; Foster et al. 2011; Smith et al. 2007; Twengstrom et al. 1998). Major management practices, relevant to this work, are discussed in detail in the following sections.

Soybean resistance. Cultivar selection is one of the most important considerations for SSR management. Disease control is limited by the lack of complete resistance to SSR; however, several partially resistant soybean genotypes have been identified (Boland and Hall 1987; Grau, Radke, and Gillespie 1982; Kim and Diers 2000). Within partially resistant cultivars, various quantitative trait loci (QTL) were found to contribute to Sclerotinia stem rot resistance. Some examples include three QTL identified by Kim and Diers (2000) and 28 QTL identified by Arahana et al. (2001) which individually explain 4-10% of the phenotypic variation of the trait. Other QTL have been associated with soluble pigments (likely containing anthocyanins) present in resistant soybean stems (Li et al. 2010). Field resistance screening sometimes identifies QTL linked to escape mechanisms, rather than physiological resistance, such as plant height, lodging, and date of flowering (Kim and Diers 2000). Using detached leaf or whole plant assays helps to identify resistance associated with physiological mechanisms which result in direct reduction of infection (Arahana et al. 2001). Other studies have used transgenic approaches to develop genetically resistant soybeans which degrade oxalic acid (*S. sclerotiorum* pathogenicity factor) (Cunha et al. 2010) or silence soybean NADPH oxidases (Ranjan et al. 2017). Transgenic forms of *S. sclerotiorum* resistance, however, have yet to be exploited commercially in soybean.

Traditionally, soybean resistance studies have been conducted in controlled environments with only one or two aggressive *S. sclerotiorum* isolates (Boland and Hall

1986; Hoffman et al. 2002; Kim and Diers 2000; Wegulo et al. 1998). The predominantly clonal population structure and regional similarities has historically justified single-isolate selections (Auclair et al. 2004). As discussed previously, however, agricultural populations may contain a conglomeration of different clones (Anderson and Kohn 1995), and diverse isolate populations have been documented in US soybean fields (Aldrich-Wolfe et al. 2015; Koga et al. 2014; Kull et al. 2004; Petrofeza and Nasser 2012). Ongoing breeding efforts should use selections of isolates that account for the overall *S. sclerotiorum* population structure in target areas.

A better understanding of physiological disease resistance in soybeans could also improve resistance development. In SSR, infection begins with ascospore colonization of soybean flowers and is rapidly followed by stem colonization and subsequent lesion formation. The colonization of floral and stem tissues is, therefore, of interest in understanding soybean resistance mechanisms. *S. sclerotiorum* colonization was monitored in the flowers and leaves of an oxalate oxidase-over expressing (OxO-OE), resistant soybean and the wild-type (WT) susceptible parent (Davidson et al. 2016). While oxalic acid (OA) accumulation differed in all tissues of OxO-OE and WT soybean, no differences in colonization of floral tissues were detected. Disease severities, integrating flower and stem infection, however, were different between resistant and susceptible plants. Differences in stem colonization could, therefore, elucidate the mechanism of soybean resistance involved in reducing *S. sclerotiorum* infection.

A variety of histopathological methods were used to differentiate the stem colonization habits of *Cadophora gregata* (formerly known as *Phialophora gregata*), the

causal agent of brown stem rot, in resistant and susceptible soybean cultivars (Impullitti and Malvick 2014). Fungal hyphae were either stained with lactophenol aniline blue and visualized using light microscopy or were expressing green fluorescent protein (GFP) or red fluorescent protein (RFP) and visualized using laser scanning confocal microscopy (LSCM). Using similar techniques, differences in *S. sclerotiorum* infection of resistant and susceptible soybean stems may be monitored. *S. sclerotiorum* infection has been visualized in dry bean, canola, soybean, and sunflower using isolates expressing GFP (de Silva et al. 2009). In these findings, fluorescent *S. sclerotiorum* hyphae were detected in susceptible soybean petiole tissues. Microscopic visualization of stem colonization, therefore, could be conducted using staining techniques and further enhanced using *S. sclerotiorum* isolates expressing fluorescent proteins.

Ergosterol is a fungus-specific lipid (Nes 1977) and has been used to quantify *in vitro S. sclerotiorum* fungal biomass (Yarden et al. 2014). Furthermore, ergosterol has been used to detect fungal pathogens, *Diaporthe phaseolorum* and *Cercospora kikuchii*, in soybean cotyledon samples (Xue et al. 2006). Colonization evidence collected in microscopic studies could be substantiated using ergosterol quantification from inoculated stem tissues. Fungal biomass assays and colonization assays using multiple histopathological techniques will help understand physiological mechanisms of resistance in soybean germplasm. These studies, in combination with studies investigating *S. sclerotiorum* populations, will improve ongoing soybean breeding efforts.

Chemical control. As no complete resistance is available in commercial cultivars, in-season management relies heavily on chemical control targeted at protecting the flowers from

S. sclerotiorum ascospore infection (Peltier et al. 2012). Soybean flowering occurs from the R1 (beginning flower) to R3 (beginning pod) growth stages (Fehr et al. 1971). Most fungicides used in SSR control are classified as methyl benzimidazole carbamates (MBC) (e.g. thiophanate-methyl), succinate dehydrogenase inhibitors (SDHI) (e.g. boscalid), demethylation inhibitors (DMI) (e.g. flutriafol, prothioconazole, tetraconazole), and quinone outside inhibitors (QoI) (e.g. fluoxastrobin, picoxystrobin, trifloxystrobin) (Armando et al. 2015; Di et al. 2016; Huzar-Novakowiski et al. 2017; Liang et al. 2015; Peltier et al. 2012). Fluazinam, an uncoupler of oxidative phosphorylation (uncouplers), has also been found to effectively inhibit *S. sclerotiorum* (Liang et al. 2015).

These fungicide classes inhibit *S. sclerotiorum* growth and development in a variety of ways. The MBC fungicides inhibit fungal cell division whereas SDHI, QoI, and uncoupler fungicides interfere with the electron transport chain inhibiting cellular respiration and energy production (Peltier et al. 2012). DMI fungicides, on the other hand, inhibit sterol biosynthesis which results in abnormal fungal cell wall development (Peltier et al. 2012). Fungicides inhibiting energy production will effectively inhibit spore germination whereas those targeting cellular structure or growth will only simply slow fungal growth. In addition to these fungicides, the herbicide lactofen has also been identified for SSR management; herbicides impact canopy development and promote systemic resistance, both of which inhibit infection by *S. sclerotiorum* and subsequent development of SSR (Peltier et al. 2012; Dann et al. 1999).

Epidemiological modeling. Soybean flowering, apothecial germination, and conducive weather conditions must occur simultaneously for SSR development. Due to this

complex array of factors, fungicide applications are often ineffective, and even unnecessary. The development of a predictive model to forecast SSR in soybeans will help effectively time fungicide applications for improved disease control. *Sclerotinia* forecasting models have been developed for other crop systems, such as peanut, carrot, lettuce, and canola. Under controlled environment conditions, ascospore density (>87 spores cm^{-2}), temperature (21.7°C optimal), and relative humidity (80-100%) were used to predict *S. sclerotiorum* infection of lettuce (Clarkson et al. 2014). In lettuce, apothecial germination occurred after 30-50 days at temperatures of 18-20°C after appropriate sclerotial conditioning (Clarkson et al. 2007). These findings suggest that temperature and moisture over a period of 30-50 days influences apothecial development. Moving averages of weather variables, therefore, will be investigated for integration into a predictive model for apothecial development in soybean.

Models incorporating soil temperature (maximum of 24°C) and moisture (≥20 kPa) were also shown to predict the development of apothecia and ascospores of Sclerotinia rot in carrot (SRC) (Foster et al. 2011). These data were incorporated into a model which also accounted for field history, canopy closure (>95%), and senescing leaves (on 70-80% of plants) to better predict the fungicide applications necessary for disease control. In a two-year field validation study, the model reduced the total number of fungicide applications and achieved equivalent control to a typical calendar-spray regime (Foster et al. 2011). Soil parameters are often difficult to simulate and acquire for site-specific predictions unless an on-site scientific weather station is feasible. Simulated virtual weather data, however, is readily available for most air temperature and moisture variables. Models generated using these publicly available data will allow the model to be accessible and functional in virtually

any growing location (Magarey et al. 2001). Using architectural and phenological initiation parameters, such as canopy closure and flowering, will nevertheless be useful in model development and will be used in SSR prediction for soybean systems.

Studies in China have investigated correlations between the numbers of apothecia present during the blossom stage, disease incidence, and yield loss (Pan et al. 2001; Saharan and Mehta 2008). Both number of apothecia and disease severity were negatively correlated with yield loss, and a control threshold of three to four apothecia per 9.75 m^2 was established. Apothecial size (approximately 0.5-2.0 mm in diameter) (Grau and Hartman 2015) and aggregated distribution (Boland and Hall 1988b), however, make this model difficult to implement for growers. A study conducted in the North-Central region of the US used logistic regression to model the prevalence of soybean SSR (Mila et al. 2004). Using total precipitation and air temperature in either April or July combined with regional tillage practices, disease prevalence was modeled at a regional level. This model, however, was not accurate at the field level. Growers in the Great Lakes region, therefore, would benefit from an accurate, site-specific model to use in risk assessment of SSR in soybean fields.

Historically, *S. sclerotiorum* apothecia and SSR incidence were both spatially aggregated and correlated within sectors of soybean fields (Boland and Hall 1988b). More recently, the distribution of SSR has been correlated with apothecia in both canola (Qandah and del Rio Mendoza 2012) and soybean (Wegulo et al. 2000). In both studies, disease incidence decreased as distance from apothecial inoculum sources increased. Furthermore, ascospores were deposited near the apothecia within soybean fields (Wegulo et al. 2000), which supports the relationship between apothecia and disease. Sclerotial load, determined

by intensive soil sampling, was not found to describe white mold incidence in bean fields (McDonald and Boland 2004). Apothecial presence, therefore, is a promising candidate to use for SSR risk assessment in soybean fields. A model to predict apothecial presence could be used in integrated SSR management to treat areas of increased risk if weather conditions are conducive.

Light has been shown to play a role in *Botrytis cinerea* growth and sporulation (Tan and Epton 1973) and in Stemphylium leaf spot, caused by *S. botryosum*, development in alfalfa (Cowling and Gilchrist 1982). Near-ultraviolet wavelengths of light have even been shown to influence conidial development in *Alternaria tomato* (Kumagai and Oda 1969). Similarly, *S. sclerotiorum* apothecial development is influenced by different light intensities (Sun and Yang 2000) and requires ultraviolet wavelengths of light between 276 and 319 nm (Thaning and Nilsson 2000). Field and controlled environment studies will be conducted to determine the effects of the soybean canopy and various light profiles on apothecial development. This information will be incorporated into an optimized model to predict apothecial presence.

Literature Cited

Abawi, G., and Grogan, R. 1979. Epidemiology of diseases caused by *Sclerotinia* species. Phytopathology. 69:899–904 Available at: http://www.apsnet.org/publications/phytopathology/backissues/Documents/1979Abstracts/Phyto69_899.htm.

Abawi, G. S., and Grogan, R. G. 1974. Source of primary inoculum and effects of temperature and moisture on infection of beans by *Whetzelinia sclerotiorum*. Phytopathology. 65:300–309.

Adams, P. B., and Ayers, W. A. 1979. Ecology of *Sclerotinia* Species. Phytopathology. 69:896–899.

Aldrich-Wolfe, L., Travers, S., and Nelson, B. D. 2015. Genetic variation of *Sclerotinia*

sclerotiorum from multiple crops in the North Central United States. PLoS One. 10:e0139188 Available at: http://dx.plos.org/10.1371/journal.pone.0139188.

Allen, T. W., Bradley, C. A., Sisson, Adam, J., Byamukama, E., Chilvers, M. I., Coker, C. M., et al. 2017. Soybean yield loss estimates due to diseases in the United States and Ontario, Canada from 2010 to 2014. Plant Heal. Prog.

Amselem, J., Cuomo, C. a, van Kan, J. a L., Viaud, M., Benito, E. P., Couloux, A., et al. 2011. Genomic analysis of the necrotrophic fungal pathogens *Sclerotinia sclerotiorum* and *Botrytis cinerea*. PLoS Genet. 7:e1002230 Available at: http://www.pubmedcentral.nih.gov/articlerender.fcgi?artid=3158057&tool=pmcentrez&rendertype=abstract [Accessed January 23, 2014].

Anderson, J. B., and Kohn, L. M. 1995. Clonality in soilborne, plant-pathogenic fungi. Annu. Rev. Phytopathol. 33:369–391.

Arahana, V. S., Graef, G. L., Specht, J. E., Steadman, J. R., and Eskridge, K. M. 2001. Identification of QTLs for resistance to Sclerotinia sclerotiorum in soybean. Crop Sci. 41:180–188.

Armando, Q., Armenta, A., Mondaca, E. C., Ángel, M., Sánchez, A., Manuel, V., et al. 2015. Efectividad de fungicidas convencionales y biorracionales sobre Sclerotinia sclerotiorum in vitro. Rev. Mex. Cienc. Agric. 11:2149–2156.

Auclair, J., Boland, G. J., Kohn, L. M., and Rajcan, I. 2004. Genetic interactions between *Glycine max* and *Sclerotinia sclerotiorum* using a straw inoculation method. Plant Dis. :891–895.

de Bary, A. 1887. *Comparative morphology and biology of the fungi, mycetozoa and bacteria (translated by Henry E.F. Garnsey; revised by Isaac B. Balfour)*. Clarendon Press.

Bateman, D. F., and Beer, S. V. 1965. Simultaneous production and synergistic action of oxalic acid and polygalacturonase during pathogenesis by *Sclerotium rolfsii*. Phytopathology. 55:204–211.

Ben-Yephet, Y., and Bitton, S. 1985. Use of a selective medium to study the dispersal of ascospores of *Sclerotinia sclerotiorum*. Phytoparasitica. 13:33–40.

Boland, G. J., and Hall, R. 1988a. Epidemiology of Sclerotinia stem rot of soybean in Ontario. Phytopathology. 78:1241.

Boland, G. J., and Hall, R. 1987. Evaluating soybean cultivars for resistance to *Sclerotinia sclerotiorum* under field conditions. Plant Dis. 71:934–936.

Boland, G. J., and Hall, R. 1986. Growthroom evaluation of soybean cultivars for resistance to *Sclerotinia sclerotiorum*. Can. J. Plant Sci. 66:559–564 Available at: http://article.pubs.nrc-cnrc.gc.ca/ppv/RPViewDoc?issn=0008-4220&volume=66&issue=3&startPage=559&ab=y.

Boland, G. J., and Hall, R. 1994. Index of plant hosts of *Sclerotinia sclerotiorum*. Can. J.

Plant Pathol. 16:93–108.

Boland, G. J., and Hall, R. 1988b. Relationships between the spatial pattern and number of apothecia of *Sclerotinia sclerotiorum* and stem rot of soybean. Plant Pathol. 37:329–336.

Bolton, M. D., Thomma, B. P. H. J., and Nelson, B. D. 2006. *Sclerotinia sclerotiorum* (Lib.) de Bary: biology and molecular traits of a cosmopolitan pathogen. Mol. Plant Pathol. 7:1–16.

Broeske, M., Gaspar, A. P., Gaska, J. M., and Conley, S. P. 2016. Soybean growth stages. Univ. Wisconsin-Madison, UW-Extension, Madison, WI.

Campbell, W. A. 1947. A new species of *Coniothyrium parasitic* on sclerotia. Mycologia. 39:190–195.

Carter, T. E., Gizlice, Z., and Burton, J. W. 1945. Coefficient-of-parentage and genetic-similarity estimates for 258 North American soybean cultivars released by public agencies during 1945-88. In *U.S. Department of Agriculture, Technical Bulletin No. 1814*, , p. 1–168.

Cessna, S. G., Sears, V. E., Dickman, M. B., and Low, P. S. 2000. Oxalic acid, a pathogenicity factor for *Sclerotinia sclerotiorum*, suppresses the oxidative burst of the host plant. Plant Cell. 12:2191–200 Available at: http://www.pubmedcentral.nih.gov/articlerender.fcgi?artid=150167&tool=pmcentrez&rendertype=abstract.

Chun, D., Kao, L. B., Lockwood, J. L., and Isleib, T. G. 1987. Laboratory and field assessment of resistance in soybean to stem rot caused by *Sclerotinia sclerotiorum*. Plant Dis. 71:811–815.

Clarkson, J. P., Fawcett, L., Anthony, S. G., and Young, C. 2014. A model for *Sclerotinia sclerotiorum* infection and disease development in lettuce, based on the effects of temperature, relative humidity and ascospore density. PLoS One. 9:e94049 Available at: http://www.pubmedcentral.nih.gov/articlerender.fcgi?artid=3988091&tool=pmcentrez&rendertype=abstract [Accessed May 27, 2014].

Clarkson, J. P., Phelps, K., Whipps, J. M., Young, C. S., Smith, J. a, and Watling, M. 2007. Forecasting Sclerotinia disease on lettuce: a predictive model for carpogenic germination of *Sclerotinia sclerotiorum* sclerotia. Phytopathology. 97:621–31 Available at: http://www.ncbi.nlm.nih.gov/pubmed/18943582.

Clarkson, J. P., Phelps, K., Whipps, J. M., Young, C. S., Smith, J. a, and Watling, M. 2004. Forecasting Sclerotinia disease on lettuce: toward developing a prediction model for carpogenic germination of sclerotia. Phytopathology. 94:268–79 Available at: http://www.ncbi.nlm.nih.gov/pubmed/18943975.

Cowling, W. A., and Gilchrist, D. G. 1982. Effect of light and moisture on severity of Stemphylium leaf spot of alfalfa. Plant Dis. 66:291–294.

Cui, Z., Carter, T. E., Burton, J. W., and Wells, R. 2001. Phenotypic diversity of modern Chinese and North American soybean cultivars. Crop Sci. 41:1954–1967.

Cui, Z., Carter, T. E., Gai, J., Qiu, J., and Nelson, R. 1999. Origin, description, and pedigree of Chinese soybean cultivars released from 1923 to 1995. In *U.S. Department of Agriculture, Agricultural Research Service, Technical Bulletin No. 1871*, , p. 1–267.

Cunha, W. G., Tinoco, M. L. P., Pancoti, H. L., Ribeiro, R. E., and Aragão, F. J. L. 2010. High resistance to *Sclerotinia sclerotiorum* in transgenic soybean plants transformed to express an oxalate decarboxylase gene. Plant Pathol. 59:654–660 Available at: http://doi.wiley.com/10.1111/j.1365-3059.2010.02279.x [Accessed June 6, 2014].

Danielson, G. A., Nelson, B. D., and Helms, T. C. 2004. Effect of Sclerotinia stem rot on yield of soybean inoculated at different growth stages. Plant Dis. 88:297–300.

Dann, E. K., Diers, B. W., and Hammerschmidt, R. 1999. Suppression of Sclerotinia stem rot of soybean by lactofen herbicide treatment. Phytopathology. 89:598–602.

Davidson, A. L., Blahut-Beatty, L., Itaya, A., Zhang, Y., Zheng, S., and Simmonds, D. 2016. Histopathology of *Sclerotinia sclerotiorum* infection and oxalic acid function in susceptible and resistant soybean. Plant Pathol. 65:878–887 Available at: http://doi.wiley.com/10.1111/ppa.12514.

Di, Y. L., Zhu, Z. Q., Lu, X. M., and Zhu, F. X. 2016. Baseline sensitivity and efficacy of trifloxystrobin against *Sclerotinia sclerotiorum*. Crop Prot. 87:31–36.

Dillard, H. R., Ludwig, J. W., and Hunter, J. E. 1995. Conditioning sclerotia of *Sclerotinia sclerotiorum* for carpogenic germination. Plant Dis. 79:411–415 Available at: http://www.apsnet.org/publications/PlantDisease/BackIssues/Documents/1995Articles/PlantDisease79n04_411.pdf.

Fall, M. F., Boyse, J. F., Wang, D., Willbur, J. F., Smith, D. L., and Chilvers, M. I. 2018. Case study of an epidemiological approach dissecting historical soybean Sclerotinia stem rot observations and identifying environmental predictors of epidemics and yield loss. Phytopathology. XX:XX–XX.

Fehr, W. R., Caviness, C. E., Burmood, D. T., and Pennington, J. S. 1971. Stage of development descriptions for soybeans, *Glycine max* (L.) Merill. Crop Sci. 11:929–931.

Foster, A. J., Kora, C., McDonald, M. R., and Boland, G. J. 2011. Development and validation of a disease forecast model for Sclerotinia rot of carrot. Can. J. Plant Pathol. 33:187–201 Available at: http://www.tandfonline.com/doi/abs/10.1080/07060661.2011.563753 [Accessed January 21, 2014].

Fuckel, L. 1869. *Beiträge zur Kenntniss der Rheinischen Pilze*.

Godoy, G., Steadman, J., Dickman, M., and Dam, R. 1990. Use of mutants to demonstrate the role of oxalic acid in pathogenicity of *Sclerotinia sclerotiorum* on *Phaseolus vulgaris*. Physiol. Mol. Plant Pathol. 37:179–191.

Gracia-Garza, J. A., Neumann, S., Vyn, T. J., and Boland, G. J. 2002. Influence of crop rotation and tillage on production of apothecia by *Sclerotinia sclerotiorum*. Can. J. Plant

Pathol. 24:137–143.

Grau, C. R., and Hartman, G. L. 2015. *Compendium of soybean diseases*. 5th ed. eds. G.L. Hartman, J.C. Rupe, E.J. Sikora, L.L. Domier, J.A. Davis, and K.L. Steffey. St Paul, MN: The American Phytopathological Society.

Grau, C., Radke, V., and Gillespie, F. 1982. Resistance of soybean cultivars to *Sclerotinia sclerotiorum*. Plant Dis. 66:506–508.

Hartman, G. L., Kull, L., and Huang, Y. H. 1998. Occurence of *Sclerotinia sclerotiorum* in soybean fields in East-Central Illinois and enumeration of inocula in soybean seed lots. Plant Dis. 82:560–564.

Hoffman, D. D., Diers, B. W., Hartman, G. L., Nickell, C. D., Nelson, R. L., Pedersen, W. L., et al. 2002. Selected soybean plant introductions with partial resistance to *Sclerotinia sclerotiorum*. Plant Dis. 86:971–980 Available at: http://apsjournals.apsnet.org/doi/abs/10.1094/PDIS.2002.86.9.971.

Hoffman, D. D., Hartman, G. L., Mueller, D. S., Leitz, R. A., Nickell, C. D., and Pedersen, W. L. 1998. Yield and seed quality of soybean cultivars infected with *Sclerotinia sclerotiorum*. Plant Dis. 82:826–829.

Huzar-Novakowiski, J., Paul, P. A., and Dorrance, A. E. 2017. Host resistance and chemical control for management of Sclerotinia stem rot of soybean in Ohio. Phytopathology. XX:XX–XX.

Impullitti, A. E., and Malvick, D. K. 2014. Anatomical response and infection of soybean during latent and pathogenic infection by Type A and B of *Phialophora gregata*. PLoS One. 9:e98311 Available at: http://www.pubmedcentral.nih.gov/articlerender.fcgi?artid=4039477&tool=pmcentrez&rendertype=abstract [Accessed June 5, 2014].

Jaccoud-Filho, D., Fadel Sartori, F., Manosso-Neto, M., Maurício Vrisman, C., da Cunha Pierre, M. L., Berger-Neto, A., et al. 2016. Influence of row spacing and plant population density on management of " white mould " in soybean in southern Brazil. Aust. J. Crop Sci. 10:161–168.

Jensen, B., and Smith, D. L. 2017. Generalized calendar of events for insects and diseases in Wisconsin: Soybean. UW-Extension Rep. :1–4.

Kabbage, M., Williams, B., and Dickman, M. B. 2013. Cell death control: the interplay of apoptosis and autophagy in the pathogenicity of *Sclerotinia sclerotiorum*. PLoS Pathog. 9:e1003287 Available at: http://dx.plos.org/10.1371/journal.ppat.1003287.

Kabbage, M., Yarden, O., and Dickman, M. B. 2015. Pathogenic attributes of *Sclerotinia sclerotiorum*: switching from a biotrophic to necrotrophic lifestyle. Plant Sci. 233:53–60 Available at: http://linkinghub.elsevier.com/retrieve/pii/S0168945214003057.

Kim, H. S., and Diers, B. W. 2000. Inheritance of partial resistance to Sclerotinia stem rot in soybean. Crop Sci. 40:55–61.

Kim, H. S., Hartman, G. L., Manandhar, J. B., Graef, G. L., Steadman, J. R., and Diers, B. W. 2000. Reaction of soybean cultivars to Sclerotinia stem rot in field, greenhouse, and laboratory evaluations. Crop Sci. 40:665–669.

Koenning, S. R., and Wrather, J. A. 2010. Suppression of soybean yield potential in the continental United States by plant diseases from 2006 to 2009. Plant Heal. Prog.

Koga, L. J., Bowen, C. R., Godoy, C. V., Oliveira, M. C. N. De, and Hartman, G. L. 2014. Mycelial compatibility and aggressiveness of *Sclerotinia sclerotiorum* isolates from Brazil and the United States. Pesqui. Agropecuária Bras. 49:265–272 Available at: http://www.scielo.br/scielo.php?script=sci_arttext&pid=S0100-204X2014000400265&lng=en&nrm=iso&tlng=en.

Kohn, L. M. 1979. A monographic revision of the genus Sclerotinia. Mycotaxon. 9:365–444.

Kohn, L. M., Carbone, I., and Anderson, J. B. 1990. Mycelial interactions in *Sclerotinia sclerotiorum*. Exp. Mycol. 14:255–267.

Kohn, L. M., Stasovski, E., Carbone, I., Royer, J., and Anderson, J. B. 1991. Mycelial incompatibility and molecular markers identify genetic variability in field populations of *Sclerotinia sclerotiorum*. Phytopathology. 81:480–485.

Korf, R. R., and Dumont, K. P. 1972. Whetzelinia, a new generic name for *Sclerotinia sclerotiorum* and *S. tuberosa*. Mycologia. 64:248–251.

Kull, L. S., Pedersen, W. L., Palmquist, D., and Hartman, G. L. 2004. Mycelial compatibility grouping and aggressiveness of *Sclerotinia sclerotiorum*. Plant Dis. 88:325–332 Available at: http://dx.doi.org/10.1094/PDIS.2004.88.4.325.

Kumagai, T., and Oda, Y. 1969. Blue and near ultraviolet reversible photoreaction in conidial development of the fungus, *Alternaria tomato*. Dev Growth Differ. 11:130–142 Available at: http://www.ncbi.nlm.nih.gov/pubmed/5392521.

Kurle, J. E., Grau, C. R., Oplinger, E. S., and Mengistu, A. 2001. Tillage, crop sequence, and cultivar effects on Sclerotinia stem rot incidence and yield in soybean. Agron. J. 93:973–982.

Lee, C. D., Renner, K. A., Penner, D., Hammerschmidt, R., and Kelly, J. D. 2005. Glyphosate-resistant soybean management system effect on Sclerotinia stem rot. Weed Technol. 19:580–588.

Lehner, M. S., Lima, R. C., Carneiro, J. E. S., Paula Júnior, T. J., Vieira, R. F., and Mizubuti, E. S. G. 2016. Similar aggressiveness of phenotypically and genotypically distinct isolates of *Sclerotinia sclerotiorum*. Plant Dis. 100:360–366 Available at: http://dx.doi.org/10.1094/PDIS-04-15-0400-RE.

Lehner, M. S., Pethybridge, S. J., Meyer, M. C., and Del Ponte, E. M. 2016. Meta-analytic modelling of the incidence-yield and incidence-sclerotial production relationships in soybean white mould epidemics. Plant Pathol.

Li, D., Sun, M., Han, Y., Teng, W., and Li, W. 2010. Identification of QTL underlying

soluble pigment content in soybean stems related to resistance to soybean white mold (*Sclerotinia sclerotiorum*). Euphytica. 172:49–57 Available at: http://link.springer.com/10.1007/s10681-009-0036-z [Accessed June 6, 2014].

Liang, H. J., Di, Y. L., Li, J. L., and Zhu, F. X. 2015. Baseline sensitivity and control efficacy of fluazinam against *Sclerotinia sclerotiorum*. Eur. J. Plant Pathol. 142:691–699.

Libert, M. A. 1837. Plante crytogamicae arduennae (Exsiccati) No. 326. Publ. by author.

Lumsden, R. D., and Dow, R. L. 1973. Histopathology of *Sclerotinia sclerotiorum* infection of bean. Phytopathology. 63:708.

Machado, F. J., Fitopatologia, D. De, and Viçosa, U. F. De. 2017. Quantitative review of the effects of triazole and benzimidazole fungicides on Fusarium head blight and wheat yield in Brazil. :1633–1641.

Madden, L. V, and Paul, P. A. 2011. Meta-analysis for evidence synthesis in plant pathology: an overview. Phytopathology. 101:16–30 Available at: http://www.ncbi.nlm.nih.gov/pubmed/21142781%5Cnhttp://apsjournals.apsnet.org/doi/abs/10.1094/PHYTO-03-10-0069.

Madden, L. V, Piepho, H., and Paul, P. A. 2016. Statistical models and methods for network meta-analysis. Phytopathology. 106:792–806.

Magarey, R., Seem, R., Russo, J., Zack, J., Waight, K., Travis, J., et al. 2001. Site-specific weather information without on-site sensors. Plant Dis. 85:1216–1226.

Maxwell, D. P., and Lumsden, R. D. 1970. Oxalic acid production by *Sclerotina sclerotiorum* in infected bean and in culture. Phytopathology. 60:1395–1398.

McDonald, M. R., and Boland, G. J. 2004. Forecasting diseases caused by *Sclerotinia* spp. in eastern Canada: fact or fiction? Can. J. Plant Pathol. 488:480–488.

Mila, A. L., Carriquiry, A. L., and Yang, X. B. 2004. Logistic regression modeling of prevalence of soybean Sclerotinia stem rot in the north-central region of the United States. Phytopathology. 94:102–110.

Mueller, D. S., Bradley, C. A., Grau, C. R., Gaska, J. M., Kurle, J. E., and Pedersen, W. L. 2004. Application of thiophanate-methyl at different host growth stages for management of Sclerotinia stem rot in soybean. Crop Prot. 23:983–988.

Mueller, D. S., Hartman, G. L., and Pedersen, W. L. 2002. Effect of crop rotation and tillage system on Sclerotinia stem rot on soybean. Can. J. Plant Pathol. 24:450–456.

Nes, W. R. 1977. *Advances in Lipid Research, Volume 15*. eds. Rodolfo Paoletti and David Kritchevsky. New York: Academic Press.

Noyes, R. D., and Hancock, J. G. 1981. Role of oxalic acid in the Sclerotinia wilt of sunflower. Physiol. Plant Pathol. 18:123–132 Available at: http://linkinghub.elsevier.com/retrieve/pii/S0048405981800331 [Accessed June 6, 2014].

Pan, H., Xi, J., Liu, W., Wan, Q., and Li, H. 2001. Optimal stage and threshold of the control of Sclerotinia rot. Acta Phytophylacica Sin. 28:199–302.

Paul, P. A., Lipps, P. E., Hershman, D. E., McMullen, M. P., Draper, M. A., and Madden, L. V. 2008. Efficacy of triazole-based fungicides for Fusarium head blight and deoxynivalenol control in wheat: a multivariate meta-analysis. Phytopathology. 98:999–1011 Available at: http://apsjournals.apsnet.org/doi/10.1094/PHYTO-98-9-0999.

Paul, P. A., Mcmullen, M. P., Hershman, D. E., and Madden, L. V. 2010. Meta-analysis of the effects of triazole-based fungicides on wheat yield and test weight as influenced by Fusarium head blight intensity. Phytopathology. 100:160–171.

Pedersen, P. 2004. *Soybean growth and development*. Iowa State University, Ames, IA.

Peltier, A. J., Bradley, C. A., Chilvers, M. I., Malvick, D. K., Mueller, D. S., Wise, K. A., et al. 2012. Biology, yield loss and control of Sclerotinia stem rot of soybean. J. Integr. Pest Manag. 3:1–7 Available at: http://openurl.ingenta.com/content/xref?genre=article&issn=2155-7470&volume=3&issue=2&spage=1.

Petrofeza, S., and Nasser, L. C. B. 2012. *Case study: Sclerotinia sclerotiorum: Genetic diversity and disease control*. Prof. Mahm. InTech. Available at: http://www.intechopen.com/books/the-molecular-basis-of- plant-genetic-diversity/case-study-sclerotinia-sclerotiorum-genetic-diversity-and-disease-control.

Phillips, A. 1986. Carpogenic germination of sclerotia of *Sclerotinia sclerotiorum* after periods of conditioning in soil. J. Phytopathol. 116:247–258.

Purdy, L. H. 1979. Sclerotinia sclerotiorum: history, diseases and symptomatology, host range, geographic distribution, and impact. Phytopathology. 69:875.

Qandah, I. S., and del Rio Mendoza, L. E. 2012. Modelling inoculum dispersal and Sclerotinia stem rot gradients in canola fields. Can. J. Plant Pathol. 34:390–400.

Ranjan, A., Jayaraman, D., Grau, C., Hill, J. H., Whitham, S. A., Ané, J. M., et al. 2017. The pathogenic development of *Sclerotinia sclerotiorum* in soybean requires specific host NADPH oxidases. Mol. Plant Pathol. :1–15.

Rousseau, G., Rioux, S., and Dostaler, D. 2007. Effect of crop rotation and soil amendments on Sclerotinia stem rot on soybean in two soils. Can. J. Plant Sci. 87:605–614.

Saharan, G. S., and Mehta, N. 2008. Sclerotinia *diseases of crop plants: biology, ecology and disease management*. Springer.

Shurtleff, W., and Aoyagi, A. 2010. *History of soybeans and soyfoods in Southeast Asia (13th Century to 2010)*. Lafayette, CA: Soyinfo Center.

de Silva, A. P., Bolton, M. D., and Nelson, B. . 2009. Transformation of *Sclerotinia sclerotiorum* with the green fluorescent protein gene and fluorescence of hyphae in four inoculated hosts. Plant Pathol. 58:487–496.

Smith, D. L., Hollowell, J. E., Isleib, T. G., and Shew, B. B. 2007. A site-specific, weather-based disease regression model for Sclerotinia blight of peanut. Plant Dis. 91:1436–1444 Available at: http://sfx.scholarsportal.info/guelph?url_ver=Z39.88-2004&rft_val_fmt=info:ofi/fmt:kev:mtx:journal&genre=article&sid=ProQ:ProQ%253Adeepindexagrsci&atitle=A+Site-Specific%252C+Weather-Based+Disease+Regression+Model+for+Sclerotinia+Blight+of+Peanut&title=Pl.

Specht, J. E., Hume, D. J., and Kumudini, S. V. 1999. Soybean yield potential - A genetic and physiological perspective. Crop Sci. 39:1560–1570.

Specht, J. E., and Williams, J. H. 1984. Contribution of genetic technology to soybean productivity - retrospect and prospect. In *Contributions to yield gains of five major crop plants*, ed. W.R. Fehr. Madison, WI: American Society of Agronomy and Crop Science Society of America, p. 49–74.

Stotz, H. U., and Guimaraes, R. L. 2004. Oxalate production by *Sclerotinia sclerotiorum* deregulates guard cells during infection. Plant Physiol. 136:3703–3711.

Suhre, J. J., Weidenbenner, N. H., Rowntree, S. C., Wilson, E. W., Naeve, S. L., Conley, S. P., et al. 2014. Soybean yield partitioning changes revealed by genetic gain and seeding rate interactions. Agron. J. 106:1631–1642.

Sumida, C. H., Canteri, M. G., Peitl, D. C., Tibolla, F., Orsini, I. P., Araújo, F. A., et al. 2015. Chemical and biological control of Sclerotinia stem rot in the soybean crop. Ciência Rural. 45:760–766 Available at: http://www.scielo.br/scielo.php?script=sci_arttext&pid=S0103-84782015000500760&lang=pt.

Sun, P., and Yang, X. B. 2000. Light, temperature, and moisture effects on apothecium production of *Sclerotinia sclerotiorum*. Plant Dis. 84:1287–1293.

Tan, K. K., and Epton, H. A. S. 1973. Effect of light on the growth and sporulation of *Botrytis cinerea*. Trans. Br. Mycol. Soc. 61:145–157 Available at: http://linkinghub.elsevier.com/retrieve/pii/S0007153673800968.

Thaning, C., and Nilsson, H.-E. 2000. A narrow range of wavelengths active in regulating apothecial development in *Sclerotinia sclerotiorum*. J. Phytopathol. 631:627–631.

Twengstrom, E., Sigvald, R., Svensson, C., and Yuen, J. 1998. Forecasting Sclerotinia stem rot in spring sown oilseed rape. Crop Prot. 17:405–411.

United States Department of Agriculture - National Agricultural Statistics Service (USDA-NASS). 2017. United States soybean prices. USDA-NASS:Washington, DC.

Vleugels, T., Baert, J., and van Bockstaele, E. 2013. Morphological and pathogenic characterization of genetically diverse *Sclerotinia* isolates from European red clover crops (*Trifolium pratense L.*). J. Phytopathol. 161:254–262 Available at: http://doi.wiley.com/10.1111/jph.12056.

Wakefield, E. M. 1924. On the names *Sclerotinia sclerotiorum* (Lib.) Massee and *S.*

libertiana Fuckel. Phytopathology. 14:126–127.

Wegulo, S. N., Sun, P., Martinson, C. a., and Yang, X. B. 2000. Spread of Sclerotinia stem rot of soybean from area and point sources of apothecial inoculum. Can. J. Plant Sci. 80:389–402.

Wegulo, S. N., Yang, X. B., and Martinson, C. A. 1998. Soybean cultivar responses to *Sclerotinia sclerotiorum* in field and controlled environment studies. Plant Dis. 82:1264–1270.

Willetts, H. J., and Wong, J. A.-L. 1980. The biology of *Sclerotinia sclerotiorum, S. trifoliorum*, and *S. minor* with emphasis on specific nomenclature. Bot. Rev. 36:101–165.

Williams, B., Kabbage, M., Kim, H.-J., Britt, R., and Dickman, M. B. 2011. Tipping the balance: *Sclerotinia sclerotiorum* secreted oxalic acid suppresses host defenses by manipulating the host redox environment. PLoS Pathog. 7:e1002107 Available at: http://www.pubmedcentral.nih.gov/articlerender.fcgi?artid=3128121&tool=pmcentrez&rendertype=abstract [Accessed June 3, 2014].

Wisconsin Soybean Association (WSA) and Wisconsin Soybean Marketing Board (WSMB). 2013. U.S. Wisconsin soybean facts. Available at: http://www.wisoybean.org/news/soybean_facts.php.

World Agricultural Production. 2017. In *United States Department of Agriculture - Foreign Agricultural Service (USDA-FAS), Circular Series 11-17*, p. 1–29. Available at: http://apps.fas.usda.gov/psdonline/circulars/production.pdf%5Cnhttp://www.fao.org/faostat/en/#data.

Wrather, A., and Koenning, S. 2009. Effects of diseases on soybean yields in the United States 1996 to 2007. Plant Heal. Prog.

Wrather, A., Shannon, G., Balardin, R., Carregal, L., Escobar, R., Gupta, G., et al. 2010. Effect of diseases on soybean yield in the top eight producing countries in 2006. Plant Heal. Prog.

Wrather, J. a., Koenning, S. R., and Anderson, T. R. 2003. Effect of diseases on soybean yields in the United States and Ontario (1999 to 2002). Plant Heal. Prog.

Xue, H. Q., Upchurch, R. G., and Kwanyuen, P. 2006. Ergosterol as a quantifiable biomass marker for *Diaporthe phaseolorum* and *Cercospora kikuchii*. Plant Dis. 90:1395–1398.

Yang, X. B., Lundeen, P., and Uphoff, M. D. 1999. Soybean varietal response and yield loss caused by *Sclerotinia sclerotiorum*. Plant Dis. 83:456–461.

Yarden, O., Veluchamy, S., Dickman, M. B., and Kabbage, M. 2014. *Sclerotinia sclerotiorum* catalase SCAT1 affects oxidative stress tolerance, regulates ergosterol levels and controls pathogenic development. Physiol. Mol. Plant Pathol. 85:34–41 Available at: http://linkinghub.elsevier.com/retrieve/pii/S0885576513000763 [Accessed October 1, 2014].

Zancan, W. L. A., Steadman, J. R., Higgins, R., Jhala, R., and Machado, J. da C. 2015.

Genetic and aggressiveness variation among *Sclerotinia sclerotiorum* dry bean isolates from Brazil fields. Biosci. J. 31:1143–1151.

CHAPTER 2: Comprehensive Sclerotinia stem rot screening of soybean germplasm requires multiple isolates of *Sclerotinia sclerotiorum*

Abstract

Sclerotinia sclerotiorum population variability directly affects Sclerotinia stem rot (SSR) resistance breeding programs. In the North Central United States, however, soybean germplasm selection has often involved only a single isolate. Forty-four *S. sclerotiorum* isolates from Illinois, Michigan, Minnesota, Wisconsin, Poland, and across 11 different host species were evaluated for variation in isolate *in vitro* growth, *in vitro* oxalate production, and *in planta* aggressiveness on the susceptible soybean cultivar Williams 82. Significant differences ($P < 0.0001$) were detected in isolate *in planta* aggressiveness, *in vitro* growth, and *in vitro* oxalate production. Furthermore, diverse isolate characteristics were observed within all hosts and locations of collection. Aggressiveness was not correlated to colony growth, and was only weakly correlated ($r = 0.26$; $P < 0.0001$) to isolate oxalate production. In addition, the host or location of collection did not explain isolate aggressiveness. Isolate oxalic acid production, however, is partially explained by the host ($P < 0.01$) and location ($P < 0.05$) of collection. Using a representative subset of nine *S. sclerotiorum* isolates and soybean genotypes exhibiting susceptible or resistant responses (determined using a single isolate), a significant interaction ($P = 0.04$) was detected between isolates and genotypes when SSR severity was evaluated. Our findings suggest that screening of *S. sclerotiorum*-resistant soybean germplasm should be performed with multiple isolates to account for the overall diversity of *S. sclerotiorum* isolates found throughout the soybean growing regions of the United States.

Introduction

Sclerotinia sclerotiorum (Lib.) de Bary, the soilborne causal agent of Sclerotinia stem rot (SSR), is a devastating fungal pathogen affecting more than 400 host species globally (Boland and Hall 1994). Soybean (*Glycine max* (L.) Merrill) is one of the most economically important hosts impacted by SSR (Peltier et al. 2012). In the United States, SSR ranked in the top ten yield reducing diseases of soybeans in 2000, 2004, 2006, and 2009, and continues to significantly contribute to soybean yield reduction (Koenning and Wrather 2010; Wrather and Koenning 2009). In both 2004 and 2009, SSR accounted for an estimated 1.6 million metric ton yield reduction (Peltier et al. 2012; Koenning and Wrather 2010; Wrather and Koenning 2009). In 2011, the United Soybean Board estimated that 94% of nationwide losses occurred in the great lakes region. Producers lost a corresponding ~$138 million according to 2011 market values (NASS).

Disease control is limited by the lack of complete resistance to SSR, however, some partially resistant soybean genotypes have been identified (Boland and Hall 1987; Grau, Radke, and Gillespie 1982; Kim and Diers 2000). Traditionally, controlled environment soybean resistance studies have been conducted with only one or two aggressive *S. sclerotiorum* isolates (Boland and Hall 1986; Hoffman et al. 2002; Kim et al. 2000; Wegulo, Yang, and Martinson 1998). Auclair et al. (2004) proposed that such practice may be justified, and considered different isolates of *S. sclerotiorum* sampled from soybean in the same geographical region as equivalent. The limited number of isolates used by this study, however, and the complexity of *S. sclerotiorum* pathogenic development coupled with our

limited understanding of the mechanisms that underpin host resistance to this pathogen justify a broader evaluation of *S. sclerotiorum* isolates.

Furthermore, while overwintering sclerotia may myceliogenically germinate in the soil, the millions of ascospores generated from the apothecial sexual fruiting body are typically the primary source of inoculum for *S. sclerotiorum* in soybean fields (Peltier et al. 2012; Willetts and Wong 1980). The limited dispersal of ascospores (Ben-Yephet and Bitton 1985) and homothallic life cycle of *S. sclerotiorum* (Willetts and Wong 1980) support regional clonality. Individual clones, however, may be more widely distributed by seed-borne transmission of sclerotia (Hartman, Kull, and Huang 1998). As a result, *S. sclerotiorum* clones are considered highly dispersive, and agricultural populations may contain a conglomeration of genotypes (Anderson and Kohn 1995).

Predictably, diverse isolate populations have been documented in US soybean fields (Aldrich-Wolfe, Travers, and Nelson 2015; Koga et al. 2014; Kull et al. 2004; Petrofeza and Nasser 2012). These findings suggest that soybean genotypes should be selected for resistance using appropriately representative isolates. The importance of characterizing *S. sclerotiorum* isolate diversity has been investigated for dry bean resistance evaluations in Brazil (Lehner et al. 2015). While the overall aggressiveness of 20 isolates on a susceptible or a resistant cultivar was similar, subtle differences in isolate performance between cultivars was detected. Certain isolates of *S. sclerotiorum,* therefore, seem better suited for evaluation of certain cultivars. *S. sclerotiorum* studies in *Brassica* spp. also considered the use of using a diverse set of isolates (one weakly and one strongly aggressive), however, were unable to detect differences due to the unreliability of using only one very weak isolate (Taylor et al.

2015). As such, resistance evaluations, should account for the full extent of regional variation within a pathogen population to ensure the development and release of a durable product. Pathogen diversity should, therefore, be investigated for use in representative resistance evaluations.

S. sclerotiorum isolate diversity has been investigated using growth characteristics, aggressiveness properties, mycelial compatibility groups (MCGs), and the production of the key pathogenicity factor oxalic acid (OA) (Koga et al. 2014; Kohn et al. 1991; Kull et al. 2004). *In vitro* mycelial compatibility is used as an indication of isolate homogeneity and may be used to detect variation within a fungal population (Kohn, Carbone, and Anderson 1990). Multiple MCGs have been detected in North America and South America (Kohn et al. 1991; Kull et al. 2004). MCGs, however, do not necessarily explain isolate aggressiveness at the regional level (Kull et al. 2004; Lehner et al. 2015).

The non-host specific key pathogenicity factor, OA, largely contributes to the extraordinarily broad host range of *S. sclerotiorum* (Godoy et al. 1990; Maxwell and Lumsden 1970; Noyes and Hancock 1981). The roles of OA in *S. sclerotiorum* infection include pH-dependent regulation of cell wall degrading enzymes (Bateman and Beer 1965), stomatal regulation (Stotz and Guimaraes 2004), and suppression of host defenses (Cessna et al. 2000; Williams et al. 2011; Kabbage, Williams, and Dickman 2013). OA production may, therefore, more accurately describe isolate aggressiveness. Indeed, OA production by *S. sclerotiorum* isolates has been previously described, and was found to explain isolate aggressiveness in European red clover populations (Vleugels, Baert, and van Bockstaele 2013).

The objectives of our research were to evaluate a diverse collection of *S. sclerotiorum* isolates, collected from the Midwestern United States and Poland as well as from a variety of hosts using a multi-pronged approach, which takes into account, colony growth, OA production, and aggressiveness on soybean. We hypothesized that isolates within our collection would exhibit highly variable levels of aggressiveness, in part due to pathogenicity factors such as OA, but also due to specific interactions with a particular soybean genotype. Furthermore, we postulate that accounting for differences in isolate characteristics would affect the overall success of resistance breeding programs. We investigated the use of a representative panel of *S. sclerotiorum* isolates as a tool to evaluate the response of several soybean recombinant inbred lines (RILs).

Materials and Methods

Isolate collection. Between 2003 and 2013, forty-four *S. sclerotiorum* isolates (Table 2.1) were collected from Indiana, Michigan, Minnesota, Wisconsin, and Poland. Isolates were collected from ten hosts including carrot (*Daucus carota*), celery (*Apium graveolens*), dwarf everlast (*Helichrysum arenium*), green bean (*Phaseolus vulgaris*), lettuce (*Lactuca sativa*), parsley (*Petroselinum crispum*), petunia (*Petunia* sp.), rapeseed (*Brassica napus*), soybean (*Glycine max*), and the common weed velvetleaf (*Abutilon theophrasti*).

Isolates were grown on carrot discs to promote sclerotial formation. Sclerotia were collected using a 2.00 mm U.S. standard sieve (American Scientific, McGaw Park, IL), dried for 48 hr at room temperature, and stored at 4 °C in sterile 15 ml polypropylene conical tubes (Becton Dickinson, Franklin Lakes, NJ) until use in characterization assays. Tubes were kept in sealed plastic bags with desiccant packs (Humidity Sponge™, Control Company, Houston,

TX) to promote dry storage (Pottinger et al. 2008). Stored sclerotia were surface disinfested in 10% (v/v) bleach for 1 min followed by 95% ethanol for 1 min, rinsed in sterile ultrapure Milli-Q® water (EMD Millipore), blotted dry on sterile filter paper (Qualitative P8, porosity coarse; Fisher Scientific), and placed onto potato dextrose agar (PDA; Fisher Scientific, Pittsburg, PA) in a Petri plate (100 by 15 mm). Active mycelia from the leading edge of colonies were used for further analysis. Isolates were regenerated from previously dry-stored sclerotia between each repetition of the characterization assays and evaluations.

Colony growth assessment. Isolate growth was determined *in vitro* by monitoring PDA cultures over time. A 5-mm plug of PDA was taken from the leading edge of an actively growing colony and transferred to the center of a standard 100-mm by 15-mm Petri plate containing PDA. Each isolate transfer was replicated 3 times and each replicate was randomized in stacks placed in a 14-hour photoperiod, 16 °C incubator for the duration of the assay. An oxalic acid deficient (A2) mutant was included to determine the role of oxalic acid in *in vitro* growth (Godoy et al. 1990). Mycelial growth was measured along two axes (x and y, at a right angle extending from the center of the plate) once a day for 3 to 4 consecutive days until mycelia reached the edge of the agar plate. Standardized areas under the growth curves (STAUGC) were used for statistical analyses. The STAUGC is analogous to the standardized area under the disease progress curve as described by Campbell and Madden (1990). The colony growth assessment was repeated once after regeneration of isolates from dry-stored sclerotia.

Oxalic acid production. OA production was determined *in vitro* in potato dextrose broth (PDB; EMD Chemicals Inc., Darmstadt, Germany) cultures. A 5-mm diameter plug

was transferred from the leading edge of an actively growing culture of each isolate to 25 ml of sterile PDB in 125-ml Erlenmeyer flasks. Broth cultures were incubated at room temperature (21-24 °C) in complete darkness for 3 days. Cultures were agitated by hand twice daily to ensure mycelia remained suspended in the broth. After 3 days, 5 ml samples of culture broth were collected for oxalic acid determination. Remaining cultures were vacuum filtered and mycelia was collected, weighed, dried at 37 °C for 2 days, and reweighed. Dry mycelial weights were used to adjust oxalic acid concentrations for each isolate to a per milligram unit for statistical analyses.

OA levels were quantified using an enzymatic assay kit (Trinity Biotech plc, Bray, Co., Wicklow, Ireland). Broth samples were diluted 1:1 using kit diluent and adjusted to a pH of 6 to 7 with either 1 N hydrochloric acid or 1 N sodium hydroxide. Enzymatic assays were conducted on activated charcoal purified samples according to the instructions in the kit. Resulting sample reactions were transferred to a 96-well microplate and absorbencies at 590 nm were recorded using a Bio-Rad iMark^{TM} (Bio-Rad Laboratories, Hercules, CA) microplate reader. Two negative controls, broth cultures with a sterile PDA plug only (technical control) or a broth culture with an OA deficient mutant, were included in all experiments; absorbencies were corrected with the mutant background. An oxalate standard curve, produced from 0.00, 0.25, 0.50, 1.00, 2.00, and 4.00 mmol/liter standards, was used to convert sample absorbencies to oxalate concentrations. Resulting concentrations were adjusted to a milligram unit using the corresponding mycelial dry weights. All isolates were replicated three times and the entire experiment was repeated once. Isolates were regenerated from dry-stored sclerotia between each repetition.

Aggressiveness evaluations. A susceptible soybean cultivar, Williams 82, was challenged with all *S. sclerotiorum* isolates to evaluate isolate aggressiveness *in planta*. Soybeans were planted in 15.25 cm pots, approximately 4 cm deep in moist potting mix (Sun Gro® Horticulture, Agawam, MA), and grown in a 14-hour photoperiod growth room set to 22 °C during the day and 18 °C at night. Soybeans were watered daily and fertilized once a week (Miracle-Gro®, Scotts Miracle-Gro Products, Marysville, OH). Soybeans grown to the V4 growth stage (four fully emerged trifoliates) were used to conduct aggressiveness evaluations.

Isolate inoculum was prepared by transferring a 5-mm plug of agar from the leading edge of an actively growing PDA culture, on a standard Petri plate, to a deep Petri plate (100 mm by 25 mm; Lab-Tek® Nunc®, Sigma-Aldrich) with PDA. Inoculations were conducted using a previously described cut petiole technique (Peltier and Grau 2008). Using 1,000 µl pipet tips (Fisher Scientific, Pittsburg, PA), a 1.5 cm thick agar core was collected from the leading edge of mycelia on each inoculum plate. Second trifoliate leaflets were excised such that petioles were 2.5 to 3 cm in length. Petioles were inserted into pipet tips of inoculum and positioned so that mycelia and cut petiole tissue were in direct contact.

Isolate inoculations were performed in triplicate (three replicates) and soybean plants were arranged in a randomized complete block design (RCBD). An oxalic acid deficient mutant was also included in every experiment to determine the role of oxalic acid *in planta*. Stem lesions were measured daily using a digital caliper (Thermo Fisher Scientific, Waltham, MA) for a duration of seven to fourteen days post-inoculation (depending on repetition). Square-roots of standardized areas under the disease progress curves (STAUDPC) were used

for statistical analyses of isolate aggressiveness. The square-root transformation was used to normalize the data, however, back-transformed means are presented graphically. Each aggressiveness evaluation was repeated once, and isolates were regenerated from previously dry-stored sclerotia between each repetition.

Multi-isolate by soybean germplasm evaluations. To investigate the response of soybean germplasm to a variety of *S. sclerotiorum* isolates, a preliminary screen was conducted in a greenhouse at the West Madison Agricultural Research Station (Madison, Wisconsin). Two putatively resistant experimental lines (determined from preliminary testing, *data not shown*), 91-38 (classified as moderately resistant; MR) and 91-145 (classified as highly resistant; HR), one susceptible (S) experimental line, 91-44, and a susceptible check, Williams 82, were selected for multi-isolate challenge. Line phenotypes were determined using the previously described cut petiole method with a single isolate, #30. These lines were evaluated using a modified 0 to 4 rating scale where 0 = no lesion on the main stem, 1 = small lesion (approximately <1 cm) on the main stem, 2 = considerable lesion (≥1 cm) development on the main stem but no associated foliar wilt, 3 = considerable lesion development and irreversible foliar wilt, and 4 = lesion development resulting in poor pod fill and plant death (Grau, Radke, and Gillespie 1982). All germplasm lines (91-38, 91-145, and 91-44) were generated from the initial cross of the soybean cyst nematode resistant line LN89-5717 (Nickell et al. 1994) and the partially SSR-resistant line W04-1002 (Peltier and Grau 2008). Experimental lines were of the F8:12 generation, i.e. from the fourth subsequent progeny of a single F8 derived soybean plant. Lines were considered highly inbred with limited genetic diversity. Soybeans were planted in 15.25 cm peat pots approximately 4 cm

deep in moist potting mix (Sun Gro® Horticulture, Agawam, MA), watered daily, and fertilized twice a week (Scotts Peters Professional® Peat-Lite Special 20-10-20, Scotts-Sierra Horticultural Products Co., Marysville, OH) until the V4 growth stage.

Representative isolates were selected from the previously characterized 44 isolates. Four strongly aggressive isolates, four weakly aggressive isolates, and the original single isolate used in previous screens (a total of 9 isolates) were included for resistance evaluations (Table 2.2). Cut petiole inoculations were conducted as described previously. Inoculated plants were arranged in a RCBD to accommodate all 4 x 9 factorial treatment combinations. Isolate-line interactions were evaluated in triplicate (3 replicates) and repeated once. Isolates were regenerated from sclerotia between each repetition. Stem lesions were measured every 2 or 3 days for 13 days post-inoculation using a digital caliper as described above.

An additional repetition (for a total of three repetitions) was conducted in the same greenhouse at the West Madison Agricultural Research Station (Madison, Wisconsin) using only the 91-145, 91-38, and 91-44 RILs. Three soybeans were planted equidistant from each other in 15.25 cm peat pots approximately 4 cm deep in moist potting mix (Sun Gro® Horticulture, Agawam, MA). The plants were watered daily and fertilized as previously described until the V5 growth stage. Second trifoliate petioles, of all plants in each pot, were excised to a length of 2.5 cm and inoculated using the pipet tip method described previously. All nine isolates of *S. sclerotiorum* used in the preceding screens were regenerated from dry-stored sclerotia and included in the evaluation. Stem lesions were measured 5, 10, and 15 days post-inoculation using the previously described digital calipers. Standardized area under the disease progress curves (STAUDPC) was analyzed to evaluate germplasm resistance

reactions to a variety of isolates in all greenhouse screens. A square root transformation was used to normalize STAUDPC data, however, back-transformed means were presented graphically.

Statistical analyses. Correlations between isolate colony growth, oxalic acid production, and aggressiveness were determined using Pearson correlation coefficients generated in SAS v. 9.3 (SAS Institute, Cary, NC) using the PROC CORR procedure. Correlations were evaluated at the α=0.05 significance level.

Isolate variation by *in vitro* growth (STAUGC), oxalic acid production, and aggressiveness (STAUDPC), were used as dependent variables in generalized linear mixed model (GLIMMIX) analysis of variance (ANOVA) using SAS 9.3 (SAS Institute, Cary, NC). Host and location of collection were also used to explain isolate variation. Replicate and repetition (run) were combined in a nested random effect [rep(run)].

Raw data from the previous analysis were extracted for the nine isolates selected for the multi-isolate evaluations and analyzed as a subset using the SAS 9.3 (SAS Institute, Cary, NC) GLIMMIX procedure. Isolate aggressiveness (STAUDPC) was the only dependent variable used in this subset analysis. Repetition (run) and replicate were treated as a nested random effect [rep(run)].

A similar GLIMMIX analysis was performed for the multi-isolate by germplasm line experiment. Isolate and germplasm line were treated as fixed effects and repetition (run) and replicate were combined in a nested random effect [rep(run)]. In order to maintain a balanced design, all Williams 82 observations were removed from the pooled analyses of runs 1, 2,

and 3. Differences between and within the remaining 91-145, 91-38, and 91-44 RILs were determined at the α=0.05 significance level.

The extracted Williams 82 observations from runs 1 and 2 of the multi-isolate by soybean germplasm evaluations were used to validate characterization of the selected isolates in the preceding growth room evaluations. Comparison of growth room and greenhouse results of isolate aggressiveness on Williams 82 soybeans was conducted using STAUDPC values generated in a GLIMMIX analysis in SAS 9.3 (SAS Institute, Cary, NC) as previously described. Isolate aggressiveness groupings were evaluated using Fisher's Least Significant Difference (LSD) letter groupings; means with the same letter were not considered different at the α=0.05 significance level.

Results

Diversity of *S. sclerotiorum* isolates. Isolate standardized area under the growth curves (STAUGC), oxalate production, and aggressiveness, measured as standardized area under the disease progress curves (STAUDPC), were used to characterize the diversity of this *S. sclerotiorum* isolate collection. *In vitro* growth, *in vitro* oxalic acid (OA) production, and *in planta* aggressiveness were significantly different ($P < 0.0001$) among all isolates (Fig. 2.1).

All wild type isolates exhibited characteristic growth on PDA; the mean STAUGC value of this collection (n=45) was 14.35, with a minimum of 7.23 and a maximum of 18.07 (Fig. 2.1A). All isolates, except the OA deficient mutant, secreted acid levels detected by a pH change from 7.10 (mean of technical control) to between 6.01 and 6.97 over the three day incubation period (*data not shown*). The mean OA concentration produced by these isolates

(n=45) was 0.13 mmol/L/mg, with a minimum of $6.34x10^{-14}$ mmol/L/mg and a maximum of 0.25 mmol/L/mg (Fig. 2.1B). In aggressiveness assays, Williams 82 stems inoculated with wild type isolates exhibited characteristic lesions ranging from light tan to dark brown. The mean STAUDPC value of the isolates evaluated (n=45) was 16.74, with a minimum of < 0.01 and a maximum value of 31.39 (Fig. 2.1C). Minimum values of all three assays resulted from the OA deficient mutant, denoted as isolate 'A'.

Correlations with aggressiveness. The OA deficient mutant, denoted as isolate 'A', exhibited a delayed growth phenotype *in vitro* (Fig. 2.1A). As expected, OA mutant *in vitro* oxalate concentrations, however, were not significantly different from background absorbance levels and are presented as 0.00 mmol/L/mg (Fig. 2.1B). On the host plant, the OA mutant was unable to progress the length of the petiole and no lesion formed on the stem resulting in an STAUDPC of 0.00 (Fig. 2.1C). These results suggest a potential correlation between *in vitro* oxalate production and *in planta* pathogenicity but do not support a correlation between *in vitro* growth and aggressiveness.

A weak positive correlation ($r = 0.26$; $P < 0.0001$) was identified between OA production and aggressiveness (Fig. 2.2). STAUGC was very weakly correlated ($r = 0.13$; $P < 0.05$) with aggressiveness in these experiments. Based on these results, *in vitro* isolate growth and OA production do not accurately describe isolate aggressiveness. Thus, despite the importance of OA in *S. sclerotiorum* pathogenicity as shown with the OA deficient mutant, natural variations in OA levels among field isolates did not fully explain the variability in isolate aggressiveness.

Effect of host or location of collection. Host and location of collection were used to further describe variation of isolate *in vitro* OA production and *in planta* aggressiveness. The diversity of isolate OA production was explained by plant host ($P < 0.05$) (Fig. 2.3) and location of collection ($P < 0.01$) (Fig. 2.4). Isolates collected from canola (n=2) and parsley (n=1) produced the highest and lowest OA levels, respectively. Additionally, isolates from Poland (n=10) and Michigan (n=3) displayed the highest OA concentrations, whereas, isolates collected from Minnesota (n=3) produced the lowest concentrations. Variability in isolate aggressiveness was observed across all hosts (Fig. 2.5) and locations (Fig. 2.6); aggressiveness on a susceptible soybean cultivar, however, was not explained by either host or location.

Representative subset of isolates. Representative isolates were selected based on *in planta* aggressiveness on a susceptible soybean cultivar as measured in previous experiments (STAUDPC). Isolate colony growth, OA production, host of origin, and location of collection were not considered due to the lack of any significant effects on isolate aggressiveness. Therefore, four strongly (#10, 19, 20, 62) and four mildly (#3, 15, 47, 60) aggressive isolates were selected to inoculate soybean RILs (Table 2.2). STAUDPC replicates from both repetitions (n=6) were extracted and pooled for each isolate to determine mean differences at the $\alpha=0.05$ level. Based on Fisher's Least Significant Difference (LSD; $\alpha=0.05$), selected isolates within an aggressiveness grouping, i.e. strong or mild, were not significantly different from one another, however, isolates from different groups were significantly different on the susceptible soybean cultivar Williams 82.

Comparison of growth room and greenhouse evaluations. Comparisons were conducted to validate isolate aggressiveness designations determined in growth chamber experiments. According to LSD letter groupings, the majority of the isolates clustered similarly to previous growth room evaluations (Supp. Table S2.1). Seven of the nine isolates successfully exhibited responses that corresponded to the previously determined aggressiveness designations. The letter groupings indicated that three of the four mildest isolates, #47, 60, and 15, were not significantly different from one another and had the lowest STAUDPC means. Likewise, four of the strongly aggressive isolates, #20, 19, 10, and 62 were not significantly different from one another and had among the highest STAUDPC means. Only isolates #3 and 30 appeared considerably more aggressive in greenhouse evaluations.

Multi-isolate by soybean germplasm evaluations. Response of several soybean RILs was previously tested using a single isolate of *S. sclerotiorum* (#30) (*data not shown*). In this study, resistant soybean lines 91-145 (HR) and 91-38 (MR), susceptible line 91-44 (S), and cultivar Williams 82 were reevaluated using the original isolate used for selection (#30), four strongly (#10, 19, 20, 62), and four mildly (#3, 15, 47, 60) aggressive isolates (Table 2.2). The isolate by line interaction was significant ($P = 0.04$) in the pooled STAUDPC analyses.

Based on the mean STAUDPC of 7.19, line 91-145 (HR) did appear highly resistant. Line 91-38 (MR) and 91-44 (S), however, do not exhibit significantly different reactions from each other based on STAUDPC means of 11.88 and 15.02, respectively. Threshold STAUDPC values were determined from these means to describe the individual isolate by

line reactions independent of previous line designations (HR, MR, or S). Germplasm reactions with STAUDPC ≤ 10 were considered resistant, STAUDPC > 10 but ≤ 15 were considered moderately susceptible, and STAUDPC > 15 were considered susceptible.

Overall, line 91-145 (HR), successfully exhibited resistant reactions to seven of the nine isolates (Fig. 2.7A). Isolates #10 and 20, however, caused a moderately susceptible and susceptible reaction in line 91-145, respectively. Line 91-38 (MR) only appeared noticeably resistant against four of the nine isolates (Fig. 2.7B). Use of isolates #3, 10, 15, 19, and 62 against soybean line 91-38 elicited moderately susceptible to susceptible reactions. Additionally, the line 91-44 (S) only checked as susceptible using seven of the nine isolates (Fig. 2.7C). The use of isolates #47 and 60 result in a resistant response. Therefore, these data show that while the overall response of the soybean lines tested in this study was predictable and confirmed previous trends, SSR severity in some instances was predicated by specific line by isolate interactions. Some isolates are better suited to produce higher SSR severity on specific soybean lines regardless of perceived aggressiveness (Fig. 2.7), thus justifying the use of multiple *S. sclerotiorum* isolates when evaluating SSR levels in breeding lines.

Discussion

The overall results of our study suggest that the representative *S. sclerotiorum* isolate collection presented here contained a range of mildly to strongly aggressive isolates on soybean. These findings corroborate other reports of variation in isolate aggressiveness (Kull et al. 2004; Li et al. 2008; Vleugels, Baert, and van Bockstaele 2013). As previously described, differences were also observed in *S. sclerotiorum* isolate oxalic acid (OA)

production (Durman, Menendez, and Godeas 2005; Li et al. 2008; Vleugels, Baert, and van Bockstaele 2013). Isolate variability in OA levels, however, did not completely explain the variability in *in planta* aggressiveness. A strong correlation between *in vivo* oxalate production and aggressiveness was reported in red clover ($r = 0.46$, $P = 0.010$) (Vleugels, Baert, and van Bockstaele 2013) and sunflower ($r = 0.74$, $P < 0.01$) (Li et al. 2008). However, the weak ($r = 0.26$; $P < 0.0001$) correlation we observed is more consistent with previous conclusions that isolate aggressiveness in common bean stem inoculations was not explained by the oxaloacetate acetylhydrolase (OAH) haplotype which is involved in OA biosynthesis (Lehner et al. 2015). It is thus conceivable that while OA is an important virulence factor, its production beyond a specific threshold does not always correlate with increased aggressiveness. In addition to OA, *S. sclerotiorum* may also require additional pathogenicity factors for successful infection, including cell wall degrading enzymes, toxins, and proteinaceous effectors (Guyon et al. 2014; Kabbage, Yarden, and Dickman 2015). A recent study showed that OAH mutants were able to induce restricted lesions on detached leaves despite their inability to produce oxalic acid (Liang et al. 2014). Clearly, OA is not the only contributing factor to *S. sclerotiorum* aggressiveness. It is not surprising, therefore, that a single pathogenicity factor, while important, does not solely describe isolate aggressiveness. Alternatively, OA production by *S. sclerotiorum* may be conditioned by environmental factors within the infection court. Thus, future studies should consider OA levels in the context of the host plant, in addition to *in vitro* production.

Our *S. sclerotiorum* isolate collection exhibited significant variation in isolate radial colony growth in accordance with previous reports (Garg et al. 2009; Li et al. 2008;

Vleugels, Baert, and van Bockstaele 2013), however, only a weak correlation was observed between colony growth and aggressiveness in our study. Previous studies reported the presence of aggressiveness-correlated colony growth in detached celery petiole assays (Durman, Menéndez, and Godeas 2003) and in red clover leaf and plant assays (Vleugels, Baert, and van Bockstaele 2013). Other studies, however, reported no significant correlation between colony radial growth and aggressiveness on either *Brassica* sp. cotyledons (Garg et al. 2009) or detached sunflower leaves (Li et al. 2008). Our results provide additional evidence that the complexity of *S. sclerotiorum* isolate aggressiveness is poorly correlated with *in vitro* growth characteristics. This is not surprising considering that disease outcome is largely based on virulence factors and host responses during pathogenic development compared to saprophytic growth.

The host and location of collection did not explain the variation observed in isolate aggressiveness. The overall variation in isolate aggressiveness was well represented within most hosts and locations. Differences between hosts or locations, however, were difficult to distinguish due to the unbalanced distribution of isolates within our collection, i.e. approximately half of the isolates originated from Wisconsin soybean plants. Despite this limitation, our findings support other reports of variation in isolate aggressiveness both within a single region, e.g. Brazil (Zancan et al. 2015), and across a more widespread geographic region, e.g. Illinois (US) and Argentina (Kull et al. 2004). Differences in bean isolate aggressiveness, however, have been attributed to their location of origin (Otto-Hanson et al. 2011). Significant differences in aggressiveness on detached celery petioles were also reported in isolates collected from soybean, lettuce, and sunflower; sunflower isolates were

determined to be the most aggressive (Durman, Menéndez, and Godeas 2003). No differences due to isolate host or location of collection were detected in our study, however, obtaining a larger sample of isolates from each location may more clearly elucidate the effects of source and origin on isolate aggressiveness.

Our results also suggest that the location of collection did somewhat explain isolate OA production. However, other studies reported that sunflower isolates collected from China, Canada, and England varied significantly in OA production regardless of geographic origin (Li et al. 2008). In our collection, isolates from Poland (n=10) and Michigan (n=3) had the highest OA production, and isolates collected in Minnesota (n=3) had the lowest OA production; samples numbers, however, were low and may not be representative of the regional population. *S. sclerotiorum* isolates from lettuce, soybean, and sunflower, also exhibited differences in OA production that was explained by the plant host origin (Durman, Menendez, and Godeas 2005). Durman et al. (2005) identified soybean isolates (n=53) to exhibit the highest level of OA production, followed by sunflower (n=19) and lettuce (n=49). The host from which our isolates were collected also had a significant effect on *in vitro* oxalic acid production. Canola (n=2) and dwarf everlast (n=3) isolates consistently exhibited a higher mean OA concentration than soybean (n=29) isolates. As mentioned previously, the unbalanced nature of our *S. sclerotiorum* isolate collection most likely contributed to the inconsistencies in these findings. While our results identified the diversity of OA production in *S. sclerotiorum* within several hosts and locations, the effect of host and location on OA production should be further investigated using a larger and more evenly distributed sample of isolates.

The differences in greenhouse and growth room performance of isolates on Williams 82 soybeans could be explained by simple light or temperature differences between the two environments. *S. sclerotiorum* infection in lettuce has been shown to be sensitive to temperature (Young et al. 2004). The growth room used in in initial aggressiveness studies was set to 22°C during the day and 18 °C at night with a 14-hour photoperiod. The greenhouse temperature was approximately 24 °C during the day, however, this environment may be more easily influenced by ambient temperatures. In addition, variability in photosynthetically active radiation (PAR) levels have been shown to affect SSR development in both growth room and field environments (Peltier and Grau 2008). While light levels were not monitored in these experiments, it is evident that probable differences could explain the poor correlation between isolate performance in the growth room and greenhouse. As mentioned previously, however, the majority of the nine isolates used in the greenhouse experiments successfully clustered according to the aggressiveness groupings determined in previous growth room evaluations. This suggests that any isolate by line interactions observed were not simply due to environmental differences.

The reactions of three soybean RILs to a diverse subset of nine *S. sclerotiorum* isolates were monitored in the greenhouse. The three RILs used in the greenhouse evaluations exhibited phenotypes consistent with the original selection designations (HR, MR, and S) during the development of these lines. Line 91-145 (HR) exhibited a highly resistant phenotype (STAUDPC < 10) in our experiments. While lines 91-38 (MR) and 91-44 (S) did not exhibit significantly different responses, line 91-44 displayed the highest STAUDPC mean (> 15), which corresponds to the lowest level of resistance in our study.

Ongoing studies of these germplasm lines recently suggested that the germplasm population from which our 3 lines are derived, were typically more resistant than other populations despite having varying resistance levels (*data not shown*). Overall, the known and consistent levels of resistance of these lines enabled us to focus on phenotypic differences solely based on *S. sclerotiorum* isolate characteristics.

Using a representative subset of isolates, including the original isolate used for germplasm selection (#30), four strongly (#10, 19, 20, 62), and four mildly (#3, 15, 47, 60) aggressive isolates, differential resistance profiles were observed in the three soybean germplasm lines tested. Our results indicate that a comprehensive evaluation of these lines required the use of several *S. sclerotiorum* isolates. Resistance assessment using only the original isolate #30, for example, would have determined line 91-44 (S) to be susceptible (STAUDPC > 15) and lines 91-38 (MR) and 91-145 (HR) to be resistant (STAUPDC < 10). Using another isolate, e.g. #20, however, we would consider 91-145 to be susceptible and 91-44 to be only moderately susceptible ($10 < \text{STAUDPC} \leq 15$). Using yet another aggressive isolate, e.g. #62, we would consider 91-44 to be susceptible, 91-145 resistant, but 91-38 to be highly susceptible (STAUDPC > 20). The use of a single mildly aggressive isolate, e.g. #47, would suggest that all three germplasm lines were resistant. Furthermore, isolate #15, is consistently one of the weakest isolates according to evaluations on the susceptible Williams 82 cultivar. This isolate performed poorly on both our 91-44 (S) and 91-145 (HR) lines, however, was among the most aggressive isolates on our line 91-38 (MR). Clearly, the resistant or susceptible outcome of these lines is directly dependent on the isolate used for evaluation. These results suggest that regardless of the perceived aggressiveness of isolates

or resistance level of the host, some isolates may be particularly equipped to overcome defense responses on a particular genotype, thus making screening for resistance using a single isolate challenging.

Our findings provide evidence that supports the use of a representative panel of *S. sclerotiorum* isolates, which includes both putatively strong and mildly aggressive isolates, especially when evaluating RILs. The differential profiles of these lines against various isolates suggests that either the lines confer different resistance mechanisms, or that different isolates potentially utilize different mechanisms to subvert host resistance. Soybean resistance mechanisms to *S. sclerotiorum* are not fully understood and QTL mapping studies have shown that resistance to *S. sclerotiorum* to be controlled by multiple genes throughout the soybean genome, revealing a complex genetic architecture of resistance to this pathogen (Kim and Diers 2000; Huynh et al. 2010). It is thus conceivable that the aggressiveness of a particular isolate may be dependent on the genetic make-up of the soybean host, and representative isolates should, therefore, be used to encourage the selection of broadly resistant lines exhibiting multiple potential mechanisms. Use of such a tool may prevent selection of lines that express a single resistance mechanism that might be easily circumvented by a diverse population of *S. sclerotiorum* isolates, as might happen if just one perceived aggressive isolate is used.

The significant interaction between isolates and soybean lines observed in our experiment corroborates reported interactions between *S. sclerotiorum* isolates and genotypes of European red clover (Vleugels, Baert, and van Bockstaele 2013) and *Brassica* sp. (Garg et al. 2009). Our findings are in disagreement with other studies reporting insignificant

interaction between cultivated host genotypes and *S. sclerotiorum* isolates in soybean (Auclair et al. 2004; Kull et al. 2004), alfalfa (Pratt and Rowe 1995), and *Brassica* sp. (Taylor et al. 2015). We hypothesize that the publicly available cultivars used in these studies A) exhibited heterogeneous Sclerotinia stem rot (SSR) reactions resulting in the failure to detect isolate by cultivar interactions, and B) were only able to confer, at most, moderate resistance to SSR. We believe that we were able to detect this interaction as a result of the consistent responses in our highly inbred germplasm lines and our ability to incorporate a line exhibiting strong SSR resistance.

Overall, the high level of diversity in *S. sclerotiorum* isolate aggressiveness within our collection was unexplained by host or location of collection. A representative subset of isolates was selected to investigate soybean SSR resistant germplasm reactions to multiple isolates, with varying levels of aggressiveness, and differential host profiles were observed. Our findings clearly demonstrate the necessity of using multiple isolates to determine the resistance profile of soybean genotypes. These results strongly suggest using a representative panel of characterized *S. sclerotiorum* isolates in SSR resistance evaluations in soybean.

Literature Cited

Aldrich-Wolfe, L., Travers, S., and Nelson, B. D. 2015. Genetic Variation of *Sclerotinia sclerotiorum* from Multiple Crops in the North Central United States. PLoS One. 10:e0139188.

Anderson, J. B., and Kohn, L. M. 1995. Clonality in soilborne, plant-pathogenic fungi. Annu. Rev. Phytopathol. 33:369–391.

Auclair, J., Boland, G. J., Kohn, L. M., and Rajcan, I. 2004. Genetic interactions between *Glycine max*and *Sclerotinia sclerotiorum* using a straw inoculation method. Plant Dis. :891–895.

Bateman, D. F., and Beer, S. V. 1965. Simultaneous production and synergistic action of oxalic acid and polygalacturonase during pathogenesis by *Sclerotium rolfsii*. Phytopathology. 55:204–211.

Ben-Yephet, Y., and Bitton, S. 1985. Use of a Selective Medium to Study the Dispersal of Ascospores of *Sclerotinia sclerotiorum*. Phytoparasitica. 13:33–40.

Boland, G. J., and Hall, R. 1987. Evaluating soybean cultivars for resistance to *Sclerotinia sclerotiorum* under field conditions. Plant Dis. 71:934–936.

Boland, G. J., and Hall, R. 1986. Growthroom evaluation of soybean cultivars for resistance to *Sclerotinia sclerotiorum*. Can. J. Plant Sci. 66:559–564.

Boland, G. J., and Hall, R. 1994. Index of plant hosts of *Sclerotinia sclerotiorum*. Can. J. Plant Pathol. 16:93–108.

Campbell, C. L., and Madden, L. V. 1990. *Introduction to Plant Disease Epidemiology*. New York: John Wiley and Sons.

Cessna, S. G., Sears, V. E., Dickman, M. B., and Low, P. S. 2000. Oxalic acid, a pathogenicity factor for Sclerotinia sclerotiorum, suppresses the oxidative burst of the host plant. Plant Cell. 12:2191–200.

Durman, S. B., Menendez, A. B., and Godeas, A. M. 2005. Variation in oxalic acid production and mycelial compatibility within field populations of *Sclerotinia sclerotiorum*. Soil Biol. Biochem. 37:2180–2184.

Durman, S. B., Menéndez, A. B., and Godeas, A. M. 2003. Mycelial compatibility groups in Buenos Aires field populations of *Sclerotinia sclerotiorum* (Sclerotiniaceae). Aust. J. Bot. 51:421–427.

Garg, H., Kohn, L. M., Andrew, M., Li, H., Sivasithamparam, K., and Barbetti, M. J. 2009. Pathogenicity of morphologically different isolates of *Sclerotinia sclerotiorum* with *Brassica napus* and *B. juncea* genotypes. Eur. J. Plant Pathol. 126:305–315.

Godoy, G., Steadman, J., Dickman, M., and Dam, R. 1990. Use of mutants to demonstrate the role of oxalic acid in pathogenicity of *Sclerotinia sclerotiorum* on *Phaseolus vulgaris*. Physiol. Mol. Plant Pathol. 37:179–191.

Grau, C., Radke, V., and Gillespie, F. 1982. Resistance of soybean cultivars to *Sclerotinia sclerotiorum*. Plant Dis. 66:506–508.

Guyon, K., Balagué, C., Roby, D., and Raffaele, S. 2014. Secretome analysis reveals effector candidates associated with broad host range necrotrophy in the fungal plant pathogen *Sclerotinia sclerotiorum*. BMC Genomics. 15:336.

Hartman, G. L., Kull, L., and Huang, Y. H. 1998. Occurence of *Sclerotinia sclerotium* in soybean fields in East-Central Illinois and enumeration of inocula in soybean seed lots. Plant Dis. 82:560–564.

Hoffman, D. D., Diers, B. W., Hartman, G. L., Nickell, C. D., Nelson, R. L., Pedersen, W. L., Cober, E. R., Graef, G. L., Steadman, J. R. Grau, C. R., Nelson, B. D., del Rio, L. E., Helms, T., Anderson, T., Poysa, V., Rajcan, I., Stienstra, W. C. 2002. Selected soybean plant introductions with partial resistance to *Sclerotinia sclerotiorum*. Plant Dis. 86:971–980.

Huynh, T. T., Bastien, M., Iquira, E., Turcotte, P., and Belzile, F. 2010. Identification of QTLs associated with partial resistance to white mold in soybean using field-based inoculation. Crop Sci. 50:969.

Kabbage, M., Williams, B., and Dickman, M. B. 2013. Cell death control: the interplay of apoptosis and autophagy in the pathogenicity of *Sclerotinia sclerotiorum*. PLoS Pathog. 9:e1003287.

Kabbage, M., Yarden, O., and Dickman, M. B. 2015. Pathogenic attributes of Sclerotinia sclerotiorum: switching from a biotrophic to necrotrophic lifestyle. Plant Sci. 233:53–60.

Kim, H. S., and Diers, B. W. 2000. Inheritance of partial resistance to Sclerotinia stem rot in soybean. Crop Sci. 40:55–61.

Kim, H. S., Hartman, G. L., Manandhar, J. B., Graef, G. L., Steadman, J. R., and Diers, B. W. 2000. Reaction of soybean cultivars to Sclerotinia stem rot in field, greenhouse, and laboratory evaluations. Crop Sci. 40:665–669.

Koenning, S. R., and Wrather, J. A. 2010. Suppression of soybean yield potential in the continental United States by plant diseases from 2006 to 2009. Plant Heal. Prog.

Koga, L. J., Bowen, C. R., Godoy, C. V., Oliveira, M. C. N. De, and Hartman, G. L. 2014. Mycelial compatibility and aggressiveness of *Sclerotinia sclerotiorum* isolates from Brazil and the United States. Pesqui. Agropecuária Bras. 49:265–272.

Kohn, L. M., Carbone, I., and Anderson, J. B. 1990. Mycelial interactions in *Sclerotinia sclerotiorum*. Exp. Mycol. 14:255–267.

Kohn, L. M., Stasovski, E., Carbone, I., Royer, J., and Anderson, J. B. 1991. Mycelial incompatibility and molecular markers identify genetic variability in field populations of *Sclerotinia sclerotiorum*. Phytopathology. 81:480–485.

Kull, L. S., Pedersen, W. L., Palmquist, D., and Hartman, G. L. 2004. Mycelial compatibility grouping and aggressiveness of *Sclerotinia sclerotiorum*. Plant Dis. 88:325–332.

Lehner, M. S., Lima, R. C., Carneiro, J. E. S., Paula Junior, T. J., Vieira, R. F., and Mizubuti, E. S. G. 2015. Similar aggressiveness of phenotypically and genotypically distinct isolates of *Sclerotinia sclerotiorum*. Plant Dis. :1–31.

Li, Z., Zhang, Y., Li, R., and Fernando, W. G. D. 2008. Mycelial compatibility group and pathogenicity variation of *Sclerotinia sclerotiorum* populations in sunflower from China, Canada and England. Plant Pathol. 7:131–139.

Liang, X., Liberti, D., Li, M., Kim, Y.-T., Hutchens, A., Wilson, R., Rollins, J. A. 2014. Oxaloacetate acetylhydrolase gene mutants of *Sclerotinia sclerotiorum* do not accumulate oxalic acid, but do produce limited lesions on host plants. Mol. Plant Pathol. 16:1–13.

Maxwell, D. P., and Lumsden, R. D. 1970. Oxalic acid production by *Sclerotina sclerotiorum* in infected bean and in culture. Phytopathology. 60:1395–1398.

Nickell, C. D., Noel, G. R., Bernard, R. L., Thomas, D. J., and Frey, K. 1994. Registration of soybean germplasm line LN89-5717, resistant to soybean cyst nematode. Crop Sci. 34:34–1133.

Noyes, R. D., and Hancock, J. G. 1981. Role of oxalic acid in the Sclerotinia wilt of sunflower. Physiol. Plant Pathol. 18:123–132.

Otto-Hanson, L., Steadman, J. R., Higgins, R., and Eskridge, K. M. 2011. Variation in *Sclerotinia sclerotiorum* bean isolates from multisite resistance screening locations. Plant Dis. 95:1370–1377.

Peltier, A. J., Bradley, C. A., Chilvers, M. I., Malvick, D. K., Mueller, D. S., Wise, K. A., Esker, P. D. 2012. Biology, yield loss and control of Sclerotinia stem rot of soybean. J. Integr. Pest Manag. 3:1–7.

Peltier, A. J., and Grau, C. R. 2008. The influence of light on relationships between Sclerotinia stem rot of soybean in field and controlled environments. Plant Dis. 92:1510–1514.

Petrofeza, S., and Nasser, L. C. B. 2012. *Case Study:* Sclerotinia sclerotiorum*: Genetic diversity and disease control*. Prof. Mahm. InTech.

Pottinger, B. M., Ridgway, H. J., Bourd̂t, G. W., and Stewart, A. 2008. Influence of storage method on the viability, mycelial growth and pathogenicity of *Sclerotinia sclerotiorum* sclerotia. Australas. Plant Pathol. 37:609–614.

Pratt, R. G., and Rowe, D. E. 1995. Comparative pathogenicity of isolates of *Sclerotinia trifoliorum* and *S. sclerotiorum* on alfalfa cultivars. Plant Dis. 79:474–477.

Stotz, H. U., and Guimaraes, R. L. 2004. Oxalate production by *Sclerotinia sclerotiorum* deregulates guard cells during infection. Plant Physiol. 136:3703–3711.

Taylor, A., Coventry, E., Jones, J. E., and Clarkson, J. P. 2015. Resistance to a highly aggressive isolate of *Sclerotinia sclerotiorum* in a *Brassica napus* diversity set. Plant Pathol. 64:932–940.

United States Department of Agriculture - National Agricultural Statistics Service. 2011. United States soybean prices. U.S. Dep. Agric./NASS, Washington, DC.

Vleugels, T., Baert, J., and van Bockstaele, E. 2013. Morphological and pathogenic characterization of genetically diverse *Sclerotinia* isolates from European red clover crops (*Trifolium pratense L.*). J. Phytopathol. 161:254–262.

Wegulo, S. N., Yang, X. B., and Martinson, C. A. 1998. Soybean cultivar responses to *Sclerotinia sclerotiorum* in field and controlled environment studies. Plant Dis. 82:1264–1270.

Willetts, H. J., and Wong, J. A.-L. 1980. The biology of *Sclerotinia sclerotiorum, S. trifoliorum*, and *S. minor* with emphasis on specific nomenclature. Bot. Rev. 36:101–165.

Williams, B., Kabbage, M., Kim, H.-J., Britt, R., and Dickman, M. B. 2011. Tipping the balance: *Sclerotinia sclerotiorum* secreted oxalic acid suppresses host defenses by manipulating the host redox environment. PLoS Pathog. 7:e1002107.

Wrather, A., and Koenning, S. 2009. Effects of diseases on soybean yields in the United States 1996 to 2007. Plant Heal. Prog.

Young, C. S., Clarkson, J. P., Smith, J. a., Watling, M., Phelps, K., and Whipps, J. M. 2004. Environmental conditions influencing *Sclerotinia sclerotiorum* infection and disease development in lettuce. Plant Pathol. 53:387–397.

Zancan, W. L. A., Steadman, J. R., Higgins, R., Jhala, R., and Machado, J. da C. 2015. Genetic and aggressiveness variation among *Sclerotinia sclerotiorum* dry bean isolates from Brazil fields. Biosci. J. 31:1143–1151.

Tables and Figures

Table 2.1. Collection information of 44 *Sclerotinia sclerotiorum* isolates.

Isolate #	Location	Host	Common Name	Year	Collector, Citation
1	WI	*Glycine max*	Soybean	2012	D. Smith
2	WI	*G. max*	Soybean	2012	D. Smith
3	WI	*G. max*	Soybean	2012	D. Smith
5	IL	*G. max*	Soybean	-[a]	C. Bradley
6	IL	*Abutilon theophrasti*	Velvetleaf	-	C. Bradley
7	IL	*A. theophrasti*	Velvetleaf	-	C. Bradley
8	MI	*G. max*	Soybean	-	M. Chilvers
9	MI	*G. max*	Soybean	-	M. Chilvers
10	MI	*G. max*	Soybean	-	M. Chilvers
15	WI	*G. max*	Soybean	-	C. Grau
16	WI	*G. max*	Soybean	-	C. Grau
17	WI	*G. max*	Soybean	-	C. Grau
18	WI	*G. max*	Soybean	-	C. Grau
19	-	*G. max*	Soybean	2012	C. Fritz
20	-	*G. max*	Soybean	2012	C. Fritz
21	-	*G. max*	Soybean	2012	C. Fritz
22	WI	*G. max*	Soybean	-	C. Grau
23	WI	*G. max*	Soybean	2003	C. Grau
24	WI	*G. max*	Soybean	2012	C. Grau/K. Lackermann
25	WI	*G. max*	Soybean	2012	C. Grau/K. Lackermann
26	WI	*G. max*	Soybean	2000	C. Grau
27	WI	*G. max*	Soybean	-	C. Grau
28	WI	*G. max*	Soybean	-	C. Grau
29	-	*G. max*	Soybean	2012	C. Fritz
30	WI	*G. max*	Soybean	2012	C. Grau/K. Lackermann
31	WI	*G. max*	Soybean	-	C. Grau
32	WI	*G. max*	Soybean	2012	C. Grau/K. Lackermann
33	WI	*G. max*	Soybean	-	C. Grau
34	-	*G. max*	Soybean	2012	C. Fritz
43	NE	*Phaseolus vulgaris*	Green bean	1980	Godoy et al. 1990
44	WI	*P. vulgaris*	Green bean	2009	D. Malvick
45	MN	*Petunia* sp.	Petunia	2009	D. Malvick
46	MN	*G. max*	Soybean	2013	D. Malvick
47	MN	*G. max*	Soybean	2013	D. Malvick
57	Poland	*B. napus*	Canola	2011	A. Baturo-Ciesniewska
58	Poland	*Helichrysum arenarium*	Dwarf everlast	2012	A. Baturo-Ciesniewska
59	Poland	*H. arenarium*	Dwarf everlast	2012	A. Baturo-Ciesniewska
60	Poland	*H. arenarium*	Dwarf everlast	2012	A. Baturo-Ciesniewska
61	Poland	*Daucus carota*	Carrot	2012	A. Baturo-Ciesniewska
62	Poland	*Brassica napus*	Canola	2013	A. Baturo-Ciesniewska
63	Poland	*D. carota*	Carrot	2013	A. Baturo-Ciesniewska
64	Poland	*Apium graveolens*	Celery	2012	A. Baturo-Ciesniewska
65	Poland	*Petroselinum crispum*	Parsley	2012	A. Baturo-Ciesniewska
66	Poland	*Lactuca sativa*	Lettuce	2013	A. Baturo-Ciesniewska

[a]Information unknown (-); highly likely that all isolates with unknown location information were collected in Wisconsin.

Table 2.2. Collection information of nine *S. sclerotiorum* isolates selected for multi-isolate resistance evaluations of soybean germplasm. Isolates selected based on consistent standardized areas under the disease progress curves (STAUDPC) across two growth room evaluations. Means are presented for four weakly aggressive isolates (#47, 60, 15, and 3), four strongly aggressive isolates (#62, 19, 10, and 20), and the original isolate used in Wisconsin soybean resistance evaluations (#30).

Isolate #	STAUDPC[x]	HOST	LOC
47	2.39 d[y]	Soybean	MN
60	6.21 cd	Dwarf everlast	Poland
15	6.72 cd	Soybean	WI
3	9.22 cd	Soybean	WI
62	25.64 ab	Canola	Poland
19	25.13 ab	Soybean	-[z]
10	29.43 ab	Soybean	MI
20	31.38 a	Soybean	-
30	14.61 bc	Soybean	WI
LSD	1.69	-	-

[x]Aggressiveness data was extracted from the existing STAUDPC data set, from experiments conducted on Williams 82 soybean, and analyzed as a subset.
[y]Means followed by the same letter are not significantly different based on Fisher's Least Significant Difference (LSD; α=0.05).
[z]Information unknown (-); highly likely that all isolates with unknown location information were collected in Wisconsin.

Supplementary Table S2.1. Greenhouse performance of nine *S. sclerotiorum* isolates, selected for multi-isolate resistance evaluations, on Williams 82 soybeans. Standardized areas under the disease progress curves (STAUDPC) indicate aggressiveness determined in two greenhouse evaluations on Williams 82 soybeans. STAUDPC means are presented for the selected panel of four weakly aggressive isolates (#47, 60, 15, and 3), the four strongly aggressive isolates (#62, 19, 10, and 20), and the original isolate used in Wisconsin soybean resistance evaluations (#30). Isolate means are grouped based on their aggressiveness designations determined in the preceding growth room evaluations.

Isolate #	STAUPDC[x]	SE	HOST	LOC
47	5.64 c[y]	7.25	Soybean	MN
60	13.13 c	7.25	Dwarf everlast	Poland
15	19.32 bc	7.25	Soybean	WI
3	36.17 a	7.94	Soybean	WI
20	31.53 ab	7.25	Soybean	-[z]
19	34.76 ab	7.25	Soybean	-
10	42.02 a	7.25	Soybean	MI
62	48.12 a	7.94	Canola	Poland
30	41.92 a	7.94	Soybean	WI

[x]Aggressiveness data was extracted from the multi-isolate by line data set, from experiments conducted on Williams 82 soybean in the greenhouse, and analyzed as a subset.
[y]Means followed by the same letter are not significantly different based on Fisher's Least Significant Difference (LSD; α=0.05).
[z]Information unknown (-); highly likely that all isolates with unknown location information were collected in Wisconsin.

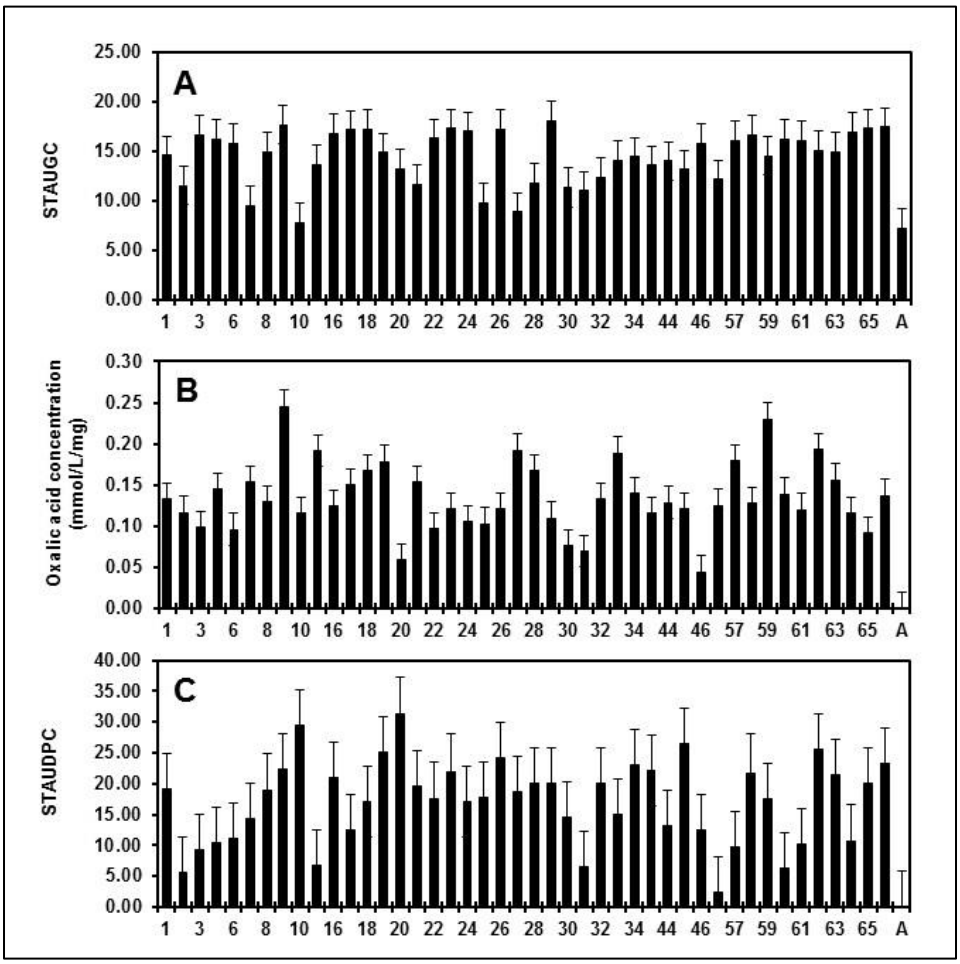

Figure 2.1. Diversity in *S. sclerotiorum* isolate **A,** *in vitro* growth on potato dextrose agar, measured as standardized areas under the growth curves (STAUGC); **B,** *in vitro* oxalic acid production in potato dextrose broth, measured oxalate concentrations determined by spectrophotometric absorbencies at 590 nm; and **C,** aggressiveness on a susceptible Williams 82 soybean, measured as standardized areas under the disease progress curves (STAUDPC). An oxalic acid deficient mutant (A) was included in every experiment. Isolate differences in STAUGC, oxalic acid production, and STAUDPC are significant ($P < 0.0001$). Error bars represent standard errors of the mean values, based on three replicates from two repetitions, for each isolate.

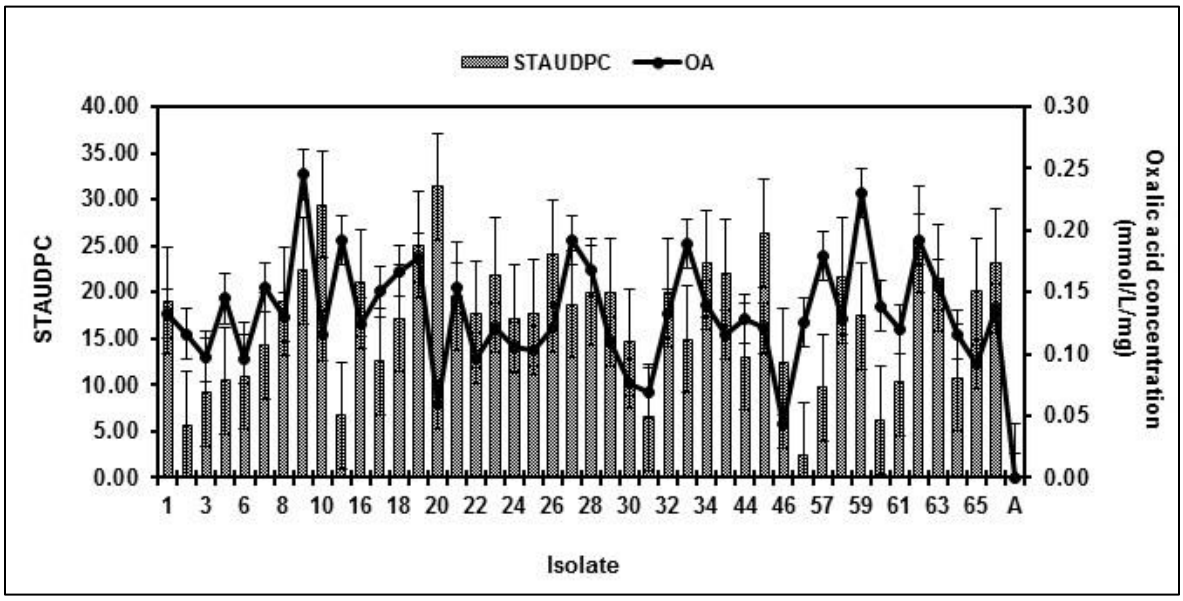

Figure 2.2. Correlations between *S. sclerotiorum* isolate aggressiveness on the susceptible Williams 82 soybean cultivar, measured as standardized area under the disease progress curves (STAUDPC), and *in vitro* oxalic acid production (shown on the secondary axis), determined using spectrophotometric absorbencies at 590 nm and an oxalate standard curve. An oxalic acid deficient mutant (A) was included in every experiment. A weakly positive correlation was detected between mean STAUDPC and oxalic acid concentrations ($r = 0.26$; $P < 0.0001$). Error bars represent standard errors of the mean values from three replicates for each isolate.

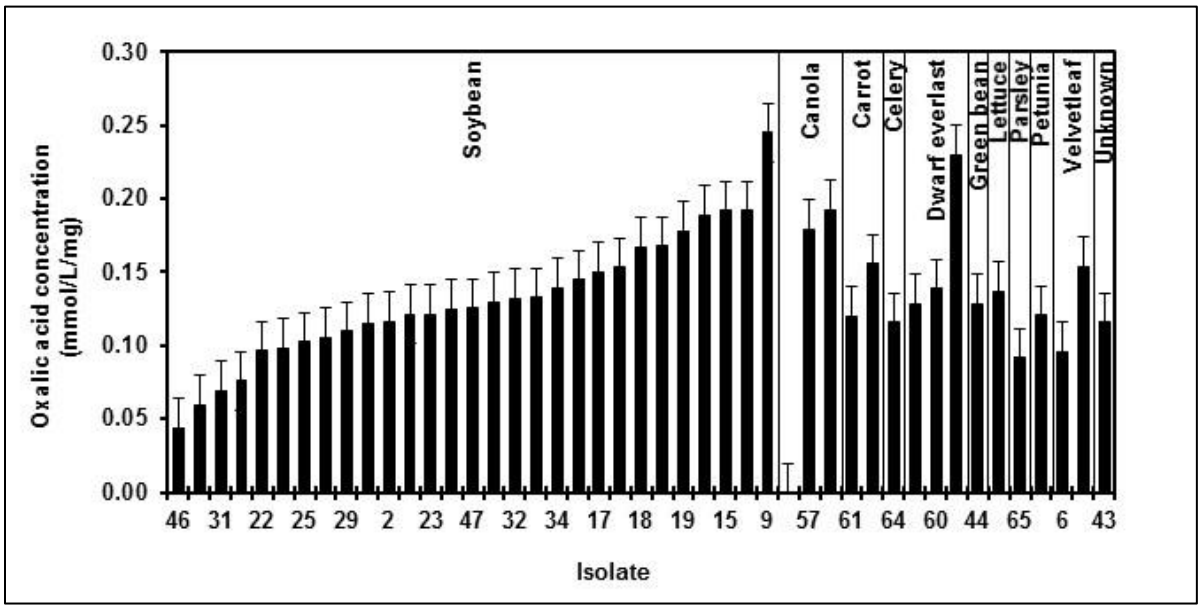

Figure 2.3. Significant effect ($P < 0.05$) of plant host of origin on isolate *in vitro* oxalic acid production, determined using spectrophotometric absorbencies at 590 nm and an oxalate standard curve. Solid bars represent means of three replicates from two repetitions. Error bars represent standard errors of the mean values for each isolate.

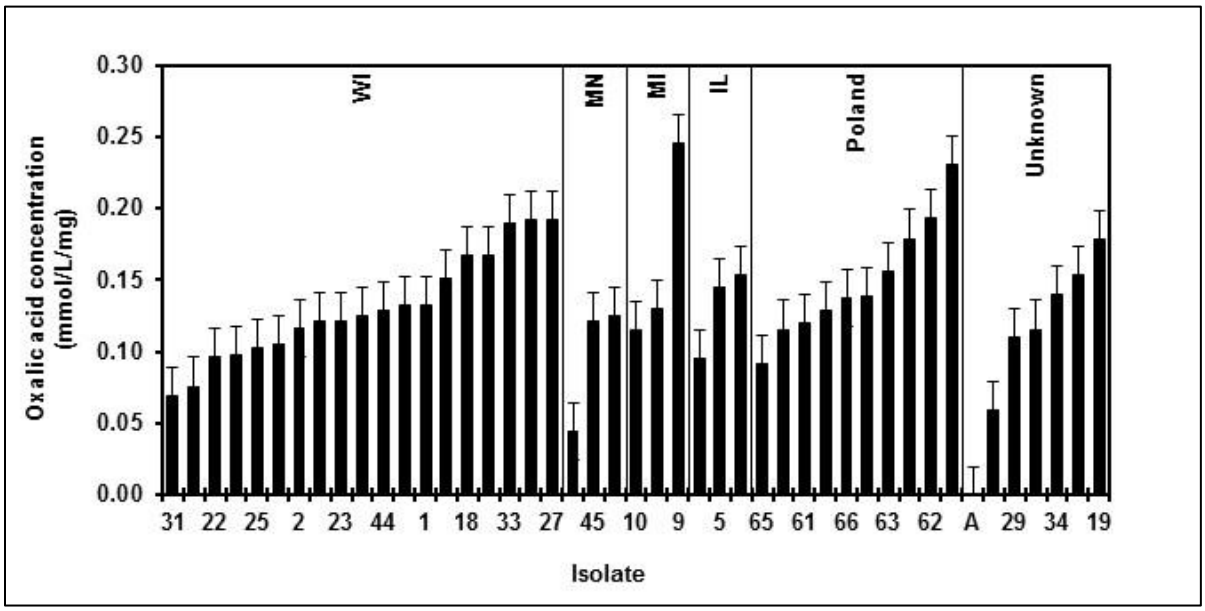

Figure 2.4. Significant effect ($P < 0.01$) of location of collection on *S. sclerotiorum* isolate *in vitro* oxalic acid production as determined using spectrophotometric absorbencies at 590 nm and an oxalate standard curve. Solid bars represent means of three replicates two repetitions. Error bars represent standard errors of the mean values for each isolate.

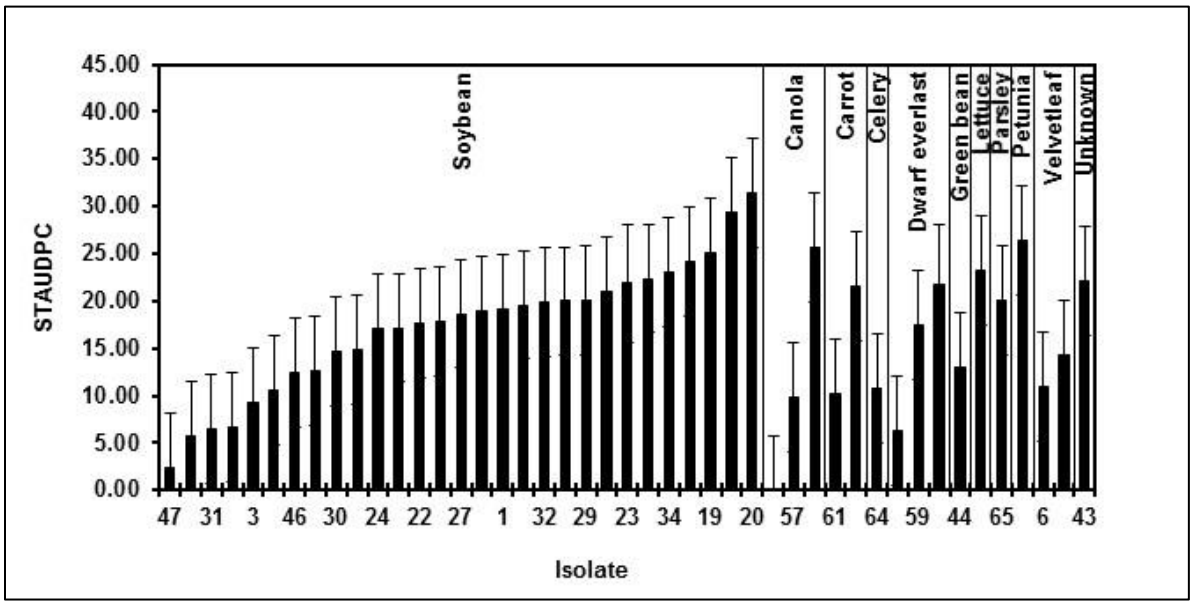

Figure 2.5. Effect of host origin on *S. sclerotiorum* isolate *in planta* aggressiveness on a susceptible soybean cultivar, Williams 82, measured as standardized area under the disease progress curves (STAUDPC). Growth room evaluations were conducted by collecting daily stem lesion (mm) measurements for 7-14 days post-inoculation. Solid bars represent means of three replicates from two repetitions. The effect of host origin within each run was not significant ($P > 0.05$). Error bars represent standard errors of the mean values for each isolate.

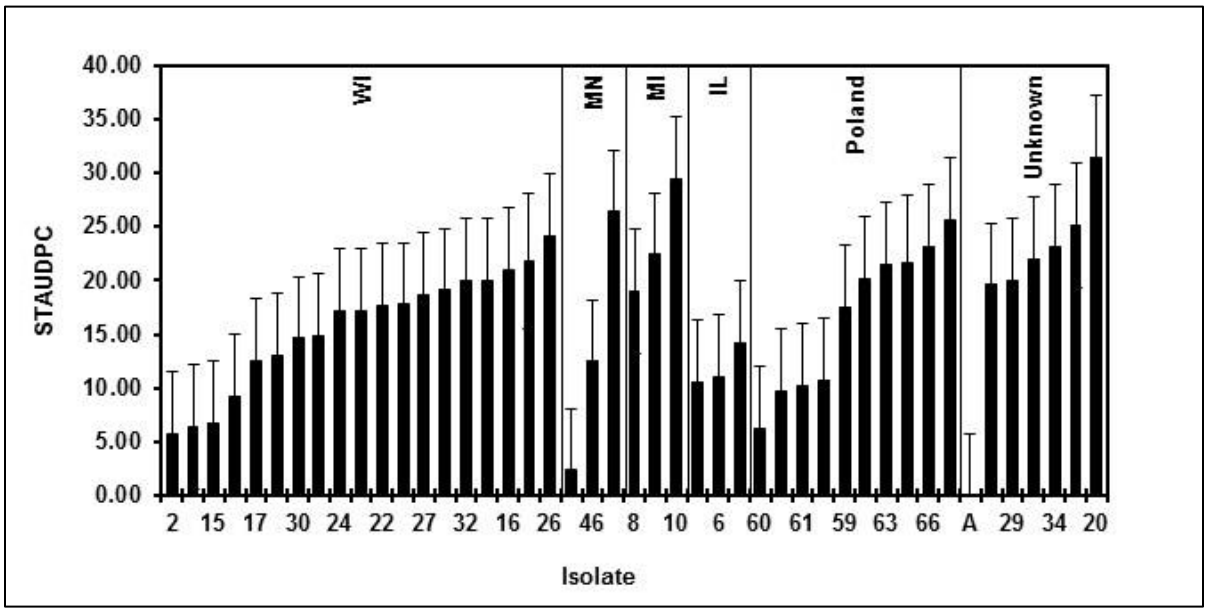

Figure 2.6. Effect of location of collection on *S. sclerotiorum* isolate *in vivo* aggressiveness on a susceptible the soybean cultivar, Williams 82, measured as standardized areas under the disease progress curves (STAUDPC). Growth room evaluations were conducted by collecting daily stem lesion (mm) measurements for 7-14 days post-inoculation. Solid bars represent means of three replicates from two repetitions. The effect of location within each run was not significant ($P > 0.05$). Error bars represent standard errors of the mean values for each isolate.

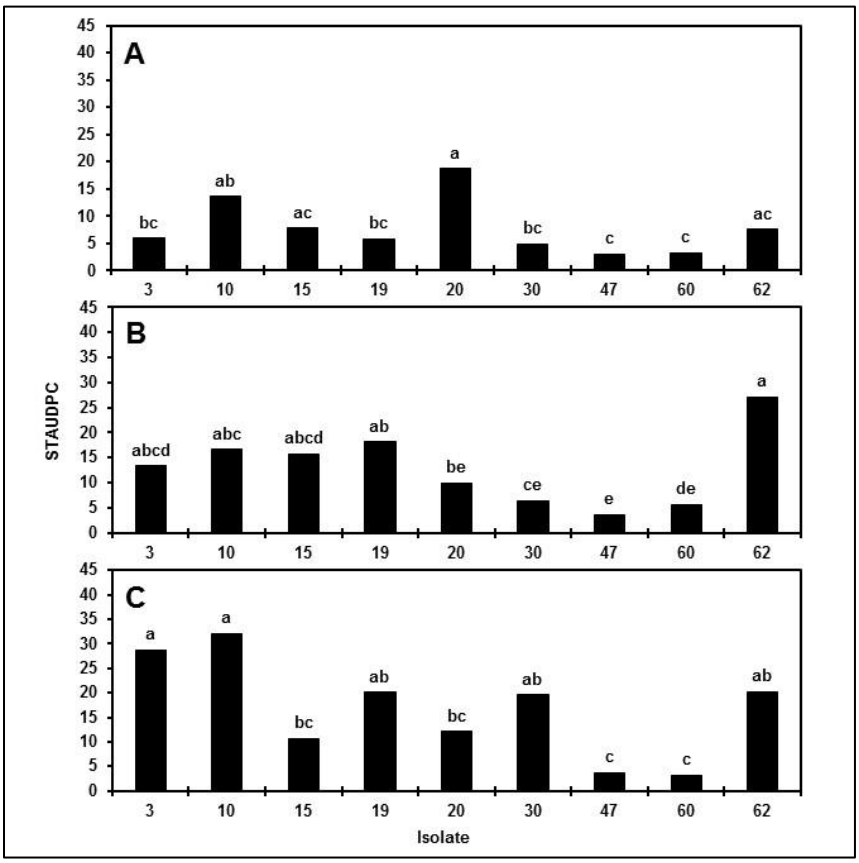

Figure 2.7. Soybean germplasm reactions, measured as standardized areas under the disease progress curves (STAUDPC), to multiple *S. sclerotiorum* isolates. Multiple isolates were used to challenge **A,** a strongly resistant germplasm line 91-145; **B,** a moderately resistant line 91-38; and **C,** a susceptible line 91-44. Greenhouse evaluations were conducted by measuring stem lesions (mm) every 1-3 days for 13 days post-inoculation, in runs 1 and 2, or every 5 days for 15 days, in run 3. Runs 1, 2, and 3 are pooled and mean comparisons by recombinant inbred line were evaluated using Fisher's Least Significant Difference (LSD). Bars designated by the same letter are not significantly different at the α=0.05 significance level. The overall isolate by line interaction was significant (P = 0.04). Reactions with STAUDPC $\leq$ 10 were considered resistant, STAUDPC > 10 but $\leq$ 15 were considered moderately susceptible, and STAUDPC > 15 were considered susceptible.

CHAPTER 3: Development and Evaluation of *Glycine max* Germplasm Lines with Quantitative Resistance to *Sclerotinia sclerotiorum*

*Primary authors M. McCaghey and J. Willbur share first authorship. In the following methods and results sections, a double-asterisk (**) indicates contributions by J.Willbur.

Abstract

Sclerotinia sclerotiorum, the causal agent of Sclerotinia stem rot, is a devastating fungal pathogen of soybean that can cause significant yield losses to growers when environmental conditions are favorable for the disease. The development of resistant varieties has proven difficult. However, poor resistance in commercial cultivars can be improved through additional breeding efforts and understanding the genetic basis of resistance. The objective of this project was to develop soybean germplasm lines that have a high level of Sclerotinia stem rot resistance to be used directly as cultivars or in breeding programs as a source of improved Sclerotinia stem rot resistance. Sclerotinia stem rot-resistant soybean germplasm was developed by crossing two sources of resistance, W04-1002 and AxN-1-55, with lines exhibiting resistance to *Heterodera glycines* and *Cadophora gregata* in addition to favorable agronomic traits. Following greenhouse evaluations of 1,076 inbred lines derived from these crosses, 31 lines were evaluated for resistance in field tests during the 2014 field season. Subsequently, 11 Sclerotinia stem rot resistant breeding lines were moved forward for field evaluation in 2015, and seven elite breeding lines were selected and evaluated in the 2016 field season. To better understand resistance mechanisms, a marker analysis was conducted to identify quantitative trait loci (QTL) linked to resistance. Thirteen markers associated with Sclerotinia stem rot resistance were identified on chromosomes 15, 16, 17, 18, and 19. Our

markers confirm previously reported chromosomal regions associated with Sclerotinia stem rot resistance as well as a novel region of chromosome 16. The seven elite germplasm lines were also re-evaluated within a greenhouse setting using a cut petiole technique with multiple *S. sclerotiorum* isolates to test the durability of physiological resistance of the lines in a controlled environment. This work presents a novel and comprehensive classical breeding method for selecting lines with physiological resistance to Sclerotinia stem rot and a range of agronomic traits. In these studies, we identify four germplasm lines; 91-38, 51-23, SSR51-70, and 52-82B exhibiting a high level of Sclerotinia stem rot resistance combined with desirable agronomic traits, including high protein and oil contents. The germplasm identified in this study will serve as a valuable source of physiological resistance to Sclerotinia stem rot that could be improved through further breeding to generate high-yielding commercial soybean cultivars.

Introduction

Soybean [*Glycine max* (L.) Merr.] is an important, globally-grown source of protein, and it is the largest source of edible oil. In 2015, U.S. agricultural exports of soybean, soybean meal, and soybean oil had a value of nearly 28 billion dollars (Economic Research Service, USDA, 2016). In that year, soybean yielded an average of 3,195 kg ha^{-1} in the United States (National Agricultural Statistics Service, 2015), which was a historical high. In 2016 in Wisconsin, seed oil concentration averaged 19.2% and protein averaged 34.3% (Miller-Garvin and Naeve, 2016), while food-grade soybean averaged 18.7% oil and 35.9% protein (Miller-Garvin and Naeve, 2016).

Among the factors limiting soybean production in the Midwestern U.S. is infection by *Sclerotinia sclerotiorum*, the causal agent of Sclerotinia stem rot (Sclerotinia stem rot). *S. sclerotiorum* is a destructive fungal pathogen in soybean and is estimated to have reduced yield by 1,606 million kilograms in 2009 (Koenning and Wrather, 2010). In other soybean growing regions such as Brazil, Sclerotinia stem rot has also become a production-limiting disease of soybean that can cause yield reductions as high as 60% (Cunha et al., 2010). Integrated management of Sclerotinia stem rot utilizes a combination of cultural, chemical, and biological control practices. Cultural practices include crop rotation, tillage, weed control, irrigation management, and modification of seeding rates and row spacing (Peltier et al., 2012). Fungicides such as picoxystrobin (Aproach®) and boscalid (Endura®) have resulted in suppression of Sclerotinia stem rot in field trials and are most effective when applied at the R1(first flower) to R3 (beginning pod development) growth stages (Smith et al., 2014). The most commonly available and well-studied biological control agent for Sclerotinia stem rot is *Coniothyrium minitans* (Contans® (Peltier, 2012). This beneficial fungus is known to degrade sclerotia, the resting structure of *S. sclerotiorum*.

Despite the existence of various tools for Sclerotinia stem rot management, a high level of control that does not rely on pesticide applications is still in dire need. Acceptable Sclerotinia stem rot control is limited by the lack of strong resistance in available commercial cultivars. Several partially resistant soybean genotypes have been identified in controlled environmental studies and field trials (Bastein et al, 2014; Boland and Hall, 1987; Grau et al., 1982; Han et al., 2008; Huynh et al., 2010; Iquira et al., 2015; Kim and Diers, 2000; Li et al., 2010; Sebastian et al., 2010; Zhao et al., 2015). Within partially resistant cultivars, various

quantitative trait loci (QTL) contributing to Sclerotinia stem rot resistance have been identified. For example, three QTL were identified by Kim and Diers (2000) and 28 QTL were identified by Arahana et al. (2001) which individually explain 4-10% of the phenotypic variation for the trait. Additionally, Vuong et al. (2008) mapped four QTL for Sclerotinia stem rot resistance that each explained from 5.5 to 12.1% of the phenotypic variance in Sclerotinia stem rot development, and Guo et al. (2008) identified seven QTLs which explained 6.0-15.7% of resistance phenotype differences in their populations. Other studies of genetic resistance include investigations of the degradation of the *S. sclerotiorum* pathogenicity factor, oxalic acid, which resulted in the successful development of Sclerotinia stem rot resistant transgenic soybean (Cunha et al., 2010; Donaldson et al., 2001); and more recently the identification that the silencing of soybean NADPH oxidases leads to enhanced resistance to this pathogen (Ranjan, et al., 2017). However, these transgenic soybeans have yet to be exploited commercially. Furthermore, a need persists to differentiate between structurally and physiologically resistant phenotypes, which are often not clearly distinguished in breeding lines.

Breeding for Sclerotinia stem rot resistance is complicated by polygenic resistance alleles, with some likely controlling structural disease avoidance phenotypes, such as plant height, and others controlling physiological resistance mechanisms, as well as complex genetic and environmental interactions. For example, Kim and Diers (2000) identified three QTL which accounted for 8-10% of disease severity index (DSI) variability. However, two were associated with disease klendusity (i.e. plant escape mechanisms) including plant height, lodging, and date of flowering. To determine physiological resistance to Sclerotinia

stem rot, QTL have been mapped in greenhouse experiments where plants were inoculated to avoid screening for escape mechanisms associated with field trials (Arahana et al., 2001; Guo et al., 2008; Vuong et al., 2008). Physiological Sclerotinia stem rot resistance has, thus far, been limited to only a few partially resistant lines (Grau et al., 1982; Kim and Diers, 2000; Vuong et al., 2008). Field testing for physiological resistance is difficult, as environmental conditions and inoculum distributions are not uniform in field trials; the resulting differential disease pressure makes line comparisons unreliable.

Furthermore, isolates of *S. sclerotiorum* have been found to differ in aggressiveness. Willbur et al. (2017) highlighted the importance of using a representative panel of mildly to strongly aggressive isolates for screening soybean lines due to disparate interactions between isolates and lines which may be attributable to varying abilities of isolates to overcome host resistance mechanisms on certain genotypes. Additional efforts are needed to evaluate physiological resistance to ascertain related QTL and to breed for resistance to a wide range of isolates and environments.

Incomplete resistance in commercial soybean cultivars can be addressed through traditional breeding efforts and improved understanding of genetic sources of resistance while preserving the agronomic and industrial qualities of soybean. Breeding efforts have primarily focused on increasing yield first, before attempting to incorporate disease resistance traits. Furthermore, trade-offs can be expected when breeding exclusively for disease resistance due to associated energy requirements that may limit yield and metabolic activities (Wang et al., 2015). For example, lower lignin content of soybean is associated with disease resistance to Sclerotinia stem rot (Peltier et al., 2009). Lignin content, as a

structural component of stems, may be inversely related to lodging which is a contributor to lower yields (Board, 2001). Furthermore, trade-offs have been observed historically when attempting to improve multiple traits simultaneously, which further complicates breeding efforts (Recker et al., 2014). Therefore, continuous evaluations of desirable traits are necessary for the development of elite soybean breeding lines.

The objectives of this project were to: 1) develop soybean germplasm lines that have a high level of Sclerotinia stem rot resistance, that yield competitively with commercial cultivars, while maintaining acceptable protein and oil profiles which would allow them to be used directly as cultivars or in breeding programs as a source of Sclerotinia stem rot resistance; 2) conduct a search for genetic markers associated with Sclerotinia stem rot resistance in the newly developed germplasm lines which can be used to select for resistance and to improve progress in breeding for Sclerotinia stem rot resistance; and 3) compare the response of the generated germplasm lines in a controlled greenhouse environment to multiple isolates of *S. sclerotiorum* and in field environments.

Materials and Methods

Breeding line generation. Six soybean populations were developed, utilizing the Sclerotinia stem rot resistance sources AxN-1-55 and W04-1002 (Table 3.1). AxN-1-55 (PI 640911) was released as public germplasm (Diers et al., 2006) with partial Sclerotinia stem rot resistance in 2006. AxN-1-55 has 75% plant survival after challenge with *S. sclerotiorum* in controlled inoculation trials (Grau *unpublished data*). W04-1002 is an inbred line derived from a single plant selection from PI 567157A (Peltier and Grau, 2008). W04-1002 has

expressed 90 to 100% survival after repeated challenges with multiple isolates of *S. sclerotiorum* and is considered highly resistant to the pathogen (Peltier and Grau, 2008).

The two aforementioned sources of resistance to *S. sclerotiorum* were selected as parents to cross with four parental lines possessing desirable agronomic and pathogen resistance traits (Table 3.1). Populations were assigned a name containing a number indicating the female parent and a "1" or "2" for the Sclerotinia stem rot resistant parent, W04-1002 or AxN-1-55, respectively. Population designations are as follows: 41 = W04-571 x W04-1002, 51 = W04-680 x W04-1002, 81 = L84-5873 x W04-1002, 91 = LN89-5717 x W04-1002, 42 = W04-571 x AxN-1-55, 52 = W04-680 x AxN-1-55.

Initial selections were made based on pod set, minimal lodging, maturity (MG0 to MGII), and absence of foliar diseases to ensure the persistence of acceptable agronomic qualities and parental *C. gregata* and *H. glycines* resistance. Six F1 seeds from each of the six populations were planted in a greenhouse; F2 seed was harvested and combined for field selection. In 2007 F2 seed was planted in a field nursery, naturally infested with *C. gregata* and *H. glycines*, at West Madison Agricultural Research Station located in Verona, Wisconsin (43.06028, -89.531667). Approximately 300 plants were selected within each population, harvested, and F3 seed was combined for planting in 2008. In 2008 field selections, the identity of progeny of each selected plant was maintained to develop sets of individual F3:4 breeding lines for each population.

Selection for resistance to *S. sclerotiorum* was conducted in greenhouse studies and in naturally infested field nurseries. Four plants per F3:4 line were challenged with *S. sclerotiorum* isolate 105HT (Peltier and Grau, 2008) in greenhouse trials to select for

physiological resistance. A cut-petiole inoculation technique was used to challenge lines at the R1 (first flower) growth stage (Peltier and Grau, 2008). One or two surviving plants were advanced to the next generation of selection and identified as a new line. Remnant seed from lines designated as susceptible (plants from lines with 100% mortality when inoculated) were planted to maintain both resistant and susceptible lines within each population in order to assess genetic gain from selection. Single plant selection of new lines continued until the F7 generation, and 1,076 F7:8 lines were advanced to the field for further selection.

After three generations of greenhouse selection, 1,076 inbred lines (F7:8) were planted in 6.1 m, single row, non-replicated plots in a field nursery naturally infested with *C. gregata* and *H. glycines*. Eight hundred and thirty lines were selected for the persistence of acceptable agronomic traits and disease resistance based on criteria previously described. All breeding lines (F7:9 generation) within the four W04-1002-descended populations were once again evaluated for resistance to *S. sclerotiorum* in greenhouse trials. Selection within population 42 was discontinued due to a lack of sustained and measurable disease resistance. By the end of this selection phase of the project, there were 109 lines for population 41, 117 lines for population 51, 224 lines for population 81 and 250 lines for population 91 for a total of 700 lines.

2013 preliminary greenhouse disease severity evaluations. Greenhouse trials were conducted in 2013 at the West Madison Greenhouse Complex located on the grounds of West Madison Agricultural Research Station. Soybean seeds were planted approximately 4 cm deep in 15.25 cm diameter pots of moist potting mix (Sun Gro Horticulture). Soybean

plants were watered daily and fertilized twice weekly (Scotts Peters Professional Peat-Lite Special 20-10-20; Scotts-Sierra Horticultural Products Co.) prior to inoculation.

Soybean plants were inoculated using the cut petiole technique (Peltier and Grau, 2008) with aggressive *S. sclerotiorum* isolate 25 (Willbur et al., 2017). A 1.5-cm-thick agar core was collected from the leading edge of mycelia on each inoculum plate with a 1,000 µl pipet tip (Fisher Scientific). At the R1 (first flower) growth stage, second or third trifoliate leaflets were excised at a petiole length of 2.5 to 3 cm. Pipet tips of inoculum were placed on petioles such that mycelia and cut petiole tissue were in direct contact. Two to three plants (sub-samples) were inoculated per pot for each line and replicated three to four times in a randomized complete block design (RCBD) blocked by replicate. The trial was repeated once. F7:9 lines were phenotyped at the R3 growth stage 14 days post-inoculation (DPI) for resistance to Sclerotinia stem rot using a rating scale of 0 (no stem lesion), 1 (small stem lesion), 2 (lesion but no wilt), 3 (wilt), and 4 (dead plant). Lines with a mean severity score of 0 to 1 were characterized as resistant.

Genetic marker analysis. This work focused on mapping genes that control Sclerotinia stem rot infection using the W04-1002 lines as a resistance source because it represents a novel and stable source of Sclerotinia stem rot resistance. Genomic DNA was extracted from a bulk sample of fresh leaf tissue from each of the 8-10 most Sclerotinia stem rot-resistant and most Sclerotinia stem rot-susceptible lines in 2013 greenhouse evaluations (Table 3.2). Seven soybean leaves for each line were used for the hexadecyltrimethylammonium bromide (CTAB) extraction protocol as described by Keim et al. (1988). The samples were tested for single nucleotide polymorphism (SNP) genetic

markers with the Illumina GoldenGate 1,536 Universal Soy Linkage Panel 1.0 (USLP 1.0) (Hyten et al., 2010). Marker data were analyzed for an association between disease resistance and the alleles from the resistant and susceptible parents for each marker. Based on chi-square analysis, SNP markers with significant segregation distortion were identified. Subsequently, microsatellite markers closely linked to the significant SNP markers from the Chi-square analysis were used to evaluate all lines in the populations. Primer sequences for microsatellite markers were obtained from the SoyBase website (http://soybase.org). Genetic markers were evaluated for 109 lines in population 41, 117 lines in population 51, 224 lines in population 81 and 250 lines in population 91, for a total of 700 lines evaluated. Lines were tested with 12 to 37 markers, depending on the population, that mapped onto three to seven chromosomes (Table 3.3).

****Field evaluations of agronomic traits and disease severity of later generation breeding lines.** Lines planted in the 2014 advanced field trials were selected based on the lowest Sclerotinia stem rot disease severity of the 336 lines trialed from the six populations in the 2013 naturally infested field trials (population 41=64 lines; population 51=51 lines; population 81=93 lines; population 91=76 lines; population 42=36 lines; population 52=16 lines). Subsequent evaluations were also performed in the greenhouse in early 2014. As mentioned previously, population 42 was not evaluated through 2015 due to a lack of performance.

The lines selected in 2013 were planted at the West Madison Agricultural Research Station in May of 2014 and the Hancock Agricultural Research Station in May of 2015 and

2016. Plots were overhead irrigated at each location 1.9-3.2 cm/ha every two to five days to facilitate disease development.

The experimental design each year was a randomized complete block (blocked by replicate) with five or six replications. Plots consisted of four 0.76 m wide rows that were 6.1 m long. Each plot was separated by a 1.5 m non-planted alley. Sowing occurred at a rate of approximately 437,500 seeds ha^{-1} using a tractor-mounted cone-type planter (Almaco, Nevada, IA). Nutrient management was conducted per University of Wisconsin-Madison Cropping Guidelines.

Plot grain weight and moisture was taken from the two center rows of each field plot using an Almaco (Nevada, IA) SPC40 small-plot combine equipped with a HarvestMaster HM800 grain gauge with Mirus software package (Juniper Systems, Logan, UT). Yield measurements were calculated and standardized to 13% moisture. Sub-samples of grain were obtained during harvest and used to assess oil (%) and protein (%) in 2015 and 2016. Oil and protein data were assessed using the average of five 50 ml subsamples of seed from each plot using a near infrared (NIR) grain analyzer (Perten Instruments Inframatic 9500, Hägersten, Sweden). Readings were calibrated by the system for a moisture content of 13%.

Sclerotinia stem rot severity index (DSI) was determined in all years by a rating 30 arbitrarily selected plants in each plot of the field nursery at the R6 soybean growth stage. Plants were scored either 0 (no infection), 1 (infection on branches), 2 (infection on, but not girdling, the main stem), or 3 (infection on the main stem resulting in death or poor pod fill). The sum of the scores of the 30 plants were totaled for each class and divided by 0.9 (Grau et al., 1982). The disease incidence (DI) was calculated by counting the number of symptomatic

plants in 12.19 m of row. Lodging was measured October 11, 2014, October 10, 2015, and October 14, 2016 using an average ranking for each plot of 1 (no leaning), 2 (25-degree lean), 3 (45-degree lean), 4 (more than a 45-degree lean), and 5 (laying on the ground) for each plot.

****Late generation multi-isolate greenhouse evaluations of AUDPC.** Multi-isolate greenhouse evaluations were conducted on soybean plants from the seed of lines tested in 2016 using the previously described cut-petiole technique (Peltier and Grau, 2008). Three soybean seeds per pot were planted approximately 4 cm deep in 15.25 cm diameter peat pots of moist potting mix (Premier Pro-Mix HP BioFungicide + Mycorrhizae). Nine *S. sclerotiorum* isolates, of 44 previously characterized isolates with varying degrees of aggressiveness (Willbur et al., 2017), were used for evaluations. As described by Willbur et al. (2017), lines were inoculated at the V4 growth stage, and lesions were measured with digital calipers (Thermo Fisher Scientific) 5, 12, and 14 DPI. Inoculations were performed in triplicate (three replicates) with three seeds planted per pot, and soybean plants were arranged in a randomized complete block design (RCBD) blocked by replicate. Line evaluations were repeated a second time. Initial inoculum was generated from dry-stored sclerotia (Willbur et al., 2017). Inoculum applied in the second repetition was generated from sclerotia reisolated from the first repetition of plants. The AUDPC was analyzed to evaluate germplasm resistance reactions to a variety of isolates in both greenhouse screens.

Statistical analysis. Mixed-model analysis of variance (ANOVA) was conducted for lodging, agronomic traits, and protein and oil using PROC GLIMMIX in the SAS statistical software package and the analysis of the markers tested for populations was conducted in

PROC GLM (v 9.4, SAS Institute, Inc. Cary NC). Means were separated using Fisher's Least Significant Difference (LSD) via an open source macro (Piepho, 2012). Prior to analysis, lodging scores for each plot were subjected to rank analysis using PROC RANK in SAS. This was done to normalize the categorical nature of lodging scores, so that mixed model ANOVA could be conducted as described above. Disease and yield data were analyzed separately for each year due to large differences in overall disease attributable to environment variability. Significance was reported at α=0.05 significance level.

******The multi-isolate-germplasm line experiments were analyzed using a generalized mixed model (PROC GLIMMIX) analysis of variance using SAS (v 9.4, SAS Institute, Inc.), as described in Willbur et al. 2017. Data were normalized using a lognormal distribution and denominator degrees of freedom for fixed effects were computed using the Kenward-Rodger degrees of freedom approximation. Differences between lines and isolates were determined at α=0.05 significance level.

Results

Germplasm generation, and 2013 greenhouse disease severity evaluations. Six populations were generated in this study by utilizing two Sclerotinia stem rot resistance sources AxN-1-55 and W04-1002. Crosses were established between these sources of resistance and six parental lines conferring other desirable pathogen resistance traits (See materials and methods for details). The resulting populations were designated as follows: 41 = W04-571 x W04-1002, 51 = W04-680 x W04-1002, 81 = L84-5873 x W04-1002, 91 = LN89-5717 x W04-1002, 42 = W04-571 x AxN-1-55, 52 = W04-680 x AxN-1-55. In 2013, 700 promising inbred lines (F7:9) derived from W04-1002, were subjected to *S. sclerotiorum*

petiole inoculations to evaluate physiological resistance to *S. sclerotiorum* and to later identify markers associated with resistance phenotypes. Responses observed among the lines ranged from resistant to highly susceptible within greenhouse trials (Fig. 3.1). After multiple greenhouse trials, 160 of 700 expressed 0 to 25% plant mortality (severity class 0-1, Figure 3.1). Concurrently, parental lines were also evaluated for Sclerotinia stem rot resistance. As expected, the resistant parent W04-1002 showed a highly resistant rating of 0.1, while the average rating of W04-571 was 3.0, W04-680 was 4.0, L84-5873 was 3.5, and LN89-5717 was 3.8. W04-1002, therefore, remained one of the most resistant lines, and a range of responses to Sclerotinia stem rot persisted among lines at the F7:9 generation. The results of 2013 greenhouse evaluations informed selection of the most resistant and susceptible lines for SNP analyses in 2013 and the selection W04-1002 lines evaluated in 2014 field trials.

Genetic markers associated with Sclerotinia stem rot resistance. The preliminary marker analysis was performed using 1,536 single nucleotide polymorphism (SNP) genetic markers (data not shown). This was done by comparing the marker pattern of the 8-10 most resistant lines with the 8-10 most susceptible lines in each population generated from a cross with W04-1002 (Table 3.2). The SNP markers data were analyzed to determine if there was an association between disease resistance and the alleles from the resistant and susceptible parents for each marker. This association was determined by testing for significant segregation distortion compared to expected random segregation. A significant distortion of segregation indicated that the marker was genetically close to a resistance allele. Based on chi-square analysis, markers were identified that had significant ($P < 0.05$) segregation distortion. Due to the high cost of testing all lines in the four populations with the 1,536 SNP

markers, microsatellite markers in regions where the distorted markers are located were then used to test all lines in the populations (Table 3.3).

The microsatellite marker results from all lines in the populations were then combined with the resistance data from the 2013 greenhouse evaluations to map QTL in each population. Using a significance threshold of $P < 0.05$, this analysis resulted in the mapping of QTL to one region on chromosome 15 in population 41, one region on chromosome 19 in population 51, regions on chromosomes 17 and 18 in population 81, and regions on chromosomes 16 and 19 in population 91 (Table 3.4). For many of these regions, multiple significant markers were identified in each population, but these areas where multiple markers arise are likely linked to a common resistance QTL (Fig. 3.2). Additionally, we mapped the physical location of our significant markers with previously published markers associated with Sclerotinia stem rot resistance. With the exception of a novel position on chromosome 16, the majority of our markers confirmed previously identified genetic hot spots associated with Sclerotinia stem rot resistance (Fig.3.2).

****Field evaluations of agronomic traits and disease severity of late generation breeding lines.** After greenhouse evaluations, 31 lines including parental lines and the susceptible controls, Dwight and 91-44, were evaluated for Sclerotinia stem rot severity and the important agronomic traits of yield and lodging. Line performance in-field provided an assessment of the use and commercialization potential of lines. Significant differences among lines were observed in 2014 field tests for Sclerotinia stem rot severity ($P < 0.0002$) and incidence ($P < 0.0001$) (Table 3.5). The experimental line most susceptible to Sclerotinia stem rot based on DSI and DI in the 2014 field test was 91-44 which had a higher DSI and DI

than all other lines. Lines SSR81-107, SSR51-70, and the parental lines had DSI and DI ratings significantly lower than 91-44 but not different from most lines (Table 3.5). AxN-1-55 yielded higher than all cultivars and lines, however, Dwight, 52-11, and 52-82B were not significantly different from this line. Therefore, all breeding lines were significantly lower in DSI and DI than the susceptible line, 91-44, and lines from population 52 had promising yields.

Similarly, lines were evaluated for Sclerotinia stem rot and agronomic traits in 2015. Differences between disease responses were also present in 2015 ($P < 0.0001$) (Table 5). In 2015, the susceptible check, Dwight, and line 91-44 had significantly greater DSI scores than any other line, 50.9 and 50.2, respectively. Lines SSR51-70, W04-1002, 52-82B, and 91-103 had among the lowest DSI scores (<5.0). Dwight, 52-14, AxN-1-55, and 52-82B were the highest yielding of all lines (>3,480 kg ha^{-1}), while the lowest yielding lines included the highly Sclerotinia stem rot-resistant lines W04-1002 and 91-145 (<2,300 kg ha^{-1}). Breeding lines again demonstrated better resistance than susceptible lines, and lines such as 52-82B exhibited both the desirable phenotypes of low disease and high yield.

Among the 10 lines evaluated in 2016, significant differences were present among lines for DSI ($P < 0.01$) and DI ($P < 0.01$) (Table 3.5). DSI and DI values were much higher in 2016 compared to previous years. The most susceptible lines were Dwight, 91-44, and 52-11 with respective DSI values of 91.8, 85.2, and 72.0. In addition to these lines, 52-82B also had a higher disease incidence compared to all but three of the lines. Lowest DSI rankings occurred in lines SSR51-70 and W04-1002 with DSI values of 23.5 and 16.5, respectively. 91-38 also exhibited low disease severity levels that were not significantly different from

SSR51-70. Yield in 2016 was greater than in previous years, and the highest yields occurred in lines AxN-1-55 and 52-82B, 3,865.2 and 3,822.9 kg ha^{-1}, respectively. Lines 91-145 and 52-11 yielded similarly to these lines. Lines with the lowest yields were Dwight and 91-44. Interestingly, results demonstrated high disease ranking for the high yielding varieties 52-11 and 52-82B and lower DSI for SSR51-70 compared to many lines, as previously observed. This outcome occurred despite unusually high disease levels in a field naturally inoculated with *S. sclerotiorum* infected sunflowers.

In 2016 field nurseries, 91-38 and AxN-1-55 had the least lodging ($P < 0.05$) with mean lodging scores that were not significantly different from high yielding lines, 52-11and 52-82B (Supplementary Table S3.2). Lines 91-145 and SSR51-70 exhibited the highest lodging scores, 3.4 and 3.2 respectively, and were not significantly different from 91-44, which had a score of 2.4. Differences in lodging ranks between lines were observed in 2014 (Supplementary Table S3.1) and 2016, but not 2015. 91-38 and 52-11 were not significantly different from AxN-1-55 in 2014 (Supplementary Table S3.1). Lodging results indicated the problematic trait of lodging was consistently present in the highly resistant line, SSR51-70. However, other lines such as 91-38 and 52-82B exhibited positive traits such as moderate disease resistance and high yield in conjunction with a good stand.

In 2015, protein and oil were added to the agronomic traits evaluated, as they are important considerations for commercialization and breeding (Supplementary Table S3.3). The selected breeding lines were also evaluated in 2016 (Supplementary Table S3.4). In 2016, the line with the highest protein content, 39.4%, was W04-1002 ($P < 0.05$), and it was not significantly different from SSR51-70 at 39.2 % and 91-44 at 38.7%. The highest

percentage of oil, 19.2%, was measured from 91-44 and 91-38. Similarly, the aforementioned lines produced high levels of protein and oil in 2015 (Supplementary Table S3.2).

Overall, after three years of evaluations for disease responses and agronomic traits, genetic gain was observed within breeding populations. Desirable observed traits include high levels of disease resistance, as observed in SSR51-70, and maintained yields, as observed with 52-82B. Additionally, moderate disease resistance was observed in conjunction with high protein and oil or moderate yield as observed in 91-38 and 51-23, respectively. Therefore, field evaluations elucidated several promising lines for future breeding or commercialization.

****Late generation multi-isolate greenhouse evaluations of AUDPC.** To determine the physiological resistance of lines, in the absence of field escape mechanisms, greenhouse inoculations of the 2016 lines were conducted using nine previously characterized (Willbur et al., 2017) *S. sclerotiorum* isolates. Previously, 2013 greenhouse evaluations used only a single aggressive isolate. However, current *S. sclerotiorum* research indicates that various isolates may elicit differential resistance responses (Willbur et al., 2017). In 2016, differences in the AUDPC of lines, measured at 5, 10, and 14 DPI, were explained by the line inoculated ($P < 0.01$) and the isolate used ($P < 0.01$). The most resistant lines, as indicated by the lowest AUDPC, were 52-82B and 91-38 ($P < 0.05$) (Fig. 3.3). AUDPC results were lower than the resistant parents', and these lines outperformed several lines considered more resistant based on results from field evaluations. For example, SSR51-70 was consistently more resistant in field experiments than 52-82B and 91-38. Genetic gain was once more observed, as 52-82B and 91-38 had lower AUDPCs than resistant parents. Additionally, 52-82B and 91-38 are

promising lines for agronomic traits, as previously observed. Therefore, high levels of Sclerotinia stem rot resistance bolsters their applicability as commercial lines. Overall, 2016 multi-isolate greenhouse evaluations demonstrated the importance of pathogen diversity and screening in a controlled environment for physiological resistance and the broad applicability of breeding efforts.

Discussion

In this study, QTL associated with reduced *S. sclerotiorum* infection were identified in the four populations of germplasm lines generated from W04-1002 as a source of Sclerotinia stem rot resistance. QTL were identified on chromosomes 15, 16, 17, 18, and 19. These QTL can be used in soybean breeding programs to facilitate the development of Sclerotinia stem rot resistant varieties through marker-assisted selection. For most the significant markers, the allele associated with a lower disease severity phenotype originates from W04-1002, the resistant parent of the populations reported here. However, for marker 1400 from population 41 and marker 0105 from population 81, the allele associated with lower disease severity originated from the susceptible parent (Table 3.4). Resistance alleles for QTL from susceptible parents have been previously identified in other studies (Toojinda et al., 1998). Associated phenotypes included a reduction in lesion size caused by *S. sclerotiorum* on soybean (Arahana et al., 2001) and resistance to BSR originating from PI88788, after crossing with another susceptible parent, potentially through epistatic interactions (Bachman and Nickel 2000; Patzolt et al., 2005). Epistatic interactions are corroborated by the findings of Moellers et al., 2017, which identified 24 significant epistatic

interactions related to Sclerotinia stem rot resistance through genome-wide associated epistatic studies.

Previously, QTL conferring resistance to Sclerotinia stem rot have been reported for the chromosomes identified in this study. Based on genomic map searches on SoyBase.org and a review of current literature on Sclerotinia stem rot resistance loci, it is possible that some of the microsatellite markers in this study correspond to previously identified Sclerotinia stem rot resistance QTL (Arahana et al., 2001; Bastein et al., 2014; Boland and Hall, 1987; Guo et al., 2008; Han et al., 2008; Huynh et al., 2010; Kim and Diers, 2000; Li et al., 2010; Sebastian et al., 2010; Vuong et al., 2008; Zhao et al., 2015). On chromosomes 15, 17, 18, and 19 markers are located between .77 and 4.5 Mega base pairs (Mbp) from the closest, previously associated markers: BARCSOYSSR_17_0507 with Satt154 (Arahana et al., 2001) and BARCSOYSSR_19_1424 with SATT166 (Sebastian et al., 2010) respectively. However, it is likely that a marker identified on chromosome 16, BARCSOYSSR_16_0290 is associated with a novel source of resistance, as it is located 31.5 Mbp from the closest, previously identified marker, Satt431 (Arahana et al., 2001) also identified chromosome 16 as an important contributor to Sclerotinia stem rot resistance. Conversely, they did not find a strong effect in a single population and only observed an association when populations were combined. In this report, we demonstrated that a single population, population 91, possesses a significant QTL on chromosome 16 (Table 3.4; Fig. 3.2). It is important to note that Arahana et al. (2001) and Han et al. (2008) did find significant associations between resistance to Sclerotinia stem rot and markers on chromosome 16 for which the physical position is not available in the literature searched or SoyBase.org. This study both confirms

the presence of QTL near regions identified in previous studies and presents a novel locus (BARCSOYSSR_16_0290), which may be useful in breeding for resistance to Sclerotinia stem rot.

These results are consistent with previous studies showing that Sclerotinia stem rot resistance QTL typically have small effects and are therefore difficult to map (Kim and Diers, 2000; Arahana et al., 2001; and Vuong et al., 2008). An important consideration with the results presented here is that the resistance testing was done in a greenhouse with a reliable inoculation technique to directly assess physiological resistance. Previous efforts to map QTL associated with field resistance have instead resulted in the identification of markers associated with architectural traits such as plant height and lodging (Kim and Diers, 2000). Plant architecture should not have had a major impact on the resistance phenotypes observed in these greenhouse studies; the QTL identified in this study, therefore, are likely not associated with architectural traits. Additionally, QTL on chromosomes 15 and 18 were previously identified in association with cut-petiole assays conducted in the field (Guo et al., 2008); QTL identified on chromosomes 16, 17, and 19, however, were associated with Sclerotinia stem rot resistance in detached leaflet assays (Arahana et al., 2001). This study confirms that QTL on chromosomes 16, 17, and 19 are associated with Sclerotinia stem rot resistance and are, furthermore, associated with physiological resistance in whole-plant, cut-petiole inoculations which is likely more representative of a true resistance phenotype. Several lines in the populations presented here, possess QTL on chromosomes 16 and 19 that were identified using our techniques. Therefore, soybean breeders may find these QTL more

useful than previously thought based on the strong response identified using our whole-plant inoculations and field screening.

The results from the multi-isolate greenhouse evaluations demonstrate the importance of selection within a controlled greenhouse environment for determining a high level of physiological resistance. Representative isolates caused a range of resistance reactions as previously described by Willbur et al. (2017) and variation in isolate aggressiveness has been reported previously (Kull et al., 2004; Li et al., 2008; Vleugels et al., 2013). These studies provide evidence that the breeding lines in this study have been confirmed to exhibit durable resistance to multiple *S. sclerotiorum* isolates, which substantiates the high level of partial resistance available in these populations.

Multi-isolate greenhouse evaluation results were consistent when repeated. However, results differed from field trials in some cases. Lines 52-82B and 91-38 exhibited the highest levels of resistance in greenhouse trials but not in field trials and SSR51-70 did not perform as well in greenhouse evaluations, indicating the importance of using controlled environment evaluations to elucidate physiological resistance phenotypes. The results of Willbur et al. (2017) corroborated moderate resistance in 91-38 against multiple *S. sclerotiorum* isolates in greenhouse evaluations. This suggests klendusity for pathogen avoidance in some germplasm lines, which become apparent in a field setting. Furthermore, partial resistance in some lines may be overcome in the field if cool, moist environments, adequate inoculum, and the correspondence of flowering with apothecial development are simultaneously met in years favorable for Sclerotinia stem rot. Marker alleles corresponding to higher DSI of Sclerotinia stem rot on soybean have also been identified in association with phenotypes of taller plant

height, greater lodging, and later flowering (Kim et al., 1999). As a result, differences in disease severity in a field setting may be a direct effect of physical, rather than physiological, attributes that prevent favorable infection conditions. These studies suggest that a combination of greenhouse inoculations for elucidating physiological resistance and subsequent field evaluations for Sclerotinia stem rot field resistance and agronomic properties contribute to a holistic method to identify lines with QTL for Sclerotinia stem rot resistance and to comprehensively characterize resistance in breeding programs.

This work demonstrates that genetic gain can be made for Sclerotinia stem rot resistance in soybean while maintaining agronomic qualities, protein and oil content, and resistance to other pathogens. Breeding efforts using a novel source of Sclerotinia stem rot resistance followed by greenhouse and field screening, resulted in the development of several promising soybean lines for release as cultivars or use as parents in breeding programs. These candidate lines include 91-38, 52-82B, SSR51-70, and 51-23. Line 91-38 achieved an average yield of 2,802.5 kg ha^{-1}, which is 360.2 kg ha^{-1} higher than W04-1002, the Sclerotinia stem rot resistant parent, and a mean DSI value of 11.4 across all field years evaluated. Line 91-38, which possessed the novel resistance-associated marker region on chromosome 16, also had one of the lowest disease severity rankings in both field and greenhouse trials compared to the susceptible check, Dwight, and other commercial lines in 2016. Additionally, line 52-82B had one of the best yields, a three-year mean of 3,547.1 kg ha^{-1}, and a low DSI mean of 27.5. Line SSR51-70 consistently exhibited among the lowest disease scores for all years in both field (mean DSI of 10.7) and greenhouse studies. With a three-year mean yield of 2,972.5 and DSI of 26.2, line 51-23 also exhibits promising yield

potential and a high level of Sclerotinia stem rot resistance. All lines yielded on average between 2,700 and 3,600 kg ha^{-1} and were consistently near or above the yearly state averages for 2014 (2,953.03 kg ha^{-1}), 2015 (3,322.15 kg ha^{-1}), and 2016 (3,691.27 kg ha^{-1}) (National Agricultural Statistics Service et al., 2014-2016). Overall, the yield performance and elevated disease resistance of these four lines provides strong evidence for their candidacy in future Sclerotinia stem rot resistance breeding programs.

Additionally, lines 91-38, 52-82B, and 51-23 exhibit reduced lodging phenotypes, another highly desirable agronomic trait. Lodging was correlated with lower yield in 2014 (-0.56, $P < 0.0001$), but it was not associated with disease severity. This is not surprising as previous findings have associated lower lignin content, a component of structural tissues in vascular plants, with a high level of resistance to Sclerotinia stem rot (Peltier et al., 2009). It has also been suggested that lower lignin content can act as a biological marker for Sclerotinia stem rot resistance; however, decreased lignin levels are likely related to increased lodging (Boland and Hall, 1987). The negative correlation between yield and lodging has been observed in other studies (Jin et al., 2010 and Recker et al., 2014). Others have also found positive correlations between Sclerotinia stem rot DSI and lodging (Kim et al., 1999). Line 91-38, however, is an example of a line exhibiting both disease resistance in multiple environments and minimal lodging characteristics. While lodging is typically associated with increased Sclerotinia stem rot resistance and reduced yield, the candidate lines presented here consistently exhibit low lodging scores with near or above average yields and strong Sclerotinia stem rot resistance.

Furthermore, lines 91-38 and 51-23 could be considered as food-grade soybean releases, possessing a yellow hilum and high protein levels. In fact, most lines developed here possessed average protein contents above 36% and oil contents that were near 20% (both on a 13% moisture basis), which is above average for soybeans grown in Wisconsin (Miller-Garvin and Naeve, 2016). Line 91-38 also had the best balance of high protein and oil content of the four lines indicated above. Considering the high level of Sclerotinia stem rot resistance, high protein and oil content, and yellow hilum trait, this line has been designated as a candidate for release as a non-GMO, food-grade soybean variety. It will be available as the variety Dane through agreements with Wisconsin Foundation Seeds (https://wisconsinfoundationseeds.wisc.edu). Other lines reported here are available for breeding purposes through an agreement with the Wisconsin Alumni Research Foundation (WARF).

The work presented here demonstrates that genetic gain can be made for Sclerotinia stem rot resistance without sacrificing agronomic qualities in soybean when a holistic approach of marker-assisted selection, greenhouse screening, and field disease nursery screening are used together. Furthermore, we have validated a proof of concept that genetic gain for physiological Sclerotinia stem rot resistance can be achieved, independent of klendusity, through selection in a controlled greenhouse environment using petiole inoculations. We were able to identify several soybean lines that have excellent potential as parents in a breeding program or as varieties themselves, as evidenced by the planned release of 91-38. In addition, crosses have been performed using lines 51-23, SSR51-70, and 52-82B

to identify new germplasm lines with even greater Sclerotinia stem rot resistance through combining sources of resistance while maintaining yield potential.

Literature Cited

Arahana, V.S., Graef, G.L., Specht, J.E., Steadman, J.R., and Eskridge, K.M. (2001). Identification of QTLs for resistance to in soybean. *Crop Sci.* 41, 180-188.

Bachman, M. S., Nickell, C. D., Stephens, P. A., and Nickell, A. D. (1997). Brown stem rot resistance in soybean germ plasm from central China. *Plant Dis.* 81, 953-956.

Bachman, M. S., and Nickell, C. D. (2000). Investigating the genetic model for brown stem rot resistance in soybean. *J. Heredity* 91, 316-321.

Bastien, M., Sonah, H. and Belzile, F. (2014). Genome wide association mapping of resistance in soybean with a genotyping-by-sequencing approach. *The Plant Genome*. *7*(1).

Board, Jim (2001). "Reduced lodging for soybean in low plant population is related to light quality." *Crop Sci.* 41, 379-384.

Boland, G.J. and R. Hall. (1987). Evaluating soybean cultivars for resistance to *Sclerotinia sclerotiorum* under field conditions. *Plant Dis*. 71, 934–936.

Cunha, W.G., Tinoco, M.L.P., Pancoti, H.L., Ribeiro, R.E., and Aragão, F.J.L. (2010). High resistance *to Sclerotinia sclerotiorum* in transgenic soybean plants transformed to express an oxalate decarboxylase gene. *Plant Pathol*. 59, 654-660.

Diers, B.W., Kopich-Obuch, F.J., Hoffman, D.D., Hartman, G.L., Pedersen, W.L., Grau, C.R., and Wang, D. (2006). Registration of AxN-1-55 soybean germplasm with partial resistance to Sclerotinia stem rot. *Crop Sci.* 46, 1403-1404.

Donaldson, P.A., Anderson, T., Lane, B.G., Davidson, A.L., and Simmonds, D.H. (2001). Soybean plants expressing an active oligomeric oxalate oxidase from the wheat gf-2.8 (germin) gene are resistant to oxalate-secreting pathogen *Sclerotinia sclerotiorum*. *Physiol. Mol. Plant Pathol.* 59, 297-307.

Economic Research Service, USDA. (2016). Outlook for U.S. Agricultural Trade/AES 92/May 26.

Guo, X., Wang, D., Gordon, S. G., Helliwell, E., Smith, T., Berry, S. A., and Dorrance, A. E. (2008). Genetic mapping of QTLs underlying partial resistance to in soybean PI 391589A and PI 391589B. *Crop Sci.* 48, 1129-1139.

Grau, C.R., Radke, V.L., and Gillespie, F.L. (1982). Resistance of soybean cultivars to *Sclerotinia sclerotiorum.* Plant Dis. 66, 506-508.

Han, F., M. Katt, W. Schuh, and D.M. Webb. (2008). *QTL controlling Sclerotinia stem rot resistance in soybean.* U.S. Patent 7250,552. Date issued: 18 September

Hughes, T.J., Kurtzweil, N.C., Diers, B.W., and Grau, C.R. (2004). Resistance to brown stem rot in soybean germ plasm with resistance to the soybean cyst nematode. *Plant Dis.* 88, 761-768.

Huynh, T.T., Bastien, M., Iquira, E., Turcotte, P. and Belzile, F. (2010). Identification of QTLs associated with partial resistance to white mold in soybean using field-based inoculation. *Crop Sci.* 50, 969-979.

Hyten, D.L., I.-Y. Choi, Q. Song, J.E. Specht, T.E. Carter, R.C. Shoemaker, E.-Y. Hwang, L.K. Matukumalli, and Cregan, P.B. (2010). A high density integrated genetic linkage map of soybean and the development of a 1,536 Universal Soy Linkage Panel for QTL mapping. *Crop Sci.* 960-968.

Iquira, E., Humira, S. and François, B. (2015). Association mapping of QTLs for Sclerotinia stem rot resistance in a collection of soybean plant introductions using a genotyping by sequencing (GBS) approach. *BMC Plant Biology* 15, 5.

Jin, J. Liu, X., Wang, G., Mi, L., Shen, Z., Chen, X., and Herbert, S.J. (2010). Agronomic and physiological contributions to the yield improvement of soybean cultivars released from 1950 to 2006 in Northeast China. *Field Crops Research* 115, 116-123.

Keim, P., Olson, T., and Shoemaker, R., (1988). A rapid protocol for isolating soybean DNA. Soybean Genet. Newslet. 12, 150-152.

Kim, H.S. and Diers, B.W. (2000). Inheritance of partial resistance to Sclerotinia stem rot in soybean. *Crop Sci.* 40, 55-61.

Kim, H.S., Sneller, C.H., and Diers, B.W. (1999). Evaluation of soybean cultivars for resistance to Sclerotinia stem rot in field environments. *Crop Science*, 39, 64-68.

Koenning, S.R. and Wrather, J.A. (2010). Suppression of soybean yield potential in the continental United States by plant diseases from 2006 to 2009. *Plant Health Prog.* http://dx. doi. org/10.1094/PHP-2010-1122-01-RS.

Kull, L.S., Pedersen, W.L., Palmquist, D., and Hartman, G.L. (2004). Mycelial compatibility grouping and aggressiveness of *Sclerotinia sclerotiorum*. *Plant Disease.* 88, 325-332.

Li, C.X., Li, H., Siddique, A.B., Sivasithamparam, K., Salisbury, P., Banga, S.S., Banga, S., Chattopadhyay, C., Kumar, A., Singh, R. and Singh, D. (2008). The importance of the type and time of inoculation and assessment in the determination of resistance in *Brassica napus* and *B. juncea* to *Sclerotinia sclerotiorum*. *Crop and Pasture Science.* 58, 1198-1203.

Li, D., Sun, M., Han, Y., Teng, W. and Li, W. (2010). Identification of QTL underlying soluble pigment content in soybean stems related to resistance to soybean white mold (*Sclerotinia sclerotiorum*). *Euphytica.* 172, 49-57.

Miller-Garvin, J. and Naeve, S.L. (2016). United States Soybean Quality, Annual Report. (2016). Retrieved from U.S. Soybean Export Council (USSEC) website:

http://ussec.org/wp content/uploads/2016/11/2016-US-Commodity-Soybean-Quality Report-11-4-16.pdf

Miller-Garvin, J. and Naeve, S.L. (2016). United States Food Soybean Quality, Annual Report. 2016. Retrieved from U.S. Soybean Export Council (USSEC) website:http://ussec.org/wp-content/uploads/2016/11/2016-US-Food-Soybean QualityReport-November.pdf

Moellers, T.C., Singh, A., Zhang, J., Brungardt, J., Kabbage, M., Mueller, D.S., Grau, C.R., Ranjan, A., Smith, D.L., Chowda-Reddy, R.V. and Singh, A.K. (2017). Main and epistatic loci studies in soybean for Sclerotinia sclerotiorum resistance reveal multiple modes of resistance in multi-environments. *Scientific Reports*. 7, doi: 10.1038/s41598 017-03695-9.

National Agricultural Statistics Services [NASS] (2014-2016). Agricultural Statistics Board, United States Department of Agriculture (USDA). Soybeans, Yield (2014, 2015, 2016). Available at: https://quickstats.nass.usda.gov/results/DF93F6A0-EAC6-334E B0362264066DFD9B

Nickell, C.D. and Bernard R.L. (1992). Registration of L84-5873 and L84-5932 soybean germplasm lines resistant to brown stem rot. *Crop Sci.* 32, 835.

Nickell, C.D., Noel, G.R., Bernard, R.L., Thomas, D.J., and Frey, K. (1994). Registration of soybean germplasm line LN89-5717, resistant to soybean cyst nematode. *Crop Sci.* 34, 1133.

Nickell, C.D., Noel, G.R. Cary, T.R., and Thomas, D.J. (1998). Registration of 'Dwight' soybean. *Crop Sci.* 38, 1398.

Patzoldt, M.E., Grau, C.R., Stephens, P.A., Kurtzweil, N.C., Carlson, S.R., and Diers, D.W. (2005). Localization of a quantitative trait locus providing brown stem rot resistance in the soybean cultivar Bell. *Crop Sci.* 45, 1241-1248

Peltier, A.J. and Grau, C.R. (2008). The influence of light on relationships between Sclerotinia stem rot of soybean in field and controlled environments. *Plant Dis.* 92, 1510-1514.

Peltier, A.J., Hatfield, R.D., and Grau, C.R. (2009). Soybean stem lignin concentration relates to resistance to *Sclerotinia sclerotiorum. Plant Disease* 9, 149-154.

Peltier, A.J., Bradley, C.A., Chilvers, M.I., Malvick, D.K., Mueller, D.S., Wise, K.A., and Esker, P.D. (2012). Biology, yield loss and control of Sclerotinia stem rot of soybean. *Journal of Integrated Pest Management*, 3, B1-B7.

Piepho, H.P. (2012). A SAS macro for generating letter displays of pairwise mean comparisons. *Communications in Biometry and Crop Science* 7, 4-13.

Ranjan, A., Jayaraman, D., Grau, C., Hill, J.H., Whitham, S.A., Ané, J.M., Smith, D.L. and Kabbage, M. (2017). The pathogenic development of Sclerotinia sclerotiorum in

soybean requires specific host NADPH oxidases. *Mol. Plant Pathol.* doi: 10.1111/mpp.12555.

Recker, J.R., Burton, J.W., Cardinal, A., and Miranda, L. (2014). Genetic and phenotypic correlations of quantitative traits in two long-term, randomly mated soybean populations. *Crop Sci*. 54, 939-943.

Sebastian, S.A., H. Lu, F. Han, D. Kyle, B.R. Hedges, et al. (2010). *Genetic loci associated with Sclerotinia tolerance in soybean*. U.S. Patent 7790,949 B2. Date issued: 7 September.

Smith, D., Chapman, S., Jensen, B. (2014). Wisconsin Field Crops Pathology Fungicide Tests Summary. Retrieved from UW Field Crop Pathology website: http://fyi.uwex.edu/fieldcroppathology/research-summaries/

Toojinda, T., Baird, E., Booth, A., Broers, L., Hayes, P., Powell, W., Thomas, W., Vivar, H. and Young, G. (1998). Introgression of quantitative trait loci (QTLs) determining stripe rust resistance in barley: an example of marker-assisted line development. *Theoretical and Applied Genetics*, 96, 123-131.

Vleugels, T., Baert, J., and Van Bockstaele, E. (2013). Morphological and pathogenic characterization of genetically diverse *Sclerotinia* isolates from European red clover crops (*Trifolium pratense* L.). *Journal of Phytopathology*, 161, 254-262.

Vuong, T.D., Diers, B.W., and Hartman, G.L. (2008). Identification of QTL for resistance to Sclerotinia stem rot in soybean plant introduction 194639. *Crop Sci.* 48, 2209-2214.

Wang, X., Jia, M.H., Ghai, P., Lee, F.N. and Jia, Y. (2015). Genome-wide association of rice blast disease resistance and yield-related components of rice. *Molecular Plant Microbe Interactions*, *28*, 1383-1392.

Wang, Y., Hobbs, H. A., Hill, C. B., Domier, L. L., Hartman, G. L., and Nelson, R. L. (2005). Evaluation of ancestral lines of U.S. soybean cultivars for resistance to four soybean viruses. *Crop Sci*. 45, 639-644.

Willbur, J. F., Ding, S., Marks, M. E., Lucas, H., Grau, C. R., Groves, C. L., and Smith, D. L. (2017). Comprehensive Sclerotinia Stem Rot Screening of Soybean Germplasm Requires Multiple Isolates of *Sclerotinia sclerotiorum*. *Plant Dis.* 101, 344-353.

Zhao, X., Han, Y., Li, Y., Liu, D., Sun, M., Zhao, Y., Lv, C., Li, D., Yang, Z., Huang, L. and Teng, W. (2015). Loci and candidate gene identification for resistance to *Sclerotinia sclerotiorum* in soybean (*Glycine max* L. Merr.) via association and linkage maps. *The Plant Journal*. 82, 245-255.

Tables and Figures

Table 3.1. Parental lines of initial crosses, desirable characteristics, plant introduction number, and line evaluation references.

Parental Lines	Characteristics	Plant Introduction[a]	Reference
W04-1002	Resistance to *S. sclerotiorum*	PI 567157A[b]	Peltier and Grau, 2008
AxN-1-55	Resistance to *S. sclerotiorum*	PI 640911	Diers et al., 2006
W04-571	High yield	Dwight x	Bachman et al., 1997
	Resistance to *C. gregata*	PI 567479[b]	Nickell et al., 1998
	Resistance to *H. glycines*		
W04-680	High yield	Dwight x	Bachman et al., 1997
	Resistance to *C. gregata*	PI 567479[b]	Nickell et al., 1998
	Resistance to *H. glycines*		
L84-5873	Resistance to *C. gregata*	PI 557536	Nickell and Bernard, 1992
LN89-5717	Resistance to *C. gregata*	PI 574542[b]	Hughes et al., 2004
	Resistance to HG type 6 of *H. glycines*		Nickell et al., 1994
Dwight[c]	High yield		Nickell et al., 1998
	Resistance to *H. glycines*		
	Sclerotinia stem rot susceptible control		

[a]Plant introduction (PI) refers to the identifying number assigned to accessions within the National Plant Germplasm System.
[b]These lines are not regarded as ancestral lines for US soybean cultivars and provided the potential for increased genetic diversity (Wang et al., 2005).
[c]Dwight was not a parental line of the populations in this paper, but it is present in pedigrees and was used as a susceptible control for Sclerotinia stem rot resistance assessments.

Table 3.2. Number of most resistant and susceptible lines in each population from 2013 Sclerotinia stem rot greenhouse evaluations used for performing SNP marker analysis.

Population (Parents)	Resistant	Susceptible
4x1 (LW04-571 x W04-1002)	9	9
5x1 (LW04-680 x W04-1002)	8	8
8x1 (L84-5873 x W04-1002)	10	10
9x1 (LN89-5717 x W04-1002)	8	7

Table 3.3. The parents of the populations tested for resistance and genetic markers, the number of lines in each population, the number of markers used to test the populations, and the chromosomes where markers are located.

Population	Parents	Number of lines	Number of markers	Chromosomes
4x1	LW04-571 x W04-1002	109	25	2, 3, 4, 8, 10, 15, 19
5x1	LW04-680 x W04-1002	117	37	2, 8, 9, 16, 18, 19
8x1	L84-5873 x W04-1002	224	12	15, 17, 18
9x1	LN89-5717 x W04-1002	250	25	6, 10, 12, 16, 19

Table 3.4. Significant genetic markers identified in the analysis of the four populations evaluated for Sclerotinia stem rot severity in 2013 greenhouse evaluations.

Marker	Chromo-some number	P value	S[a]	R[b]	Chromosome position (bp)[c]
41 Population					
BARCSOYSSR_15_1382	15	0.05	2.2	1.7	47,656,624
BARCSOYSSR_15_1400	15	<0.01	1.6	2.2	48,070,447
51 Population					
BARCSOYSSR_19_1314	19	0.04	3.1	2.7	44,933,476
BARCSOYSSR_19_1367	19	<0.01	3.1	2.7	45,777,597
BARCSOYSSR_19_1424	19	0.04	3.1	2.7	47,118,641
81 Population					
BARCSOYSSR_17_0460	17	<0.01	2.5	2.0	7,841,443
BARCSOYSSR_17_0471	17	<0.01	2.5	2.1	8,064,099
BARCSOYSSR_17_0476	17	0.05	2.5	2.1	8,281,145
BARCSOYSSR_17_0500	17	0.04	2.4	2.1	8,706,906
BARCSOYSSR_17_0507	17	0.02	2.4	2.1	8,799,234
BARCSOYSSR_18_0105	18	0.02	2.1	2.5	1,808,801
91 Population					
BARCSOYSSR_16_0290	16	0.04	2.2	1.9	4,716,256
BARCSOYSSR_19_0908	19	0.05	2.2	1.9	37,423,905

[a]S column contains the disease severity phenotypic means of the lines that are homozygous for the marker allele from the susceptible parent.
[b]R column contains the disease severity phenotypic means of lines that are homozygous for the marker allele from the Sclerotinia stem rot resistant parent of the populations (W04-1002).
[c]The chromosome positions for Sclerotinia stem rot markers are from the Glyma.Wm82.a2 assembly at soybase.org.

Table 3.5. Sclerotinia stem rot severity and incidence, and yield of soybean breeding lines and cultivars tested in a Sclerotinia stem rot nursery at University of Wisconsin's Hancock Agricultural Research Station, 2014-2016.

Breeding Line or Cultivar	Sclerotinia stem rot DSI (0-100)[a, c]			Disease Incidence (# of plants) [b, c]			Yield (kg ha^{-1})[c]		
	2014	2015	2016	2014	2015	2016	2014	2015	2016
91-44	59.1 a	50.2 a	85.2 ab	36.8 a	32.0 cd	34.9 ab	2,215.9 gh	3,058.2 cde	2617.0 c
52-14	22.7 b	15.6 bd	-	9.8 b	10.0 bc	-	2,915.5 bcd	3,541.6 ac	-
41-39	22.2 b	6.6 bc	-	9.2 bc	3.5 cd	-	2,495.0 efg	2,932.6 de	-
51-23	17.1 bc	6.9 bc	59.7 cd	8.4 bc	3.0 a	21.6 bcd	2,625.6 df	3,156.2 bcd	3135.6 b
91-103	16.2 bc	4.7 cd	-	7.2 bc	2.8 cd	-	2,355.0 fg	2,662.2 df	-
Dwight	15.3 bc	50.9 a	91.8 a	8.6 bc	26.6 cd	41.9 a	3,102.0 ab	3,486.5 ac	2621.0 c
52-11	14.0 bc	11.8 bc	72.0 ac	10.0 b	5.2 cd	33.0 ab	3,232.6 ab	3,134.3 cd	3522.8 ab
52-82B	13.1 bc	4.0 cd	65.4 bc	5.6 bc	1.4 c	28.7 abc	3,075.7 ac	3,742.8 a	3822.9 a
91-145	10.9 bc	5.4 bc	56.2 cd	3.8 bc	2.4 a	15.8 d	2,336.6 fh	2,246.5 f	3459.9 ab
91-38	9.3 bc	10.7 bc	38.9 de	3.2 bc	4.8 cd	14.2 de	2,456.4 efg	2,605.5 ef	3345.6 b
SSR81-62	8.4 bc	14.6 bc	-	4.8 bc	8.4 bd	-	2,753.6 cde	2,880.3 de	-
SSR51-70	5.6 c	2.9 cd	23.5 ef	1.8 bc	1.2 d	8.7 e	2,252.5 gh	2,801.8 de	3187.7 b
AxN-1-55	3.8 c	7.8 bc	-	1.2 bc	3.6 cd	17.8 cd	3,356.9 a	3,667.8 ab	3865.2 a
W04-1002	3.8 c	2.9 c	16.5 f	1.6 bc	1.0 cd	4.1 f	1,994.7 h	2,258.3 f	3073.8 bc
SSR81-107	2.0 c	17.1 b	-	0.6 c	10.4 cd	-	2,226.5 gh	2,612.0 ef	-

[a]Sclerotinia stem rot severity was measured using the disease severity index (DSI) which was generated by rating 30 arbitrarily selected plants in each plot and scoring plants on a 0-3 scale: 0 = no infection; 1 = infection on branches; 2 = infection on main stem with little effect on pod fill; 3 = infection on main stem resulting in death or poor pod fill. The scores of the 30 plants were totaled for each class and divided by 0.9.

[b]Average number of symptomatic plants in 12.19 m of row.

[c]Means followed by the same letter are not significantly different based on Fisher's Least Significant Difference (LSD; α=0.05)

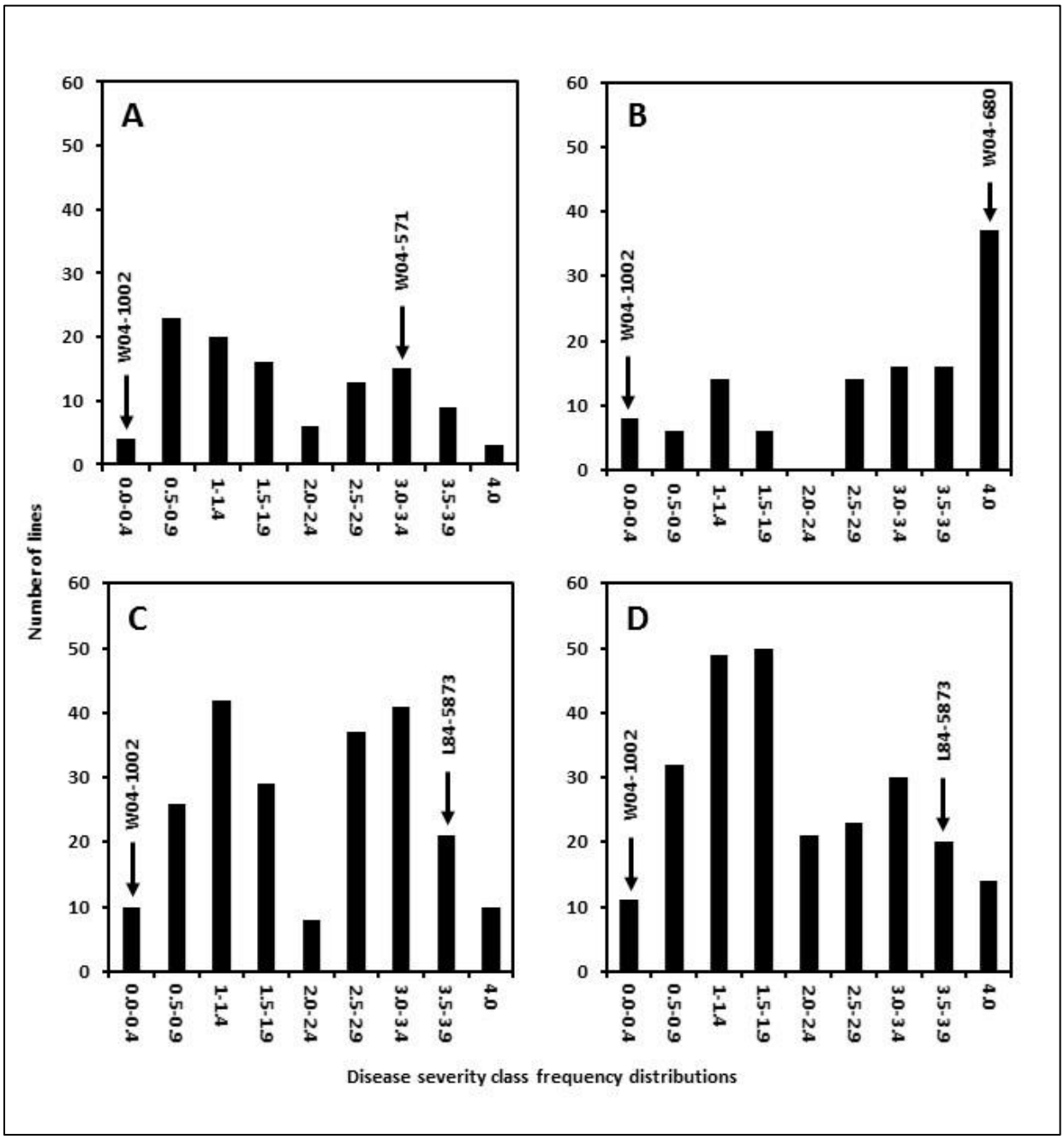

Figure 3.1. Frequency distribution of disease severity classes in populations 41 (A), 51 (B), 81 (C), and 91 (D) from 2013 greenhouse evaluations. The resistant parent line W04-1002 showed a highly resistant rating of 0.1 while the average rating of other parental lines was 3.0 for W04-571, 4.0 for W04-680, 3.5 for L84-5873, and 3.8 for LN89-5717.

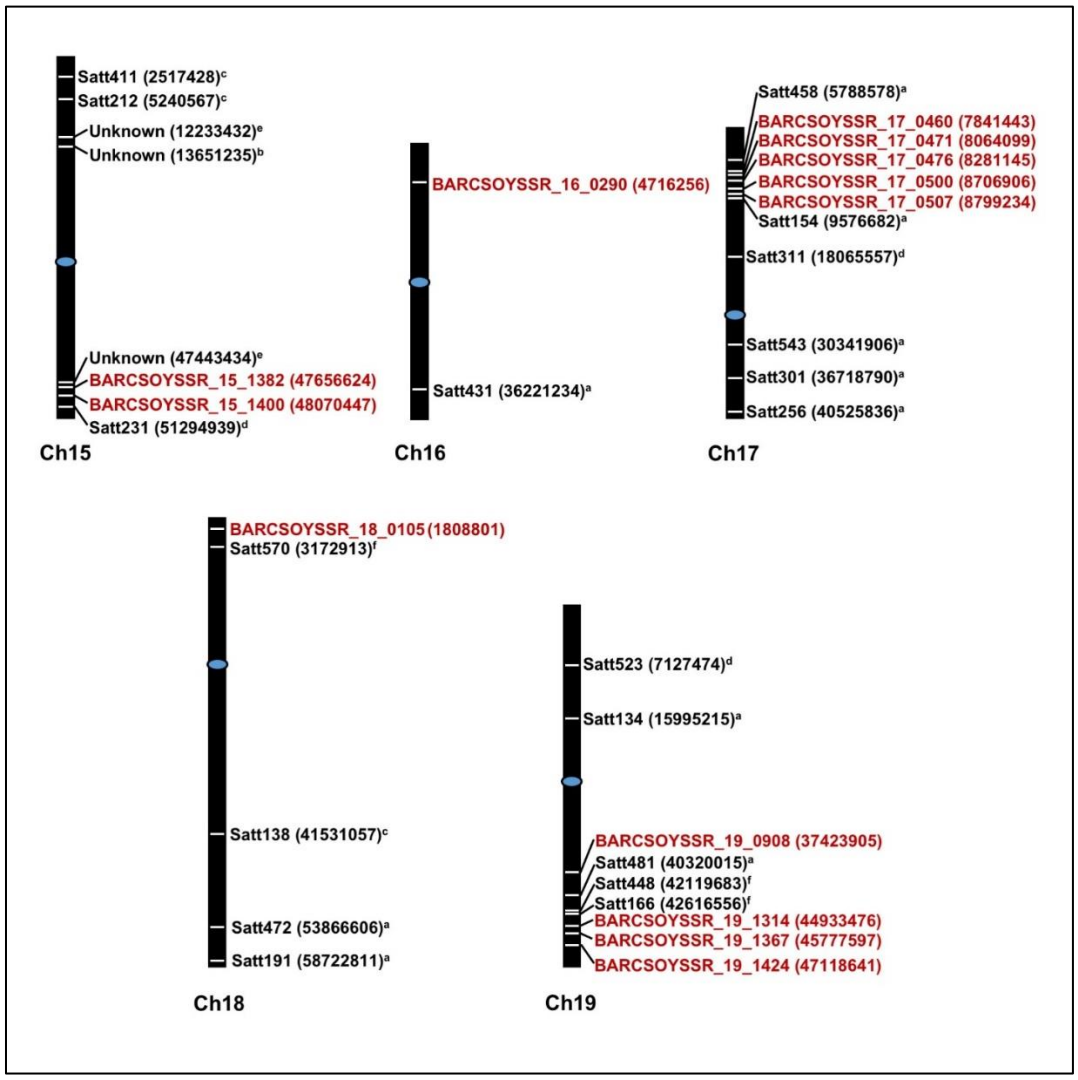

Figure 3.2. Physical starting positions of markers associated with disease resistance in previous studies and this study. Chromosome numbers are displayed under each chromosome. Markers locations are indicated by white lines placed directly on chromosomes and are placed relative to physical positions. Physical starting position of the microsatellite markers are shown in parenthesis. Markers in red text are from the present study while markers from previous study are shown in black text. Centromeres are indicated by blue ovals. [a]Arahana et al., 2001; [b]Bastein et al., 2014; [c]Guo et al 2008; [d]Han et al., 2008; [e]Iquira et al., 2015; [f]Sebastian et al., 2010

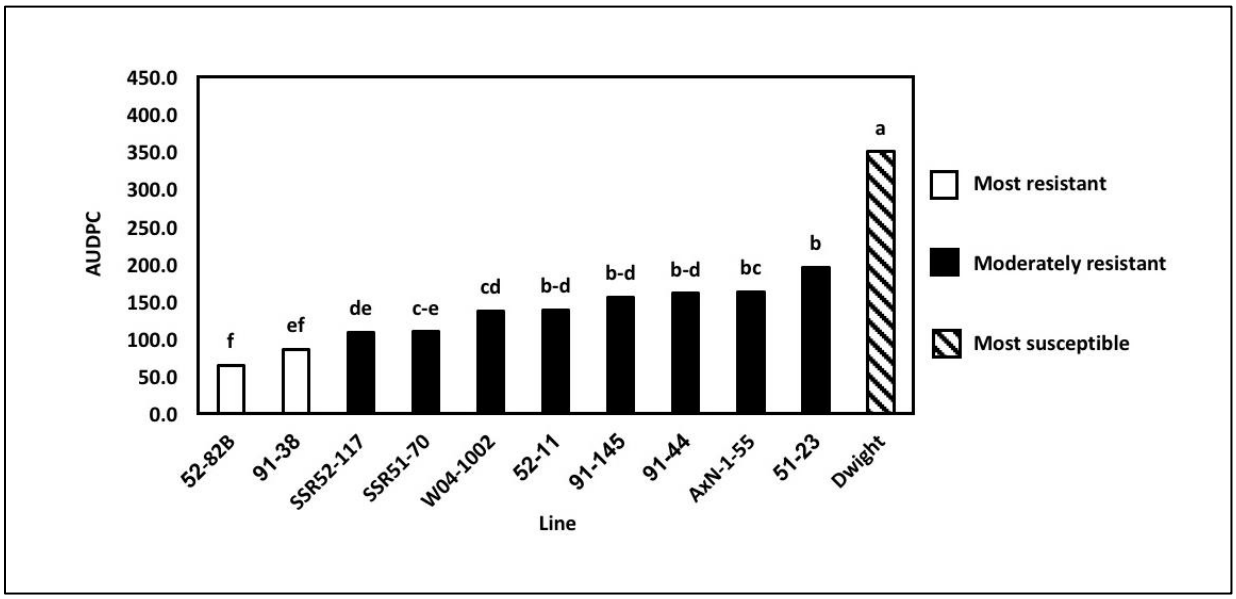

****Figure 3.3.** Area under the disease progress curve (AUDPC) of multi-isolate greenhouse evaluations. Means followed by the same letter are not significantly different based on Fisher's Least Significant Difference (LSD; α=0.05). LSD values were calculated based on the lognormal transformed AUDPC values.

Supplementary Materials

Supplementary Table S3.1. Mean lodging scores for breeding lines in 2014

Variety	Mean Lodging Score[z]	Rank Estimate[y]
91-145	3.4	62.4 a
51-23	3.0	56.0 ab
91-103	3.0	56.0 ab
SSR51-70	3.0	53.8 abc
W04-1002	3.0	51.6 abcd
SSR81-62	2.8	50.6 abc
41-39	2.6	45.2 bcd
52-14	2.2	35.6 cdef
SSR81-107	2.2	34.4 de
91-44	2.0	29.0 e
52-82B	1.6	20.6 ef
Dwight	1.6	20.6 ef
52-11	1.5	18.5 efg
91-38	1.4	16.4 fg
AxN-1-55	1.0	8.0 g

[z]Soybean lodging was scored on a 1-5 scale: 1= upright. 2 = 25-degree lean. 3 = 45-degree lean. 4 = more than 45-degree lean and 5 = laying on the ground. This scale represents the approximate average rating for the whole plot.

[y]Rank estimates were generated to compare categorical lodging scores. Values followed by the same letter are not significantly different based on Fisher's Least Significant Difference (LSD; α=0.05).

Supplementary Table S3.2. Mean lodging scores for breeding lines in 2016

Variety	Mean Lodging Score[a]	Rank Estimate[b]
91-145	3.4	48.3 a
SSR51-70	3.2	46.2 a
91-44	2.4	36.5 ab
W04-1002	2.0	29.4 bc
51-23	2.0	33.0 b
Dwight	1.6	26.8 bc
52-82B	1.3	21.3 bcd
52-11	1.2	17.9 cd
AxN-1-55	1.0	14.5 d
91-38	1.0	14.5 d

[a]Soybean lodging was scored on a 1-5 scale: 1= upright. 2 = 25-degree lean. 3 = 45-degree lean. 4 = more than 45-degree lean and 5 = laying on the ground. This scale represents the approximate average rating for the whole plot.

[b]Rank estimates were generated to compare categorical lodging scores. Values followed by the same letter are not significantly different based on Fisher's Least Significant Difference (LSD; α=0.05).

Supplementary Table S3.3. Total protein and total oil content of grain from soybean breeding lines harvested in 2015 calibrated to 13% moisture

Breeding Line	Protein (%)[z]	Oil (%)[z]
91-103	38.4 a	18.2 h
W04-1002	38.1 ab	17.8 i
91-38	37.8 abc	19.0 bc
SSR51-70	37.5 bd	18.6 df
52-14	37.3 cde	18.7 cde
91-44	37.1 de	19.6 a
52-11	37.1 de	18.5 efgh
91-145	37.1 de	18.2 gh
52-82B	37.0 df	18.5 dg
AxN-1-55	37.0 df	18.4 efgh
SSR81-62	36.8 ef	18.2 h
SSR81-107	36.4 fg	19.2 b
Dwight	35.7 gh	18.8 cd
51-23	35.5 h	18.3 fgh
41-39	35.3 h	19.3 ab

[z]Means followed by the same letter are not significantly different based on Fisher's Least Significant Difference (LSD; α=0.05).

Supplementary Table S3.4. Total protein and total oil content of grain from soybean breeding lines harvested in 2016 calibrated to 13% moisture.

Breeding Line	Protein (%)[a]	Oil (%)[a]
W04-1002	39.4 a	17.9 c
SSR51-70	39.2 ab	18.6 b
91-44	38.7 ac	19.2 a
91-38	38.6 bc	19.2 a
52-82B	38.5 bc	18.1 c
52-11	38.5 c	18.4 b
AxN-1-55	38.3 c	18.4 b
91-145	37.6 d	18.7 b
Dwight	37.6 d	18.5 b
51-23	37.3 d	18.5 b

[a]Means followed by the same letter are not significantly different based on Fisher's Least Significant Difference (LSD; α=0.05).

CHAPTER 4: Weather-based models for assessing the risk of *Sclerotinia sclerotiorum* apothecial presence in soybean (*Glycine max*) fields

Abstract

Sclerotinia stem rot (SSR) epidemics in soybean, caused by *Sclerotinia sclerotiorum,* are currently responsible for up to one million metric ton annual yield reductions in the United States. In-season disease management is largely dependent on chemical control, but its efficiency and cost-effectiveness depends both on the chemistry used and the risk of apothecia formation, germination and further dispersal of ascospores during susceptible soybean growth stages. Hence, accurate prediction of the *S. sclerotiorum* apothecial risk during the soybean flowering period could enable farmers to improve in-season SSR management. From 2014 to 2016, apothecial presence or absence was monitored in three irrigated (n = 1,505 plot-level observations) and six non-irrigated (n = 2,361) field trials located in Iowa (n = 156), Michigan (n = 1,400), and Wisconsin (n = 2,310) for a total of 3,866 daily plot observations. Hourly air temperature, relative humidity, dew point, wind speed, leaf wetness, and rainfall were also monitored continuously, throughout the season, at each location using high-resolution gridded weather data. Logistic regression models were developed, for irrigated and non-irrigated conditions, using apothecial presence as a binary response variable. Agronomic variables (row width) and weather-related variables (defined at 30-day moving averages, prior to apothecial germination) were tested for their predictive ability. In irrigated soybean fields, apothecial risk was best explained by row width (r = -0.41, $P < 0.0001$) and 30-day moving averages of daily maximum air temperature (r = 0.27, $P < 0.0001$) and daily maximum relative humidity (r = 0.16, $P < 0.05$). In non-irrigated

fields, apothecial risk was best predicted using moving averages of daily maximum air temperature (r = -0.30, P < 0.0001) and wind speed (r = -0.27, P < 0.0001). These models correctly predicted (overall accuracy = 67-70%) apothecial risk during the soybean flowering period for four independent datasets (n = 1,102 plot observations; 30 daily mean observations).

Introduction

Sclerotinia stem rot (SSR), also known as white mold, is caused by *Sclerotinia sclerotiorum* and consistently ranks in the top ten diseases plaguing soybean crops worldwide (Allen et al. 2017; Lehner et al. 2017; Wrather et al. 2010). In 2014, SSR was responsible for a 1.1 million metric ton yield reduction in soybean growing regions which cost farmers ~$511 million according to market prices (Allen et al. 2017; Bradley et al. 2016; USDA-NASS 2017). *Sclerotinia sclerotiorum* is infamously characterized by its broad host range (> 400 host species), longevity in the soil (as soilborne sclerotia), and by the subsequently devastating crop losses (Boland and Hall 1994; Peltier et al. 2012). Thus, SSR management is justifiably ranked high in significance and concern in the North Central region of the U.S.

Ascospores produced from *S. sclerotiorum* apothecia are the primary source of inoculum for infection by this fungus in soybean (Abawi and Grogan 1974; Grau and Hartman 2015; Peltier et al. 2012; Saharan and Mehta 2008). Ascospores are wind-dispersed onto senescing flowers, which provide a source of nutrients for successful mycelial colonization (Grau et al. 1982; Grau and Hartman 2015; Saharan and Mehta 2008). Despite the variety of strategies used in SSR management (Peltier et al. 2012), effective in-season control depends on chemical applications, which are primarily targeted at protecting flowers

from ascospore infection. Since environmental conditions conducive for apothecial germination often coincide with soybean flowering, or between the R1 (first bloom) to R3 (first pod forming) growth stages (Fehr et al. 1971), the risk of disease onset should be assessed and addressed during this period. It would be beneficial to farmers if they were informed of 1) risk of apothecial formation during the flowering period, and 2) if and when fungicides should be applied for economic and optimal control during the flowering period.

Soybean flowering, apothecial germination, and weather conditions conducive for infection must occur simultaneously for SSR development. Due to this complex array of factors, and the difficulty for farmers to assess these factors efficiently during the season, fungicide applications may be unnecessary or ineffective as a result of unsuitable timing (Mueller et al. 2004). Accordingly, the development of a model to predict the risk of disease development in soybeans is key to effectively timing fungicide applications for SSR control. Disease forecasting models have been developed and tested for predicting diseases caused by *Sclerotinia spp.* in other crops, such as peanut (Smith et al. 2007), carrot (Foster et al. 2011), lettuce (Clarkson et al. 2007, 2014), dry bean (Harikrishnan and del Río 2008), and canola (Twengstrom et al. 1998). In lettuce, under controlled environment conditions, ascospore density (> 87 spores cm^{-2}), temperature (21.7°C optimal), and relative humidity (80-100%) were all important to predict *S. sclerotiorum* infection (Clarkson et al. 2014). In another study, 30-50 days at temperatures of 18-20°C was found to be optimal for apothecial germination, dependent on the *S. sclerotiorum* isolate (Clarkson et al. 2007). Collectively, these findings suggest that temperature and moisture, over a period of 30-50 days prior to sclerotial germination, influence apothecial development.

Models incorporating soil temperature (maximum of 24°C) and moisture (≥ 20 kPa) were able to predict development of apothecia and ascospores of Sclerotinia rot in carrot (Foster et al. 2011). In a two-year field evaluation study, the model reduced the total number of fungicide applications compared to a typical calendar-spray regime and achieved an equivalent level of control (Foster et al. 2011). Soil parameters are often difficult to simulate and acquire for site-specific predictions unless an on-site meteorological-grade weather station is used. Simulated, model-derived weather data, however, are readily available for most air temperature and moisture variables. In the United States, simulated downscaled weather data are created by numerical weather models that use weather station data and remote sensing to generate weather data at grid resolutions of 5 km (Benjamin et al. 2007). Models generated using these publicly available data allow the disease prediction models to be more widely accessible to farmers and functional in virtually any growing location (Magarey et al. 2001).

Studies in China have investigated correlations between the numbers of apothecia present during the soybean blossom stage and disease index with yield loss measurements (Pan et al. 2001; Saharan and Mehta 2008). Both number of apothecia and disease index were negatively correlated with yield, and an action threshold for implementing chemical control was established at three to four apothecia per 9.75 m^2 (Pan et al. 2001). Apothecial size (approximately 0.5-10 mm in diameter) (Grau and Hartman 2015; Kohn 1979) and aggregated distribution within a field (Boland and Hall 1988b), however, make this model difficult to implement for soybean farmers. A study conducted in the North-Central region of the U.S. used logistic regression to model the prevalence (proportion of diseased fields

within a large production region) of soybean SSR (Mila et al. 2004). Using total precipitation and air temperature in either April or July combined with regional tillage practices, disease prevalence was modeled at a regional level. This model, however, while useful at the regional level, was not accurate at the field level (Mila et al. 2004). Farmers in the Great Lakes region, therefore, would benefit from an accurate, site-specific model to predict the risk of SSR at the soybean field level where management decisions are applied.

Historically, *S. sclerotiorum* apothecia and SSR incidence were both spatially aggregated and correlated within sectors of white bean and soybean fields (Boland and Hall 1988a, b). More recently, the spatial distribution of SSR has been correlated with apothecia in both canola (Qandah and del Rio Mendoza 2012) and soybean (Wegulo et al. 2000). In both studies, disease incidence (DI) decreased as distance from apothecial inoculum sources increased. Furthermore, the majority of ascospores were deposited near apothecia (Wegulo et al. 2000) which supports the relationship between apothecia and disease. Therefore, apothecial presence is a promising candidate to use for SSR risk assessment in soybean fields.

The ultimate goal of this research is to develop and test the usefulness of a risk prediction model, which can be further integrated into a decision-support system, to help farmers make economic and environmentally-friendly decisions related to fungicide use and timing. To address this goal, empirically-derived logistic regression models were developed using downscaled gridded weather data to predict the risk of *S. sclerotiorum* apothecial presence in soybean fields.

Materials and Methods

Study area and experimental conditions.

Wisconsin. In 2014, 2015, and 2016 apothecial populations were intensively monitored in small-plot field trials established at University of Wisconsin – Madison Agricultural Research Stations (Table 4.1), in fields with a known history of *S. sclerotiorum* infestation. Trials used in this study were planted in locations with soil types representative of the state and using cultivars with typical flowering periods for the region (Table 4.1). In 2014 and 2015, trials located in West Madison, WI were planted on May 30 and May 13, respectively. Small four-row plots, 6.1 m long by 3.0 m wide, were planted at a 0.76-m row spacing and at a density of 375,000 seeds/ha in 2014 or 350,000 seeds/ha in 2015.

In 2016, small plots were planted on May 18 at 350,000 seeds/ha with a 0.76-m row spacing in trials located in Arlington, WI. An additional trial subjected to overhead irrigation was planted on May 17 in Hancock, WI. This trial was planted at 350,000 seeds/ha with a 0.76-m row spacing. Plots were generally irrigated every two to five days at a rate of 1.9 to 3.2 cm/ha.

Field trials used for apothecial monitoring were established as cultivar and/or fungicide evaluations; treatments were replicated five times and arranged in a randomized complete block design. Trials were surrounded by at least 3.0 m of buffer soybean plants, 1.5-m alleys were cleared between each block, and data were collected in the center two rows of each plot. Inoculum in field sites was augmented by planting sunflower crops inoculated with three *S. sclerotiorum* isolates (collected in Wisconsin). The sunflower crops were planted and inoculated one or two years prior to the soybean crop being planted. Shallow-depth field cultivation was used to uniformly incorporate sclerotia into the upper soil profile

after sunflower harvest. SSR nursery infestations were maintained with yearly rotations of soybean and sunflower and repeated sunflower inoculations.

Michigan. Trials used in this study were conducted with cultivars and soil types representative of the state (Table 4.1). In 2015, apothecial observations were collected from four field trials, planted on May 21 at the Michigan State University Research Center in Montcalm, MI. All Montcalm trials were overhead irrigated to supplement local rainfall.

In 2015, trials were irrigated approximately once a week between July 06 and August 12 with 5.4 to 6.4 cm/ha of water. One trial was planted at 0.76-m row spacing and contained ten plots which were 12.2 m long by 6.1 m wide. A second trial was planted at 0.36-m row spacing containing nine plots which were 12.2 m long by 6.1 m wide. The two other trials were planted at either a 0.76- or 0.36-m row spacing, with each containing eight four- or six-row plots, which were 12.2 m long and 3.0 m wide. These trials also doubled as replicated fungicide evaluations. Fungicide treatments were replicated four times and arranged in a randomized complete block design.

In 2016, apothecial counts were collected from two non-fungicide-treated, irrigated trials. Trials were planted May 17 at either a 0.76- or 0.38-m row spacing. Small, four- or six-row plots, which were 6.1 m long by 3.0 m wide, were planted at a target density of 400,000 seeds/ha. Plots were irrigated approximately once per week, similarly to 2015.

In 2016, additional apothecial observations were collected in an on-farm trial located in Ionia, MI; this trial was non-irrigated, not treated with fungicide, and planted at a 0.38-m row spacing. The field was divided into five 21.0- by 21.0-m square plots.

Iowa. In 2016, apothecial presence data were collected from two non-irrigated trials located in Manilla and Nashua, IA (Table 4.1). Manilla and Nashua trials were planted on May 08 at a row spacing of 0.76 m and at seeding rates of 375,000 and 475,000 seeds/ha, respectively. In Manilla, apothecia were monitored in a fungicide trial with 24 replicated treatments. In Nashua, the trial evaluated six fungicide treatments. Treatments in both trials were arranged in a randomized complete block design with four replicates. Small, four-row plots were 6.1 m long by 3.0 m wide and blocks were separated by 1.5-m alleys. The trials used for this research were conducted with cultivars and soil types representative of the state (Table 4.1).

Data collection and response variables.

Apothecia counts.

Wisconsin. Scouting for apothecia began prior to the R1 growth stage (first flower) and typically continued twice weekly until either complete apothecial senescence or until plants reached the R7 growth stage (beginning maturity). At each observation day, three 0.76- by 0.76-m square areas were examined between the center two rows (yield rows) in each plot. Squares were arbitrarily placed at three locations throughout the 6.1-m length of the plot and apothecial numbers were recorded at each stop. In 2014, scouting was conducted for seven weeks from 52 to 102 days after seeding (DAS) between the R3 (beginning pod) and R7 growth stages (n = 520). In 2015, scouting was conducted for eight weeks from 48 to 105 DAS, between the V4 (fourth trifoliate) to R6 (full pod) growth stages (n = 400). In 2016, the trial in Arlington, WI was scouted for eight weeks from 37 to 97 DAS, or from the V5 (fifth trifoliate) to R5 (beginning seed) growth stages (n = 1,125). At the Hancock trial in

2016, scouting was conducted three times at 44, 57, and 78 DAS, which were at the V6 (sixth trifoliate), R2 (full flowering), and R5 growth stages (n = 225).

Michigan. In 2015, apothecial counts were taken twice weekly in eight 0.76-m squares placed arbitrarily throughout each plot, of the four total trials, and daily totals recorded per plot. In the two non-treated trials, ten plots were scouted in the 0.76-m row spacing and nine plots in the 0.36-m spacing trial. In the two fungicide trials, all eight plots were scouted for every observation day. Scouting was conducted in every trial for 12 weeks from 36 to 125 DAS, which began prior to the R1 growth stage and continued through the R6 growth stage (n = 720).

In 2016 in Montcalm, four plots per trial were scouted twice weekly for ten weeks from 28 to 100 DAS (n = 560). Apothecial counts were taken in four 0.76-m squares placed arbitrarily throughout the plot and totals were recorded for each stop. Daily apothecial means for this study were generated for each day per trial as previously described.

In 2016 in Ionia, apothecial counts were collected in four 0.76-m squares arbitrarily placed throughout the square plots and totals were recorded for each stop. Counts were collected on six days over the course of four weeks beginning just prior to R1 and continuing until the R4 (full pod) growth stage (n = 120).

Iowa. Apothecial counts were taken in three 0.76-m squares placed arbitrarily throughout the center two rows of each non-treated plot of each trial. The total apothecia in each square were recorded per plot. Both Manilla and Nashua locations were scouted once a week for five to six weeks, including the approximate two week flowering period, from around 53 to 96 DAS (n = 156).

Ascospore trapping.

Wisconsin. Ascospore presence was monitored in Wisconsin trials from 2014 to 2016. Spores were detected using bromophenol blue semi-selective media (SSM) in Petri plates (Steadman, Marcinkowska, and Rutledge 1994; Foster et al. 2011). These "spore-trapping" plates consisted of standard 90-mm Petri plates containing potato dextrose agar (PDA) amended with 25 mg L^{-1} 75% pentachloronitrobenzene (PCNB), 150 mg L^{-1} penicillin G (potassium salt), 150 mg L^{-1} streptomycin sulfate, and 50 mg L^{-1} bromophenol blue indicator. As in the Foster et al. (2011) study, SSM plates were placed beneath the soybean canopy at a 45-degree angle, facing upwind, and were exposed between 09:00 and 14:00 h. In Wisconsin, plates were exposed beneath the soybean canopy for three consecutive hours. Plates were incubated at room temperature (21–24°C) for two to three days and then evaluated for the presence of *S. sclerotiorum* colony forming units (CFUs). CFUs were distinguishable by the characteristic yellow halo surrounding the small, circular, translucent white colonies. Colonies were best visualized using backlighting or a dissecting microscope in the case of heavily infested plates. Discrete CFUs were considered to result from a single ascospore, and *S. sclerotiorum* detection was confirmed by formation of subsequent characteristic sclerotia after sub-culturing representative colonies.

In Wisconsin trials, seven or eight SSM plates were placed evenly across two perpendicular transects, oriented north to south and east to west. Spores were monitored twice a week in the trial that was also monitored for apothecial presence. To avoid disturbance of apothecia, plates were placed in non-yield rows during the time of exposure. In 2014, ascospore presence was monitored from 62 to 80 DAS, between the R4 and R5

growth stages. In 2015 and 2016, spores were monitored for six to seven weeks from the V4/5 to R5 growth stages.

Michigan. Ascospore presence was also monitored in Michigan trials from 2015 to 2016. The spore plates were used as previously described, however, in Michigan, spore plates were exposed between one and three hours. In 2015, ascospores were monitored in eight plots of the non-treated trial planted at a 0.76-m row spacing. One plate was placed in each of the eight plots and spores were monitored from 55 to 118 DAS. In 2016, ascospore observations were collected from eight spore plates placed in non-treated trials, four in the 0.76-m row spacing trial and four placed in the 0.38-m spacing trial. Spores were monitored from 51 to 70 DAS.

Descriptive and correlation analysis. All statistical analyses throughout this study were conducted in SAS v. 9.4 (SAS Institute, Cary, NC). Daily apothecial means for this study were estimated for each treatment using a mixed model analysis of variance in PROC GLIMMIX; treatment was used as the fixed effect and replicate was considered a random effect. A binary irrigation variable was generated based on the absence (0) or presence (1) of over-head irrigation during the season. A binary fungicide variable was generated based on the absence (0) or presence (1) of a fungicide application during the season.

Two and three years of apothecial observations from Michigan and Wisconsin (n = 557), respectively, were used with corresponding ascospore observations (n = 399) in correlation analyses. Ascospore numbers were correlated with apothecial numbers taken from the same trials on the same days of plate exposure. Daily means of apothecial counts and corresponding ascospore CFUs were estimated using a mixed model analysis of variance

in PROC GLIMMIX; the LSMEANS estimates for each day were used in correlation analyses. Kendall correlation coefficients were calculated using the PROC CORR procedure and by specifying the Kendall option for non-parametric analyses. Correlations were evaluated at the $\alpha = 0.05$ significance level. Simple linear regression models, using PROC REG, were fitted to the relationship between apothecia and ascospore counts.

Weather and agronomic variable selection. Numerical gridded weather data, at a 5-km resolution, were obtained through cooperation with the integrated pest information platform for extension and education (iPiPE) project (Isard et al. 2015). This platform uses high-resolution real-time mesoscale analysis (RTMA) data (Benjamin et al. 2007), supplied by the information technology company ZedX, Inc. (Bellefonte, PA); data were sourced from the National Oceanic and Atmospheric Administration National Centers for Environmental Prediction. Site-specific weather data were generated for each trial year and location using coordinates obtained from a global positioning system (Table 4.1). Hourly estimates of air temperature, relative humidity, dew point, wind speed, leaf wetness, and rainfall were obtained for each location. Two additional variables were created from the raw data to describe: 1) the duration of time (hours) for which relative humidity was ≥ 86% (RH86) and 2) the duration of time (hours) for which air temperature was ≥ 10°C and ≤ 25°C (ATD). The ATD thresholds were established based on the germination data provided by Clarkson et al. (2007). From the relative humidity range in Clarkson et al. (2014), on-site leaf wetness durations were used to determine the locally adjusted relative humidity threshold (data not shown) (Rowlandson et al. 2015).

Daily mean, minimum, maximum, and sum values of all variables were generated in SAS using the UNIVARIATE procedure. From the resulting daily predictor values, 30-, 40-, 50-, and 60-day moving averages (mean, min, max data) or sums (sum data) were generated by day and treatment (n = 444) (Clarkson et al. 2007). Moving averages or sums were calculated using the EXPAND procedure with MOVAVE or MOVSUM transformation options of 30, 40, 50, and 60. All moving average and moving sum variables were used as potential independent variables in the model building process.

Additionally, binary prediction variables were created for row, fungicide, and irrigation data and tested in the model. If data were collected in a plot with 0.36- or 0.38-m row spacing, then row was equal to 0; if collected in a plot with 0.76-m row spacing, then row was equal to 1. The fungicide variable was equal to 1 if any fungicide was applied in a plot or equal to 0 if no fungicide was applied. The irrigation variable was equal to 0 if plots were not overhead irrigated and to 1 if any overhead irrigation was used to supplement natural rainfall.

All gridded predictor variables, for each moving-average duration, and binary descriptors were used in Kendall correlation analyses with raw apothecial means using the PROC CORR procedure. Correlations were evaluated at the $\alpha = 0.05$ significance level. The best moving average duration was selected based on number and strength of predictor variables which were significantly correlated to mean apothecial counts. The selected moving average duration variables were used as independent variables in all modeling steps.

Subsequently, apothecial binary variables, defined based on thresholds of daily apothecial means, were used as potential response variables for the selected moving average

predictors. Nine thresholds were defined: 0.1, 0.2, 0.3, 0.4, 0.5, 0.6, 0.7, 0.8, and 0.9 apothecia per plot. For example, for the 0.1 threshold, 0 was assigned when the mean apothecia per plot was < 0.1 and 1 if the mean was ≥ 0.1. The best threshold was defined using the Kendall correlation analyses described previously and was used further as the dependent binary variable in the analysis.

On-site validation of gridded RTMA weather data. In Wisconsin in 2015 and 2016, on-site weather was monitored using a variety of sensors connected to a measurement datalogger for automatic data-acquisition (Campbell Scientific, Model CR1000). Air temperature and relative humidity (Vaisala T/RH probe, Model HMP155A, Campbell Scientific) were measured at 3 m above the soil to remain at least 2 m above the soybean canopy throughout the season. Rainfall (Texas Electronics Tipping Bucket Gauge, Model TE 525WS, Campbell Scientific) was monitored 1 m above the ground with the bucket positioned on the south side of the mounting post. Leaf wetness was measured above and below the canopy using two dielectric sensors (Decagon Devices, Model LWS-L, Campbell Scientific) positioned at a 45-degree angle, facing north, and at heights of 0.9 m and 5 cm above the soil, respectively. The below canopy sensor was placed in a soybean row to better mimic leaf wetness within the lower canopy. Soil moisture was also monitored using a volumetric water content reflectometer probe (Campbell Scientific, Model CS655) buried 10 cm below the soil surface and inserted horizontally into the soybean root zone. In 2016, a wind sentry sensor anemometer and vane (R.M. Young Wind Sentry, Model 3002, Campbell Scientific) was added to monitor wind speed and direction. The sentry was positioned 2.4 m above the soil surface and calibrated 2.73 ± 0.6 degrees to true north.

All sensors were connected to the datalogger, which was attached to a 10-ft tripod (Campbell Scientific, Model CM106B) constructed in border rows surrounding intensively monitored trials, in West-Madison and Arlington, WI (Table 4.1), where apothecia and ascospore presence was monitored. Measurements were taken every 5 min and averaged to calculate hourly surface and near-surface conditions. All sensors were located in the soybean field trial were positioned within or above the soybean canopy and situated less than 25 m from the tripod station. In 2015, data were collected between Jun 10 and Oct 07, or 28 to 147 DAS. In 2016, data were collected between Jun 10 and Oct 10, which was 23 to 145 DAS. In both years, weather data collection began prior to first detection of apothecia and continued from approximately the V1 (first trifoliate) to the R8 (full maturity) growth stage.

Campbell scientific weather station data were not used during model development. However, data were used to validate the accuracy of site-specific gridded RTMA data. Station data for air temperature, relative humidity, rainfall, leaf wetness (using the above canopy sensor), and wind speed (in 2016) were used with gridded weather data in correlations analyses in SAS. Bias coefficients were calculated from the mean difference (generated using PROC MEANS) between hourly on-site Campbell weather station data and gridded RTMA data; bias coefficient = hourly on-site data – hourly gridded data (Charney et al. 2013). Pearson correlation and Lin's concordance agreement analyses (Lin 1989) were also conducted using SAS code available through the Pennsylvania State University, Eberly College of Science (Lengerich 2017).

Logistic regression model development. In model development, weather variables of the selected moving average duration were used as independent variables, and the binary

apothecial variable from the selected threshold for apothecia presence was used as the dependent variable. A mixed model using PROC GLIMMIX in SAS was used to evaluate the effects of fungicide, row, irrigation, and their interactions on apothecial presence. Additionally, all variables were included in Kendall correlation analyses using PROC CORR with the Kendall option; correlations were used to measure the degree of association between apothecial presence and biologically significant moisture and temperature variables.

Due to unexpectedly weak relationships between apothecial presence and temperature variables, Kendall correlations were re-evaluated by the binary irrigation variable (0 or 1). Subsequently, models were fitted separately for irrigated and non-irrigated data. Correlations were evaluated at the $\alpha = 0.05$ significance level and significant variables with correlation coefficients typically > |0.2| were considered in logistic regression unless a variable was determined to be biologically important.

Logistic regressions were performed using the PROC LOGISTIC procedure with the descending option (to predict apothecia = 1). All possible predictor variables were included in initial analyses using stepwise, forward, backwards, and score selection methods. Variables with odds ratio point estimates of > 999.999 or < 0.001 were typically removed from subsequent analyses. Akaike's information criterion (AIC), percent concordant observations, and the area under the receiver operating characteristic (ROC) curve, or the c-statistic, were used to evaluate models of interest.

Models containing commonly selected biologically significant variables, across model selection methods, were evaluated for goodness of fit using the Hosmer-Lemeshow test in an additional LACKFIT analysis in PROC LOGISTIC (Allison 1999; Hosmer and

Lemeshow 2000). The max-rescaled R-square statistic (Allison 1999) was also considered in model selection. The classification table (Hosmer and Lemeshow 2000), using the CTABLE option, was also used to: 1) determine an appropriate apothecial probability action threshold (probability at which sensitivity and specificity converged), and 2) to evaluate potential models for percentages of correctness, sensitivity, specificity, false positives, and false negatives at the selected threshold.

Final models were evaluated for collinearity using a weighted regression procedure (Allison 1999) in PROC REG. Tolerance and variation inflation factors (VIFs) were evaluated to assess collinearity between variables using the TOL and VIF options, respectively. Collinear variables were determined at tolerance values < 0.40 and VIF values of > 3.0. Final model selection considered all described model selection criteria, to assess explanatory power, as well as model parsimony, to obtain the simplest set of model parameters.

Model validation datasets. Model validations were conducted using four datasets from Michigan and Wisconsin, which were not used to develop the model. In Wisconsin in 2014, additional apothecial observations were collected from an irrigated breeding germplasm SSR nursery located at the West Madison Agricultural Research Station (n = 525 plot observations). The trial consisted of five replicates of 35 soybean lines or cultivars (total of 175 small plots) planted on a 0.76-m row spacing. Observations were collected on three days, at the R3, R4, and R5 growth stages, in three 0.76- by 0.76-m squares per plot (total area of 1.73 m^2). In 2016, additional observations were collected from an irrigated germplasm nursery at the Hancock Agricultural Research Station (n = 168 plot observations)

and in a small, non-irrigated validation trial at the Arlington Agricultural Research Station (n = 400 plot observations). The irrigated trial contained six replicates of 14 lines or cultivars (total of 84 small plots) planted on a 0.76-m row spacing. Observations were collected on two days, at the R2 and R4/5 growth stages, using the same method as described previously. In the non-irrigated Arlington validation trial, five treatments were replicated five times (total of 25 small plots) and planted on a 0.76-m row spacing. Observations were collected on 16 days using the previously described method. Disease incidence observations were also collected near the end of the season, between R4 and R6. The number of diseased plants in the center two rows were counted and divided by the total number of plants in the stand to obtain disease incidence (%); mean disease incidence was calculated for each location. All three of the described trials were located either adjacent to, within the same fields, or within 2 km of the epidemiology trials where model building data were collected. Weather data used in validations, therefore, were taken from previously described data sets.

In Michigan in 2015, additional observations were obtained from an on-farm trial located in Ionia, MI (n = 9 daily observations). These observations were collected in the same location as the 2016 apothecia observations which were included for model building. In 2015, however, only apothecial presence (1) or absence (0) was noted on nine days between the R3 and R6 growth stages. No disease measurements were collected at this location, however, absence or presence of disease was noted. Including this dataset, a total of 1,102 plot observations were made and 30 observation days were considered in model validations. In irrigated trials, a total of five daily observations were collected. In non-irrigated trials, a total of 25 daily observations were used in validations.

Daily mean apothecial observations were compared to the predicted probabilities to evaluate model accuracy. If the daily model probability correctly predicted the presence of apothecia (at the established action threshold) above or below the disease control threshold of 3 to 4 apothecia per 9.75 m^2 (Pan et al. 2001), or a mean of 0.5-0.7 apothecia in the total 1.73-m^2 area scouted per plot, then the observation was determined a success (1); if incorrectly predicted, e.g. observed a mean of > 0.5 apothecia per plot and model prediction was less than the established action threshold, then the observation was determined a failure (0). The total number of successes observed out of the total number of observations was used to calculate the percentage of correct observations.

Results

Correlation analyses. Using the daily mean counts (n = 50), mean ascospore counts were strongly and positively associated with mean apothecial counts (r = 0.65, P < 0.0001) (Supp. Figure S4.1). Daily mean ascospore counts were found to increase by 24 for each additional mean apothecia observed. Three daily mean observations were found to be influential and were removed based on residuals greater than five standard deviations from the mean and Cook's distance values of greater than 0.6.

On-site validation of gridded weather data. Gridded weather data, derived for trial site based on site-specific GPS coordinates, were in agreement with on-site weather station data, but the level of agreement varied according to the weather variable (Table 4.2). Bias coefficients indicated gridded weather data typically overestimated average hourly on-site weather variables except for relative humidity which was underestimated. However, differences between gridded and on-site hourly averages were typically small (bias

coefficients of -0.005 to -0.752); relative humidity was estimated to differ by 3.6%. Gridded air temperature and relative humidity data were in higher agreement with on-site data – concordance correlation coefficients (ccc) > 0.90, compared to rainfall and wind speed – ccc > 0.70. The poorest agreement was found between estimated and on-site leaf wetness data – ccc = 0.47.

Selection of response variables. Moving average durations were evaluated for number and strength of predictor variables (n = 34) significantly correlated with apothecial means (Table 4.3). Apothecial means were determined to be most correlated with 30-day moving averages with 24 of 34, or 73% of, predictors having significant ($P < 0.05$) correlations. Additionally, of the significantly correlated variables, 18 of 34 (55%) had correlation coefficients > |0.10|. Therefore, 30-day moving average durations were used in all subsequent analyses as potential independent variables.

Various apothecial mean thresholds, used to generate a binary apothecial response variable, were evaluated in correlation analyses with the previously selected 30-day moving average predictor variables (n = 34) (Table 4.4). The chosen 30-day parameters were found to best describe the binary apothecial observations generated from a mean threshold of 0.3. The resulting apothecial binary variable was significantly ($P < 0.05$) correlated to 23 of 34, or 68% of, predictor variables. Furthermore, 50% of the correlated variables resulted in Kendall coefficients > |0.10|. The apothecial binary variable based on the 0.3 mean threshold best described the mean apothecial counts observed and was used in all subsequent analyses as the dependent variable.

Correlations between predictors and responses. Among the agronomic variables, only row spacing was determined to be a significant predictor ($P < 0.0001$). Row was therefore included as a class variable during model development. In preliminary analyses, Kendall correlations determined the apothecial presence to be negatively correlated with row width ($r = -0.25$, $P < 0.0001$) and fungicide application ($r = -0.10$, $P = 0.03$) and positively correlated with irrigation ($r = 0.15$, $P = 0.0009$). These were all expected effects of these predictors.

Additionally, Kendall correlations were used to identify gridded weather variables of interest for use in model development. As expected, apothecial presence was positively correlated with moisture variables such as the 30-day moving averages of daily mean relative humidity ($r = 0.12$, $P = 0.0016$) and leaf wetness ($r = 0.17$, $P < 0.0001$). Also, apothecial presence was found to be negatively correlated with the 30-day moving average of daily mean wind speed ($r = -0.14$, $P = 0.0008$), interpreted here as a measure of "dryness". The 30-day moving average of daily mean temperature, however, was only found to be very weakly, correlated (negatively) to apothecial presence ($r = -0.08$, $P = 0.05$). The weak correlations observed (coefficients < |0.2|) and the unexpectedly weak effect of temperature (a biologically significant variable) on apothecial presence prompted separate analysis of data obtained from irrigated and non-irrigated sites.

When data from irrigated and non-irrigated sites were analyzed separately, the variables of interest had stronger and more significant correlations, with coefficients generally > |0.2| and $P < 0.0001$. Strong differences in temperature effect between systems also became quite apparent (Table 4.5). For non-irrigated fields, apothecial presence was

positively correlated with the 30-day moving averages of the daily mean air temperature duration between 10 and 25°C ($r = 0.35$, $P < 0.0001$), mean leaf wetness ($r = 0.22$, $P < 0.0001$), and mean relative humidity ($r = 0.18$, $P < 0.0001$). Negative correlations were observed for 30-day moving average variables of maximum air temperature ($r = -0.30$, $P < 0.0001$) and maximum wind speed ($r = -0.27$, $P < 0.0001$). The row variable was not applicable for predicting apothecial presence under no irrigation as data were mostly collected in fields with 0.76-m row spacing.

For irrigated fields, apothecial presence was found to be highly correlated with row width ($r = -0.41$, $P < 0.0001$) and 30-day moving averages of daily mean air temperature ($r = 0.31$, $P < 0.0001$), maximum dew point ($r = 0.28$, $P < 0.0001$), maximum air temperature ($r = 0.27$, $P < 0.0001$), and maximum leaf wetness ($r = 0.26$, $P = 0.0006$). In both irrigated and non-irrigated cases, mean dew point and air temperature were positively correlated ($r = 0.60$, $P < 0.0001$); mean relative humidity and mean leaf wetness were also positively correlated ($r > 0.70$, $P < 0.0001$). In addition, mean air temperature duration, between 10 and 25ºC, was negatively correlated with mean air temperature ($r > -0.60$, $P < 0.0001$) and mean relative humidity ≥ 86% was positively correlated to mean relative humidity ($r \geq 0.70$, $P < 0.0001$).

Logistic regression model development and selection. Non-irrigated models tended to include relative humidity, air temperature, leaf wetness, and wind speed variables. Irrigated models tended to include row width, air temperature, leaf wetness, and dew point variables. Final model selection was conducted for combinations of one to four of these parameters with preference given to variables with strong correlations to apothecial presence (Table 4.6). Duration variables of optimal air temperatures, between 10 and 25ºC, and

relative humidity, ≥ 86%, were not used in final model selection due to atypical point estimates and 95% Wald's confidence limits. The 30-day moving averages of daily minimums and 30-day moving sums averages of daily sums were also not included in final models as other variables were more explanatory and biologically relevant. Additionally, highly correlated variables were not selected together as sole parameters in final models (data not shown).

Models were assessed using the predicted model accuracy (% correct), sensitivity, and specificity, as well as the tendency toward false positives and negatives. These percentages were determined from the PROC LOGISTIC classification table at the probability level of 0.40. Model sensitivity and specificity tended to converge at a probability between 0.45 and 0.47, but the lower 0.40 threshold was selected to reduce the percentages of predicted false negative errors. The 0.40 probability level was selected as a potential action threshold for model validation. Using this threshold, sites with model probabilities ≥ 0.40 would be predicted to have an elevated risk of detecting apothecia in fields with a history of SSR.

For non-irrigated fields, one of the most parsimonious, best-fitting models used the 30-day moving averages of daily maximum air temperature and wind speed to predict the probability of apothecial presence (Equation 4.1). The models containing only the 30-day moving average of daily maximum air temperature (Equation 4.2) or the 30-day moving averages of daily maximum air temperature, relative humidity, and wind speed (Equation 4.3) were also models of interest.

$$Logit\ (\mu) = -0.47(MaxAT_{30MA}) - 1.01(MaxWS_{30MA}) + 16.65 \quad (4.1)$$

$$Logit\ (\mu) = -0.68(MaxAT_{30MA}) + 17.19 \quad (4.2)$$

$$Logit\ (\mu) = -0.56(MaxAT_{30MA}) + 0.10(MaxRH_{30MA}) - 0.75(MaxWS_{30MA}) + 8.20 \quad (4.3)$$

These models possessed c-statistics between 0.7-0.8, indicating acceptable discrimination (Hosmer and Lemeshow 2000), greater than 62% model accuracy, greater than 67% sensitivity, and greater than 57% specificity. The Hosmer-Lemeshow test, however, indicated a weak fit for all models presented ($P < 0.05$). The two-variable model had a relatively high c-statistic (0.74), max-rescaled R^2 (0.2), and overall predicted model accuracy (65.7%). This model also correctly predicted both epidemics (72.5%) and non-epidemics (62.0%). Thus, the two-variable model (Equation 4.1) was selected for further model validations based on parsimony and fit. In this case, fit was defined as models that satisfied the majority of test statistics, forming a concensus, rather than passing a single test.

For irrigated fields, the model containing a row width variable and 30-day moving averages of maximum air temperature and relative humidity was one of the most parsimonious and best-fitting models (Equation 4.4). Other models of interest were those containing a row width variable and the 30-day moving averages of maximum air temperature and leaf wetness (Equation 4.5), or containing a row width variable and only the 30-day moving average maximum of air temperature (Equation 4.6). The row width variable was equal to 0 or 1 when the row spacing was 0.38 or 0.76 m, respectively.

$$Logit\ (\mu) = -2.38(Row) + 0.65(MaxAT_{30MA}) + 0.38(MaxRH_{30MA}) - 52.65 \quad (4.4)$$

$$Logit\ (\mu) = -2.39(Row) + 0.57(MaxAT_{30MA}) + 7.95(MaxLW_{30MA}) - 20.67 \quad (4.5)$$

$$Logit\ (\mu) = -2.34(Row) + 0.69(MaxAT_{30MA}) - 16.82 \quad (4.6)$$

These models possessed c-statistics indicating excellent discrimination, between 0.8-0.9 (Hosmer and Lemeshow 2000), greater than 0.35 max-rescaled R^2 values, and greater than 73% predicted model accuracies. The Hosmer-Lemeshow test, however, indicated potentially weak model fits for all models presented ($P < 0.05$). Both three variable models had c-statistics of 0.85, greater than 0.4 max-rescaled R^2 values, and relatively high predicted model accuracies (73-75%), sensitivities (81-84%), and specificities (64.5%). Based on strong accuracy of the weather variables selected, the model considering air temperature and relative humidity, along with row spacing, was selected for further model validation analyses (Equation 4.4).

Model evaluation. Four small datasets, a total of 30 mean daily observations, were used to validate the selected non-irrigated (Equation 4.1) and irrigated (Equation 4.4) models. For each validation site, the probability of apothecial presence was generated using the following calculation (Equation 4.7) with the appropriate model logit equation:

$$Probability = \frac{e^{logit(\mu)}}{(1+ e^{logit(\mu)})} \quad (4.7)$$

Using probability thresholds of 40% and 30%, the models successfully predicted the risk for 67 and 70% of the daily observations, respectively (Table 4.7). Furthermore, the models successfully predicted the risk in 82 and 91% of the daily observations between the R1 and R3 soybean growth stages at the respective 30 and 40% thresholds.

The model predictions during the R1 and R3 flowering growth stages were also able to explain the end of season disease incidence observed at three of the four validation sites (Figure 4.1). In 2016, the irrigated Hancock trial (Figure 4.1A) was predicted to have elevated risk, probability of apothecial presence > 40%, at the end of the R1 to R3 period. At this location, apothecia were confirmed during and after the flowering period and a mean disease incidence of 23.94% was observed. Conversely, very low risk (< 10%) was predicted during flowering in the 2014 irrigated West Madison trial (Figure 4.1B) and very low apothecial counts and disease incidence (0.04%) were observed. In 2016, very low levels of apothecia were observed in the non-irrigated Arlington trial (Figure 4.1C); risk during the flowering period was not predicted to be above 30%. At this location, and a mean observed disease incidence of 0.00% verified the low predicted risk. In 2015, the non-irrigated trial in Ionia, MI (Figure 4.1D) was predicted to have elevated risk (> 40%) from R1 to R3, apothecia were confirmed during this period, and disease was observed at this location (*data not shown*).

Discussion

Several models are presented here to accurately predict the risk of apothecial presence in irrigated and non-irrigated soybean fields using high-resolution gridded weather data. We have identified two of these models to be further evaluated to assist farmers with fungicide

application decisions. To our knowledge, these are the first reported weather-driven apothecial risk assessment models for use in SSR management of soybean. These models incorporate 30-day moving averages of maximum air temperature, relative humidity, and/or wind speed to predict the risk of apothecia in soybean fields. Model testing confirmed the models developed here accurately predicted apothecial presence during the flowering growth stages and explain the overall disease observed in all four locations.

The association between apothecial and ascospore counts found in our study agrees with previous studies in sunflower (McCartney and Lacey 1991). Apothecial observations were usually associated with overall disease intensity, but this is not consistent across studies (Foster et al. 2011; Schwartz and Steadman 1978) likely due to the probable aggregated distribution of inoculum (Boland and Hall 1988a, b). In the North Central region, short corn-soybean rotations are common and distribution of inoculum likely becomes more uniform with each subsequent epidemic. These models, therefore, are most appropriate for use in soybean fields with a prior history of SSR epidemics. Apothecia were, nonetheless, found to be useful to explain disease development during soybean flowering.

Gridded remote sensing data, whenever accurate, are the best choice for risk assessment at a field or farm resolution without the constraint of purchasing and maintaining on-site sensors for each location (Magarey et al. 2001). The accuracy of some of the gridded weather variables are a suitable surrogate for on-site weather data. Continuous variables, such as temperature and relative humidity, are typically easier to simulate as confirmed by the correlation results presented in Table 4.2. Discontinuous variables, such as precipitation and leaf wetness, are more difficult to simulate again apparent through correlation analyses

(Table 4.2). The minor biases or disagreements observed between on-site and gridded weather data, however, did not impact the development of the models presented here since only gridded data were considered in model building and two robust models were identified. Gridded weather data circumvents both the costly implementation of on-site weather stations and the possibility of on-site sensor failure or miscalibration, which would impede accurate model predictions (Magarey and Isard 2016). Using high-resolution gridded data, especially taking advantage of advances in the field, will facilitate the integration of these models into widely accessible algorithms, e.g. through the iPiPE (Isard et al. 2015), for dissemination and adoption into SSR management programs.

Logistic regression modeling was conducted separately for irrigated and non-irrigated fields to preserve biologically important relationships between apothecia, temperature, and moisture variables. The effect of air temperature on apothecial germination and disease development has been recently well documented in studies of Sclerotinia disease on lettuce (Clarkson et al. 2004, 2007, 2014). Historically, it was well established that *S. sclerotiorum* apothecia may form at low temperatures, between 10-25°C (Abawi and Grogan 1974; Bedi 1962; Coley-Smith and Cooke 1971; Willetts and Wong 1980). These findings support the negative effects of daily maximum air temperature on apothecial presence in non-irrigated fields, which was observed here. In irrigated fields, however, air temperature was found to be positively correlated with apothecial presence. Irrigation is expected to alter the canopy environment, and studies have shown that irrigated bean canopies exhibit cooler temperatures and prolonged leaf wetness (Blad, Steadman, and Weiss 1978). Additionally, irrigation also influences canopy structure by promoting fuller canopies which are also more favorable to

apothecial production (Schwartz and Steadman 1978). In irrigated fields, therefore, apothecial presence is likely promoted by the cooler temperatures within fuller canopies even though air temperatures are steadily increasing throughout the growing season. Warmer air temperatures in this scenario are believed to represent cooler canopy temperatures, which are favorable for apothecial development.

While soil moisture is readily recognized as important for apothecial production (Abawi and Grogan 1974; Clarkson et al. 2004, 2007; Foster et al. 2011; Morrall 1977; Sun and Yang 2000; Wu and Subbarao 2008), the effects of relative humidity and wind speed (a potential measure of "dryness") on carpogenic germination are less well studied. The findings of this study do, however, confirm the results of previous research on peanut, carrot, and lettuce reporting the positive effects of relative humidity on diseases caused by *Sclerotinia* spp. (Clarkson et al. 2014; Foster et al. 2011; Smith et al. 2007; Young et al. 2004). Relative humidity has also been shown to affect ascospore dispersal of *S. sclerotiorum* in canola canopies (Qandah and del Rio Mendoza 2012); and recently, changes in relative humidity have also been shown to affect *B. cinerea* conidia and *S. sclerotiorum* ascospore release in seed alfalfa fields (Reich et al. 2017). The observed negative effect of wind speed on apothecial presence also verifies findings in grape and lettuce of wind speed affecting conidial sporulation and lettuce drop incidence (Thomas et al. 1988; Wu and Subbarao 2006). Furthermore, air temperature, relative humidity, and wind speed are generally known to affect leaf surface moisture conditions which often promotes pathogen and disease development (Magarey et al. 2005; Huber and Gillespie 1992). Narrow row spacing was also confirmed to promote apothecial presence (Grau and Radke 1984; Jaccoud-Filho et al.

2016). Thus, the models presented here demonstrate the positive effects of high relative humidity and low wind speed, and narrow row spacing in irrigated fields, on apothecial presence. These variables are likely representative of increased moisture in the canopy microclimate which is favorable for apothecial development.

During model selection, most criteria indicate strong fit, discrimination, and accuracy of the selected irrigated and non-irrigated models. Goodness-of-fit was not supported by Hosmer-Lemeshow tests ($P < 0.05$), however, some evidence against the strength of this statistic are presented by Allison (1999). In this study, the consensus of statistical tests was evaluated for model fitness rather than using only a single test. The irrigated model statistics indicate a stronger fit and higher predictive power than the non-irrigated model, however, fewer daily mean apothecial observations were collected from irrigated fields (n = 158) than from non-irrigated fields (n = 286). The larger (non-irrigated) dataset, therefore, is expected to have more variability and would result in more challenging model fit. Despite the challenging model fits attributable to inherent variability between sites and years, these models possess acceptable or excellent discrimination as indicated by the area under the ROC (c = 0.7-0.9) as well as promising predicted accuracies (66-75%), sensitivities (73-84%), and specificities (62-65%).

Furthermore, both models performed successfully in model validations, with an 82-91% accuracy during the R1 to R3 flowering period, dependent on the established risk threshold. As a result, these models predicted periods of elevated risk during which fungicide applications could have been applied for targeted SSR control. At two validation sites where low disease was observed (< 0.04% DI), the models predicted no spray applications during

R1-R3 which would have resulted in a one to two spray savings compared to standard SSR management programs. At another validation site, where considerable disease was observed (24% DI), the model predicted elevated risk at the R3 growth stage, which would have indicated a single application of fungicide was appropriate at this location. In a standard two-spray fungicide program, this would have reduced management to a single application *and* would have effectively timed the fungicide treatment to target a critical elevated-risk event for improved SSR management. Additional field studies are required to further confirm these results.

Foster et al. (2011) presented evidence for using architectural and phenological initiation parameters, such as canopy closure, in SSR prediction models for carrot systems. In soybean, SSR development is known to be dependent on canopy closure, to promote a favorable environment for apothecial germination, as well as soybean flowering, to provide a nutrient source for infectious ascospores (Boland and Hall 1988a; Grau and Hartman 2015; Peltier et al. 2012; Saharan and Mehta 2008; Schwartz and Steadman 1978). In soybean, we plan to integrate the models presented here into a risk assessment algorithm which also considers canopy closure and soybean flowering. This algorithm will be deployed as a mobile- or web-accessible tool for users to assist in making SSR management decisions. Ultimately, site-specific model probabilities would be generated and management recommendations would be contingent on soybean flowering (R1-R3) and canopy development using row closure thresholds (M.L. Fall, *personal communication*). These models are currently available to authorized extension personnel via iPiPE for development and evaluation of these algorithms.

The model is currently limited by the number and size of validation datasets, as well as the absence of well-tested action threshold. In the future, however, additional multi-state and year model validations will be conducted using versions of the described algorithm. Model performance will be evaluated in irrigated and non-irrigated soybean fields with intensive monitoring of apothecial presence and subsequent disease development. Furthermore, validations will be used to determine appropriate probability action thresholds for a variety of scenarios. Common fungicide programs and regional cultivar resistance are also important considerations in the development of the proposed risk assessment tool.

Overall, extensive apothecial observations from nine site-years and subsequent logistic regression analyses resulted in the identification of novel models which accurately predict apothecial presence, in irrigated and non-irrigated soybean fields, using high-resolution gridded weather data. Validated models will be integrated into an algorithm considering soybean phenology and canopy architecture to provide risk assessment information for incorporation into integrated SSR management programs.

Literature Cited

Abawi, G. S., and Grogan, R. G. 1974. Source of primary inoculum and effects of temperature and moisture on infection of beans by *Whetzelinia sclerotiorum*. Phytopathology. 65:300–309.

Allen, T. W., Bradley, C. A., Sisson, A.J., Byamukama, E., Chilvers, M. I., Coker, C. M., Collins, A.A., Damicone, J.P., Dorrance, A.E., Dufault, N.S., Esker, P.D., Faske, T.R., Grybauskas, A.P., Hershman, D.E., Hollier, C.A., Hollier, C.A., Isakeit, T., Jardine, D.J., Kelly, H.M., Kemerait, R.C., Kleczewski, N.M., Koenning, S.R., Kurle, J.E., Malvick, D.K., Markell, S.G., Mehl, H.L., Mueller, D.S., Mueller, J.D., Mulrooney, R.P., Nelson, B.D., Newman, M.A., Osborne, L., Overstreet, C., Padgett, G.B., Phipps, P.M., Price, P.P., Sikora, E.J., Smith, D.L., Spurlock, T.N., Tande, C.A., Tenuta, A.U., Wise, K.A., and Wrather, J.A. 2017. Soybean yield loss estimates due to diseases in the United States and Ontario, Canada from 2010 to 2014. Plant Heal. Prog. 18(1):19-27.

Allison, P. D. 1999. *Logistic regression using the SAS system: Theory and application*. Cary,

NC: SAS Institute Inc.

Bedi, K. S. 1962. Temperature in relation to the formation of apothecia of *Sclerotinia sclerotiorum* (Lib.) de Bary. Proc. Indian Acad. Sci. 55:244–250.

Benjamin, S., Brown, J., and Manikin, G. 2007. The RTMA background – hourly downscaling of RUC data to 5-km detail. 23rd Conf. IIPS. :1–4.

Blad, B. L., Steadman, J. R., and Weiss, A. 1978. Canopy structure and irrigation influence white mold disease and microclimate of dry edible beans. Phytopathology. 68:1431–1437.

Boland, G. J., and Hall, R. 1988a. Epidemiology of Sclerotinia stem rot of soybean in Ontario. Phytopathology. 78:1241.

Boland, G. J., and Hall, R. 1994. Index of plant hosts of *Sclerotinia sclerotiorum*. Can. J. Plant Pathol. 16:93–108.

Boland, G. J., and Hall, R. 1988b. Relationships between the spatial pattern and number of apothecia of *Sclerotinia sclerotiorum* and stem rot of soybean. Plant Pathol. 37:329–336.

Bradley, C. A., Allen, T., and Esker, P. D. 2016. Estimates of soybean yield reductions caused by diseases in the United States. Univ. Illinois - Dep. Crop Sci. Ext. Outreach. http://extension.cropsciences.illinois.edu/fieldcrops/diseases/yield_reductions.php.

Charney, J. J., Service, U. F., and Kiefer, M. T. 2013. An investigation of the differences between Real Time Mesoscale Analysis and observed meteorological conditions at RAWS stations in the northeast United States. JFSP Res. Proj. Reports.

Clarkson, J. P., Fawcett, L., Anthony, S. G., and Young, C. 2014. A model for *Sclerotinia sclerotiorum* infection and disease development in lettuce, based on the effects of temperature, relative humidity and ascospore density. PLoS One. 9:e94049.

Clarkson, J. P., Phelps, K., Whipps, J. M., Young, C. S., Smith, J. A., and Watling, M. 2007. Forecasting Sclerotinia disease on lettuce: a predictive model for carpogenic germination of *Sclerotinia sclerotiorum* sclerotia. Phytopathology. 97:621–31.

Clarkson, J. P., Phelps, K., Whipps, J. M., Young, C. S., Smith, J. A., and Watling, M. 2004. Forecasting sclerotinia disease on lettuce: toward developing a prediction model for carpogenic germination of sclerotia. Phytopathology. 94:268–79.

Coley-Smith, J., and Cooke, R. 1971. Survival and germination of fungal sclerotia. Annu. Rev. Phytopathol. :65–92.

Fehr, W. R., Caviness, C. E., Burmood, D. T., and Pennington, J. S. 1971. Stage of development descriptions for soybeans, *Glycine max* (L.) Merill. Crop Sci. 11:929–931.

Foster, A. J., Kora, C., McDonald, M. R., and Boland, G. J. 2011. Development and validation of a disease forecast model for Sclerotinia rot of carrot. Can. J. Plant Pathol. 33:187–201.

Grau, C. R., and Hartman, G. L. 2015. *Compendium of soybean diseases*. 5th ed. eds. G.L.

Hartman, J.C. Rupe, E.J. Sikora, L.L. Domier, J.A. Davis, and K.L. Steffey. St Paul, MN: The American Phytopathological Society.

Grau, C., and Radke, V. 1984. Effects of cultivar and cultural practices on Sclerotinia stem rot of soybean. Plant Dis. 68:56–58.

Grau, C., Radke, V., and Gillespie, F. 1982. Resistance of soybean cultivars to *Sclerotinia sclerotiorum*. Plant Dis. 66:506–508.

Harikrishnan, R., and del Río, L. E. 2008. A logistic regression model for predicting risk of white mold incidence on dry bean in North Dakota. Plant Dis. 92:42–46.

Hosmer, D. W., and Lemeshow, S. 2000. *Applied logistic regression*. Second. John Wiley and Sons.

Huber, L., and Gillespie, T. J. 1992. Modeling leaf wetness in relation to plant disease epidemiology. Annu. Rev. Phytopathol. :553–577.

Isard, S. A., Russo, J. M., Magarey, R. D., Golod, J., and Vankirk, J. R. 2015. Integrated pest information platform for extension and education (iPiPE): progress through sharing. J. Integr. Pest Manag. 6:1–8.

Jaccoud-Filho, D., Fadel Sartori, F., Manosso-Neto, M., Maurício Vrisman, C., da Cunha Pierre, M. L., Berger-Neto, A., et al. 2016. Influence of row spacing and plant population density on management of " white mould " in soybean in southern Brazil. Aust. J. Crop Sci. 10:161–168.

Kohn, L. M. 1979. A monographic revision of the genus Sclerotinia. Mycotaxon. 9:365–444.

Lengerich, R. 2017. Concordance correlation coefficient for measuring agreement. In Statistics 509: Design and Analysis of Clinical Trials. Online publication. The Pennsylvania State University, Eberly College of Science. https://onlinecourses.science.psu.edu/stat509/sites/onlinecourses.science.psu.edu.stat509/files/lesson18/19.2_agreement_concordanc.sas.

Lin, L. I. 1989. A concordance correlation coefficient to evaluate reproducibility. Biometrics. 45:255–268.

Magarey, R. D., and Isard, S. A. 2016. A troubleshooting guide for mechanistic plant pest forecast models. J. Integr. Pest Manag. :1–7.

Magarey, R. D., Seem, R. C., Weiss, A., Gillespie, T., and Huber, L. 2005. Estimating surface wetness on plants. Agron. Hortic. - Fac. Publ. :199–226.

Magarey, R., Seem, R., Russo, J., Zack, J., Waight, K., Travis, J., et al. 2001. Site-specific weather information without on-site sensors. Plant Dis. 85:1216–1226.

McCartney, H. A., and Lacey, M. E. 1991. The relationship between the release of ascospores of *Sclerotinia sclerotiorum*, infection and disease in sunflower plots in the United Kingdom. Grana. 30:486–492.

Mila, A. L., Carriquiry, A. L., and Yang, X. B. 2004. Logistic regression modeling of prevalence of soybean Sclerotinia stem rot in the north-central region of the United States. Phytopathology. 94:102–110.

Morrall, R. A. A. 1977. A preliminary study of the influence of water potential on sclerotium germination in *Sclerotinia sclerotiorum*. Can. J. Bot. 55:8–11.

Mueller, D. S., Bradley, C. A., Grau, C. R., Gaska, J. M., Kurle, J. E., and Pedersen, W. L. 2004. Application of thiophanate-methyl at different host growth stages for management of Sclerotinia stem rot in soybean. Crop Prot. 23:983–988.

Pan, H., Xi, J., Liu, W., Wan, Q., and Li, H. 2001. Optimal stage and threshold of the control of Sclerotinia rot. Acta Phytophylacica Sin. 28:299–302.

Peltier, A. J., Bradley, C. A., Chilvers, M. I., Malvick, D. K., Mueller, D. S., Wise, K. A., et al. 2012. Biology, yield loss and control of Sclerotinia stem rot of soybean. J. Integr. Pest Manag. 3:1–7.

Qandah, I. S., and del Rio Mendoza, L. E. 2012. Modelling inoculum dispersal and Sclerotinia stem rot gradients in canola fields. Can. J. Plant Pathol. 34:390–400.

Reich, J., Chatterton, S., and Johnson, D. 2017. Temporal dynamics of *Botrytis cinerea* and *Sclerotinia sclerotiorum* in seed alfalfa fields of Southern Alberta, Canada. Plant Dis. 101:331–343.

Rowlandson, T., Gleason, M., Sentelhas, P., Gillespie, T., Thomas, C., and Hornbuckle, B. 2015. Reconsidering leaf wetness duration determination for plant disease management. Plant Dis. 99:310–319.

Saharan, G. S., and Mehta, N. 2008. Sclerotinia *diseases of crop plants: biology, ecology and disease management*. Netherlands: Springer Science & Business Media B.V.

Schwartz, H. F., and Steadman, J. R. 1978. Factors affecting sclerotium populations of, and apothecium production by, *Sclerotinia sclerotiorum*. Phytopathology. 68:383.

Smith, D. L., Hollowell, J. E., Isleib, T. G., and Shew, B. B. 2007. A site-specific, weather-based disease regression model for Sclerotinia blight of peanut. Plant Dis. 91:1436–1444.

Steadman, J. R., Marcinkowska, J., and Rutledge, S. 1994. A semi-selective medium for isolation of *Sclerotinia sclerotiorum*. Can. J. Plant Pathol. :68–70.

Sun, P., and Yang, X. B. 2000. Light, temperature, and moisture effects on apothecium production of *Sclerotinia sclerotiorum*. Plant Dis. 84:1287–1293.

Thomas, C., Marois, J., and English, J. 1988. Effects of wind speed, air temperature, and relative humidity on development of aerial mycelium and conidia of *Botrytis cinerea* on grape. Phytopathology. 78:260–265.

Twengstrom, E., Sigvald, R., Svensson, C., and Yuen, J. 1998. Forecasting Sclerotinia stem rot in spring sown oilseed rape. Crop Prot. 17:405–411.

United States Department of Agriculture - National Agricultural Statistics Service (USDA-NASS). 2017. United States soybean prices. USDA-NASS:Washington, DC.

Wegulo, S. N., Sun, P., Martinson, C. a., and Yang, X. B. 2000. Spread of Sclerotinia stem rot of soybean from area and point sources of apothecial inoculum. Can. J. Plant Sci. 80:389–402.

Willetts, H. J., and Wong, J. A.-L. 1980. The biology of *Sclerotinia sclerotiorum*, *S. trifoliorum*, and *S. minor* with emphasis on specific nomenclature. Bot. Rev. 36:101–165.

Wrather, A., Shannon, G., Balardin, R., Carregal, L., Escobar, R., Gupta, G., et al. 2010. Effect of diseases on soybean yield in the top eight producing countries in 2006. Plant Heal. Prog.

Wu, B. M., and Subbarao, K. V. 2006. Analyses of lettuce drop incidence and population structure of *Sclerotinia sclerotiorum* and *S. minor*. Phytopathology. 96:1322–9.

Wu, B. M., and Subbarao, K. V. 2008. Effects of soil temperature, moisture, and burial depths on carpogenic germination of *Sclerotinia sclerotiorum* and *S. minor*. Phytopathology. 98:1144–1152.

Young, C. S., Clarkson, J. P., Smith, J. a., Watling, M., Phelps, K., and Whipps, J. M. 2004. Environmental conditions influencing *Sclerotinia sclerotiorum* infection and disease development in lettuce. Plant Pathol. 53:387–397.

Tables and Figures

Table 4.1. Years and locations of apothecial data collection with corresponding GPS coordinates (used to obtain high-resolution, site-specific downscaled gridded RTMA weather data), irrigation specification (IR), row spacing designation (Row), number of observations (*N*), cultivar information, and soil properties.

Year, State	Location	GPS Coordinates	IR	Row (m)	*N*	Cultivar	FP[a]	Soil Type[a]	Slope (%)	Content (%)			
										OM[c]	Clay	Sand	Silt
2014													
WI	West Madison	43.0637, -89.5335	-	0.76	560	BSR-101 (S); 91-145 (R)	11	Kegonsa silt loam	2-6	1.0	13.4	50.2	36.5
2015													
MI	Montcalm	43.3525, -85.1788	+	0.76, 0.36	720	AG2535	14	Tekenink-Elmdale loamy sands	2-6	0.3	9.9	69.4	20.7
WI	West Madison	43.0692, -89.5424	-	0.76	400	AG2031	20	Plano silt loam, gravelly substratum	0-2	1.4	20.9	33.3	45.8
2016													
IA	Manilla	41.8495, -95.1751	-	0.76	72	P25T51R	14	Judson-Ackmore-Colo, overwash complex	1-5	2.1	29.2	5.5	65.3
IA	Nashua	42.9382, -92.5696	-	0.76	84	P24T93R	14	Clyde silty clay loam	0-3	2.2	25.0	32.4	42.6
MI	Ionia	43.0222, -84.9974	-	0.38	120	P92Y91R	14	Marlette loam	0-6	0.5	21.6	44.3	34.1
MI	Montcalm	43.3525, -85.1788	+	0.76, 0.38	560	AG2535	17	Tekenink-Elmdale loamy sands	2-6	0.3	9.9	69.4	20.7
WI	Arlington	43.3191, -89.3312	-	0.76	1,125	AG2031	13	Joy silt loam	0-4	1.3	20.5	10.1	69.4
WI	Hancock	44.1132, -89.5463	+	0.76	225	AG2031	15	Plainfield sand	0-2	0.3	2.4	94.9	2.7

[a]Approximate flowering period (FP) in days.
[b]Soil types and properties at the GPS coordinates provided, according to the National Cooperative Soil Survey, available through the web soil survey tool, and operated by the United States Department of Agriculture, Natural Resources Conservation Service.
[c]Organic matter.

Table 4.2. Bias, Pearson and concordance coefficients with corresponding standard deviations (SD) or 95% confidence intervals (CI) for correlation analyses of gridded real-time mesoscale analysis (RTMA) data and on-site Campbell Scientific weather station data.

Weather variable	Bias[a]	Pearson Correlation		Concordance Correlation	
	Coefficient ± SD	Coefficient, *r*	95% CI	Coefficient, r_c	95% CI
Air temperature	-0.752 ± 0.691	0.99	(0.990, 0.991)	0.98	(0.978, 0.979)
Relative humidity	3.658 ± 4.715	0.96	(0.956, 0.961)	0.93	(0.924, 0.931)
Rainfall	-0.035 ± 0.738	0.83	(0.820, 0.838)	0.83	(0.817, 0.836)
Leaf wetness	-0.005 ± 0.510[b]	0.47	(0.444, 0.489)	0.47	(0.444, 0.489)
Wind speed	-0.735 ± 0.845	0.84	(0.832, 0.854)	0.74	(0.722, 0.752)

[a]Bias coefficients were calculated from the mean difference between hourly on-site Campbell weather station data and gridded RTMA data; bias coefficient = on-site data – gridded data.
[b]Leaf wetness data was collected as binary data, and recorded as 1 if wetness was observed during the hour, and 0 if no wetness was observed. A bias coefficient close to 0 would indicate good agreement between observed and gridded leaf wetness data.

Table 4.3. Number of significant predictor variables (n=33 total) for each moving average duration correlated to apothecial means.

Criteria	**Number of correlated variables for each moving average duration**			
	30-day	**40-day**	**50-day**	**60-day**
$p < 0.05$[a]	24	22	20	23
coefficient > |0.1|	18	16	15	13

[a]Significance was determined at $\alpha=0.05$.

Table 4.4. Number of significant 30-day moving average variables (n=33 total) correlated to apothecial binary response variables established at various thresholds.

Criteria	**Number of correlated predictor variables for each apothecial binary threshold**[a]									
	0.1	**0.2**	**0.3**	**0.4**	**0.5**	**0.6**	**0.7**	**0.8**	**0.9**	**1.0**
$p < 0.05$[b]	21	18	23	18	19	15	17	14	17	17
coefficient > |0.1|	14	12	17	16	15	10	11	11	10	10

[a]Binary apothecial observations were generated for each designated mean threshold.
[b]Significance was determined at $\alpha=0.05$.

Table 4.5. Weather or agronomic parameters significantly correlated to the apothecial binary variable in irrigated (1) and non-irrigated (0) fields, generated using a 0.3 apothecia per treatment mean threshold, with correlation coefficients typically > |0.2|

Irrig.	Variable	Parameter description[a]	CC[b]	*p*-value[c]
0	MA_MinATD	30-day average of daily minimum ATD, ≥10°C and ≤25°C	0.35	<0.0001
0	MA_MeanATD	30-day average of daily mean ATD, ≥10°C and ≤25°C	0.35	<0.0001
0	MA_MaxAT	30-day average of daily maximum AT	-0.30	<0.0001
0	MS_SumATD	30-day sum of daily sum ATD, ≥10°C and ≤25°C	0.29	<0.0001
0	MS_SumAT	30-day sum of daily sum AT	-0.28	<0.0001
0	MA_MeanAT	30-day average of daily mean AT	-0.28	<0.0001
0	MA_MaxWS	30-day average of daily maximum WS	-0.27	<0.0001
0	MA_MinRH86	30-day average of daily minimum RH ≥86°C	-0.26	<0.0001
0	MA_MeanLW	30-day average of daily mean LW	0.22	<0.0001
0	MA_MinRH	30-day average of daily minimum RH	0.22	<0.0001
0	MA_MeanWS	30-day average of daily mean WS	-0.19	0.0002
0	MA_MeanRH	30-day average of daily mean RH	0.18	0.0002
0	MA_MaxDP	30-day average of daily maximum DP	-0.15	0.0027
0	MA_MaxRH	30-day average of daily maximum RH	0.13	0.0070
1	Row	Binary variable, 0=0.36- or 0.38-m row spacing and 1=0.76-m row spacing	-0.41	<0.0001
1	MA_MinLW	30-day average of daily minimum LW	-0.31	<0.0001
1	MS_SumAT	30-day sum of daily sum AT	0.31	<0.0001
1	MA_MeanAT	30-day average of daily mean AT	0.31	<0.0001
1	MA_MinAT	30-day average of daily minimum AT	0.29	<0.0001
1	MA_MaxDP	30-day average of daily maximum DP	0.28	<0.0001
1	MA_MinATD	30-day average of daily minimum ATD, ≥10°C and ≤25°C	-0.28	0.0001
1	MS_SumDP	30-day sum of daily sum DP	0.27	<0.0001
1	MA_MaxAT	30-day average of daily maximum AT	0.27	<0.0001
1	MA_MaxLW	30-day average of daily maximum LW	0.26	0.0006
1	MA_MinDP	30-day average of daily minimum DP	0.25	0.0002
1	MA_MaxRH86	30-day average of daily maximum RH ≥86°C	0.24	0.0021
1	MA_MeanATD	30-day average of daily mean ATD, ≥10°C and ≤25°C	-0.23	0.0021
1	MS_SumATD	30-day sum of daily sum ATD, ≥10°C and ≤25°C	-0.21	0.0015
1	MA_MinRH86	30-day average of daily minimum RH ≥86°C	-0.21	0.0097
1	MA_MaxRH	30-day average of daily maximum RH	0.16	0.0180

[a]Abbreviations: air temperature (AT), air temperature duration (ATD), dew point (DP), leaf wetness (LW), relative humidity (RH), relative humidity duration (RH86), wind speed (WS).
[b]Correlation coefficient.
[c]Significance was determined at α=0.05.

Table 4.6. Model selection parameters for final irrigated (1) or non-irrigated (0) models of interest, containing one to four predictors of 30-day moving average weather variables and/or an agronomic row spacing variable (row1)[a].

Variables[b]	IR	Con (%)	AIC	c	R^2	Corr (%)	Sens (%)	Spec (%)	FPos (%)	FNeg (%)
MaxAT[cd]	**0**	**70.5**	**342.08**	**0.72**	**0.16**	**75.2**	**67.6**	**79.3**	**35.5**	**18.4**
MaxAT, MaxWS	**0**	**73.6**	**334.45**	**0.74**	**0.19**	**65.7**	**72.5**	**62.0**	**48.6**	**19.7**
MaxAT, MaxLW	0	72.1	322.12	0.72	0.19	69.6	72.5	67.9	44.4	18.3
MaxAT, MaxRH, MaxWS	**0**	**75.4**	**336.72**	**0.76**	**0.20**	**62.6**	**72.5**	**57.1**	**51.6**	**21.1**
MaxAT, MeanRH, MeanWS	0	74.9	326.40	0.75	0.24	62.9	66.7	60.9	51.4	23.3
MaxAT, MaxRH, MaxLW	0	74.2	320.19	0.75	0.26	67.1	59.8	71.2	46.5	23.8
MaxAT, MeanRH, MaxWS	0	74.1	332.71	0.75	0.21	64.7	72.5	60.3	49.7	20.1
MaxAT, MeanRH, MaxLW	0	73.2	323.18	0.74	0.25	70.3	72.5	69.0	43.5	18.1
MaxAT, MeanRH, MeanLW	0	73.0	335.0	0.74	0.20	65.4	67.6	64.1	48.9	21.9
MeanAT, MeanRH, MeanWS	0	70.0	339.83	0.70	0.18	61.9	52.9	66.8	53.0	28.1
MeanAT, MeanRH, MeanLW	0	68.5	346.09	0.69	0.16	65.0	67.6	63.6	49.3	22.0
Row1, MeanAT	1	83.9	165.78	0.85	0.42	75.9	85.4	65.8	27.1	19.4
Row1, MaxAT	**1**	**83.5**	**169.84**	**0.84**	**0.39**	**76.6**	**87.8**	**64.5**	**27.3**	**16.9**
Row1, MaxAT, MaxLW	**1**	**84.8**	**165.18**	**0.85**	**0.43**	**74.7**	**84.1**	**64.5**	**28.1**	**21.0**
Row1, MeanAT, MaxRH	1	84.8	166.02	0.85	0.43	74.1	84.1	63.2	28.9	21.3
Row1, MeanRH, MeanDP	1	84.6	164.80	0.85	0.43	73.4	82.9	63.2	29.2	22.6
Row1, MeanRH, MaxDP	1	84.5	164.46	0.85	0.44	71.5	82.9	59.2	31.3	23.7
Row1, MaxAT, MaxRH	**1**	**84.3**	**166.60**	**0.85**	**0.42**	**73.4**	**81.7**	**64.5**	**28.7**	**23.4**
Row1, MeanAT, MaxLW	1	84.3	164.87	0.85	0.43	72.2	80.5	63.2	29.8	25.0
Row1, MeanAT, MeanLW	1	83.9	167.73	0.84	0.42	75.3	84.1	65.8	27.4	20.6
Row1, MaxRH, MaxDP	1	83.7	170.12	0.84	0.40	71.5	80.5	61.8	30.5	25.4
Row1, MaxRH, MeanDP	1	82.7	172.64	0.83	0.39	70.3	79.3	60.5	31.6	27.0
Row1, MeanAT, MeanRH, MeanLW	1	86.3	162.44	0.87	0.46	74.7	84.1	64.5	28.1	21.0
Row1, MaxAT, MeanRH, MeanLW	1	86.1	163.98	0.86	0.45	76.6	87.8	64.5	27.3	16.9
Row1, MaxAT, MaxRH, MaxDP	1	85.3	167.37	0.86	0.43	71.5	81.7	60.5	30.9	24.6
Row1, MaxAT, MaxRH, MaxLW	1	84.9	167.14	0.85	0.43	74.7	84.1	64.5	28.1	21.0
Row1, MaxAT, MeanRH, MaxLW	1	84.9	167.17	0.85	0.43	74.7	84.1	64.5	28.1	21.0
Row1, MeanAT, MeanRH, MaxDP	1	84.9	166.32	0.85	0.44	74.1	86.6	60.5	29.7	19.3
Row1, MeanAT, MaxRH, MaxDP	1	84.7	167.67	0.85	0.43	72.2	84.1	59.2	31.0	22.4
Row1, MaxAT, MeanRH, MaxDP	1	84.7	166.45	0.85	0.44	70.3	82.9	56.6	32.7	24.6
Row1, MaxAT, MeanRH, MeanDP	1	84.7	166.76	0.85	0.43	72.8	82.9	61.8	29.9	23.0
Row1, MeanAT, MeanRH, MeanDP	1	84.6	162.62	0.85	0.46	72.8	80.5	64.5	29.0	

[a]Abbreviations: IR = irrigation, Con = concordant, AIC = Akaike's information criterion for intercept and covariates, c = c statistic (area under the receiver operating characteristic curve), and R^2 = maximum rescaled R^2. Percents correct (Corr), sensitivity (Sens), specificity (Spec), false positives (FPos), and false negatives (FNeg) determined at a probability threshold of 0.40.
[b]Maximum (max) and mean air temperature (AT), dew point (DP), leaf wetness (LW), relative humidity (RH), wind speed (WS). Models of interest, indicated in bold, were determined to be some of the most parsimonious and best-fitting; model equations are included in the results section.

Table 4.7. Model validation results from two irrigated and two non-irrigated trials in Wisconsin and Michigan, 2014-2016[a].

									Success or failure[b]	
Year	**State**	**Location**	**IR**	**Row (m)**	**Prob (0-1)[c]**	**Obs[d]**	**GS**	**DI (%)[e]**	**Pr 0.40**	**Pr 0.30**
2015	MI	Ionia	0	0.38	0.57	1	R3	1	1	1
2015	MI	Ionia	0	0.38	0.45	1	R3	1	1	1
2015	MI	Ionia	0	0.38	0.48	1	R4	1	1	1
2015	MI	Ionia	0	0.38	0.41	1	R4	1	1	1
2015	MI	Ionia	0	0.38	0.32	1	R5	1	0	1
2015	MI	Ionia	0	0.38	0.14	1	R5	1	0	0
2015	MI	Ionia	0	0.38	0.15	1	R5	1	0	0
2015	MI	Ionia	0	0.38	0.13	1	R5-R6	1	0	0
2015	MI	Ionia	0	0.38	0.12	0	R5-R6	1	1	1
2016	WI	Arlington	0	0.76	0.19	0.00	V5	0.00	1	1
2016	WI	Arlington	0	0.76	0.19	0.00	V5/6	0.00	1	1
2016	WI	Arlington	0	0.76	0.21	0.00	V6	0.00	1	1
2016	WI	Arlington	0	0.76	0.26	0.00	R1	0.00	1	1
2016	WI	Arlington	0	0.76	0.20	0.00	R1	0.00	1	1
2016	WI	Arlington	0	0.76	0.19	0.32	R2	0.00	1	1
2016	WI	Arlington	0	0.76	0.21	0.04	R2	0.00	1	1
2016	WI	Arlington	0	0.76	0.17	0.00	R3	0.00	1	1
2016	WI	Arlington	0	0.76	0.17	0.08	R3	0.00	1	1
2016	WI	Arlington	0	0.76	0.16	1.84	R3	0.00	0	0
2016	WI	Arlington	0	0.76	0.14	1.28	R4	0.00	0	0
2016	WI	Arlington	0	0.76	0.13	1.44	R5	0.00	0	0
2016	WI	Arlington	0	0.76	0.16	1.60	R5	0.00	0	0
2016	WI	Arlington	0	0.76	0.20	0.84	R5	0.00	0	0
2016	WI	Arlington	0	0.76	0.30	0.04	R5	0.00	1	0
2016	WI	Arlington	0	0.76	0.39	0.84	R6	0.00	1	1
2014	WI	West Madison	1	0.76	0.03	0.00	R3	0.04	1	1
2014	WI	West Madison	1	0.76	0.02	0.23	R4	0.04	1	1
2014	WI	West Madison	1	0.76	0.03	0.34	R5	0.04	1	1
2016	WI	Hancock	1	0.76	0.38	2.26	R2	23.94	0	1
2016	WI	Hancock	1	0.76	0.68	3.26	R4/5	23.94	1	1

[a]Model accuracy determined using the daily model probabilities and corresponding daily apothecial observations.
Abbreviations: IR = irrigation, Row = row spacing, and GS = growth stage.

[b]Model success or failure determined by comparing daily model probabilities, using either a 0.40 or 0.30 risk threshold (Pr 0.40 or 0.30, respectively), with corresponding daily apothecial observations. If model probabilities corresponded to the daily apothecial observations, then a success (1) was recorded; if model probabilities did not correspond to daily apothecial observations, then a failure (0) was recorded. Percent correct = 67 and 70% for Pr 0.40 or Pr 0.30, respectively and percent correct at R1 to R3 growth stages = 82 to 91% for Pr 0.40 and 0.30, respectively.

[c]Daily probability of apothecial presence calculated using the selected models for irrigated (Logit (μ) = -2.38*Row + 0.65*MaxAT + 0.38*MaxRH – 52.65, where row = 1 if 0.76-m row spacing or 0 if 0.38-m row spacing) and non-irrigated (Logit (μ) = -0.47*MaxAT – 1.01*MaxWS + 16.65) fields; probability = (e^logit(μ)/[1+ e^logit(μ)].

[d]Daily apothecial presence observed (presence = 1 or absence = 0). Apothecial means were evaluated for presence or absence at the mean disease control threshold of 0.5-0.7 apothecia observed per a 1.73-m^2 area, or the total area scouted per plot.

[e]Average end of season disease incidence was calculated from the total number of diseased plants in the two center rows of each plot divided by the total number of plants in the two center rows, as determined by stand counts, and multiplied by 100 to obtain a percentage.

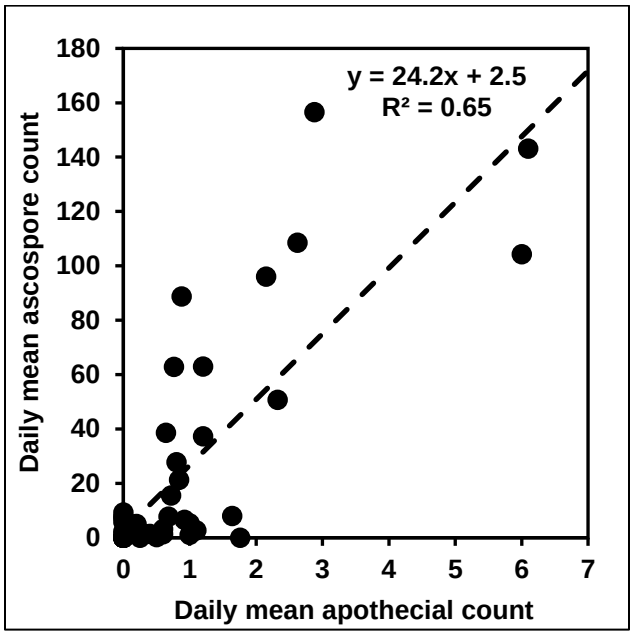

Supplementary Figure S4.1. Correlation between daily mean ascospore counts and corresponding daily mean apothecial counts taken from Michigan (2 years) and Wisconsin (3 years) (total n = 50). Daily means were generate from apothecial (n = 557) and ascospore (n = 399) observations collected in epidemiology trial plots. Observations were typically conducted beginning prior to soybean flowering and continued until either complete apothecial senescence or soybean maturity. Daily mean ascospores observed were highly correlated to daily mean apothecial presence (r = 0.65, P < 0.0001).

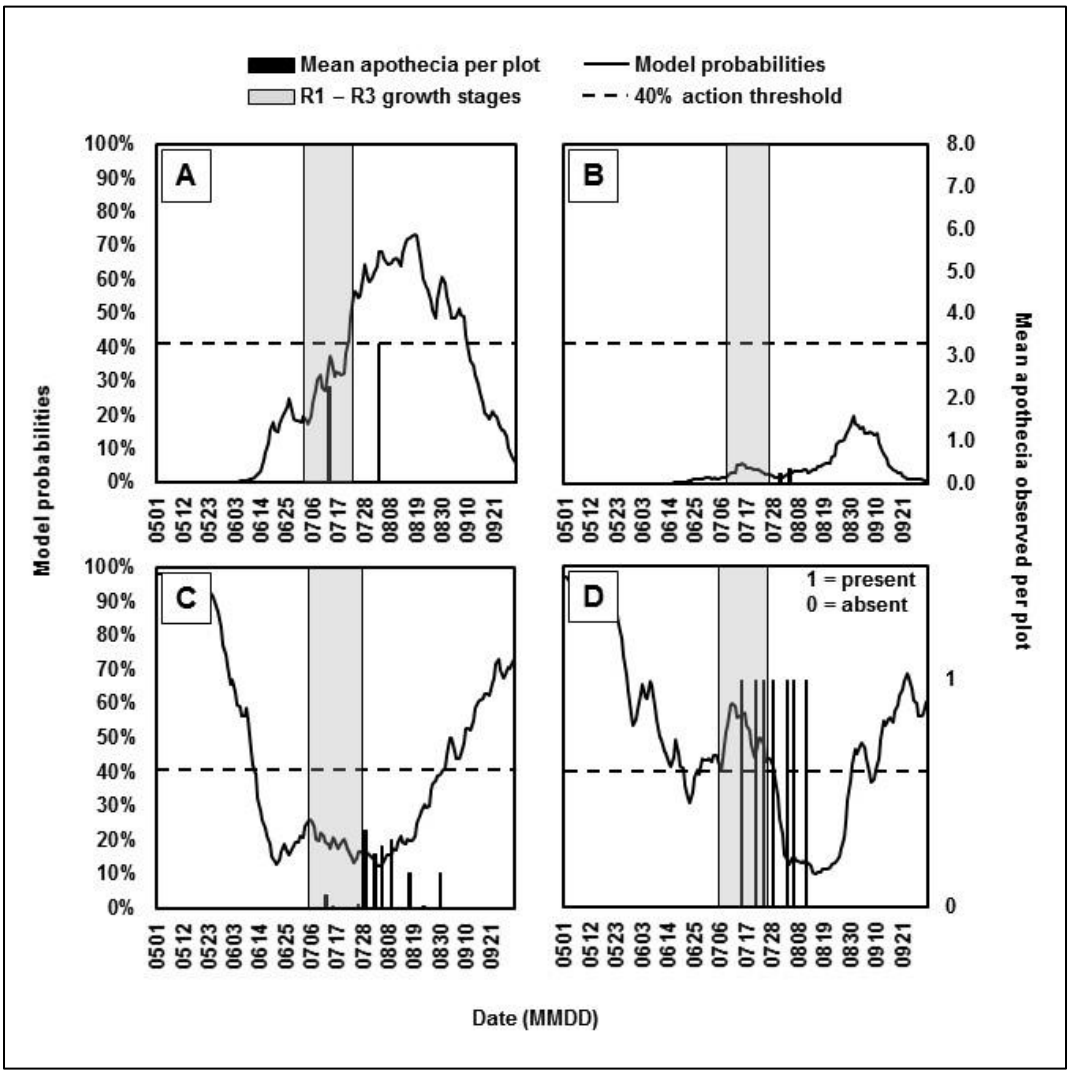

Figure 4.1. Model validations for irrigated trials in **A,** Hancock, WI 2016 and **B,** West Madison, WI 2014; and non-irrigated trials in **C,** Arlington, WI 2016 and **D,** Ionia, MI 2015. The solid line shows probabilities of apothecial presence which were calculated between May 01 and Oct 01 using the selected models for irrigated (Logit (μ) = -2.38*Row + 0.65*MaxAT + 0.38*MaxRH – 52.65, where row = 1 if 0.76-m row spacing or 0 if 0.38-m row spacing) and non-irrigated (Logit (μ) = -0.47*MaxAT - 1.01*MaxWS + 16.65) fields; probability = (e^logit(μ)/[1+ e^logit(μ)]. Solid bars in A, B, and C indicate daily apothecial

means per plot, in a total scouted area of 1.73 m^2; in D, bars indicate apothecial presence (1) or absence (0). The gray box represents the R1 to R3 flowering period. The dotted line represents the preliminary action threshold of 40% probability. SSR incidence of 0.04% was observed at location B and 0.00% at location C. At location A, 23.94% incidence was observed; at location D, incidence data were not collected, however, SSR was present.

CHAPTER 5: Validation of weather-based models for assessing the apothecial presence of *Sclerotinia sclerotiorum* in soybean (*Glycine max*) fields

Abstract

Sclerotinia stem rot (SSR), caused by *Sclerotinia sclerotiorum*, is one of the most destructive diseases of soybean crops. In soybean, *S. sclerotiorum* apothecia are the sources of primary inoculum (ascospores) critical for SSR development. Recently, logistic regression models were developed to predict the presence of apothecia in irrigated and non-irrigated soybean fields. The purpose of these studies was to validate two weather-based models (one for irrigated fields and one for non-irrigated fields) to elucidate the infection risk window and action thresholds for fungicide application for effective SSR management. In 2017, efficacy trials were conducted at agricultural research stations in Iowa, Michigan, and Wisconsin (n = 242 plot-level observations) to identify fungicide programs and thresholds for model implementation. Additionally, apothecial scouting (n = 1,007 apothecial observations) and disease monitoring (n = 1,129 SSR observations) were conducted in a total of 60 commercial grower fields in Michigan, Nebraska, and Wisconsin between 2016 and 2017 to evaluate model accuracy across the growing region. Site-specific air temperature, relative humidity, and wind speed data were obtained through the integrated pest information platform (iPiPE) and Dark Sky weather networks. Across all irrigated and non-irrigated locations, iPiPE-driven model predictions during the soybean flowering period (R1 to R4 growth stages) were found to explain end-of-season disease observations with an accuracy of 81.8% using a risk action-threshold of 35%. Dark Sky data, incorporating bias corrections for weather variables, were found to predict apothecial risk with an 87.9% accuracy (in 2017 commercial locations

in Wisconsin) using a 40% risk-threshold. Overall, these validations indicate these two weather-based apothecial models provide risk predictions, which both reduce unnecessary chemical application and accurately advise applications at critical times. Additionally, an alternative site-specific source of weather data (Dark Sky) was identified to enable further development of useful model tools for farmers.

Introduction

Soybean [*Glycine max* (L.) Merr.] is one of the most economically important hosts impacted by Sclerotinia stem rot (SSR) (Peltier et al. 2012). Sclerotinia stem rot (SSR), caused by *Sclerotinia sclerotiorum*, continues to rank in the top ten most destructive diseases of global soybean crops (Allen et al. 2017; Wrather et al. 2010). The development of *S. sclerotiorum* is favored by cool, moist conditions (Grau and Hartman 2015). In the North Central United States, these climatic conditions, combined with high yield soybean growing practices cause SSR to be particularly persistent and problematic in this region.

Apothecia that arise from soilborne sclerotia are the primary source of inoculum in soybean, producing wind-borne ascospores which infect soybean flowers (Saharan and Mehta 2008). The simultaneous presence of apothecia during both soybean flowering and weather conditions favorable for infection and disease development, is critical for SSR later in the growing season. Predictive models and risk algorithms are often used to assess the risk of SSR development, by considering these host-pathogen-environment factors, and to help growers make management decisions (Clarkson et al. 2014; Foster et al. 2011; Harikrishnan and del Río 2008; Smith et al. 2007; Twengstrom et al. 1998). We previously described weather-based models to predict apothecial development in soybean fields (Willbur et al.

2017). These models were subject to preliminary validations during development; however, further validation across a larger geography is needed to determine their accuracy.

Model validation is important to provide growers with reliable management tools. Validation may include testing the models or algorithms at additional research and commercial sites over a larger growing area and outside of the locations where the model was developed (Foster et al. 2011). Other validations may investigate other aspects of risk algorithms such as the host susceptibility window, inoculum pressure, model cut-off probabilities or action thresholds (Bondalapati and Stein 2010; Foster et al. 2011). Crowd-sourcing data over a wide region, through personal and social media communications, could be a powerful source of information for validations. Data from a variety of locations help to ensure the models will work over the wide range of growing conditions and practices present in a region.

Additionally, for models to be adopted and implemented by growers, the tools used to deliver these predictions should be easily accessible to farmers. While site-specific data is readily available (Magarey et al. 2001), the risk algorithms often consider many factors which may complicate the delivery and use of these tools. Successful web-based systems have been developed for other diseases, such as late blight in potato (Wharton et al. 2008). Ultimately, these models would be most useful to farmers if they could be repeatedly accessed at site-specific field locations over the entire growing season. Based on these predictions, farmers could then make “real-time” management decisions which are not impeded by reliance of information released through researchers or cooperative extension personnel.

The objectives of this research were 1) to validate two weather-based apothecial prediction models throughout the North Central soybean growing region in both research and commercial fields, 2) to evaluate fungicide programs as a part of model implementation, 3) to identify the host susceptibility period for incorporation into the model algorithm, and 4) to determine appropriate action thresholds (i.e. when to apply fungicide sprays) for incorporation of these models in an effective integrated management system.

Materials and Methods

Research trials used for model validations.

Iowa. In 2017, two validation trials were monitored by researchers at Iowa State University near Manilla, IA and Nashua, IA (Table 5.1). In each location, an SSR susceptible soybean variety, Pioneer 25T51R (Pioneer 2017), was planted on 13 May at 370,000 seeds ha^{-1}. The plots were 3.0 m wide by 5.3 m long and contained four rows planted at a 0.76-m row spacing. These trials were used to evaluate 11 different fungicide treatments: boscalid (Endura®, BASF, Research Triangle Park, NC) applied at R1 (beginning flower), 7 days after R1, 14 days after R1, or 21 days after R1; picoxystrobin (Aproach®, DuPont, Wilmington, DE) applied at R1, 7 days after R1, 14 days after R1, or at R1 and 14 days after R1; lactofen (Cobra®, Valent U.S.A., Walnut Creek, CA) applied at V5 or at V5 followed by picoxystrobin applied at R1; and a non-treated check (Table 5.2). These treatments were replicated four times and arranged in a randomized complete block design (RCBD) at each location, for a total of 88 plots. These trials were non-irrigated and only natural inoculum was relied upon for infection by *S. sclerotiorum*. The flowering period was approximately 14 days for all research trials in Iowa, Michigan, and Wisconsin.

Michigan. In 2017, model validation was conducted by researchers at Michigan State University in trials at the Montcalm Research Center in Montcalm, MI (Table 5.1). Soybeans were planted at two row spacings, 0.76 and 0.38 m, on 19 May and 22 May, respectively. The moderately SSR-tolerant soybean variety Asgrow 2535 (Monsanto 2017) was planted at a population of 400,000 plants ha^{-1}. Plots were 6.1 m long and 2.3 m wide at the 0.38-m row spacing and 5.3 m long and 3.0 m wide at the 0.76-m row spacing. Eleven fungicide and timing treatments, similar to those tested in Iowa, were evaluated at both row spacings (Table 5.2). These treatments were replicated five times and arranged in a randomized complete block design (RCBD) at each row spacing, for a total of 110 plots.

Four additional site areas were used for apothecial monitoring. Within each row spacing, two sampling sites were designated, and four plots were constructed within each site (for a total of 16 plots, 8 at each row spacing). The plots were the same size as the Michigan research trial plots previously mentioned (0.38-m row spacing: 6.1 x 2.3 m and 0.76-m spacing: 5.3 x 3.0 m). The variety AG2535 was planted in all the plots at the 0.38-m spacing. The plots at 0.76-m spacing were planted with two different susceptible soybean varieties. No fungicide treatments were applied to these areas. These trials were irrigated and relied on natural inoculum.

Wisconsin. In 2017, research trials used for model validations were conducted by researchers at University of Wisconsin-Madison agricultural research stations (ARS) in Arlington and Hancock, WI (Table 5.1). Trials were planted using a 0.76-m row spacing at a population density of 350,000 plants ha^{-1}. The soybean variety AG2031, which has shown

greenhouse susceptibility and moderate field resistance (*data not shown*), was planted in four-row plots that were 3.0 m wide by 6.1 m long.

In Arlington, the trial was planted on 30 May and used to evaluate seven fungicide treatments (Table 5.2) including a non-treated control as well as boscalid (Endura®) and picoxystrobin (Aproach ®) treatments applied using plant physiology or using the newly developed models to schedule fungicide applications. The treatments were replicated four times and arranged in an RCBD (for a total of 28 plots). The trial was non-irrigated and only natural levels of inoculum were used for *S. sclerotiorum* infection.

In Hancock, the trial was planted on 25 May and used to evaluate four fungicide treatments (Table 5.2) including a non-treated control and three different treatments of picoxystrobin applied at either phenology- or model-based timings. These treatments were evaluated in an RCBD with four replications (for a total of 16 plots). This trial was irrigated to promote SSR development. Soybean trials were in areas previously planted with sunflowers, which had been inoculated to increase available inoculum load in the soil.

Apothecial data collection from research trials.

Iowa. Apothecia were counted in 0.76-m by 0.76-m squares placed in three arbitrary locations of each non-treated check plot (four plots per trial). In Manilla, apothecial scouting was conducted on five days, 06 June, 11 July, 17 July, 24 July, and 31 July, which began prior to R1 and continued through the R3 (beginning pod) growth stage. In Nashua, scouting was conducted on two days, 25 July and 03 August, which began 14 days after R1 and continued through the R3 growth stage. Number of apothecia observed in each square was

recorded for each non-treated plot for a total of 60 observations in Manilla and 24 observations in Nashua (n = 84 total Iowa observations).

Michigan. Within each apothecial monitoring plot (not in fungicide validation trial), observations were recorded in four arbitrarily selected 0.74-m by 0.74-m squares. In 0.38-m row spacing plots data were collected between the third and fifth row. At 0.76-m row spacing, the data were collected between the center rows (second and third). Thirteen days of observations were collected from apothecial monitoring plots, and numbers of apothecia were recorded for each sampling of the four locations in each of the 16 plots. Observations were collected every 3-6 days beginning 20 July and continuing to 01 September (n = 832 total Michigan observations).

Wisconsin. Apothecia were counted in three 0.76-m by 0.76-m squares in the center two rows of each plot. Weekly scouting was conducted on four days between the R1 and R4 (full pod) growth stages. In Arlington, scouting was conducted on 12 July, 18 July, 27 July, and 03 August. The Hancock trial was scouted on 13 July, 19 July, 26 July, and 03 August. In Arlington, a total of 336 sample observations were recorded; in Hancock, a total of 192 sample observations were recorded (n = 528 total Wisconsin observations).

Disease and yield data collection from research trials.

Iowa. SSR incidence and/or severity was evaluated at the R6 (full seed) growth stage. Disease incidence (DI) was determined by recording the number of symptomatic plants out of 30 arbitrarily selected plants in the center two rows of each plot and converting to a percentage. Disease severity (DS) was determined by rating these 30 plants on a 0-3 scale where, 0 = no disease, 1 = disease only on the petioles or secondary stems, 2 = disease on but

not girdling the main stem, and 3 = disease girdling the main stem resulting in plant wilt or death (Grau et al. 1982). Severity ratings of symptomatic plants were averaged, divided by 3, and multiplied by the percent DI to obtain the disease severity index (DIX) value.

Yield data was collected using a small-plot combine to harvest the center two rows of each plot. Trials were harvested on 09 October and 18 October in Nashua and Manilla, respectively. Yield data was adjusted to 13% moisture and a test weight of 60 lbs bushel^{-1} to convert data from bushels acre^{-1} (bu a^{-1}) to kilograms hectare^{-1} (kg ha^{-1}). DI or DIX values and yield data were used to evaluate fungicide treatment efficacy. DI values were also used in site-specific validations of model predictions over the entire season.

Michigan. SSR incidence and severity were evaluated in the fungicide validation trials on 19 September (not in the apothecial monitoring sites). DI was determined by recording the number of symptomatic plants out of 40 arbitrarily selected plants in the center two rows of each plot and converting to a percentage. DS was determined by rating these 40 plants on the previously described 0-3 scale. Severity ratings of symptomatic plants were averaged, divided by 3, and multiplied by the percent DI to obtain the disease severity index (DIX) value. Yield data was collected from the center two or four rows (dependent on row spacing) of each plot on 20 October. DIX values and yield data were used to evaluate fungicide treatment efficacy. DI values were used in site-specific validations of model predictions.

Wisconsin. SSR incidence, severity, and DIX data were collected at R6 or R7 (beginning maturity). Severity data was collected according to the protocols previously described. The true DI was collected by counting the total number of symptomatic plants in

the center two row and converting to a percentage of the total stand count. The DIX was calculated as previously described using the true DI and average DS of symptomatic plants. Yield was collected in the center two rows of each plot, adjusted to 13% moisture. DIX and yield were used to evaluate the various fungicide treatments and the mean DI of the non-treated plots was used in full-season model validations.

Commercial fields used for model validations, 2016.

Wisconsin. In 2016, 22 commercial fields were scouted for apothecia and monitored for disease development. Fields were located throughout the state. Apothecial scouting occurred between the R1-R4 growth stages between 14 July and 01 August. Observations were made in 10 to 30 sites, at intervals of 50 to 100 paces (or approximately 38-76 m) dependent on the size of the field, using a W or Z sampling pattern. At each sampling site, a 0.76-m by 0.76-m square area was scouted for apothecia. Number of apothecia per sampling square was recorded and converted to binary presence or absence data for each site. Soybean variety, row width, irrigation, canopy closure, SSR history, typical crop rotation, and fungicide applications were noted at the time of the visit (Table 5.3). A total of 397 individual site observations were collected in Wisconsin.

Follow-up visits were conducted between the R5-R7 growth stages between 08 August and 14 September. Observations were made at 10 to 21 sites, at intervals of 38 to 76 m, using a W or Z sampling pattern. At each site within a field, a 1.0-m length in each of two rows (for a total of 2.0 m) was rated for DI (total symptomatic plants) and DS (30 plants per site were rated using the previously described scale). The DI and DS scores were used to calculate the DIX; the field DI and DIX values were averaged for each field location. The

total number of plants in the 2.0-m stand was also recorded for 2-4 sites within the field to estimate the total population of plants ha^{-1}. A total of 343 disease observations were made in Wisconsin.

Commercial fields used for model validations, 2017.

Michigan. In 2017, three additional commercial fields were used in model validations. The location, variety, row width, irrigation, SSR history, R1 and estimated R3 date were recorded for each field location (Table 5.3). SSR incidence was estimated for these fields, however, no individual site data within the field was collected and no apothecial scouting was conducted.

Nebraska. Two commercial fields were scouted for apothecia and disease in 2017 (Table 5.3). Observations were collected in 20 sites throughout the field, at intervals of 50-100 paces (or 38-76 m) dependent on the size of the field, using a W or Z sampling pattern. SSR ratings were collected on either 24 August in Scribner or 29 August in the Ord location. The ratings were taken as previously described in a 1.0-m length of row in two rows and incidence and severity data were collected. Data were used to calculate the average field DI and DIX, which were used in model validations. Typically, the soybean cultivar, row spacing, irrigation, SSR history, crop rotation, fungicide applications, and estimated R1 and R3 dates were recorded for both locations (Table 5.3).

Wisconsin. In 2017, 32 commercial fields were monitored for apothecial and SSR development. Again, fields were representative of the entire soybean growing region. Apothecial scouting occurred between the R1-R4 growth stages between 13 July and 03 August. Observations were made in 20 to 23 sites, typically at intervals of 100 paces (or 76

m) dependent on the size of the field, using the previously described pattern. Once again, a 0.76-m by 0.76-m square area was scouted for apothecia at each sampling site. Data were collected as in 2016 (Table 5.3). A total of 608 apothecial observations were recorded in Wisconsin grower fields.

Follow-up visits were conducted during the R5-R7 growth stages between 18 August and 12 September. Observations were collected at 20 to 24 sites, at intervals of 76 m, using a W or Z sampling pattern. At each site within a field, a 1.0-m length in each of two rows (for a total of 2.0 m) was again rated for DI and DS. The field DI, DIX, and population were recorded for each field location and used in model validations. A total of 633 disease observations were made in grower fields in 2017.

iPiPE weather-based risk predictions. Through cooperation with the integrated pest information platform for extension and education (iPiPE) project, gridded weather data at a 5-km resolution were obtained for each research and commercial validation site (Isard et al. 2015). The high-resolution real-time mesoscale analysis (RTMA) data (Benjamin et al. 2007) were supplied by ZedX, Inc. (Bellefonte, PA). Data were sourced from the National Oceanic and Atmospheric Administration National Centers for Environmental Prediction. As in Willbur et al. (2017), site-specific weather data were generated for each site using GPS coordinates (Table 5.3). Hourly estimates of air temperature (AT), relative humidity (RH), and wind speed (WS) were used to generate daily maximum values; daily maximums were then used to calculate 30-day moving averages of maximum AT, RH, and WS ($MaxAT_{30MA}$, $MaxRH_{30MA}$, or $MaxWS_{30MA}$). Moving averages were used in previously developed logistic regression models, either the non-irrigated model:

$$Logit\ (\mu) = -0.47(MaxAT_{30MA}) - 1.01(MaxWS_{30MA}) + 16.65 \quad (5.1)$$

or the irrigated model:

$$Logit\ (\mu) = -2.38(Row) + 0.65(MaxAT_{30MA}) + 0.38(MaxRH_{30MA}) - 52.65 \quad (5.2)$$

where the row width variable was equal to 0 or 1 when the row spacing was 0.38 or 0.76 m, respectively (Willbur et al. 2017). For each validation site, the probability of apothecial presence was generated using the following calculation with the appropriate model logit equation:

$$Probability = \frac{e^{logit(\mu)}}{(1 + e^{logit(\mu)})} \quad (5.3)$$

Validation of model accuracy in research trials. The accuracy of the apothecial probability models presented in equations 5.1 and 5.2 was evaluated at all research locations. At each site, a binary DI variable was constructed, DI5 and DI10 (DI-thresholds of 5 and 10%). If the mean DI in the non-treated plots was ≥ 5%, then DI5 was 1. If the mean DI was < 5%, then DI5 was 0. Likewise, the DI10 variable was set to 1 if the mean DI in the non-treated plots was ≥ 10% and 0 if < 10%. For each site, the probability of apothecial presence (calculated in equation 5.3) was monitored throughout the growing season at risk-thresholds of 30, 35, and 40%. If the probability was greater than the risk-threshold during the R1 to R3 period, then the site was given a 1 to indicate risk was present. If the calculated probability was less than the risk-threshold during this flowering period, then the site was assigned a 0 to indicate risk was low. If there was agreement between disease observations and risk observations (during the flowering period) then a model success (1) was recorded. If there

was disagreement between these observations, then a model failure (0) was recorded. Model accuracy was calculated as the percentage of successes out of the total number of site observations, and was calculated for all risk-thresholds (30, 35, and 40%) using both DI5 and DI10 observations. Type 1 (over prediction) or 2 (under prediction) errors were also recorded for each model failure. Six research trial sites, where disease observations were recorded, were used to validate apothecial model accuracy.

Validation of model accuracy in commercial fields. For each field, the binary DI variables DI5 and DI10 were generated. Risk-thresholds of 30, 35, and 40% were again used to determine the risk (1 or 0) during the R1 to R3 period. Agreement between model observations and end-of-season SSR observations were used to determine if the model at a site was a success (1) or failure (0). Model accuracy, or the percentage of successes out of the total number of sites, was calculated for all risk-thresholds (30, 35, and 40%) using both DI5 and DI10 thresholds. Once again, type 1 (over prediction) or 2 (under prediction) errors were recorded for each model failure. Accuracy was evaluated at 22 commercial sites in 2016 and 38 sites in 2017.

Dark Sky weather-based risk predictions. Hyperlocal hourly weather data for AT, RH, and WS were also obtained using the Dark Sky weather data network (Dark Sky Company, Cambridge, MA), accessible through darksky.net. These data were used to generate 30-day moving average of weather variables. Moving averages were used in equations 5.1-5.3 to generate apothecial risk probabilities. These weather data were compared to high-resolution RTMA weather data (sourced from iPiPE) from UW-Madison research sites at the West Madison ARS in 2015, the Arlington ARS 2016 and 2017, and the

Hancock ARS in 2017 (Willbur et al. 2017). These data were also used in correlation analyses with on-site data collected using a Campbell Scientific (Logan, Utah) weather station and sensors (Willbur et al. 2017). The weather station and sensors described in Willbur et al. (2017) were used at the 2017 Arlington site (Table 5.1) and replicated at the 2017 Hancock site (Table 5.1). As an additional test of Dark Sky weather data accuracy, data (corrected with the identified biases) were also used to validate apothecial model accuracy in 33 Wisconsin commercial sites.

Statistical analysis. All statistical analyses were conducted in SAS v 9.4 (SAS Institute, Cary, NC). Efficacy evaluations of fungicides and timings were analyzed using an analysis of variance (ANOVA) in a generalized linear mixed model (GLIMMIX) procedure. Response variables DI, DIX, and yield were evaluated using treatment as a fixed effect. The normal distribution was used, and confirmed using diagnostic plots, and the Kenward-Roger degrees of freedom approximation was used. Replicate (rep) or block was considered a random effect in all efficacy evaluations. Differences between treatment means were evaluated using Fisher's least significant different at the $\alpha = 0.05$ significance level. If the treatment effect was significant, then all pair-wise comparisons were considered using the 'mult' macro (Piepho 2004).

Comparisons of hourly Dark Sky, iPiPE, and on-site weather data were conducted using the Pearson correlation analyses with the CORR procedure. Bias coefficients were calculated from the mean difference (generated using PROC MEANS) between hourly RTMA data or on-site Campbell weather station data and Dark Sky data; bias coefficient = hourly Dark Sky RTMA or on-site data – hourly Dark Sky data (Charney et al. 2013). These

bias coefficients were used to correct Dark Sky data for further model validations (Dark Sky moving average + Bias + SD). As in Willbur et al. (2017), Lin's concordance analyses (Lin 1989) were conducted using code available through the Pennsylvania State University, Eberly College of Science (Lengerich 2017).

Results

Evaluation of fungicide efficacy and timing for model validation. In Iowa in 2017, no significant differences ($P > 0.05$) between treatments were detected for DI, DIX, or yield in Manilla (Table 5.4) or Nashua (Table 5.5) trials. The apothecial risk during the R1 to R4 period was correspondingly low (< 10%) for non-irrigated fields (Fig. 5.1A-B).

The trials in Montcalm, Michigan (Table 5.6) differences were detected between yield ($P < 0.001$) and DIX ($P < 0.05$) at row spacings of 0.76-m and 0.38-m, respectively. At the 0.76-m row width, the non-treated plots resulted in a yield of 3,284.4 kg ha^{-1} and applications of Endura at R2, R3, and R4 or Aproach at R3 resulted in the highest yields (3,750.8-4,412.5 kg ha^{-1}) despite high DI. In the trial at 0.38-m row spacing, the non-treated plots had 70.3% DIX and all Endura applications or Aproach applied at R3 resulted in the lowest DIX (43.3-62.2%). The corresponding model probabilities for Montcalm (Figure 1C) indicated risk in irrigated 0.38-m fields was > 30% between R1 and R4. Risk in irrigated 0.76-m fields was > 5% at R1 and reached 10% near R2.

No significant differences between true DI, DIX, or yield of different treatments ($P > 0.05$) were detected at trials in Arlington (Table 5.7) or Hancock (Table 5.8). The non-irrigated Arlington validation site had low levels of disease (2.0% DI and 1.5% DIX in non-treated plots). While not significantly different, Endura treatments resulted in lower DI and

DIX and higher yields than those of the non-treated control or Aproach treatments. At this non-irrigated site, slightly lower disease levels and higher yields were achieved using a 15% risk-threshold, however, neither were significantly different from not treating. In Hancock trials, DI in the non-treated plots was 17.7% and yield was 3,099.3 kg ha^{-1} (Table 5.8). Again, while not significant, treatments applied at a risk-threshold of 15% resulted in lower DI and DIX than those applied at a 30% threshold. No notable trends were observed in yield of different treatments at Hancock. The model probabilities for the non-irrigated Arlington site (Fig. 5.1D) indicated low apothecial risk (<20%) during the R1 to R3 period; the predicted risk at the irrigated Hancock site (Fig. 5.1E) indicated apothecial risk was greater than 25% near the R3 growth stage.

Validation of apothecial model accuracy in research and commercial fields. Apothecia were observed in five of the six research trials used to validate model accuracy (Table 5.9). Three sites had SSR above the DI-thresholds previously established above (5 and 10%) and three sites had low SSR levels, below the DI-thresholds. For all three risk-thresholds, 30, 35, and 40%, as many as five out of six research sites were recorded as model successes. Model failure was typically due to type 2 error, or failure of the model to predict risk where disease was present.

In commercial fields, apothecia were only detected in two of the fields in 2016 (Table 5.10). No apothecia were detected in 2017 grower-fields. Mean disease observations ranged from 0.0 to 40.2% in 2016 and 0.0 to 80% (the maximum was based on a single visual field estimate) in 2017. In 2016, 18 successes were recorded using a disease-threshold of 10% and a risk-threshold for action of 35%. In 2017, 31 successes were recorded using the DI10

threshold and risk-thresholds of 35 or 40%. Both type 1 and 2 errors were observed; however, the majority of the errors were due to model underprediction (type 2 error).

In 2017 research trials, model predictions during soybean flowering accurately explained end-of-season SSR in 83.3% of examined cases, using all risk- and disease-thresholds (Table 5.11). In commercial fields, models accurately explained SSR levels in 81.7% of cases examined using a 10% disease-threshold and 35% risk-threshold for action. Using a 5% disease-threshold and the risk-threshold of 35% models accurately predicted SSR in 76.7% commercial field cases. Across all years and locations (commercial and research), apothecial models accurately predicted SSR in 81.8% of the cases examined, when using the 10% DI-threshold and 35% risk-threshold for action. Using a 40% action threshold resulted in accurately predicting SSR 78.8% of the time. Using a 5% DI-threshold and 35% risk-threshold for action resulted in models predicting SSR 77.3% of the time across all locations.

Correlations between Dark Sky, on-site, and RTMA weather data. Dark Sky weather data was strongly correlated with both on-site and gridded RTMA data (Table 5.12). For air temperature and relative humidity, Pearson (r) and concordance (r_c) coefficients were ≥ 0.91 compared with on-site data and ≥ 0.97 compared with RTMA data (used to develop the apothecial models). For wind speed, r was 0.85 or 0.87 when compared with on-site or RTMA data, respectively. The concordance analyses indicate Dark Sky wind speed r_c was 0.72 for on-site data or 0.86 for RTMA data. Dark Sky data had bias coefficients of 0.069 (± 0.786) for wind speed, 0.642 (± 3.897) for relative humidity, and 0.116 (± 0.749) for air temperature when compared with RTMA data. These bias coefficients were used to modify the model equations for non-irrigated fields

$$Logit\ (\mu) = \ -0.47(MaxAT_{30MA} + 0.865) - 1.01(MaxWS_{30MA} + 0.855) + 16.65 \quad (5.4)$$

and irrigated fields

$$Logit\ (\mu) = \ -2.38(Row) + 0.65(MaxAT_{30MA} + 0.865) + 0.38(MaxRH_{30MA} + 4.539) - 52.65 \quad (5.5)$$

These model equations were then used in equation 5.3 to generate probabilities for tests of Dark Sky-driven model accuracy at 2017 commercial locations.

Model accuracy using Dark Sky weather data. In the subset of commercial field sites used for validation of model prediction, model accuracy was 87.9% when Dark Sky-driven (bias-corrected) model predictions were used with a 10% DI-threshold and a 40% risk-threshold to explain SSR in the cases examined. Of the four model failures at this threshold, type 1 and 2 errors occurred equally. At a 5% DI-threshold, a 40% risk-threshold for action was again most accurate with models explaining SSR at an 81.8% success rate. Use of a 30 or 35% risk-threshold at either disease-threshold resulted in < 70% model accuracy.

Discussion

Extensive validation of two weather-based models for *S. sclerotiorum* apothecial presence indicated these models result in highly accurate (81.8%) predictions of SSR in both research trials and commercial fields. The later timings of fungicide treatments (R2 to R4) were most effective in Michigan. The corresponding model-predicted risk in fields with 0.38-m spacing was greater than 35 and 40% after R1 and before R2. In all three non-irrigated research sites, the model-predicted risk was below 35 and 40% during the R1 to R3 period

and also had correspondingly low levels of observed SSR. The 35 and 40% risk-thresholds for action repeatedly resulted in the highest accuracy for predicting SSR whether a 5 or 10% disease-threshold was used. The model accuracies (Table 5.11) generated from research and commercial sites confirm that these are appropriate thresholds for SSR management. Reasonable control, however, was achieved when this disease threshold was used to determine accuracy in non-irrigated and irrigated, 0.38-m spacing environments. Most of the sites used in these validations were non-irrigated, dryland fields which were representative for this growing region.

The irrigated sites at 0.76-m row spacing (Fig. 5.1C and 5.1E), however, were not predicted to have risk above the action thresholds (35 or 40%). If a probability risk-threshold of 10% was used in these situations, then the model predictions would have resulted in appropriately timed fungicide applications for SSR management. Based on the results presented in these studies, the irrigated model at the wider row spacing should be adjusted using lower risk-thresholds for effective SRR management. Further validation of these models should be conducted in locations where irrigation is a prevalent management practice in soybeans.

While low disease pressure interfered with the fungicide evaluations at sites in Iowa and Arlington, Wisconsin, model predictions of low risk during the flowering period at all three sites helped to explain the low levels of disease observed. Low levels of SSR ultimately contributed to the inability to detect differences between the different fungicide treatments and timings. With low SSR incidence and severity and little yield impact, the low risk model predictions would have prevented costly applications, approximately \$115-136 USD ha^{-1} for

an effective program (Anonymous, *personal communication*), and unnecessary fungicide applications in these locations.

Additionally, the validation conducted in Arlington suggested boscalid may be more effective than picoxystrobin, perhaps due to longer lasting protection, despite having similar modes of action (FRAC 2017). Both fungicides inhibit fungal respiration, however, boscalid inhibits a different complex earlier in the fungal respiration cycle; we speculate that the inhibition of a different complex may increase the efficacy of this active ingredient. Picoxystrobin is also at high-risk for fungicide resistance development while boscalid is only at medium- to high-risk. Resistance to either of these active ingredients has not yet been identified in natural *S. sclerotiorum* populations.

The site in Hancock, Wisconsin had higher disease pressure, however, no differences in treatments were detected at this location either. Only picoxystrobin was applied at the Hancock site, and similar effects of this active ingredient observed in the Arlington trial could explain this lack of efficacy at this location. Apothecial risk was predicted to be greatest at and after the R3 growth stage (Figure 5.1). The R3 application of picoxystrobin may not have provided enough protection for the extended risk period at the end of the flowering period. In Michigan research trials (Table 5.6), where the risk was highest after R2, the boscalid applications between R2 and R4 were most effective. The soybean varieties typically grown in the Midwest are indeterminate, with flowering occurring over a four week period (Fehr et al. 1971). While the R1 to R3 period typically designates the flowering period, which is usually around 14 days in this region (Table 5.1), some flowers may be present and become infected after this window if risk remains high. In the Midwest, the

soybean SSR-risk window may need re-evaluation to include the R4 growth stage for adequate SSR management.

Typically, SSR management requires one or two fungicide applications during the R1 to R3 growth period. These results, however, indicate that the prediction models validated here can both reduce unnecessary fungicide input and improve application timing during the flowering period. For instance, in the areas of high disease pressure included in this study, a two-spray program may have been most effectively applied at R2 and R4 growth stages as estimated by the models. Using the determined risk-thresholds, these models could be very effective and impactful in SSR management. An accessible, mobile application for growers would be most useful in implementing these models for SSR management.

Unfortunately, the RTMA data while available as regional maps are not easily available for site-specific app development. The Dark Sky data, however, are available through an application programming interface (Dark Sky Company). These data were, therefore, evaluated for site-specific weather and model predictions. As shown, the Dark Sky data were strongly correlated to both on-site and RTMA weather data. Additionally, these data, when corrected with biases, provided accurate model predictions in 2017 Wisconsin commercial sites, with an 81.8 or 87.9% accuracy at a risk-threshold for action of 40%. These results suggest that while the Dark Sky may be an acceptable surrogate for use in mobile applications of these models, risk-thresholds for action may require slight adjustment to correct for inflated model predictions.

Based on the results presented here, the non-irrigated and irrigated, 0.38-m spacing models should be used with a 35% risk-threshold. Irrigated, 0.76-m spacing environments

should use a 10% risk-threshold. When flowers are present on soybeans (potentially R1-R4), fungicide applications should be applied according to these action thresholds for effective SSR management. Furthermore, Dark Sky data may be an acceptable surrogate for RTMA data by using adjusted risk-thresholds for model implementation. If Dark Sky data is used, action thresholds of 40% and 15% may be appropriate for non-irrigated or narrow-row, irrigated environments and irrigated wide-row environments, respectively.

Literature Cited

Allen, T. W., Bradley, C. A., Sisson, A. J., Byamukama, E., Chilvers, M. I., Coker, C. M., et al. 2017. Soybean yield loss estimates due to diseases in the United States and Ontario, Canada from 2010 to 2014. Plant Heal. Prog. 18:19.

Benjamin, S., Brown, J., and Manikin, G. 2007. The RTMA background – hourly downscaling of RUC data to 5-km detail. 23rd Conf. IIPS. :1–4 Available at: http://ams.confex.com/ams/22WAF18NWP/techprogram/paper_124825.htm.

Bondalapati, K. D., and Stein, J. M. 2010. Validation of barley DON risk prediction model. In *Proceedings of the 2010 national Fusarium head blight forum*, Milwaukee, WI: Univerity of Kentucky, p. 71.

Charney, J. J., Service, U. F., and Kiefer, M. T. 2013. An investigation of the differences between Real Time Mesoscale Analysis and observed meteorological conditions at RAWS stations in the northeast United States. JFSP Res. Proj. Reports.

Clarkson, J. P., Fawcett, L., Anthony, S. G., and Young, C. 2014. A model for *Sclerotinia sclerotiorum* infection and disease development in lettuce, based on the effects of temperature, relative humidity and ascospore density. PLoS One. 9:e94049 Available at: http://www.pubmedcentral.nih.gov/articlerender.fcgi?artid=3988091&tool=pmcentrez&rendertype=abstract [Accessed May 27, 2014].

Fehr, W. R., Caviness, C. E., Burmood, D. T., and Pennington, J. S. 1971. Stage of development descriptions for soybeans, *Glycine max* (L.) Merill. Crop Sci. 11:929–931.

Foster, A. J., Kora, C., McDonald, M. R., and Boland, G. J. 2011. Development and validation of a disease forecast model for Sclerotinia rot of carrot. Can. J. Plant Pathol. 33:187–201 Available at: http://www.tandfonline.com/doi/abs/10.1080/07060661.2011.563753 [Accessed January 21, 2014].

FRAC. 2017. Fungicde resistance action committee code list 2017: fungicides sorted by mode of action. :1–12.

Grau, C. R., and Hartman, G. L. 2015. *Compendium of soybean diseases*. 5th ed. eds. G.L. Hartman, J.C. Rupe, E.J. Sikora, L.L. Domier, J.A. Davis, and K.L. Steffey. St Paul, MN: The American Phytopathological Society.

Grau, C., Radke, V., and Gillespie, F. 1982. Resistance of soybean cultivars to *Sclerotinia sclerotiorum*. Plant Dis. 66:506–508.

Harikrishnan, R., and del Río, L. E. 2008. A logistic regression model for predicting risk of white mold incidence on dry bean in North Dakota. Plant Dis. 92:42–46 Available at: http://apsjournals.apsnet.org/doi/abs/10.1094/PDIS-92-1-0042.

Isard, S. A., Russo, J. M., Magarey, R. D., Golod, J., and Vankirk, J. R. 2015. Integrated pest information platform for extension and education (iPiPE): progress through sharing. J. Integr. Pest Manag. 6:1–8.

Lengerich, R. 2017. Concordance correlation coefficient for measuring agreement. In *Statistics 509: Design and Analysis of Clinical Trials*, The Pennsylvania State University, Eberly College of Science. Available at: https://onlinecourses.science.psu.edu/stat509/sites/onlinecourses.science.psu.edu.stat509/files/lesson18/19.2_agreement_concordanc.sas.

Lin, L. I. 1989. A concordance correlation coefficient to evaluate reproducibility. Biometrics. 45:255–268.

Magarey, R., Seem, R., Russo, J., Zack, J., Waight, K., Travis, J., et al. 2001. Site-specific weather information without on-site sensors. Plant Dis. 85:1216–1226.

Monsanto. 2017. Soybean Product Library. Available at: http://www.agseedselect.com/product-library.

Peltier, A. J., Bradley, C. A., Chilvers, M. I., Malvick, D. K., Mueller, D. S., Wise, K. A., et al. 2012. Biology, yield loss and control of Sclerotinia stem rot of soybean. J. Integr. Pest Manag. 3:1–7 Available at: http://openurl.ingenta.com/content/xref?genre=article&issn=2155-7470&volume=3&issue=2&spage=1.

Piepho, H.-P. 2004. An algorithm for a letter-based representation of all-pairwise comparisons. J. Comput. Graph. Stat. 13:456–466 Available at: http://www.tandfonline.com/doi/abs/10.1198/1061860043515.

Pioneer. 2017. Soybean Product Information. Available at: https://ca.pioneer.com/east/en/products/soybeans/ [Accessed December 12, 2017].

Saharan, G. S., and Mehta, N. 2008. *Sclerotinia diseases of crop plants: biology, ecology and disease management*. Springer.

Smith, D. L., Hollowell, J. E., Isleib, T. G., and Shew, B. B. 2007. A site-specific, weather-based disease regression model for Sclerotinia blight of peanut. Plant Dis. 91:1436–1444 Available at: http://sfx.scholarsportal.info/guelph?url_ver=Z39.88-2004&rft_val_fmt=info:ofi/fmt:kev:mtx:journal&genre=article&sid=ProQ:ProQ%253Adeep

indexagrsci&atitle=A+Site-Specific%252C+Weather-Based+Disease+Regression+Model+for+Sclerotinia+Blight+of+Peanut&title=Pl.

Twengstrom, E., Sigvald, R., Svensson, C., and Yuen, J. 1998. Forecasting Sclerotinia stem rot in spring sown oilseed rape. Crop Prot. 17:405–411.

Wharton, P. S., Kirk, W. W., Baker, K. M., and Duynslager, L. 2008. A web-based interactive system for risk management of potato late blight in Michigan. Comput. Electron. Agric. 61:136–148.

Willbur, J. F., Fall, M. L., Bloomingdale, C., Byrne, A. M., Chapman, S. A., Isard, S. A., et al. 2017. Weather-based models for assessing the risk of *Sclerotinia sclerotiorum* apothecial presence in soybean (*Glycine max*) fields. Plant Dis. 102:73–84 Available at: https://apsjournals.apsnet.org/doi/10.1094/PDIS-04-17-0504-RE.

Wrather, A., Shannon, G., Balardin, R., Carregal, L., Escobar, R., Gupta, G., et al. 2010. Effect of diseases on soybean yield in the top eight producing countries in 2006. Plant Heal. Prog.

Tables and Figures

Table 5.1. Research trial locations and GPS coordinates (Coord.), including information for cultivar, irrigation (IR), row spacing (Row), number of plots per trial (Plots), number of squares scouted per plot (Sq), number of days observations were collected (D), and total number of observations (*N*), used to validate models predicting the presence of apothecia, 2017.

Field ID	State	Location	County	Coord.	Cultivar	IR	Row (m)	Plots	Sq	D	*N*
R17-I1	IA	Manilla	Shelby	41.8495, -95.1751	P25T51R	-	0.76	4	3	5	60
R17-I2	IA	Nashua	Black Hawk	42.9382, -92.5696	P25T51R	-	0.76	4	3	2	24
R17-M1	MI	Montcalm	Montcalm	43.3525, -85.1788	AG2535	+	0.76	55	.	.	.
R17-M2	MI	Montcalm	Montcalm	43.3525, -85.1788	AG2535	+	0.38	55	.	.	.
R17-M3	MI	Montcalm	Montcalm	43.3525, -85.1788	AG2535	+	0.76	8	4	13	416
R17-M4	MI	Montcalm	Montcalm	43.3525, -85.1788	AG2535	+	0.38	8	4	13	416
R17-W1	WI	Arlington	Dane	43.3266, -89.3271	AG2031	-	0.76	28	3	4	336
R17-W2	WI	Hancock	Waushara	44.1219, -89.5379	AG2031	+	0.76	16	3	4	192

Table 5.2. Fungicide treatments, including various active ingredients (AI) and application timings evaluated in Iowa, Michigan, and Wisconsin research trials used for model validation, 2017.

Trt	Product	AI	Rate[a]	Application Timing	Growth Stage[b]	Date of Application
Iowa: *Manilla and Nashua*						
1	Non-treated	-	-	-	-	-
2	Cobra	lactofen	0.44	V5	V5	6 July
3	Endura	boscalid	0.56	R1	R1	11 July
4	Endura	boscalid	0.56	7 days post-R1	R2	18 July
5	Endura	boscalid	0.56	14 days post-R1	R3	25 July
6	Endura	boscalid	0.56	21 days post-R1	R4	01 August
7	Aproach	picoxystrobin	0.66	R1	R1	11 July
8	Aproach	picoxystrobin	0.66	7 days post-R1	R2	18 July
9	Aproach	picoxystrobin	0.66	14 days post-R1	R3	25 July
10	Aproach	picoxystrobin	0.66	R1	R1	11 July
	Aproach	picoxystrobin	0.66	14 days post-R1	R3	25 July
11	Cobra	lactofen	0.44	V5	V5	6 July
	Aproach	picoxystrobin	0.66	R1	R1	11 July
Michigan: *Montcalm*						
1	Non-treated	-	-	-	-	-
2	Cobra	lactofen	0.44	V5	V5	6 July
3	Endura	boscalid	0.56	R1	R1	17 July
4	Endura	boscalid	0.56	7 days post-R1	R2	24 July
5	Endura	boscalid	0.56	14 days post-R1	R3	24 July
6	Endura	boscalid	0.56	21 days post-R1	R4	31 July
7	Aproach	picoxystrobin	0.66	R1	R1	17 July
8	Aproach	picoxystrobin	0.66	7 days post-R1	R2	24 July
9	Aproach	picoxystrobin	0.66	14 days post-R1	R3	24 July
10	Aproach	picoxystrobin	0.66	R1	R1	17 July
	Aproach	picoxystrobin	0.66	14 days post-R1	R3	24 July
11	Cobra	lactofen	0.44	V5	V5	6 July
	Aproach	picoxystrobin	0.66	R1	R1	17 July
Wisconsin: *Arlington*						
1	Non-treated	-	-	-	-	-
2	Aproach	picoxystrobin	0.66	R1	R1	14 July
	Aproach	picoxystrobin	0.66	R3	R3	28 July

3	Endura	boscalid	0.56	R1	R1	14 July
4	Aproach	picoxystrobin	0.66	at model threshold #1[c]	R1	14 July
	Aproach	picoxystrobin	0.66	at model threshold #1	R3	28 July
5	Aproach	picoxystrobin	0.66	at model threshold #2	-	-
6	Endura	boscalid	0.56	at model threshold #1	R1	14 July
	Endura	boscalid	0.56	at model threshold #1	R3	28 July
7	Endura	boscalid	0.56	at model threshold #2	-	-
Wisconsin: *Hancock*						
1	Non-treated	-	-	-	-	-
2	Aproach	picoxystrobin	0.66	R1	R1	14 July
	Aproach	picoxystrobin	0.66	R3	R3	28 July
3	Aproach	picoxystrobin	0.66	at model threshold #1	R1	14 July
	Aproach	picoxystrobin	0.66	at model threshold #1	R3	28 July
4	Aproach	picoxystrobin	0.66	at model threshold #2	R3	28 July

[a]Lactofen (6 fl oz a^{-1}) and picoxystrobin (9 fl oz a^{-1}) application rates reported in L ha^{-1} and boscalid (8 oz a^{-1}) reported in kg ha^{-1}.

[b]Growth stages: V5 (fifth trifoliate), R1 (beginning flower), R2 (full flower), R3 (beginning pod), R4 (full pod).

[c]In Wisconsin trials, phenology-based fungicide programs were compared with programs applied between the R1 and R3 growth stages when risk was above action threshold #1 equal to 15%, or action threshold #2 equal to 30%. In some cases, low risk resulted in no applications, designated by a hyphen (-).

Table 5.3. Commercial field locations used to validate apothecial risk models, including information for variety, row spacing (Row), irrigation (IR), SSR history (H), rotation, fungicide application (Fung) and active ingredient, estimated dates of the R1 and R3 growth stages, apothecial scouting and SSR rating dates, and corresponding number of observations collected (*N*) for each visit, 2016-2017.

Year, State	Field ID	County	Variety	Row (m)	IR	H	Rotation[a]	Fung	Active Ingredient	R1[b]	R3	Apothecia Scouting Date	*N*[c]	SSR Rating Date	*N*
2016															
WI	C16-W1	Dodge	Pioneer 24T05	0.38	-	-	C, L, P, S	+	picoxystrobin	11-Jul	25-Jul	18-Jul	20	14-Sep	.
	C16-W2	Walworth	Asgrow 2035	0.38	-	+	C, S	+	lactofen	7-Jul	21-Jul	14-Jul	20	18-Aug	20
	C16-W3	Walworth	Asgrow 2035	0.38	-	+	C, S	+	lactofen	7-Jul	21-Jul	14-Jul	20	18-Aug	20
	C16-W4	Walworth	Dairyland 2909	0.76	-	+	C, S, W	-	.	7-Jul	21-Jul	14-Jul	15	17-Aug	20
	C16-W5	Walworth	Dairyland 2909	0.38	-	+	C, S, W	-	.	7-Jul	21-Jul	14-Jul	15	17-Aug	20
	C16-W6	Walworth	Dairyland 2909	0.76	-	+	C, S	-	.	7-Jul	21-Jul	14-Jul	15	17-Aug	20
	C16-W7	Walworth	Dairyland 2909	0.38	-	+	C, S	-	.	7-Jul	21-Jul	14-Jul	15	17-Aug	20
	C16-W8	Barron	Pioneer 91M10	0.76	-	+	C, S	-	.	6-Jul	20-Jul	27-Jul	20	8-Aug	21
	C16-W9	Barron	Pioneer 91M10	0.76	-	+	C, S	-	.	6-Jul	20-Jul	27-Jul	20	8-Aug	21
	C16-W10	Fond du Lac	Northrup King S20-T6	0.76	-	+	C, S	+	lactofen	12-Jul	26-Jul	26-Jul	10	23-Aug	20
	C16-W11	Fond du Lac	Northrup King S20-T6	0.76	-	+	C, S	-	.	12-Jul	26-Jul	26-Jul	15	23-Aug	10
	C16-W12	Sheboygan	Channel 2108	0.38	-	+	C, S	+	lactofen	18-Jul	1-Aug	25-Jul	20	22-Aug	20
	C16-W13	Dane	Asgrow 1733	0.48	-	+	C, S	-	.	6-Jul	20-Jul	20-Jul	21	11-Aug	19

	C16-W14	Dane	Asgrow 1733	0.48	-	+	C, S	+	tetraconazole	6-Jul	20-Jul	20-Jul	19	30-Aug	21
	C16-W15	Dodge	Renk 241	0.76	-	-	C, S	+	fluxapyroxad, pyraclostrobin	6-Jul	20-Jul	20-Jul	16	18-Aug	20
	C16-W16	Dodge	Renk 241	0.76	-	-	C, S	+	fluxapyroxad, pyraclostrobin	6-Jul	20-Jul	20-Jul	30	18-Aug	20
	C16-W17	Richland	Munsen 8284, 8245	0.76	-	+	C, S	-	.	7-Jul	21-Jul	28-Jul	21	26-Aug	21
	C16-W18	Richland	Munsen 8284, 8245	0.51	-	+	C, S	-	.	30-Jun	14-Jul	28-Jul	15	26-Aug	14
	C16-W19	Outagamie	.	0.19	-	+	C, S	-	.	5-Jul	19-Jul	26-Jul	20	23-Aug	20
	C16-W20	Outagamie	.	0.19	-	+	C, S	-	.	5-Jul	19-Jul	26-Jul	20	23-Aug	20
	C16-W21	Grant	Pioneer 92Y51, 28T08	0.76	-	+	C, S	+	azoxystrobin, propiconazole	11-Jul	25-Jul	1-Aug	20	26-Aug	21
	C16-W22	Grant	Pioneer 28T08	0.76	-	+	C, S	+	azoxystrobin, propiconazole	11-Jul	25-Jul	1-Aug	10	26-Aug	15
2017															
MI	C17-M1	Tuscola	Stine	0.71	-	+	.	.	.	10-Jul	24-Jul	.	.	.	1
	C17-M2	Huron	DynaGro	0.51	-	+	.	.	.	15-Jul	29-Jul	.	.	.	1
	C17-M3	Huron	Cropplan 1950	0.51	-	+	.	.	.	15-Jul	29-Jul	.	.	.	1
NE	C17-N1	Valley	.	0.38	-	-	C, S	-	.	25-Jul	8-Aug	.	1	29-Aug	20
	C17-N2	Scribner	Hoegemeyer 3220NRR	0.76	-	+	C, S	+	tetraconazole	20-Jul	3-Aug	.	1	24-Aug	20
WI	C17-W1	Walworth	Dairyland 2909	0.76	-	+	C, S	-	.	13-Jul	28-Jul	13-Jul	21	18-Aug	20
	C17-W2	Walworth	Dairyland 2909	0.76	-	+	C, S, W	-	.	13-Jul	28-Jul	13-Jul	20	18-Aug	20
	C17-W3	Walworth	Dairyland 3028	0.76	-	+	C, S	-	.	13-Jul	28-Jul	13-Jul	21	18-Aug	20
	C17-W4	Richland	Munson 8284	0.51	-	+	C, S	-	.	17-Jul	1-Aug	17-Jul	22	23-Aug	20
	C17-W5	Richland	Munson 8284	0.51	-	-	C, S	-	.	17-Jul	1-Aug	17-Jul	20	23-Aug	20
	C17-W6	Lafayette	Pioneer 28T08	0.76	-	+	C, S	-	.	10-Jul	24-Jul	17-Jul	20	23-Aug	21
	C17-W7	Grant	Pioneer 28T08	0.76	-	-	C, S	-	.	10-Jul	24-Jul	17-Jul	21	23-Aug	22

C17-W8	Racine	Pioneer 27T07	0.38	-	-	C, S	+	azoxystrobin	11-Jul	25-Jul	18-Jul	21	18-Aug	20
C17-W9	Kenosha	Pioneer 24XX	0.38	-	+	C, S	+	azoxystrobin	11-Jul	25-Jul	18-Jul	22	18-Aug	20
C17-W10	Kenosha	Jung 23XX, Pioneer 24XX	0.38	-	+	C, S	+	azoxystrobin	11-Jul	25-Jul	18-Jul	23	18-Aug	20
C17-W11	Dane	IS24850	0.76	-	+	C, S	-	.	11-Jul	25-Jul	18-Jul	20	30-Aug	20
C17-W12	Columbia	IS24850	0.19	-	+	C, S	-	.	11-Jul	25-Jul	18-Jul	20	30-Aug	24
C17-W13	Dodge	Pioneer 24T05	0.38	-	+	C, S	-	.	11-Jul	25-Jul	18-Jul	20	30-Aug	21
C17-W14	Marathon	Pioneer 08T96R	0.38	-	+	C, S	+	picoxystrobin	14-Jul	1-Aug	25-Jul	20	31-Aug	23
C17-W15	Marathon	Renk 096NR2 (CruiserMaxx +Headsup)	0.38	-	+	C, S	+	picoxystrobin	14-Jul	1-Aug	25-Jul	21	31-Aug	24
C17-W16	Marathon	Jung 1711 RR2	0.76	-	+	C, S	+	lactofen	10-Jul	25-Jul	25-Jul	21	31-Aug	22
C17-W17	Marathon	Jung 1711 RR2	0.76	-	+	C, S	+	lactofen	10-Jul	25-Jul	25-Jul	20	31-Aug	21
C17-W18	Green Lake	Pioneer 24T05R	0.38	-	+	C, S	+	lactofen, azoxystrobin, propioconazole	12-Jul	26-Jul	26-Jul	21	23-Aug	20
C17-W19	Dodge	Pioneer 22T41R2/22T 41R2 Ilevo	0.38	-	+	C, S	+	lactofen, azoxystrobin, propioconazole	12-Jul	26-Jul	26-Jul	21	23-Aug	20
C17-W20	Sheboygan	Channel 1808RR2	0.76	-	+	C, S	-	.	13-Jul	27-Jul	27-Jul	21	24-Aug	20
C17-W21	Sheboygan	.	0.38	-	+	C, S	-	.	13-Jul	27-Jul	27-Jul	21	24-Aug	21
C17-W22	Dodge	Renk 175	0.76	-	+	C, S	-	.	12-Jul	27-Jul	27-Jul	21	23-Aug	20
C17-W23	Dodge	Renk 246	0.76	-	+	C, S	-	.	12-Jul	27-Jul	27-Jul	20	23-Aug	20
C17-W24	Dodge	Renk 213	0.76	-	+	C, S	-	.	12-Jul	27-Jul	27-Jul	21	23-Aug	20
C17-W25	Lafayette	Jung 1211RR2	0.76	-	+	C, S	+	lactofen	14-Jul	28-Jul	28-Jul	21	6-Sep	21
C17-W26	Lafayette	Jung 1231RR2	0.76	-	+	C, S	+	lactofen	14-Jul	28-Jul	28-Jul	21	6-Sep	22
C17-W27	Sauk	Pioneer 22T69R	0.38	-	+	C, S	-	.	26-Jul	9-Aug	2-Aug	23	12-Sep	20

C17-W28	Sauk	Pioneer 22T69R	0.38	-	+	C, S	-	.	26-Jul	9-Aug	2-Aug	23	12-Sep	20
C17-W29	Barron	Asgrow 09XX	0.76	-	+	C, S	+	azoxystrobin, propiconazole	20-Jul	3-Aug	3-Aug	21	29-Aug	20
C17-W30	Grant	Pioneer 28T08	0.76	-	+	C, S	+	fluoxastrobin, flutriafol	20-Jun	4-Jul	.	.	6-Sep	21
C17-W31	Dane	Croplan 2124RR	0.76	-	+	C, S	.	.	7-Jul	24-Jul	.	.	12-Sep	20
C17-W32	Dane	Croplan 2124RR	0.76	-	+	C, S	.	.	7-Jul	24-Jul	.	.	12-Sep	20
C17-W33	Dane	.	0.19	-	.	C, S	.	.	14-Jul	28-Jul	.	.	24-Aug	20

[a]Crop rotations included corn (C), lima bean (L), pea (P), soybean (S), and wheat (W) or a combination of each.

[b]Estimated R1 and R3 growth stages, either based on grower records or growth stages at time of scouting visits. Soybeans were estimated to grow to the next growth stage every 7 days.

[c]The total number of apothecial observations collected was 1,007 and the total number of SSR observations collected were 1,129.

Table 5.4. Validation of various fungicide treatments and application timings, evaluated using disease incidence (DI) and yield (kg ha^{-1}), in Manilla, Iowa 2017.

Trt	Treatment	Rate[a]	Application Timing	DI (%)	Yield (kg ha^{-1})
1	Non-treated	-	-	1.3	4626.7
2	Cobra	0.44	V5	4.0	4834.9
3	Endura	0.56	R1	1.3	4755.4
4	Endura	0.56	R2	3.3	4833.4
5	Endura	0.56	R3	2.7	4997.3
6	Endura	0.56	R4	2.0	4690.5
7	Aproach	0.66	R1	0.0	4626.0
8	Aproach	0.66	R2	2.0	4531.5
9	Aproach	0.66	R3	0.7	4740.8
10	Aproach	0.66	R1	4.0	4706.5
	Aproach	0.66	R3		
11	Cobra	0.44	V5	0.7	4524.1
	Aproach	0.66	R1		
			F	1.13	0.7
			P-value[b]	0.36	0.72

[a]Cobra (6 fl oz a^{-1}) and Aproach (9 fl oz a^{-1}) application rates reported in L ha^{-1} and Endura (8 oz a^{-1}) reported in kg ha^{-1}.

[b]Treatment effects were evaluated at the $\alpha = 0.05$ significance level.

Table 5.5. Validation of various fungicide treatments and application timings, evaluated using disease incidence (DI), disease severity index (DIX), and yield (kg ha^{-1}), in Nashua, Iowa 2017.

Trt	Treatment	Rate[a]	Application Timing	DI (%)	DIX (%)	Yield (kg ha^{-1})
1	Non-treated	-	-	5.0	3.9	3978.7
2	Cobra	0.44	V5	12.5	11.7	3911.0
3	Endura	0.56	R1	15.0	13.6	3357.3
4	Endura	0.56	R2	6.7	6.1	3810.0
5	Endura	0.56	R3	13.3	13.1	3946.0
6	Endura	0.56	R4	14.2	13.3	3648.6
7	Aproach	0.66	R1	12.5	11.9	3888.7
8	Aproach	0.66	R2	12.5	12.2	3578.7
9	Aproach	0.66	R3	8.3	7.2	3971.9
10	Aproach	0.66	R1	5.0	4.5	3662.0
	Aproach	0.66	R3			
11	Cobra	0.44	V5	15.8	15.0	3535.2
	Aproach	0.66	R1			
			F	0.86	0.95	1.25
			P-value[b]	0.58	0.50	0.30

[a]Cobra (6 fl oz a^{-1}) and Aproach (9 fl oz a^{-1}) application rates reported in L ha^{-1} and Endura (8 oz a^{-1}) reported in kg ha^{-1}.

[b]Treatment effects were evaluated at the $\alpha = 0.05$ significance level.

Table 5.6. Validation of various fungicide treatments and application timings at 0.76- and 0.38-m row spacings, evaluated using disease incidence (DI), disease severity index (DIX), and yield (kg ha^{-1}), in Montcalm, Michigan 2017.

Trt	Treatment	Rate[a]	Application Timing	0.76-m spacing				0.38-m spacing			
				DI (%)	DIX (%)	Yield (kg/ha)		DI (%)	DIX (%)		Yield (kg ha^{-1})
1	Non-treated	-	-	42.0	31.1	3284.4	cd[b]	80.0	70.3	a-d	4641.0
2	Cobra	0.44	V5	46.7	30.4	3352.8	cd	95.8	84.7	ab	4159.5
3	Endura	0.56	R1	52.7	35.6	3723.2	bc	75.8	62.2	bde	2713.3
4	Endura	0.56	R2	64.7	32.2	4412.5	a	56.7	43.3	e	4426.6
5	Endura	0.56	R3	68.0	38.0	4260.7	ab	65.8	50.8	de	4668.8
6	Endura	0.56	R4	63.3	34.7	4238.3	ab	67.5	56.1	cde	2948.4
7	Aproach	0.66	R1	50.0	32.9	3078.7	cd	95.8	87.8	a	4183.0
8	Aproach	0.66	R2	44.0	33.3	3317.7	cd	90.0	80.8	abc	3933.8
9	Aproach	0.66	R3	55.3	32.9	3750.8	abc	67.5	58.1	cde	4333.0
10	Aproach Aproach	0.66 0.66	R1 R3	50.7	31.1	3698.8	bc	70.0	55.8	cde	4472.1
11	Cobra Aproach	0.44 0.66	V5 R1	56.7	31.8	2965.7	d	76.7	63.3	a-e	5306.0
			F	0.99	0.30	4.28		1.91	2.69		1.71
			P-value[c]	0.47	0.98	<0.01		0.08	0.02		0.13

[a]Cobra (6 fl oz a^{-1}) and Aproach (9 fl oz a^{-1}) application rates reported in L ha^{-1} and Endura (8 oz a^{-1}) reported in kg ha^{-1}.

[b]Means followed by the same letter, in each column, were not significantly different based on Fisher's least significant difference at the $\alpha = 0.05$ significance level.

[c]Treatment effects were evaluated at the $\alpha = 0.05$ significance level.

Table 5.7. Validation of various fungicide treatments and applications timings evaluated using true disease incidence (DI)[a], disease severity index (DIX), and yield (kg ha^{-1}), in Arlington, Wisconsin 2017.

Trt	Treatment	Threshold (%)[b]	Rate[c]	Application Timing	True DI (%)	DIX (%)	Yield (kg ha^{-1})
1	Non-treated	-	-	-	2.0	1.5	4254.6
2	Aproach	-	0.66	R1	1.0	0.8	4270.7
	Aproach	-	0.66	R3			
3	Endura	-	0.56	R1	0.0	0.0	4514.5
4	Aproach	15	0.66	R1	2.5	1.8	4291.7
	Aproach	15	0.66	R3			
5	Aproach	30	0.66	-	2.5	1.4	3888.1
6	Endura	15	0.56	R1	0.2	0.1	4557.3
	Endura	15	0.56	R3			
7	Endura	30	0.56	-	0.7	0.7	4164.9
				F	0.85	0.71	0.99
				P-value[d]	0.55	0.65	0.46

[a]True DI was calculated using the number of symptomatic plants in the center two rows, divided by the total stand count of the center two rows, and multiplied by 100.

[b]Phenology-based fungicide programs were compared with programs applied between the R1 and R3 growth stages when risk was above threshold #1 (equal to 15%), or threshold #2 (equal to 30%). In some cases, low predicted risk resulted in no applications, designated by a hyphen (-).

[c]Aproach (9 fl oz a^{-1}) application rates reported in L ha^{-1} and Endura (8 oz a^{-1}) reported in kg ha^{-1}.

[d]Treatment effects were evaluated at the $\alpha = 0.05$ significance level.

Table 5.8. Validation of various fungicide treatments and application timings evaluated using true disease incidence (DI)[a], disease severity index (DIX), and yield (kg ha^{-1}), in Hancock, Wisconsin 2017.

Trt	Treatment	Threshold (%)[b]	Rate (fl oz a^{-1})	Applica-tion Timing	True DI (%)	DIX (%)	Yield (kg ha^{-1})
1	Non-treated	-	-	-	17.7	17.6	3099.3
2	Aproach	-	0.66	R1	16.7	16.4	3602.5
	Aproach	-	0.66	R3			
3	Aproach	15	0.66	R1	14.8	14.7	3337.9
	Aproach	15	0.66	R3			
4	Aproach	30	0.66	R3	20.6	20.6	3627.0
				F	0.37	0.41	2.23
				P-value[c]	0.77	0.75	0.15

[a]True DI was calculated using the number of symptomatic plants in the center two rows, divided by the total stand count of the center two rows, and multiplied by 100.

[b]Phenology-based fungicide programs were compared with programs applied between the R1 and R3 growth stages when risk was above threshold #1 (equal to 15%), or threshold #2 (equal to 30%). In some cases, low predicted risk resulted in no applications, designated by a hyphen (-).

[c]Treatment effects were evaluated at the $\alpha = 0.05$ significance level.

Table 5.9. Validations of apothecial risk models in research trials, including information on row spacing (Row), irrigation status (IR), fungicide applications (Fung), apothecial presence or absence (Apo), mean disease incidence (DI), 2017.

Field ID	Row (m)	IR	Fung	Apo	Mean DI (%)	DI 5[a]	DI 10[b]	Risk ≥ Threshold (%) Between R1 and R3[c]			Success (1) or Failure (0) [DI 5%][d]			Success (1) or Failure (0) [DI 10%][d]			Type 1 or 2 Error[e] [DI10]	
								30	35	40	30	35	40	30	35	40	35	40
R17-I1	0.76	-	-	0	1.3	0	0	0	0	0	1	1	1	1	1	1	0	0
R17-I2	0.76	-	-	1	5.0	0	0	0	0	0	1	1	1	1	1	1	0	0
R17-M1	0.76	+	-	.	42.0	1	1	0	0	0	0	0	0	0	0	0	2	2
R17-M2	0.38	+	-	.	80.0	1	1	1	1	1	1	1	1	1	1	1	0	0
R17-M3	0.76	+	-	1	.	.	.	0	0	0	.	.	.	.	.	.	.	.
R17-M4	0.38	+	-	1	.	.	.	1	1	1	.	.	.	.	.	.	.	.
R17-W1	0.76	-	-	1	2.0	0	0	0	0	0	1	1	1	1	1	1	0	0
R17-W2	0.76	+	-	1	17.7	1	1	1	1	1	1	1	1	1	1	1	0	0

[a]If the mean DI was ≥ 5%, then DI5 was given a 1. If not, then the DI5 was 0.

[b]If the mean DI was ≥ 10%, then DI10 was given a 1. If not, then the DI10 was 0.

[c]If the modeled apothecial risk (equations 5.1, 5.2, and 5.3), during the R1 to R3 growth stages, was predicted above the indicated probability thresholds (30, 35, or 40%), the observation was given a 1. If the apothecial risk did not reach above these thresholds, then the observation was given a 0.

[d]If the binary risk predictions matched the corresponding binary disease observations at 5 or 10%, then the validation location was determined a success (1). If the risk predictions did not match disease observations, then the validation was determined a failure (0). Successes and failures were used to calculate model accuracy across all locations.

[e]If the validation was determined a failure and disease was under the disease threshold (5 or 10%), i.e. the model over-predicted risk in that location, then the error was considered type 1 (1). If the failure occurred in an area where disease was above threshold (5 or 10%), i.e. the model under-predicted risk in the area, then the error was considered type 2 (2).

Table 5.10. Validations of apothecial risk models in commercial grower fields, including information on row spacing (Row), irrigation status (IR), fungicide applications (Fung), apothecial presence or absence (Apo), mean disease incidence (DI), 2016-2017.

Year	Field ID	Row (m)	IR	Fung	Apo	Mean DI (%)	DI 5[a]	DI 10[b]	Risk ≥ Threshold (%) Between R1 and R3[c]			Success (1) or Failure (0) [DI 5%][d]			Success (1) or Failure (0) [DI 10%][d]			Type 1 or 2 Error[e] [DI10]	
									30	35	40	30	35	40	30	35	40	35	40
2016	C16-W1	0.38	-	+	0	low	0	0	0	0	0	1	1	1	1	1	1	0	0
	C16-W2	0.38	-	+	0	1.3	0	0	1	0	0	0	1	1	0	1	1	0	0
	C16-W3	0.38	-	+	0	0.3	0	0	1	0	0	0	1	1	0	1	1	0	0
	C16-W4	0.76	-	-	0	0.0	0	0	1	0	0	0	1	1	0	1	1	0	0
	C16-W5	0.38	-	-	0	0.0	0	0	1	0	0	0	1	1	0	1	1	0	0
	C16-W6	0.76	-	-	0	0.0	0	0	1	0	0	0	1	1	0	1	1	0	0
	C16-W7	0.38	-	-	0	0.2	0	0	1	0	0	0	1	1	0	1	1	0	0
	C16-W8	0.76	-	-	0	14.0	1	1	1	1	1	1	1	1	1	1	1	0	0
	C16-W9	0.76	-	-	0	3.8	0	0	1	1	1	0	0	0	0	0	0	1	1
	C16-W10	0.76	-	+	1	2.1	0	0	0	0	0	1	1	1	1	1	1	0	0
	C16-W11	0.76	-	-	0	2.4	0	0	0	0	0	1	1	1	1	1	1	0	0
	C16-W12	0.38	-	+	0	9.8	1	0	0	0	0	0	0	0	1	1	1	0	0
	C16-W13	0.48	-	-	0	19.4	1	1	1	1	0	1	1	0	1	1	0	0	2
	C16-W14	0.48	-	+	1	39.0	1	1	1	1	0	1	1	0	1	1	0	0	2
	C16-W15	0.76	-	+	0	1.5	0	0	0	0	0	1	1	1	1	1	1	0	0
	C16-W16	0.76	-	+	1	29.6	1	1	0	0	0	0	0	0	0	0	0	2	2
	C16-W17	0.76	-	-	0	11.7	1	1	0	0	0	0	0	0	0	0	0	2	2
	C16-W18	0.51	-	-	0	4.6	0	0	0	0	0	1	1	1	1	1	1	0	0
	C16-W19	0.19	-	-	0	0.8	0	0	0	0	0	1	1	1	1	1	1	0	0

	C16-W20	0.19	-	-	0	40.2	1	1	0	0	0	0	0	0	0	0	0	2	2
	C16-W21	0.76	-	+	0	3.3	0	0	0	0	0	1	1	1	1	1	1	0	0
	C16-W22	0.76	-	+	0	1.5	0	0	0	0	0	1	1	1	1	1	1	0	0
2017	C17-M1	0.71	-	.	.	40.0	1	1	0	0	0	0	0	0	0	0	0	2	2
	C17-M2	0.51	-	.	.	80.0	1	1	0	0	0	0	0	0	0	0	0	2	2
	C17-M3	0.51	-	.	.	40.0	1	1	0	0	0	0	0	0	0	0	0	2	2
	C17-N1	0.38	-	-	0	5.7	1	0	0	0	0	0	0	0	1	1	1	0	0
	C17-N2	0.76	-	+	0	6.5	1	0	0	0	0	0	0	0	1	1	1	0	0
	C17-W1	0.76	-	-	0	0.8	0	0	0	0	0	1	1	1	1	1	1	0	0
	C17-W2	0.76	-	-	0	0.0	0	0	0	0	0	1	1	1	1	1	1	0	0
	C17-W3	0.76	-	-	0	0.6	0	0	0	0	0	1	1	1	1	1	1	0	0
	C17-W4	0.51	-	-	0	0.3	0	0	0	0	0	1	1	1	1	1	1	0	0
	C17-W5	0.51	-	-	0	0.2	0	0	0	0	0	1	1	1	1	1	1	0	0
	C17-W6	0.76	-	-	0	0.5	0	0	0	0	0	1	1	1	1	1	1	0	0
	C17-W7	0.76	-	-	0	0.9	0	0	0	0	0	1	1	1	1	1	1	0	0
	C17-W8	0.38	-	+	0	0.7	0	0	0	0	0	1	1	1	1	1	1	0	0
	C17-W9	0.38	-	+	0	0.0	0	0	0	0	0	1	1	1	1	1	1	0	0
	C17-W10	0.38	-	+	0	0.1	0	0	0	0	0	1	1	1	1	1	1	0	0
	C17-W11	0.76	-	-	0	1.3	0	0	0	0	0	1	1	1	1	1	1	0	0
	C17-W12	0.19	-	-	0	1.7	0	0	0	0	0	1	1	1	1	1	1	0	0
	C17-W13	0.38	-	-	0	6.3	1	0	0	0	0	0	0	0	1	1	1	0	0
	C17-W14	0.38	-	+	0	2.1	0	0	1	1	1	0	0	0	0	0	0	1	1
	C17-W15	0.38	-	+	0	19.7	1	1	1	1	1	1	1	1	1	1	1	0	0
	C17-W16	0.76	-	+	0	20.3	1	1	1	1	1	1	1	1	1	1	1	0	0
	C17-W17	0.76	-	+	0	15.3	1	1	1	1	1	1	1	1	1	1	1	0	0
	C17-W18	0.38	-	+	0	0.9	0	0	0	0	0	1	1	1	1	1	1	0	0
	C17-W19	0.38	-	+	0	0.2	0	0	0	0	0	1	1	1	1	1	1	0	0
	C17-W20	0.76	-	-	0	0.3	0	0	0	0	0	1	1	1	1	1	1	0	0
	C17-W21	0.38	-	-	0	11.9	1	1	0	0	0	0	0	0	0	0	0	2	2

C17-W22	0.76	-	-	0	4.6	0	0	0	0	0	1	1	1	1	1	1	0	0
C17-W23	0.76	-	-	0	2.6	0	0	0	0	0	1	1	1	1	1	1	0	0
C17-W24	0.76	-	-	0	0.5	0	0	0	0	0	1	1	1	1	1	1	0	0
C17-W25	0.76	-	+	0	0.0	0	0	0	0	0	1	1	1	1	1	1	0	0
C17-W26	0.76	-	+	0	0.1	0	0	0	0	0	1	1	1	1	1	1	0	0
C17-W27	0.38	-	-	0	0.2	0	0	1	0	0	0	1	1	0	1	1	0	0
C17-W28	0.38	-	-	0	0.0	0	0	1	0	0	0	1	1	0	1	1	0	0
C17-W29	0.76	-	+	0	8.9	1	0	1	1	1	1	1	1	0	0	0	1	1
C17-W30	0.76	-	+	0	39.7	1	1	1	1	1	1	1	1	1	1	1	0	0
C17-W31	0.76	-	.	0	2.0	0	0	0	0	0	1	1	1	1	1	1	0	0
C17-W32	0.76	-	.	0	4.4	0	0	0	0	0	1	1	1	1	1	1	0	0
C17-W33	0.19	-	.	0	15.5	1	1	0	0	0	0	0	0	0	0	0	2	2

[a]If the mean DI was ≥ 5%, then DI5 was given a 1. If not, then the DI5 was 0.

[b]If the mean DI was ≥ 10%, then DI10 was given a 1. If not, then the DI10 was 0.

[c]If the modeled apothecial risk (equations 5.1, 5.2, and 5.3), during the R1 to R3 growth stages, was predicted above the indicated probability thresholds (30, 35, or 40%), the observation was given a 1. If the apothecial risk did not reach above these thresholds, then the observation was given a 0.

[d]If the binary risk predictions matched the corresponding binary disease observations at 5 or 10%, then the validation location was determined a success (1). If the risk predictions did not match disease observations, then the validation was determined a failure (0). Successes and failures were used to calculate model accuracy across all locations.

[e]If the validation was determined a failure and disease was under the disease threshold (5 or 10%), i.e. the model over-predicted risk in that location, then the error was considered type 1 (1). If the failure occurred in an area where disease was above threshold (5 or 10%), i.e. the model under-predicted risk in the area, then the error was considered type 2 (2).

Table 5.11. Accuracy[a] of apothecial model predictions from validations conducted in research trials or commercial fields, 2016-2017.

Accuracy (%)	**Success (1) or Failure (0) [DI 5%]**			**Success (1) or Failure (0) [DI 10%]**		
	30	35	40	30	35	40
in research trials, 2017	83.3	83.3	83.3	83.3	83.3	83.3
in commercial fields, 2016-17	63.3	76.7	73.3	68.3	81.7	78.3
Total	65.2	77.3	74.2	69.7	81.8	78.8

[a]Binary model successes (1) or failures (0), for each model action threshold (30, 35, or 40%) using disease incidence thresholds of 5 or 10% (Tables 5.9 and 5.10), were used to determine model accuracy across all locations and years. The number of successes were divided by the total number of field validations and multiplied by 100.

Table 5.12. Bias, Pearson, and concordance coefficients with corresponding standard deviations (SD) or 95% confidence intervals (CI) for correlation analyses of Dark Sky weather data and on-site Campbell Scientific weather station or gridded real-time mesoscale analysis (RTMA) data

Weather Variable	**Bias[a]**	**Pearson Correlation**		**Concordance Correlation**	
	Coefficient ± SD	Coefficient, r	95% CI	Coefficient, r_c	95% CI
On-site Campbell Weather Station					
Air Temperature	-0.633 ± 0.965	0.98	(0.979, 0.981)	0.97	(0.970, 0.973)
Relative Humidity	4.312 ± 5.140	0.94	(0.943, 0.949)	0.91	(0.907, 0.912)
Wind Speed	-0.814 ± 0.790	0.85	(0.834, 0.856)	0.72	(0.704, 0.735)
Gridded RTMA Data (sourced iPiPE)					
Air Temperature	0.116 ± 0.749	0.99	(0.988, 0.989)	0.99	(0.987, 0.989)
Relative Humidity	0.642 ± 3.897	0.97	(0.969, 0.972)	0.97	(0.968, 0.971)
Wind Speed	0.069 ± 0.786	0.87	(0.861, 0.875)	0.86	(0.857, 0.871)

[a]Bias coefficients were calculated from the mean difference between hourly Dark Sky data and on-site Campbell Scientific or gridded RTMA data; bias coefficient = Dark Sky data – onsite or RTMA data.

Table 5.13. Validations of apothecial risk models in commercial grower fields, including information on row spacing (Row), irrigation status (IR), fungicide applications (Fung), apothecial presence or absence (Apo), mean disease incidence (DI), using Dark Sky weather data 2017.

Field ID	DI 5[a]	DI 10[b]	Risk ≥ Threshold (%) Between R1 and R3[c]			Success (1) or Failure (0) [DI 5%][d]			Success (1) or Failure (0) [DI 10%][d]			Type 1 or 2 Error[e] [DI10]
			30	35	40	30	35	40	30	35	40	40
C17-W1	0	0	0	0	0	1	1	1	1	1	1	0
C17-W2	0	0	0	0	0	1	1	1	1	1	1	0
C17-W3	0	0	0	0	0	1	1	1	1	1	1	0
C17-W4	0	0	0	0	0	1	1	1	1	1	1	0
C17-W5	0	0	0	0	0	1	1	1	1	1	1	0
C17-W6	0	0	0	0	0	1	1	1	1	1	1	0
C17-W7	0	0	0	0	0	1	1	1	1	1	1	0
C17-W8	0	0	0	0	0	1	1	1	1	1	1	0
C17-W9	0	0	0	0	0	1	1	1	1	1	1	0
C17-W10	0	0	0	0	0	1	1	1	1	1	1	0
C17-W11	0	0	0	0	0	1	1	1	1	1	1	0
C17-W12	0	0	1	0	0	0	1	1	0	1	1	0
C17-W13	1	0	1	1	0	1	1	0	0	0	1	0
C17-W14	0	0	1	1	1	0	0	0	0	0	0	1
C17-W15	1	1	1	1	1	1	1	1	1	1	1	0
C17-W16	1	1	1	1	1	1	1	1	1	1	1	0
C17-W17	1	1	1	1	1	1	1	1	1	1	1	0
C17-W18	0	0	1	1	0	0	0	1	0	0	1	0
C17-W19	0	0	1	1	0	0	0	1	0	0	1	0
C17-W20	0	0	1	1	1	0	0	0	0	0	0	1
C17-W21	1	1	1	1	1	1	1	1	1	1	1	0
C17-W22	0	0	1	1	0	0	0	1	0	0	1	0
C17-W23	0	0	1	1	0	0	0	1	0	0	1	0
C17-W24	0	0	1	1	0	0	0	1	0	0	1	0
C17-W25	0	0	0	0	0	1	1	1	1	1	1	0
C17-W26	0	0	0	0	0	1	1	1	1	1	1	0
C17-W27	0	0	0	0	0	1	1	1	1	1	1	0
C17-W28	0	0	0	0	0	1	1	1	1	1	1	0
C17-W29	1	0	0	0	0	0	0	0	1	1	1	0
C17-W30	1	1	0	0	0	0	0	0	0	0	0	2

C17-W31	0	0	0	0	0	1	1	1	1	1	1	0
C17-W32	0	0	0	0	0	1	1	1	1	1	1	0
C17-W33	1	1	0	0	0	0	0	0	0	0	0	2
			Accuracy (%)			**66.7**	**69.7**	**81.8**	**66.7**	**69.7**	**87.9**	**50/50**

[a]If the mean DI was ≥ 5%, then DI5 was given a 1. If not, then the DI5 was 0.

[b]If the mean DI was ≥ 10%, then DI10 was given a 1. If not, then the DI10 was 0.

[c]If the modeled apothecial risk (equations 5.3, 5.4, and 5.5), during the R1 to R3 growth stages, was predicted above the indicated probability thresholds (30, 35, or 40%), the observation was given a 1. If the apothecial risk did not reach above these thresholds, then the observation was given a 0.

[d]If the binary risk predictions matched the corresponding binary disease observations at 5 or 10%, then the validation location was determined a success (1). If the risk predictions did not match disease observations, then the validation was determined a failure (0). Successes and failures were used to calculate model accuracy across all locations.

[e]If the validation was determined a failure and disease was under the disease threshold (5 or 10%), i.e. the model overpredicted risk in that location, then the error was considered type 1 (1). If the failure occurred in an area where disease was above threshold (5 or 10%), i.e. the model underpredicted risk in the area, then the error was considered type 2 (2). Of the cases examined, 50% of the errors were type 1 and 50% were type 2.

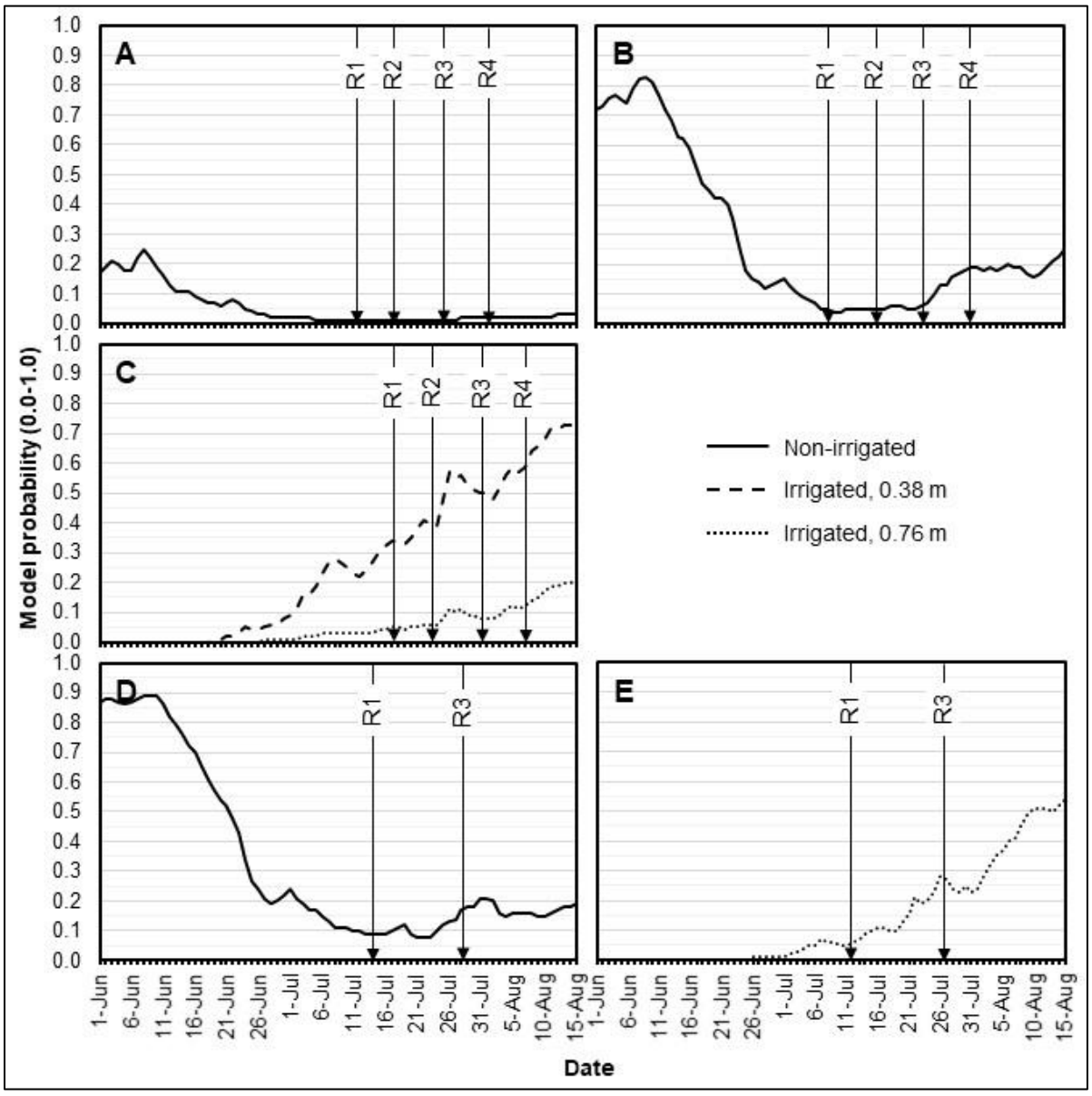

Figure 5.1. Model validations conducted in research trials 2017 located in **A,** Nashua and **B,** Manilla, Iowa, **C,** Montcalm, Michigan, and **D,** Arlington, and **E,** Hancock, Wisconsin. The solid line (—) indicates model probabilities for non-irrigated soybean fields; the logit was calculated using equation 5.1. The dashed line (---) indicates model probabilities for irrigated soybean fields at a narrow, 0.38-m row spacing; the logit was calculated using equation 5.2 where the row variable is equal to 0. The dotted line (···) indicates model probabilities for

irrigated soybean fields at a wide, 0.76-m row spacing; the logit was calculated using equation 5.2 where the row variable is equal to 1. All probabilities were calculated from the logit using equation 5.3. All weather data used in these validations were provided by the iPiPE weather network and were generated using GPS coordinates for each location. The dates of the growth stages R1 (beginning flower), R2 (full flower), R3 (beginning pod), and R4 (full pod), often where fungicide treatments were applied in efficacy trials, are indicated by the vertical labelled arrows.

CHAPTER 6: Meta-analytic and economic approaches for evaluation of fungicide impact on Sclerotinia stem rot and soybean yield in the North Central U.S.

Abstract

Sclerotinia stem rot (SSR) is caused by the fungal pathogen *Sclerotinia sclerotiorum* and consistently ranks in the top diseases plaguing global soybean crops. As complete resistance in soybean has not been achieved, and SSR continues to be of economic concern, chemical control remains a prevalent disease management strategy. Studies from multiple site-years evaluating the efficacy of fungicide treatments and application timings can provide current, regional management recommendations. Fungicide evaluations were conducted in Illinois, Iowa, Michigan, Minnesota, New Jersey, and Wisconsin from 2009 to 2016, for a total of 25 site-years (n = 2057 plot-level observations). These studies were used to test 10 active ingredients and seven common application timings. Active ingredient significantly affected disease severity index (DIX) reduction and yield benefit ($P < 0.0001$). Application timing also significantly affected disease reduction ($P < 0.0001$) and yield benefit ($P = 0.0009$). The moderator variable of disease pressure (or baseline disease in non-treated plots), while not significant ($P = 0.07$), was useful in evaluating the impact of different active ingredients on soybean yield benefit. These studies were also used in nonlinear regression analyses to determine the effect of disease severity index (DIX) on soybean yield. A three-parameter logistic model best described soybean yield loss (pseudo-$R^2 = 0.309$). In modern soybean cultivars, yield loss due to SSR does not appear to occur until 20-25% DIX and considerable yield loss (-697 kg ha^{-1} or -10 bu a^{-1}) is observed beginning at 68% DIX. Further analyses determined an 80-95% probability for return on investment using programs including one application of lactofen, two applications of picoxystrobin, and one application of boscalid.

These studies will help growers select cost effective fungicide programs for use in integrated management of SSR.

Introduction

Soybean (*Glycine max* L. Merrill) is the second largest agricultural crop grown (by acreage) in the United States, and in 2016, production reached a value of $40.9 billion USD (USDA-NASS, 2017). While soybeans are grown across 31 states from the Southern to the Northeastern US, production is concentrated in the North Central region. This region of 12 Midwestern states accounts for 84.5% of US soybean production, totaling 98 million metric tons with a farmgate value of $34.2 billion USD in 2016 (USDA-NASS, 2017). Production, however, is severely limited by more than 20 diseases affecting soybean.

Sclerotinia stem rot (SSR), more commonly known as white mold, ranks in the top ten most destructive diseases of soybean (Allen et al., 2017; Koenning and Wrather, 2010; Wrather and Koenning, 2009). From 2010 to 2014, SSR was responsible for almost 2.8 million metric tons of yield loss in soybeans, which cost growers $1.2 billion USD based on USDA market prices (Allen et al., 2017; USDA-NASS, 2017). *Sclerotinia sclerotiorum*, a necrotrophic fungal pathogen, is the causal agent of SSR (Grau and Hartman, 2015). *S. sclerotiorum* primarily infects soybean through the flowers via infectious, wind-dispersed ascospores (Grau and Hartman, 2015; Peltier et al., 2012). A major management challenge is the persistence of SSR in a field once introduced, largely due to the long-term survival of soilborne sclerotia and broad host range of *S. sclerotiorum* (Boland and Hall, 1994; Grau and Hartman, 2015; Peltier et al., 2012). As little resistance is available in commercial cultivars, in-season management relies heavily on chemical control targeted at protecting the flowers

from *S. sclerotiorum* infection by ascospores (Peltier et al., 2012). Soybean flowering occurs from the R1 (beginning flower) to R3 (beginning pod) growth stages (Fehr et al., 1971).

Most fungicides used in SSR control are classified as methyl benzimidazole carbamates (thiophanate-methyl), succinate dehydrogenase inhibitors (boscalid), demethylation inhibitors (flutriafol, prothioconazole, tetraconazole), and quinone outside inhibitors (fluoxastrobin, picoxystrobin, trifloxystrobin) (Armando et al., 2015; Di et al., 2016; Huzar-Novakowiski et al., 2017; Liang et al., 2015; Peltier et al., 2012). Fluazinam, an uncoupler of oxidative phosphorylation, also inhibits *S. sclerotiorum* (Liang et al., 2015). In addition to these fungicides, the herbicide lactofen has also been identified for SSR management. Some protoporphyrinogen oxidase (PPO) inhibitor herbicides can impact soybean canopy development and promote systemic resistance, both of which inhibit *S. sclerotiorum* infection and SSR development (Dann et al., 1999; Peltier et al., 2012).

Each year, these fungicides and herbicides are tested across the soybean growing region. Madden and Paul (2011) described meta-analysis of multiple independent trials, and further methods have been developed and implemented to analyze multiple treatments simultaneously (Machado et al., 2017; Madden et al., 2016; Paul et al., 2008, 2010). Network, or multivariate analyses, are especially useful to synthesize results from multiple treatments, whether evaluated together, separately, or in various combinations across multiple independent studies, while accounting for between- and within-study variability (Madden et al., 2016). Compilation of independent SSR fungicide efficacy trial results using these methods has not been previously performed and so would provide powerful data-driven recommendations for growers when making management decisions.

Fungicide efficacy trials generally evaluate treatments by a measure of disease, e.g. disease severity or incidence, and agronomic qualities, e.g. yield. For SSR, disease incidence and severity data are typically recorded using a rating scale and often combined into a disease severity index score (DSI or DIX; we will use DIX in this study) (Grau et al., 1982; Kim et al., 2000). These data when combined with yield information in subsequent yield loss analyses help identify control thresholds for cost-effective disease management. While studies of the relationship between incidence and yield have been conducted (Chun et al., 1987; Danielson et al., 2004; Hoffman et al., 1998; Lehner et al., 2016; Yang et al., 1999), few studies have reported the impact of DIX on soybean yield (Fall et al., 2018) and none have been conducted across an entire growing region.

Almost 100 years of extensive breeding efforts have resulted in soybean cultivars with significantly higher yield performance, approximately double that of historical cultivars (Suhre et al., 2014). These yield improvements are largely due to the enhanced branching capacity in modern soybean cultivars (Suhre et al., 2014). Quantification of SSR impact on soybean yield, therefore, should account for the architectural changes in modern varieties. The Grau 0-3 disease severity rating scale distinguishes between SSR on the main stem and SSR on the branches or secondary stems (1982). Use of this severity rating, represented by the DIX score, in yield loss analysis would provide a model that appropriately describes the impact of SSR on modern soybean varieties.

This study compiles independent fungicide trials from across the North Central soybean growing region to 1) investigate the impact of SSR on soybean yield, using disease scoring appropriate for modern soybean architecture, 2) evaluate the efficacies and yield

benefits of multiple fungicides and timings in a comprehensive network meta-analysis, and 3) conduct return on investment analyses for effective fungicide programs.

Materials and Methods

Study selection and data compilation for analyses. The data used in this study were collected from fungicide evaluations conducted by university researchers in Illinois, Iowa, Michigan, Minnesota, New Jersey, and Wisconsin from 2009 to 2016, for a total of 25 site-years (n = 2057 plot-level data points). Raw, plot-level observations from the studies, or individual participant data, were available and used in this meta-analysis (Madden and Paul, 2011). A study was defined as an independent experimental trial consisting of four or more pesticide treatments, including a non-treated control treatment, replicated four or five times, and conducted in a randomized complete block design. Fungicides were evaluated in small four or six row plots ranging from 1.5-3.0 m in width and 4.6-9.1 m in length, with row spacing between 0.19-m and 0.76-m. In each site-year, a regionally representative susceptible soybean cultivar was used. Pesticides were applied using either tractor or backpack sprayers. These studies evaluated the effects of various combinations of pesticide class, active ingredient, rate, and application timing on SSR incidence and severity. Forty-four named products were included, with 27 known active ingredients, and were applied at one or a combination of ten different soybean growth stages. The pesticide products included in this study represented 10 fungicide classes, however, also included were three protoporphyrinogen oxidase (PPO) herbicides, one 5-enolpyruvylshikimate-3-phosphate (EPSP) synthase inhibitor herbicide, two insecticides, and one biocontrol. Including all the different combinations of products, rates, and timings there were 216 unique treatments within the dataset. For this study, application rate and the inclusion or exclusion of a non-

ionic surfactant were not considered. To be included in the analyses conducted here, 1) SSR must have been observed in one or more plots in the study, and 2) a measure of disease (incidence, severity, and/or severity index) and yield must have been recorded at the plot level.

Measurements of SSR and soybean yield. Disease data were typically collected in the center two or four rows of four- or six-row plots. For all locations, the disease severity index (DIX) was calculated as follows:

$$DIX = DI \times \frac{DS}{3} \quad (6.1)$$

where disease incidence (DI) was estimated as a percentage of diseased plants (of the rated plants) in the center rows, and disease severity (DS) of symptomatic plants was calculated by arbitrarily rating 10-80 plants in the center rows of each plot on a 0-3 scale, where 0 = no disease, 1 = infection on a secondary stem or branch, 2 = disease on the main stem not resulting in plant wilt or death, 3 = disease girdling the main stem and resulting in plant wilt or death (Grau et al., 1982), then the average rating of only the symptomatic plants was used in equation 6.1. In multiplying the percent DI by the average DS rating, the resulting DIX value is a percentage ranging from 0 to 100.

Yield data were typically collected in the center two to four rows of four- to six-row plots. Soybeans were harvested using research-plot combines and yield data were adjusted to 13% moisture.

Analysis of SSR impact on soybean yield loss. All analyses in this study were conducted using SAS 9.4 (SAS Institute, Cary, NC). SSR impact on soybean yield was analyzed using raw plot data from the above studies. For this analysis, plot-level DIX data

(equation 6.1) were adjusted to a 0 to 1 scale, by dividing DIX by 100, for the nonlinear regression analyses with the associated yield data (kg ha^{-1}). Data for nineteen plots were removed from this analysis due to missing DIX or yield data (n = 2038). Nonlinear regression analyses were conducted using the NLIN procedure with a specified Marquardt option. Parameters were defined with initial estimates and then incorporated into the model statement.

A two-parameter Weibull model (Madden et al., 2007) and a three-parameter modified logistic model (Graybill and Iyer, 1994) were investigated and results are presented here based on the shape and fit of the regression line compared to the raw plot data. The equation used for the Weibull model was

$$Yield = Yield_o \times \left(\frac{1 - DIX}{[(1 - a) + a(1 - DIX)]^2} \right) \quad (6.2)$$

where *Yield* is the individual plot yield in kg ha^{-1}, $Yield_o$ is the estimated yield potential (y-intercept), *DIX* is the DIX adjusted to a 0 to 1 scale, and *a* is a shape parameter. Initial estimates were given for $Yield_o$ and *a*, and were 4000 and 0.56, respectively.

The equation used for the modified logistic model was

$$Yield = Yield_o / \left[1 + e^{-(b + c * DIX)}\right] \quad (6.3)$$

where *Yield* is the individual plot yield in kg ha^{-1}, $Yield_o$ is the estimated yield potential (y-intercept), *b* and *c* are shape parameters, and *DIX* is the DIX adjusted to a 0 to 1 scale. Initial estimates were given for $Yield_o$, *b*, and *c*, and were 4000, 5, and -15, respectively.

Nonlinear regression goodness-of-fit was compared between models using the pseudo-R^2 calculated as follows (Carey, 2013; Chism et al., 1992):

$$Pseudo - R^2 = 1 - \frac{SSE}{CTSS} \quad (6.4)$$

where *SSE* is the sum of the squared errors as reported in the NLIN output table and the *CTSS* is the corrected total sum of squares generated using PROC MEANS for the yield variable with the corrected sum of squares option (css). The model with the larger pseudo-R^2 value was considered to have better fit.

Generation of treatment means and distributions. Prior to the network meta-analyses, the raw plot data were condensed to treatment means in a generalized linear mixed model (GLIMMIX) primary analysis of variance (ANOVA) conducted for each site-year. For each study, the yield (Y) and DIX (X) means were generated for each treatment, including the non-treated check. Replicate was considered a random effect and the Kenward-Roger degrees of freedom correction was used. The mean, standard error, mean squared error (the residual estimate from the covariance parameter output table), and study non-treated mean were recorded for yield and DIX. Treatments were considered "common" if there were ≥ 10 mean observations (N). The means generated were separated into two data subsets. One subset contained all common fungicide active ingredients (N = 359): boscalid (BOSC), boscalid and fluxapyroxad/pyraclostrobin (BOSC+FLUX/PYRA), fluazinam (FLUA), fluoxastrobin and flutriafol (FLUO+FLUT), lactofen (LACT), picoxystrobin (PICO), prothioconazole (PROT), prothioconazole and trifloxystrobin (PROT+TRIF), tetraconazole (TETR), and thiophanate methyl (THIM) (Table 6.1). The other subset contained all common fungicide application timings (N = 454), shown as soybean growth stages: V5, R1 (beginning flower), R2 (full flower), R3 (beginning pod), R5 (beginning seed), R1+R2 (beginning and full flower),

R1+R3 (beginning flower and pod) (Table 6.1). Each data subset was used in the following network meta-analyses. These data were also analyzed using the SAS BOXPLOT procedure to examine the distributions of DIX and yield for each treatment (active ingredient and application timing). The summary output table was used with corresponding plots to describe these distributions.

Response variables of interest. The treatment means were used to generate response variables of interest for a network meta-analysis of the effects of fungicide active ingredient and timing on soybean disease and yield. The response variables of interest were: 1) the DIX reduction (D_t), which is the difference in mean DIX (%) for each fungicide treatment and the non-treated control, and 2) the yield benefit (B_t), which is the difference in mean yield of the treatment and the non-treated control, relative to the non-treated yield. Treatment *t* corresponds to either individual common active ingredients (BOSC, BOSC+FLUX/PYRA, FLUA, FLUO+FLUT, LACT, PICO, PROT, PROT+TRIF, TETR, THIM, and CONTROL) or common fungicide application timings (V5, R1, R2, R3, R5, R1+R2, R1+R3, and CONTROL). For each study, DIX reduction for treatment *t* (D_t) is described by the equation

$$D_t = \bar{X}_t - \bar{X}_{nt} \tag{6.5}$$

where $\bar{X}_t$ is the mean DIX of the fungicide treatment and $\bar{X}_{nt}$ is the mean DIX of the non-treated control (Machado et al., 2017; Madden et al., 2016; Madden and Paul, 2011; Paul et al., 2010). Greater negative values indicate increased disease reduction, or control, by the fungicide treatment. $\bar{D}_t$ would indicate the mean DIX reduction across all studies. For each study, yield benefit for treatment *t* (B_t) is described by the equation

$$B_t = \left(\frac{\bar{Y}_t - \bar{Y}_{nt}}{\bar{Y}_{nt}}\right) \times 100 = \left(\frac{\bar{Y}_t}{\bar{Y}_{nt}} - 1\right) \times 100 \quad (6.6)$$

where $\bar{Y}_t$ is the mean yield of the fungicide treatment and $\bar{Y}_{nt}$ is the mean yield of the non-treated control (Machado et al., 2017; Madden et al., 2016; Madden and Paul, 2011; Paul et al., 2008). $\bar{B}_t$ would indicate the mean yield benefit, across all studies, of treatment *t*. Greater values indicate greater yield gains from a fungicide treatment.

Variables used in the network meta-analysis. To evaluate the above response variables the following variables were generated for the meta-analysis: 1) the DIX reduction (D) described by equation 6.5, and 2) the yield response ratio (R), which is the mean yield of the treatment relative to the non-treated yield. For each study, the response ratio for treatment *t* (R_t), was calculated by

$$R_t = \frac{\bar{Y}_t}{\bar{Y}_{nt}} \quad (6.7)$$

Due to the statistical complication of treatments of the same study sharing a denominator (Hedges et al., 1999; Machado et al., 2017; Madden and Paul, 2011; Paul et al., 2008), the log of the response ratio (L_t) was calculated and the equivalent difference in log means, for a single study, was used in the analysis

$$L_t = \ln(R_t) = \ln\left(\frac{\bar{Y}_t}{\bar{Y}_{nt}}\right) = \ln(\bar{Y}_t) - \ln(\bar{Y}_{nt}) \quad (6.8)$$

$\bar{L}_t$ would indicate the mean log response ratio, across all studies, of treatment *t*. For each study, the within-study variance for *D* was calculated as in Paul et al. (2010):

$$Var_D = \frac{V_D}{n} \quad (6.9)$$

where V_D is the DIX mean square error, or the residual estimate obtained from the covariance parameter GLIMMIX output, and *n* is the number of replicates (4 or 5) in a study. The within-study variance for *L* was calculated as in Paul et al. (2008), for each treatment *t*:

$$Var_L = \frac{V_L}{n(\bar{Y}_t{}^2)} \tag{6.10}$$

where V_L is the yield mean square error, or the residual estimate obtained from the covariance parameter GLIMMIX output, $\bar{Y}_t$ is the mean yield of the fungicide treatment, and *n* is the number of replicates (4 or 5) in a study.

A categorical moderator variable, disease pressure group (DIXG), was also generated using the study mean non-treated DIX (Madden et al., 2016). For each study, if the non-treated mean DIX was <40%, then the study was considered to have low disease pressure and was assigned to group 1. If the non-treated mean DIX was ≥40%, then the study was considered to have high disease pressure and was assigned to DIX group 2.

Network meta-analysis of main effects. As multiple treatments of interest were evaluated simultaneously in some trials, a network or multivariate model was fitted to the data (Machado et al., 2017; Paul et al., 2010). The summary results can be described as Y_{ij} for the i^{th} study ($i = 1, \ldots, K$) and j^{th} treatment ($j = 1, \ldots, M$); the vector of responses for the i^{th} study is $\mathbf{Y_i}$ with elements $\bar{X}_t$ (D_t or L_t). For a single study, the response vector is given by:

$$\mathbf{Y} = \begin{bmatrix} \bar{X}_{t1} \\ \bar{X}_{t2} \\ \vdots \\ \bar{X}_{tM} \end{bmatrix}$$

The responses were used in the following network meta-analytic model:

$$\mathbf{Y_i} \sim N(\boldsymbol{\mu}, \boldsymbol{\Sigma} + \mathbf{S_i}) \quad (6.11)$$

where $\mathbf{Y_i}$ has a multivariate normal distribution with a $K \times 1$ mean vector $\boldsymbol{\mu}$ (over K studies) and variance-covariance matrix $\boldsymbol{\Sigma} + \mathbf{S_i}$; $\boldsymbol{\Sigma}$ is either an eight-by-eight or 11-by-11 between-study variance-covariance matrix for fungicide timing or active ingredient treatments, respectively (Machado et al., 2017; Madden et al., 2016; Paul et al., 2010). Vector $\mathbf{S_i}$ is the within-study variance-covariance matrix for the i^{th} study, where the diagonal elements are the within-study variances for each study i and treatment j (s_{ij}^2 = *VarD* or *VarL* see equations 6.9 and 6.10) and the off-diagonal elements are 0 (Madden et al., 2016). The dimensions $\mathbf{Y_i}$ are different for each study i, and are dependent on the number of treatments (either active ingredients or timings) evaluated in that study.

Significant between-study variability was expected due to the large number of studies and variation in methods used at different locations. Study, therefore, was considered a random effect ($\boldsymbol{\Sigma} \neq 0$) in the following analyses, and a random-effects model was used for all subsequent analyses to account for the between-study variability likely present. Heterogeneity assessment was not examined as little advantage from using a fixed-effects model was expected (Madden and Paul, 2011).

Due to the large number of treatments in this study, a heterogeneous variance-covariance structure for $\boldsymbol{\Sigma}$ was used, based on the heterogeneous compound symmetry (CSH) model (Madden et al., 2016). The data from the 25 studies were fitted to the equation 6.11 using the GLIMMIX procedure in SAS, which considered fungicide timing or active ingredient as fixed effects and study as a random effect (Madden et al., 2016). Treatments with $N \geq 10$ mean observations were evaluated, so restricted maximum likelihood was used

to account for the relatively small number of N for some treatments (Madden and Paul, 2011). The within-study variances, the elements of $\mathbf{S_i}$ calculated using equations 6.9 and 6.10, were incorporated into the meta-analytic model by weighting each study by the inverse of the variance ($1/Var_D$ or $1/Var_L$) (Madden and Paul, 2011; Paul et al., 2010). In the parameter statement, the initial estimate for the correlation term was 0.5 and the residual variance was held constant at 1 (Madden et al., 2016).

The standard type III test of fixed effects was performed to evaluate whether the fungicide timing or active ingredient treatment effect was significant at the 5% level. The *lsmeans* statement in GLIMMIX was used to obtain estimates of $\bar{D}_t$ and $\bar{L}_t$, which represent the mean effect sizes of interest across all studies, as well as corresponding standard errors and 95% confidence intervals. The "mult" macro was used to generate letter groupings for all-pairwise comparisons of treatment means according to Fisher's least significant difference determined at the 5% significance level (Piepho, 2004). The means of the log of the response ratio ($\bar{L}_t$) and the corresponding confidence limits, were back-transformed to estimate the mean yield benefit ($\bar{B}_t$) and confidence intervals (across all studies) using the following equation (Machado et al., 2017; Paul et al., 2008)

$$\bar{B}_t = ((\exp(\bar{L}_t)) - 1) \times 100 \quad (6.12)$$

A standard normal test statistic was used to determine whether the mean DIX reductions ($\bar{D}_t$) and yield benefits ($\bar{B}_t$) were significantly different from zero for each treatment (Paul et al., 2008, 2010).

Network meta-analysis of moderator variable. Using the random-effects model, the network analysis was expanded to evaluate the influence of the categorical moderator

variable, DIXG, on the effects of fungicide timing and active ingredient on disease reduction and yield benefit (Madden et al., 2016). The standard type III test of fixed effects was performed to evaluate the whether the treatment x moderator interaction was significant at the α=0.05 significance level. If a significant interaction was identified, then the analysis was conducted separately by DIXG and the means, standard errors, and confidence intervals for $\overline{D}_t$ and/or $\bar{B}_t$ were presented separately by disease pressure group (1 or 2).

Return on investment analyses. Economic analyses were conducted for three of the best-performing fungicide treatment programs. Treatments means for $\bar{L}_t$ values and corresponding between-study variances (or MSE, taken from the covariance parameter estimate output) were used to calculate break-even probabilities over different soybean price scenarios, \$9-14 USD kg^{-1} (\$7-16 USD bu^{-1}). Program prices were calculated for each selected active ingredient by summing the list price (per unit area) and application cost (per unit area), based on the typical application recommendations for each product. The program prices were used to determine the yields required to break even at each soybean price, which were then used to calculate the percentage gain required to break even, using the mean yield across studies of 3,766 kg ha^{-1} (56 bu a^{-1}). The log transformation of the break-even percent gain was used with the treatment $\bar{L}_t$ values and standard deviations [calculated as the sqrt(MSE)] to calculate standard normal z-statistics and corresponding break-even probabilities for a particular fungicide program.

Results

SSR impact on soybean yield. In the 25 site-years (n = 2038 individual plots) used in this analysis, SSR was found to significantly impact soybean yield using a Weibull or

modified logistic model (equations 6.2 and 6.3) ($P < 0.0001$), despite considerable variability across the dataset (Fig. 6.1). The individual plot data appeared nonlinear in nature with an estimated mean upper and lower asymptote at around 4,000 kg ha^{-1} and 1,000 kg ha^{-1}, respectively. Due to these limits, the modified 3-parameter logistic model was found to best describe these data.

The nonlinear regression analysis using the logistic model resulted in the equation:

$$Yield = 4225.3 \text{ kg ha}^{-1} / \left[1 + e^{-(6.86 - 7.72 \times DIX)}\right] \quad (6.13)$$

where yield is expressed in kg ha^{-1}, 4225.3 kg ha^{-1} is the estimated yield potential across the region ($Yield_o$; y-intercept), 6.86 and -7.72 correspond to shape parameters *b* and *c*, and *DIX* is the DIX adjusted to a 0 to 1 scale (see equation 6.3). Model fitting resulted in a pseudo-R^2 of 0.309. According to this model, little yield loss (26-60 kg ha^{-1} or 0.4-0.9 bu a^{-1}) occurred between 25-35% DIX. After 40% DIX, yield decreased more dramatically with considerable yield loss (-697 kg ha^{-1} or -10 bu a^{-1}) beginning at 68% DIX. For every approximate 10% increase in DIX after 65%, there was a corresponding approximate 650 kg ha^{-1} (10 bu a^{-1}) reduction in soybean yield.

The Weibull model resulted in the equation:

$$Yield = 4147.0 \text{ kg ha}^{-1} \times \left(\frac{1 - DIX}{[(1 - 0.57) + 0.57 \times (1 - DIX)]^2}\right) \quad (14)$$

where yield is expressed in kg ha^{-1}, 4147.0 kg ha^{-1} is the estimated yield potential ($yield_o$; y-intercept), 0.57 is the estimate of shape parameter *a*, and *DIX* is the DIX adjusted to a 0 to 1 scale (see equation 6.2). Model fitting resulted in a pseudo-R^2 of 0.298, however, the lower asymptote of the data was not represented by this model. Based on overall model fit and

shape, the modified 3-parameter logistic model was selected to describe the relationship between DIX and soybean yield loss.

DIX and yield distributions for different fungicide active ingredients. Mean DIX and yield varied significantly across the studies (Fig. 6.2A and 6.2B). Despite the variability, treatments which successfully reduced DIX and increased yield, relative to the non-treated control, were identified. The mean non-treated DIX across all studies was 32.8% with a median of 30.5%. Five treatments had mean and median DIX levels lower than the non-treated control (mean: 24.7-29.6%; median: 17.1-28.1%), these include the active ingredients: lactofen (LACT), boscalid (BOSC), picoxystrobin (PICO), prothioconazole and trifloxystrobin (PROT+TRIF), and boscalid and fluxapyroxad/pyraclostrobin (BOSC+FLUX/PYRA). The lowest mean DIX levels were observed from the BOSC and LACT treatments, 27.4% and 24.7%, respectively. The remaining active ingredients, fluazinam (FLUA), fluoxastrobin and flutriafol (FLUO+FLUT), prothioconazole (PROT), tetraconazole (TETR), and thiophanate-methyl (THIM), resulted in means and median DIX levels higher than the non-treated control (mean: 34.2-39.5%; median: 32.5-35.3%).

The mean non-treated yield across all the studies was 3,883.6 kg ha^{-1} (57.7 bu a^{-1}) with a median of 3,850.3 kg ha^{-1} (57.3 bu a^{-1}). Once again, half the treatments resulted in mean yields which were greater than the non-treated control (3,925.6-4,216.6 kg ha^{-1}; 58.4-62.7 bu a^{-1}). These treatments included PICO, PROT, PROT+TRIF, BOSC, and BOSC+FLUX/PYRA. Treatments PICO and BOSC resulted in the highest yields, with means of 4,195.2 and 4,216.6 kg ha^{-1} (62.4 and 62.7 bu a^{-1}), respectively. The remaining active ingredients resulted in mean yields lower than the non-treated control, 3310.7-3,813.3

kg ha^{-1} (49.2-56.7 bu a^{-1}). Only three of these remaining treatments, FLUO+FLUT, LACT, and THIM, also resulted in median yields lower than the non-treated control median yield of 3,850.3 kg ha^{-1} (57.3 bu a^{-1}).

DIX and yield distributions for different fungicide application timings. Mean DIX and yield varied significantly across the studies (Fig. 6.3A and 6.3B). Despite the variability, application timings were identified which successfully reduced DIX and increased yield, relative to the non-treated control. The mean non-treated control DIX, across all studies in the common application timing dataset, was 32.8% with a median of 30.4%. Most application timings resulted in mean and median DIX which were less than the non-treated control (means: 25.6-29.1%; medians: 16.1-29.2%). Only single applications at R1 (beginning flower) and R3 (beginning pod) resulted in means of 33.4 and 40.2% DIX, respectively. Likewise, all fungicide application timings resulted in yields higher than the mean non-treated yield (3,882.9 kg ha^{-1}; 57.7 bu a^{-1}), except the R1 and R2 (full flowering) timings. The R1+R2 double application timing resulted in the highest mean yield (4,249.4 kg ha^{-1}; 63.1 bu a^{-1}) and among the lowest mean DIX levels (27.4%).

Effects of active ingredient on DIX reduction and yield benefit. In this study, significant effects of active ingredient were observed for both DIX reduction ($P < 0.0001$) and yield benefit ($P < 0.0001$). While all active ingredients resulted in overall mean DIX reductions (Table 6.2), LACT, BOSC, PICO, and BOSC+FLUX/PYRA resulted in the highest mean reductions, -19.4 to -13.8% DIX. These treatments were significantly different from 0.00 ($P < 0.0001$) and were not statistically different from one another at the α=0.05

significance level. TETR was the only treatment which resulted in a mean DIX reduction not significantly different from 0.0% or the non-treated control.

All active ingredients were also found to result in positive yield benefits (Supp. Table 6.1). In this analysis, BOSC+FLUX/PYRA, BOSC, PICO, and PROT+TRIF resulted in the highest mean yield benefits (10.7-16.0%) and were not statistically different from one another at the α=0.05 significance level. The LACT treatment, however, resulted in a mean yield benefit of only 5.7% which was not statistically different from 0.0% (P = 0.0753). As this treatment resulted in significant DIX reductions, the yield benefit analyses were conducted using the moderator variable of disease pressure (DIXG) (Table 6.3). While the moderator did not significantly influence the active ingredient effect on yield benefit (χ^2: P = 0.0737), the analysis helped explain the lack of yield benefit observed by LACT. In a high disease pressure situation (non-treated DIX $\geq$ 40%), the LACT treatment resulted in a yield benefit of 16.3% and was significantly different from 0.0% (P = 0.0030). In a low disease pressure situation (non-treated DIX < 40%), however, the LACT herbicide treatment negatively impacts yield (-3.7% benefit). Overall, all active ingredients evaluated resulted in higher mean yield benefits in high disease pressure situations.

Effects of fungicide application timing on DIX reduction and yield benefit. In this study, significant effects of timing were observed for both DIX reduction (P < 0.0001) and yield benefit (P = 0.0009). All fungicide timings resulted in mean disease reductions significantly different from the non-treated control (Table 6.4). The double application timings, R1+R2 and R1+R3, resulted in the greatest DIX reductions, -12.7 and -14.6%, respectively. Applications outside the flowering period, V5 and R5, resulted in among the

least control (-5.7 and -4.8%). While all applications resulted in positive mean yield benefits (Table 6.5), the combination timings also resulted in the highest mean yield benefits (10.8 and 13.2%). Again, the V5 and R5 applications result in the lowest yield benefits of 6.1 and 4.0%, respectively. No significant effects of treatment x moderator were observed (P = 0.9096); treatments, therefore, were evaluated separately but not by disease pressure grouping.

Farmer returns on investment. In return on investment analyses, the three programs of interest were boscalid (single application, R1), picoxystrobin (two applications, R1 and R3), and lactofen (single application). These active ingredients were selected based on their consistent performance in disease reduction and yield benefit, in high disease pressure situations. The calculated list prices were \$115.10 USD ha^{-1} (\$46.04 a^{-1}), \$136.26 ha^{-1} (\$54.50 a^{-1}), and \$40.79 ha^{-1} (\$16.32 a^{-1}) for boscalid (R1), picoxystrobin (R1+R3), and lactofen, respectively. In both high and low disease pressure situations, the lactofen program had the highest probability for farmers to break even on an investment (Fig. 6.4). At low pressure, lactofen had approximately 60% chance of breaking even across all soybean prices; the boscalid and picoxystrobin programs resulted in probabilities between 35 and 50% (Fig. 6.4A). At high pressure, all three programs resulted in break-even probabilities between 80 and 95% across all soybean price scenarios (Fig. 6.4B).

Discussion

Considering the wide variety of chemical products used in SSR management and the substantial number of independent state-specific fungicide trials, a network meta-analysis was desirable to synthesize these evaluations into regionally relevant results. Individual states may experience variable levels of disease, possess unique soybean yield potentials, and all

rely on similar programs for controlling SSR. This study presents standardized yield benefits, relative to each location, and disease control, corrected for local disease pressure, from 25 total site-years such that results are applicable across a growing region. These results can be helpful to researchers and growers when research trials, in a particular location and year, fail to produce results but disease persists in other fields within the state.

Our modified 3-parameter logistic regression model suggests that the increased branching capacity of modern varieties (Suhre et al., 2014) circumvents significant yield impact to SSR at lower disease indices. The selected 3-parameter logistic model (Graybill and Iyer, 1994) appropriately represents the shape of these data, despite wide variability across the dataset, and accounts for the lower asymptote which presumably represents the lower limit of soybean research harvesters. Recently, a similar non-linear model was identified by Fall et al. (2018) to describe soybean yield loss due to SSR in Michigan; these results corroborate with the logistic model identified here which represents 25 site-years of data. Biologically, our model also supports that lower indices (<40%) are indicative of disease on the secondary stems and higher indices (>40%) represent disease affecting the main stem. These observations appropriately reflect the use of the Grau severity rating scale, which distinguishes between disease on the main and secondary stems (1982). Yield impacts, therefore, are greater when disease reaches the main soybean stem, as suggested by the model presented in Figure 6.1. The model also helps us better understand the thresholds for effective SSR control. In low disease pressure situations (<40%), in-season control measures may not be cost effective. Breeding efforts may also benefit from this information, which suggests varieties that consistently result in <40% DIX will likely have competitive yield

performance. The model offers important considerations in an integrated SSR management system.

Furthermore, all products evaluated in this study resulted in overall mean disease reductions, offering some level of control, and potential yield benefits. It is worthwhile to note that while disease pressure was not found to significantly influence treatment effect (P = 0.07), all products resulted in higher yield benefits when used in higher pressure situations. In particular, the lactofen treatment was only found to have positive yield benefits under high SSR pressure, a previously observed phenomenon in soybeans (Dann et al., 1999). These results are also evident in the yield loss model presented, which suggests greater yield impacts are observed at higher disease pressure. In the absence of considerable SSR pressure, no active ingredients evaluated here resulted in a yield benefit over the non-treated yield, with the slight exception of the prothioconazole and trifloxystrobin program. However, it is difficult to assess any potential plant health benefits of this program, other than disease-driven uses, as these results were not observed for fungicides in similar classes. In soybean, strobilurin fungicides were not found to have associated yield benefits in the absence of disease (Swoboda and Pedersen, 2009); the findings presented here further refute the use of fungicides for nonfungicidal effects. Treatments, therefore, will be most effective if applied in areas of high disease potential, i.e. in fields where severe SSR has historically been observed.

In the North Central region, a single application of boscalid (Endura, BASF, Research Triangle Park, NC) or two applications of picoxystrobin (Aproach, DuPont, Wilmington, DE) are standard recommendations for SSR management. In this study, these active

ingredients along with lactofen (Cobra, Valent U.S.A., Walnut Creek, CA) consistently resulted in the highest reductions in SSR and yield benefits, under high disease pressure. According to our model, the potential SSR reductions of 14-19% would sufficiently reduce disease and minimize yield impacts in areas of disease up to 60% DIX. These active ingredients were also found to reduce disease severity indices in fungicide trials conducted in Ohio (Huzar-Novakowiski et al., 2017). No yield benefits were identified in Ohio studies, however, in our studies across six other states yield benefits of 16-23% were observed under high disease pressure. With a mean yield across studies of approximately 3,700 kg ha^{-1} (55 bu a^{-1}), these products could result in potential 850 kg ha^{-1} (13 bu a^{-1}) increases over the non-treated control. Prothioconazole with trifloxystrobin (Proline and Stratego YLD, Bayer Crop Science, Research Triangle Park, NC) and boscalid with fluxapyroxad/pyraclostrobin (Endura and Priaxor, BASF Corporation, Research Triangle Park, NC) also resulted in comparable efficacies and yield gains. These products represent the succinate dehydrogenase inhibitors (SDHI), demethylation inhibitors (DMI), and quinone outside inhibitors (QoI), as well as a protoporphyrinogen oxidase herbicide. These chemical classes are known to prevent infection by acting directly on fungal development or indirectly by either delaying canopy development or promoting plant resistance responses (Dann et al., 1999; Peltier et al., 2012).

The active ingredients fluoxastrobin with flutriafol (Fortix, Arysta Lifescience, Cary, NC), tetraconazole (Domark, Isagro USA, Morrisville, NC), and thiophanate-methyl (Cerexagri-Nisso, King of Prussia, PA) were consistently found to have among the lowest efficacies and yield benefits. Limited SSR control or yield benefit by thiophanate-methyl has

also been observed (Huzar-Novakowiski et al., 2017), and thiophanate-methyl insensitivity has been previously identified as a concern (Lehner et al., 2015; Mueller et al., 2002). However, to our knowledge no *S. sclerotiorum* insensitivity to tetraconazole or fluoxastrobin with flutriafol has been reported. Treatment efficacy may have been affected by a variety of application characteristics (Huzar-Novakowiski et al., 2017). With the high degree of variability observed in the trials analyzed here, including but not limited to sprayer equipment, application rates, varieties, and environments, there may have been factors which impacted the efficacy of these products. Other products tested in similar trials throughout these studies, however, performed well so this variability is unlikely to be the limiting factor. Even though fungicide rate and variety were not considered in these analyses, recommended label rates were most frequently evaluated and susceptible varieties were used in these trials. Further studies should be conducted, using isolates representative of the current regional populations, to identify possible fungicide insensitivity to the less effective active ingredients identified here.

The timing of fungicide applications is also known to be critical in SSR management (Peltier et al., 2012). In these studies, the timing of applications significantly impacted both disease reduction and yield benefit ($P < 0.001$) with double applications during the soybean flowering period resulting in the most control and highest yield gains. Within the flowering window, single applications at R1 and R2 resulted in more disease control than those applied at R3. Applications applied outside the flowering period resulted in the least SSR control and associated yield benefits. These findings corroborate other studies which identified effective application programs within the flowering period (Huzar-Novakowiski et al., 2017; Mueller

et al., 2004). The economics of single and double spray programs were further considered for the best performing products at recommended rates and timings. Under high disease pressures, i.e. in areas with a history of severe SSR epidemics, the two-application picoxystrobin program had comparable probabilities of return on investment to the lactofen and boscalid single application programs. Products which require two applications for effective control, therefore, could be competitive options when the price per unit area is less expensive.

Overall this study generated powerful regional SSR fungicide recommendations, including efficacy and yield benefit information, for incorporation into a grower decision-making tool. In addition, a novel yield loss model was identified that biologically describes SSR epidemics in modern soybean varieties, by considering DIX measurements.

Literature Cited

Allen, T. W., Bradley, C. A., Sisson, Adam, J., Byamukama, E., Chilvers, M. I., Coker, C. M., et al. (2017). Soybean yield loss estimates due to diseases in the United States and Ontario, Canada from 2010 to 2014. *Plant Heal. Prog.* doi:10.1094/PHP-RS-16-0030.

Armando, Q., Armenta, A., Mondaca, E. C., Ángel, M., Sánchez, A., Manuel, V., et al. (2015). Efectividad de fungicidas convencionales y biorracionales sobre *Sclerotinia sclerotiorum* in vitro. 2149–2156.

Boland, G. J., and Hall, R. (1994). Index of plant hosts of *Sclerotinia sclerotiorum*. *Can. J. Plant Pathol.* 16, 93–108.

Carey, G. (2013). "Nonlinear models," in *Quantitative methods in neuroscience* (Boulder, CO), 289–310.

Chism, W. J., Birch, J. B., and Bingham, S. W. (1992). Nonlinear regressions for analyzing growth stage and quinclorac interactions. *Weed Technol.* 6, 898–903.

Chun, D., Kao, L. B., Lockwood, J. L., and Isleib, T. G. (1987). Laboratory and field assessment of resistance in soybean to stem rot caused by *Sclerotinia sclerotiorum*. *Plant Dis.* 71, 811–815.

Danielson, G. A., Nelson, B. D., and Helms, T. C. (2004). Effect of Sclerotinia stem rot on yield of soybean inoculated at different growth stages. *Plant Dis.* 88, 297–300.

Dann, E. K., Diers, B. W., and Hammerschmidt, R. (1999). Suppression of Sclerotinia stem rot of soybean by lactofen herbicide treatment. *Phytopathology* 89, 598–602. doi:10.1094/PHYTO.1999.89.7.598.

Di, Y. L., Zhu, Z. Q., Lu, X. M., and Zhu, F. X. (2016). Baseline sensitivity and efficacy of trifloxystrobin against Sclerotinia sclerotiorum. *Crop Prot.* 87, 31–36. doi:10.1016/j.cropro.2016.04.020.

Fall, M. F., Boyse, J. F., Wang, D., Willbur, J. F., Smith, D. L., and Chilvers, M. I. (2018). Case study of an epidemiological approach dissecting historical soybean Sclerotinia stem rot observations and identifying environmental predictors of epidemics and yield loss. *Phytopathology* XX, XX–XX.

Fehr, W. R., Caviness, C. E., Burmood, D. T., and Pennington, J. S. (1971). Stage of development descriptions for soybeans, *Glycine max* (L.) Merill. *Crop Sci.* 11, 929–931.

Grau, C. R., and Hartman, G. L. (2015). *Compendium of soybean diseases*. 5th ed. , eds. G. L. Hartman, J. C. Rupe, E. J. Sikora, L. L. Domier, J. A. Davis, and K. L. Steffey St Paul, MN: The American Phytopathological Society.

Grau, C., Radke, V., and Gillespie, F. (1982). Resistance of soybean cultivars to *Sclerotinia sclerotiorum*. *Plant Dis.* 66, 506–508.

Graybill, F. a, and Iyer, H. K. (1994). "Nonlinear regression," in *Regression analysis: concepts and applications* (Duxbury Pr), 599–625.

Hedges, L. V., Gurevitch, J., and Curtis, P. S. (1999). The meta-analysis of response ratios in experimental ecology. *Ecology* 80, 1150–1156. doi:10.2307/177062.

Hoffman, D. D., Hartman, G. L., Mueller, D. S., Leitz, R. A., Nickell, C. D., and Pedersen, W. L. (1998). Yield and seed quality of soybean cultivars infected with *Sclerotinia sclerotiorum*. *Plant Dis.* 82, 826–829.

Huzar-Novakowiski, J., Paul, P. A., and Dorrance, A. E. (2017). Host resistance and chemical control for management of Sclerotinia stem rot of soybean in Ohio. *Phytopathology* XX, XX–XX. doi:10.1165/rcmb.2012-0347OC.

Kim, H. S., Hartman, G. L., Manandhar, J. B., Graef, G. L., Steadman, J. R., and Diers, B. W. (2000). Reaction of soybean cultivars to Sclerotinia stem rot in field, greenhouse, and laboratory evaluations. *Crop Sci.* 40, 665–669.

Koenning, S. R., and Wrather, J. A. (2010). Suppression of soybean yield potential in the continental United States by plant diseases from 2006 to 2009. *Plant Heal. Prog.* doi:10.1094/PHP-2010-1122-01-RS.Abstract.

Lehner, M. S., Paula Júnior, T. J., Silva, R. A., Vieira, R. F., Carneiro, J. E. S., Schnabel, G., et al. (2015). Fungicide sensitivity of Sclerotinia sclerotiorum: A thorough assessment using discriminatory dose, EC50, high-resolution melting analysis, and description of new point mutation associated with thiophanate-methyl resistance. *Plant Dis.* 99, 1537–1543. doi:10.1094/PDIS-11-14-1231-RE.

Lehner, M. S., Pethybridge, S. J., Meyer, M. C., and Del Ponte, E. M. (2016). Meta-analytic modelling of the incidence-yield and incidence-sclerotial production relationships in soybean white mould epidemics. *Plant Pathol.* doi:10.1111/ppa.12590.

Liang, H. J., Di, Y. L., Li, J. L., and Zhu, F. X. (2015). Baseline sensitivity and control efficacy of fluazinam against Sclerotinia sclerotiorum. *Eur. J. Plant Pathol.* 142, 691–699. doi:10.1007/s10658-015-0644-5.

Machado, F. J., Fitopatologia, D. De, and Viçosa, U. F. De (2017). Quantitative review of the effects of triazole and benzimidazole fungicides on Fusarium head blight and wheat yield in Brazil. 1633–1641. doi:10.1094/PDIS-03-17-0340-RE.

Madden, L. V, Hughes, G., and van den Bosch, F. (2007). "Epidemics and crop yield," in *The study of plant disease epidemics* (St Paul, MN: The American Phytopathological Society), 353–366.

Madden, L. V, and Paul, P. A. (2011). Meta-analysis for evidence synthesis in plant pathology: an overview. *Phytopathology* 101, 16–30. doi:10.1094/PHYTO-03-10-0069.

Madden, L. V, Piepho, H., and Paul, P. A. (2016). Statistical models and methods for network meta-analysis. *Phytopathology* 106, 792–806.

Mueller, D. S., Bradley, C. A., Grau, C. R., Gaska, J. M., Kurle, J. E., and Pedersen, W. L. (2004). Application of thiophanate-methyl at different host growth stages for management of Sclerotinia stem rot in soybean. *Crop Prot.* 23, 983–988. doi:10.1016/j.cropro.2004.02.013.

Mueller, D. S., Dorrance, A. E., Derksen, R. C., Ozkan, E., Kurle, J. E., Grau, C. R., et al. (2002). Efficacy of fungicides on Sclerotinia sclerotiorum and their potential for control of Sclerotinia stem rot on soybean. *Plant Dis.* 86, 26–31. doi:10.1094/PDIS.2002.86.1.26.

Paul, P. A., Lipps, P. E., Hershman, D. E., McMullen, M. P., Draper, M. A., and Madden, L. V. (2008). Efficacy of triazole-based fungicides for Fusarium head blight and deoxynivalenol control in wheat: a multivariate meta-analysis. *Phytopathology* 98, 999–1011. doi:10.1094/PHYTO-98-9-0999.

Paul, P. A., Mcmullen, M. P., Hershman, D. E., and Madden, L. V (2010). Meta-analysis of the effects of triazole-based fungicides on wheat yield and test weight as influenced by Fusarium head blight intensity. *Phytopathology* 100, 160–171.

Peltier, A. J., Bradley, C. A., Chilvers, M. I., Malvick, D. K., Mueller, D. S., Wise, K. A., et al. (2012). Biology, yield loss and control of Sclerotinia stem rot of soybean. *J. Integr. Pest Manag.* 3, 1–7. doi:10.1603/IPM11033.

Piepho, H.-P. (2004). An algorithm for a letter-based representation of all-pairwise comparisons. *J. Comput. Graph. Stat.* 13, 456–466. doi:10.1198/1061860043515.

Suhre, J. J., Weidenbenner, N. H., Rowntree, S. C., Wilson, E. W., Naeve, S. L., Conley, S. P., et al. (2014). Soybean yield partitioning changes revealed by genetic gain and

seeding rate interactions. *Agron. J.* 106, 1631–1642. doi:10.2134/agronj14.0003.

Swoboda, C., and Pedersen, P. (2009). Effect of fungicide on soybean growth and yield. *Agron. J.* 101, 352–356. doi:10.2134/agronj2008.0150.

Tinsley, N. A., Estes, R. E., and Gray, M. E. (2012). Validation of a nested error component model to estimate damage caused by corn rootworm larvae. *J. Appl. Entomol.*, 1–9. doi:10.1111/j.1439-0418.2012.01736.x.

United States Department of Agriculture - National Agricultural Statistics Service (USDA-NASS) (2017). *United States soybean prices* USDA-NASS, Washington, DC.

Wrather, A., and Koenning, S. (2009). Effects of diseases on soybean yields in the United States 1996 to 2007. *Plant Heal. Prog.* doi:10.1094/PHP-2009-0401-01-RS.Abstract.

Yang, X. B., Lundeen, P., and Uphoff, M. D. (1999). Soybean varietal response and yield loss caused by *Sclerotinia sclerotiorum*. *Plant Dis.* 83, 456–461.

Tables and Figures

Table 6.1. Common (N ≥ 10) fungicide active ingredients and fungicide timings, evaluated in Sclerotinia stem rot fungicide efficacy trials in the North Central US from 2009-2016, and used in network meta-analyses of treatment effects on disease severity index (DIX) reduction and soybean yield benefit.

Fungicide Treatments	**Abbreviation**	***K*[a]**	**N[b]**
Active ingredient			
boscalid	BOSC	23	60
boscalid+fluxapyroxad/pyraclostrobin	BOSC+FLUX/PYRA	8	12
fluazinam	FLUA	11	17
fluoxastrobin+flutriafol	FLUO+FLUT	7	15
lactofen	LACT	14	26
picoxystrobin	PICO	21	63
prothioconazole	PROT	14	30
prothioconazole+trifloxystrobin	PROT+TRIF	13	26
tetraconazole	TETR	15	30
thiophanate-methyl	THIM	15	42
non-treated control	CONTROL	25	38
Timing			
fifth trifoliate	V5	7	13
beginning flower	R1	24	211
full flower	R2	4	20
beginning pod	R3	19	71
beginning seed	R5	5	10
beginning and full flower	R1+R2	6	10
beginning flower and pod	R1+R3	18	81
non-treated control	CONTROL	25	38

[a]Total number of studies (trials) used to evaluate each treatment.

[b]Total number of mean observations, generated from the primary analysis of variance, and used to evaluate each treatment in network meta-analyses.

Table 6.2. Network meta-analytic estimates of effect size ($\bar{D}_t$) which is the mean reduction of disease severity index (DIX) in treated soybean plots, relative to non-treated plots, and corresponding statistics for common active ingredients used in Sclerotinia stem rot fungicide efficacy trials in the North Central US from 2009-2016.

AI[a]	K[b]	N[c]	$\bar{D}_t$[d]	SE($\bar{D}_t$)[e]	Z[f]	P[g]	CL_L[h]	CL_U[i]
LACT	14	26	-19.35 g[j]	4.07	4.75	<0.0001	-27.40	-11.30
BOSC	23	60	-15.82 fg	2.57	6.15	<0.0001	-20.90	-10.73
PICO	21	63	-13.83 efg	2.48	5.58	<0.0001	-18.72	-8.94
BOSC+FLUX/PYRA	8	12	-13.81 eg	2.97	4.65	<0.0001	-19.68	-7.94
FLUA	11	17	-12.50 def	2.48	5.05	<0.0001	-17.39	-7.61
PROT+TRIF	13	26	-11.38 cde	2.52	4.52	<0.0001	-16.35	-6.41
PROT	14	30	-8.23 bcd	2.01	4.09	<0.0001	-12.20	-4.25
THIM	15	42	-7.75 bc	1.62	4.79	<0.0001	-10.95	-4.55
FLUO+FLUT	7	15	-7.20 bcd	2.46	2.92	0.0017	-12.07	-2.33
TETR	15	30	-2.90 ab	3.11	0.93	0.1758	-9.03	3.24
CONTROL	25	38	0.05 a	0.16	0.28	0.3896	-0.28	0.37

[a]Active ingredients LACT = lactofen, BOSC = boscalid, PICO = picoxystrobin, BOSC+FLUX/PYRA = boscalid and fluxapyroxad+pyraclostrobin, FLUA = fluazinam, PROT+TRIF = prothioconazole and trifloxystrobin, PROT = prothioconazole, THIM = thiophanate-methyl, FLUO+FLUT = fluoxastrobin and flutriafol, TETR = tetraconazole, CONTROL = non-treated control.

[b]Total number of studies (trials) used in the analysis.

[c]Total number of mean observations used in the analysis.

[d]Effect size ($\bar{D}$) is the mean difference in DIX (%) across all studies for each fungicide treatment relative to the non-treated check calculated (see equation 6.5).

[e]Standard error of $\bar{D}_t$ (SE($\bar{D}_t$)) generated from the network meta-analysis.

[f]Standard normal (Z) statistic, calculated by mean effect size divided by the standard error of the effect size or $\bar{D}_t$/ SE($\bar{D}_t$).

[g]Probability (P) value against the null hypothesis that a mean estimate is equal to zero (at the α=0.05 significance level); $P < 0.0001$ indicates strong evidence of a mean estimate significantly different from zero.

[h]Lower (CL_L) limit of the 95% confidence interval around $\bar{D}_t$.

[i]Upper (CL_U) limit of the 95% confidence interval around $\bar{D}_t$.

[j]Means evaluated using Fisher's least significant difference; means followed by the same letter are not different at the $\alpha = 0.05$ significance level.

Table 6.3. Moderator influence of disease severity index grouping (G) on network meta-analytic estimates of the log of response ratio ($\bar{L}_t$), or effect size, and back-calculated percent yield benefit ($\bar{B}_t$) in treated soybean plots, relative to non-treated plots, with corresponding statistics for common active ingredients used in Sclerotinia stem rot fungicide efficacy trials in the North Central US from 2009-2016.

			Effect size[d]						**Mean Yield Benefit (%)[e]**		
AI[a]	**G[b]**	**N[c]**	$\bar{L}_t$	**SE($\bar{L}_t$)**	**Z**	***P***	CL_L	CL_U	$\bar{B}_t$	CL_L	CL_U
BOSC+FLUX/ PYRA	1	7	0.08	0.05	1.75	0.0404	-0.02	0.18	8.20	-2.34	19.87
BOSC	1	29	0.06	0.04	1.62	0.0525	-0.02	0.13	5.90	-1.59	13.96
PICO	1	33	0.05	0.04	1.37	0.0857	-0.03	0.13	5.17	-2.58	13.53
LACT	1	15	-0.04	0.05	0.74	0.2285	-0.15	0.07	-3.71	-13.60	7.32
FLUA	1	7	0.04	0.04	1.15	0.1244	-0.04	0.12	4.48	-3.45	13.07
PROT+TRIF	1	12	0.07	0.03	2.17	0.0149	0.00	0.14	7.51	0.27	15.27
FLUO+FLUT	1	7	0.04	0.03	1.45	0.0739	-0.03	0.11	4.26	-2.60	11.59
PROT	1	14	0.03	0.02	1.26	0.1030	-0.02	0.08	3.04	-1.93	8.27
THIM	1	15	0.05	0.03	1.52	0.0638	-0.02	0.11	4.74	-1.73	11.63
TETR	1	16	0.00	0.03	0.13	0.4477	-0.07	0.08	0.44	-6.67	8.10
CONTROL	1	23	0.00	0.01	0.25	0.4028	-0.02	0.02	0.25	-1.75	2.30
BOSC+FLUX/ PYRA	2	5	0.23	0.05	4.32	<0.0001	0.11	0.34	25.32	12.00	40.23
BOSC	2	31	0.20	0.04	5.72	<0.0001	0.13	0.28	22.64	13.86	32.10
PICO	2	30	0.19	0.04	5.21	<0.0001	0.12	0.27	21.48	12.41	31.30
LACT	2	11	0.15	0.05	2.74	0.0030	0.03	0.27	16.25	3.45	30.63

FLUA	2	10	0.14	0.04	3.74	0.0001	0.06	0.22	14.84	6.36	24.02
PROT+TRIF	2	14	0.13	0.03	4.09	<0.0001	0.06	0.20	13.94	6.59	21.80
FLUO+FLUT	2	8	0.11	0.03	3.68	0.0001	0.04	0.19	11.91	3.95	20.48
PROT	2	16	0.10	0.02	4.60	<0.0001	0.06	0.15	10.88	5.75	16.26
THIM	2	27	0.09	0.03	2.71	0.0033	0.02	0.16	9.22	2.03	16.92
TETR	2	14	0.03	0.04	0.83	0.2044	-0.05	0.12	3.37	-5.07	12.56
CONTROL	2	15	0.01	0.01	0.53	0.2985	-0.02	0.04	0.75	-2.00	3.57

[a]Active ingredients BOSC+FLUX/PYRA = boscalid and fluxapyroxad+pyraclostrobin, BOSC = boscalid, PICO = picoxystrobin, LACT = lactofen, FLUA = fluazinam, PROT+TRIF = prothioconazole and trifloxystrobin, FLUO+FLUT = fluoxastrobin and flutriafol, PROT = prothioconazole, THIM = thiophanate-methyl, TETR = tetraconazole, CONTROL = non-treated control.

[b]Disease severity index (DIX) grouping (G): 1 indicates the mean DIX of the non-treated control < 40% (low disease pressure), and 2 indicates a non-treated mean DIX ≥ 40% (high disease pressure).

[c]Total number of mean observations used in the analysis.

[d] Mean log of the response ratio ($\bar{L}_t$), across all studies, for each fungicide treatment relative to the non-treated check (individual study L_t calculated using equation 6.8); standard error of $\bar{L}_t$ (SE($\bar{L}_t$)); Z (standard normal) statistic and the probability (*P*) value against the null hypothesis that a mean estimate is equal to zero (at the α=0.05 significance level); lower (CL_L) and upper (CL_U) limits of the 95% confidence interval around $\bar{L}_t$.

[e]Mean estimated yield benefit ($\bar{B}_t$), across all studies, and lower (CL_L) and upper (CL_U) limits of the 95% confidence interval around $\bar{B}_t$, back-calculated using equation 6.12.

Table 6.4. Network meta-analytic estimates of effect size ($\overline{D}_t$) which is the mean reduction of disease severity index (DIX) in treated soybean plots, relative to non-treated plots, and corresponding statistics for common fungicide timings (shown as soybean growth stages) used in Sclerotinia stem rot fungicide efficacy trials in the North Central US from 2009-2016.

TIMING[a]	K[b]	N[c]	$\overline{D}_t$[d]		SE($\overline{D}_t$)[e]	Z[f]	P[g]	CL_L[h]	CL_U[i]
V5	7	13	-5.72	bc[j]	1.52	3.76	0.0001	-8.74	-2.70
R1	24	211	-9.94	cd	1.97	5.04	<0.0001	-13.85	-6.03
R2	4	20	-8.74	bcde	3.71	2.36	0.0092	-16.09	-1.38
R1+R2	6	10	-12.75	de	1.95	6.55	<0.0001	-16.61	-8.89
R1+R3	18	81	-14.60	e	2.26	6.47	<0.0001	-19.08	-10.13
R3	19	71	-7.66	bc	1.51	5.06	<0.0001	-10.66	-4.66
R5	5	10	-4.76	b	1.22	3.90	<0.0001	-7.19	-2.34
CONTROL	25	38	-0.10	a	0.17	0.59	0.2776	-0.43	0.23

[a]Soybean growth stages at which fungicides were applied: V5 (fifth trifoliate), R1 (beginning flower), R2 (full flower), R1+R2 (beginning and full flower), R1+R3 (beginning flower and pod), R3 (beginning pod), R5 (beginning seed), CONTROL (non-treated control).

[b]Number of studies (trials) used in the analysis.

[c]Number of mean observations used in the analysis.

[d]Effect size ($\overline{D}_t$) or the mean difference in DIX (%), across all studies, for each fungicide treatment relative to the non-treated check (individual study D_t calculated using equation 6.5).

[e]Standard error of $\overline{D}_t$ (SE($\overline{D}_t$)) generated from the network meta-analysis.

[f]Standard normal (Z) statistic, calculated by mean effect size divided by the standard error of the effect size or $\overline{D}_t$ / SE($\overline{D}_t$).

[g]Probability (*P*) value against the null hypothesis that a mean estimate is equal to zero (at the α=0.05 significance level); $P < 0.0001$ indicates strong evidence of a mean estimate significantly different from zero.

[h]Lower (CL_L) limit of the 95% confidence interval around $\overline{D}_t$.

[i]Upper (CL_U) limit of the 95% confidence interval around $\overline{D}_t$.

[j]Means were evaluated using Fisher's least significant difference; means followed by the same letter are not different at the $\alpha = 0.05$ significance level.

Table 6.5. Network meta-analytic estimates of effect size ($\bar{L}_t$), or effect size, and back-calculated percent yield benefit ($\bar{B}_t$) in treated soybean plots, relative to non-treated plots, with corresponding statistics for fungicide timings (shown as soybean growth stages) used in Sclerotinia stem rot fungicide efficacy trials in the North Central US from 2009-2016.

			Effect size[d]						Mean Yield Benefit (%)[e]		
TIMING[a]	K[b]	N[c]	$\bar{L}_t$		SE($\bar{L}_t$)	Z	*P*	CL_L	CL_U	$\bar{B}_t$	CL_L	CL_U
V5	7	13	0.06	bcd[f]	0.04	1.69	0.0458	-0.01	0.13	6.14	-1.04	13.85
R1	24	211	0.09	abc	0.02	3.62	0.0001	0.04	0.14	9.28	4.09	14.73
R2	4	20	0.06	abcd	0.03	1.84	0.0332	0.00	0.13	6.26	-0.49	13.46
R1+R2	6	10	0.10	ab	0.02	4.60	<0.0001	0.06	0.15	10.83	6.02	15.86
R1+R3	18	81	0.12	a	0.03	4.17	<0.0001	0.07	0.18	13.24	6.74	20.13
R3	19	71	0.06	bc	0.02	2.97	0.0015	0.02	0.10	6.31	2.05	10.75
R5	5	10	0.04	c	0.01	2.60	0.0046	0.01	0.07	3.97	0.93	7.11
CONTROL	25	38	0.00	d	0.01	0.51	0.3036	-0.01	0.02	0.43	-1.21	2.09

[a]Soybean growth stages at which fungicides were applied: V5 (fifth trifoliate), R1 (beginning flower), R2 (full flower), R1+R2 (beginning and full flower), R1+R3 (beginning flower and pod), R3 (beginning pod), R5 (beginning seed), CONTROL (non-treated control).

[b]Number of studies (trials) used in the analysis.

[c]Number of mean observations used in the analysis.

[d]Mean log of the response ratio ($\bar{L}_t$), across all studies, for each fungicide treatment relative to the non-treated check (individual study L_t calculated using equation 6.8); standard error of $\bar{L}_t$ (SE($\bar{L}_t$)); Z (standard normal) statistic and the probability (*P*) value against the null hypothesis that a mean estimate is equal to zero (at the α=0.05 significance level); lower (CL_L) and upper (CL_U) limits of the 95% confidence interval around $\bar{L}_t$.

[e]Back-calculated mean estimated yield benefit ($\bar{B}_t$), across all studies, and lower (CL_L) and upper (CL_U) limits of the 95% confidence interval around $\bar{B}_t$, calculated from $\bar{L}$ using equation 6.12.

[f]Means were evaluated using Fisher's least significant difference; means followed by the same letter are not different at the α = 0.05 significance level.

Supplementary Table 6.1. Network meta-analytic estimates of log of response ratio ($\bar{L}_t$), or effect size, and back-calculated percent yield benefit ($\bar{B}_t$) in treated soybean plots, relative to non-treated plots, with corresponding statistics for common active ingredients used in Sclerotinia stem rot fungicide efficacy trials in the North Central US from 2009-2016.

			Effect size[d]						Mean Yield Benefit (%)[e]		
AI[a]	K[b]	N[c]	$\bar{L}_t$	SE($\bar{L}_t$)	*Z*	*P*	CL_L	CL_U	$\bar{B}_t$	CL_L	CL_U
BOSC+ FLUX/ PYRA	8	12	0.15	a[f]	0.04	4.16	<0.0001	0.08	0.22	16.01	8.11	24.50
BOSC	23	60	0.13	ab	0.03	4.56	<0.0001	0.07	0.19	13.92	7.66	20.53
PICO	21	63	0.12	ac	0.03	4.15	<0.0001	0.06	0.18	12.83	6.54	19.49
PROT+ TRIF	13	26	0.10	a-d	0.02	4.50	<0.0001	0.06	0.15	10.72	5.88	15.78
FLUA	11	17	0.09	b-d	0.03	3.35	0.0004	0.04	0.14	9.20	3.68	15.00
FLUO+ FLUT	7	15	0.08	cd	0.02	4.32	<0.0001	0.04	0.11	8.04	4.29	11.93
THIM	15	42	0.07	d	0.02	2.99	0.0014	0.02	0.11	7.08	2.34	12.04
PROT	14	30	0.07	d	0.02	4.01	<0.0001	0.03	0.10	7.04	3.51	10.69
LACT	14	26	0.06	de	0.04	1.44	0.0753	-0.02	0.13	5.70	-2.05	14.08
TETR	15	30	0.03	e	0.02	1.27	0.1019	-0.02	0.07	2.91	-1.58	7.61
CONT-ROL	25	38	0.00	e	0.01	0.52	0.3011	-0.01	0.02	0.43	-1.20	2.09

[a]Active ingredients BOSC+FLUX/PYRA = boscalid and fluxapyroxad+pyraclostrobin, BOSC = boscalid, PICO = picoxystrobin, PROT+TRIF = prothioconazole and trifloxystrobin, FLUA = fluazinam, FLUO+FLUT = fluoxastrobin and flutriafol, THIM = thiophanate-methyl, PROT = prothioconazole, LACT = lactofen, TETR = tetraconazole, CONTROL = non-treated control.

[b]Number of studies (trials) used in the analysis.

[c]Number of mean observations used in the analysis.

[d]Mean log of the response ratio ($\bar{L}_t$), across all studies, for each fungicide treatment relative to the non-treated check (individual study L_t calculated using equation 6.8); standard error of $\bar{L}_t$ (SE($\bar{L}_t$)); Z (standard normal) statistic and the probability (P) value against the null hypothesis that a mean estimate is equal to zero (at the α=0.05 significance level); lower (CL_L) and upper (CL_U) limits of the 95% confidence interval around $\bar{L}_t$.

[e]Back-calculated mean estimated yield benefit ($\bar{B}_t$), across all studies, and lower (CL_L) and upper (CL_U) limits of the 95% confidence interval around $\bar{B}_t$, calculated from $\bar{L}_t$ using equation 6.12.

[f]Means were evaluated using Fisher's least significant difference; means followed by the same letter are not different at the α = 0.05 significance level.

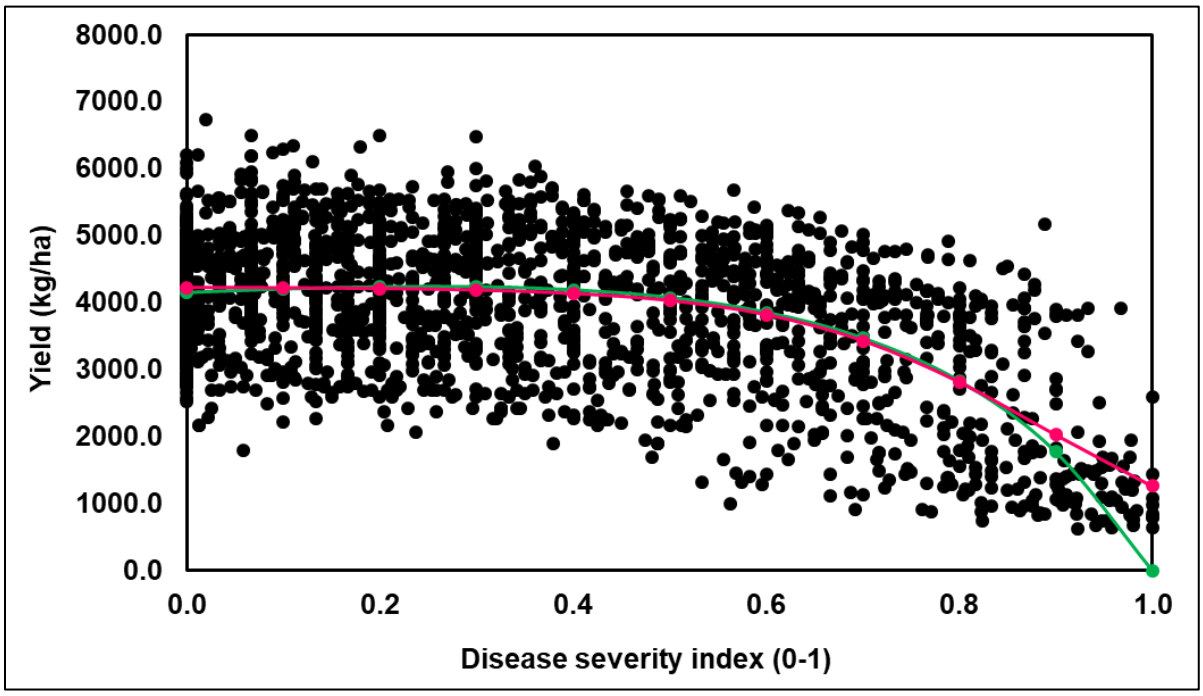

Figure 6.1. Soybean yield (kg/ha) results for raw plot data (n = 2038) collected in 25 site-years of Sclerotinia stem rot (SSR) fungicide evaluations, conducted from 2009 to 2016 and in Illinois, Iowa, Michigan, Minnesota, New Jersey, and Wisconsin. Disease severity index (DIX) was calculated using percent disease incidence (DI) and disease severity of symptomatic soybeans (DS), see equation 6.1. Percent DIX was converted to a 0-1 scale (X) for this analysis. The 3-parameter logistic model used to describe soybean yield as DIX increases is represented by the pink trendline (Equation 13): yield = 4,225.3 kg/ha ÷ (1 + exp(-(6.86 – 7.72×*DIX*))) (Pseudo-R^2 = 0.309). The 2-parameter Weibull model is represented by the green trendline (Equation 14): yield = (4147.0 kg/ha) × [(1 - *DIX*) ÷ ((1 – 0.57) + 0.57×(1 – *DIX*))^2] (Pseudo-R2 = 0.298).

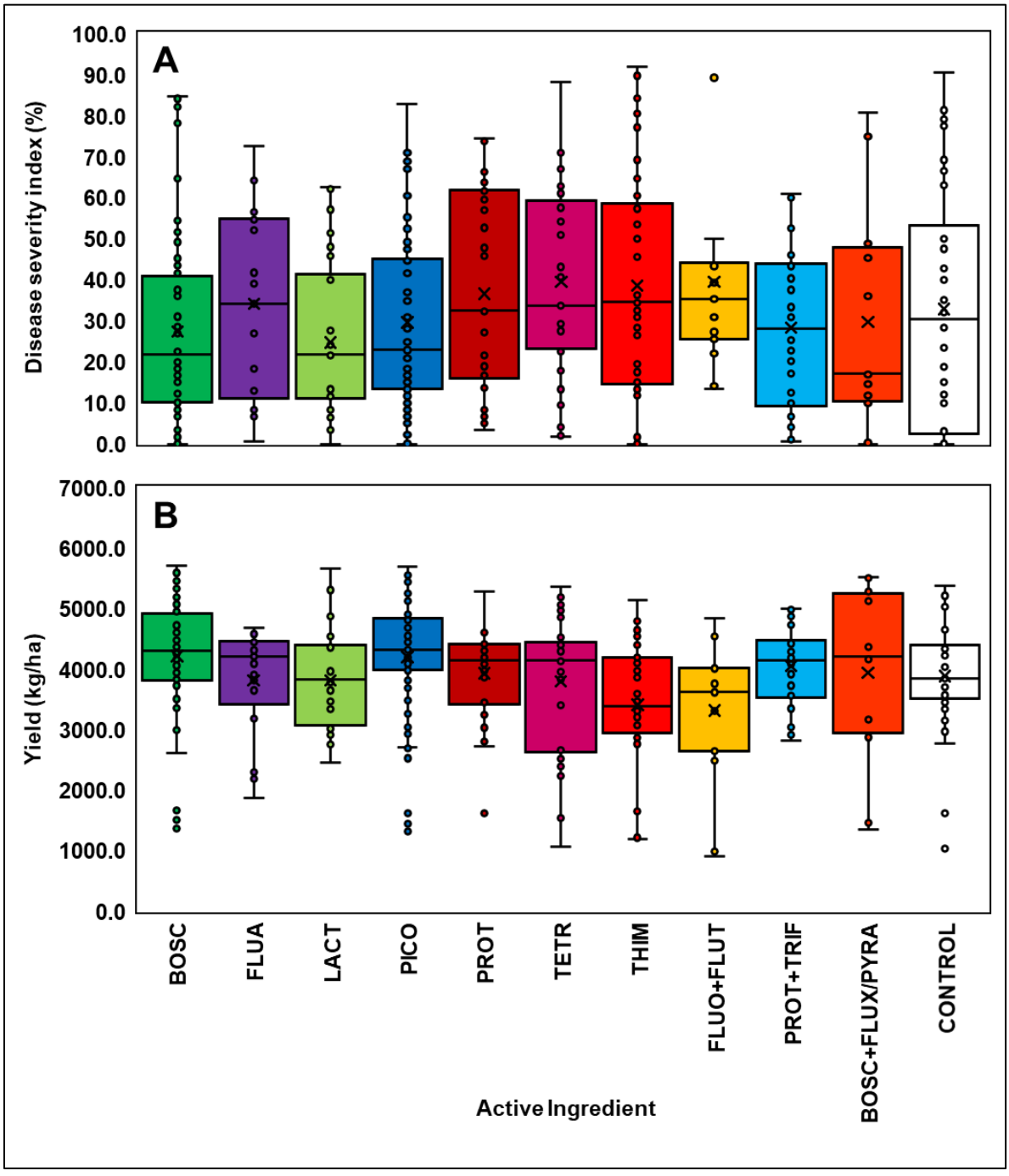

Figure 6.2.

Box plot distributions of mean **A,** disease severity index (DIX) and **B,** yield (kg/ha) for common ($k \geq 10$ mean observations) active ingredients used in 25 site-years of replicated (4

to 5) Sclerotinia stem rot (SSR) fungicide evaluations. Treatments shown include boscalid (BOSC), fluazinam (FLUA), lactofen (LACT), picoxystrobin (PICO), prothioconazole (PROT), tetraconazole (TETR), thiophanate-methyl (THIM), fluoxastrobin and flutriafol (FLUO+FLUT), prothioconazole and trifloxystrobin (PROT+TRIF), boscalid and fluxapyroxad+pyraclostrobin (BOSC+FLUX/PYRA), and a non-treated control (CONTROL). Disease severity index (DIX) was calculated using percent disease incidence (DI) and disease severity of symptomatic soybeans, see equation 6.1. The line within the box indicates the median, the x corresponds to the mean, the box represents 50% of the data (between the 1^{st} and 3^{rd} quartiles), the vertical bars represent the minimum and maximum values, and the circles outside the vertical bars indicate outliers.

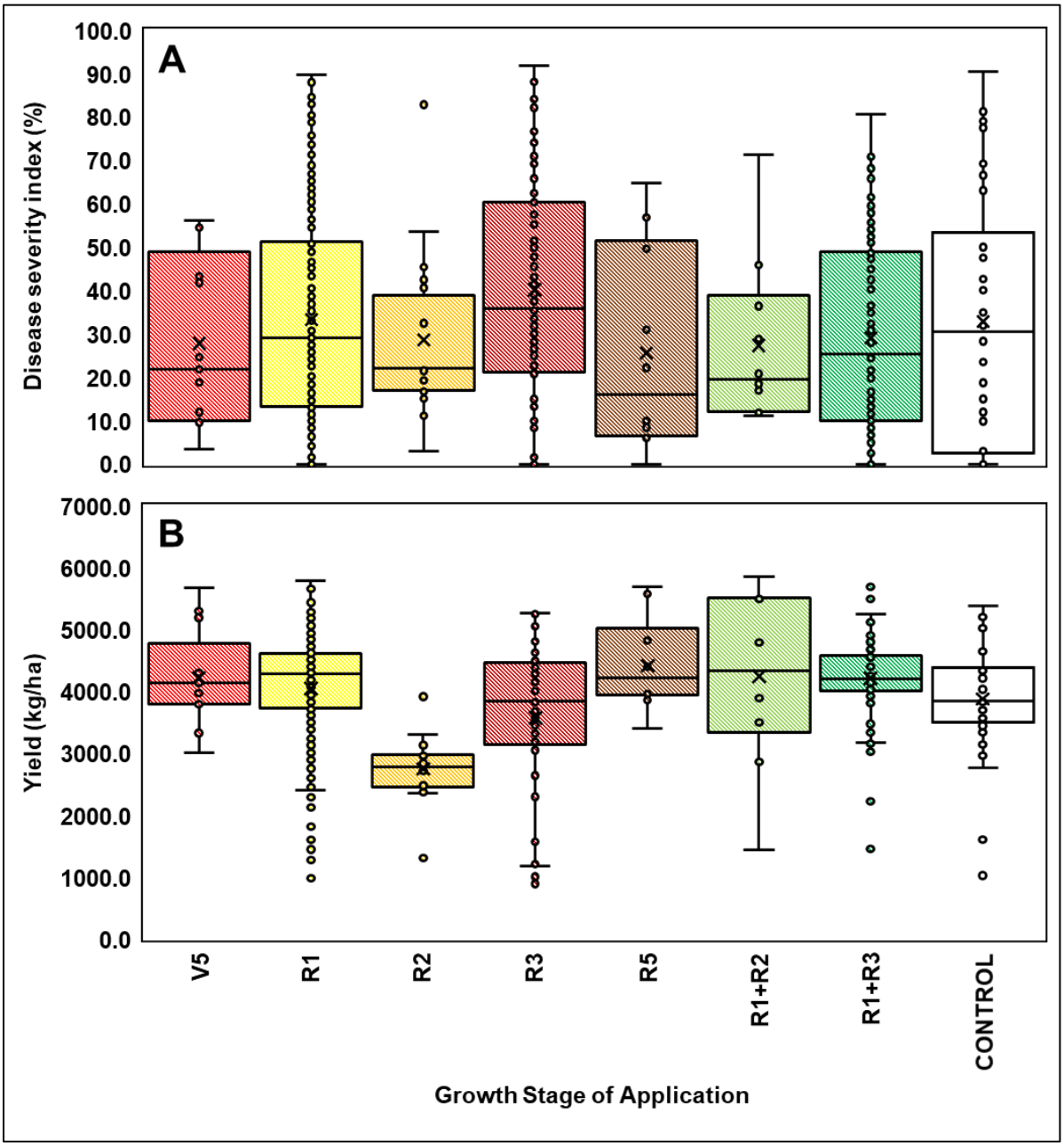

Figure 6.3. Box plot distributions of mean **A,** disease severity index (DIX) and **B,** yield (kg/ha) for common ($k \geq 10$ mean observations) fungicide timings used in 25 site-years of replicated (4 to 5) Sclerotinia stem rot (SSR) fungicide evaluations. Fungicides were applied at the fifth trifoliate (V5), beginning flower (R1), full flower (R2), beginning pod (R3),

beginning seed (R5), beginning and full flower (R1+R2), beginning flower and pod (R1+R3), or non-treated (CONTROL). Disease severity index (DIX) was calculated using percent disease incidence (DI) and disease severity (DS) of symptomatic soybeans, see equation 6.1. The line within the box indicates the median, the x corresponds to the mean, the box represents 50% of the data (between the 1st and 3rd quartiles), the vertical bars represent the minimum and maximum values, and the circles outside the vertical bars indicate outliers.

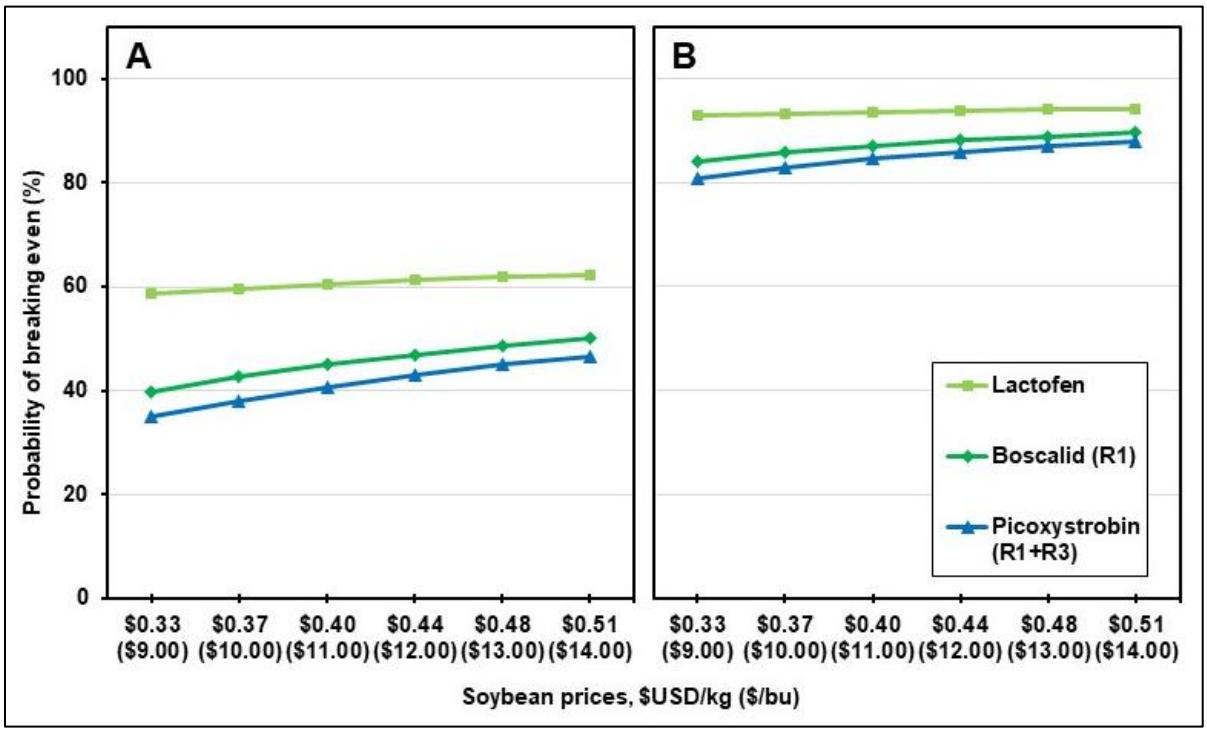

Figure 6.4. The probability of breaking even using three selected fungicide programs in **A,** high Sclerotinia stem rot (SSR) pressure and **B,** low SSR pressure scenarios. Program prices, combined list price and application cost, and yield benefit results were used to calculate the probability of farmers breaking even on an investment using these well-performing active ingredients. Probabilities were calculated over soybean prices from $0.33 to $0.51 USD/kg (or $9.00 to $14.00 USD/bu).

CHAPTER 7: Characterizing the effect of foliar lipo-chitooligosaccharide application on sudden death syndrome and Sclerotinia stem rot in soybean

D.A. Marburger and J.F. Willbur share first authorship. In the following chapter, a double-asterisk (**) indicates contributions by J.F. Willbur.

Abstract

Lipo-chitooligosaccharides (LCOs) are signal molecules produced by plant root endosymbionts and have been identified, formulated, and marketed as growth promoting adjuvants for soybean [*Glycine max* (L.) Merr.]. Experiments were conducted under controlled environmental conditions to characterize the effects of foliar LCO applications on early symptom development of sudden death syndrome (SDS), caused by *Fusarium virguliforme*, and Sclerotinia stem rot (SSR), caused by *Sclerotinia sclerotiorum*. Treatment factors for the SDS experiment included two soybean cultivars (Sloan and CH2105R2), two inoculation levels (non-inoculated control and inoculated), and two LCO applications (control and foliar LCO application); whereas, two experimental soybean lines (91-38 and 91-44) and two LCO applications (water control and foliar LCO application) were used in the SSR experiment. The LCO application did not significantly influence SDS root symptom severity or early-season growth characteristics. However, on the susceptible line ($P = 0.01$) and with LCO application ($P = 0.03$) significantly larger SSR lesions developed compared to the non-treated control and resistant line. These results suggest foliar-applied LCOs have a limited effect on early root symptom development caused by *F. virguliforme* but increase stem symptom development caused by *S. sclerotiorum*.

Introduction

Lipo-chitooligosaccharides (LCOs) are signal molecules involved in the early stages of the rhizobia-legume symbiosis development (Venkateshwaran et al. 2013). Plant roots exude signal molecules, mainly flavonoids, isoflavonoids, and betaines (Cesco et al. 2010; Mandal et al. 2010). The perception of these signals by the rhizobia, through nucleotide oligomerization domain (NOD)-like receptor proteins, induces the expression of structural *nod* genes, which leads to the production of LCOs (also known as Nod factors when produced by rhizobia). These diffusible LCOs are perceived by legume hosts at very low concentrations (micromolar to picomolar concentrations), are the main basis of host specificity in the rhizobia-legume association, and are generally required for root infection, nodule development, and subsequent N_2 fixation. Lipo-chitooligosaccharides are composed of a tri- to penta-chitin backbone with an *N*-acyl group at the non-reducing end and can possess a variety of substitutions along the chitin backbone. In soybean [*Glycine max* (L.) Merrill], a symbiotic relationship is often formed with the soil bacterium *Bradyrhizobium japonicum*, and the main Nod factor produced by the bacterium is Bj-V ($C_{18:1}$, MeFuc) (Duzan et al. 2005). Lipo-chitooligosaccharides are also produced by arbuscular mycorrhizal fungi (Maillet et al. 2011) and perceived by rice and legumes (Sun et al. 2014).

Lipo-chitooligosaccharides have been found to stimulate seed germination (Zhang and Smith 2001), promote seedling development (Smith et al. 2002), stimulate root colonization by arbuscular mycorrhizal fungi (Xie et al. 1995), and cause cell division and embryogenesis (Spaink 1996). Furthermore, foliar-applied LCOs have been shown to increase the photosynthetic rates of soybean, common bean (*Phaseolus vulgaris* L.), corn (*Zea mays* L.), rice (*Oryza sativa* L.), canola (*Brassica napus* L.), apple (*Malus domestica*

Borkh), and grape (*Vitis vinifera* L.) (Smith et al. 2002). This increase in photosynthetic rate led to a 40% soybean seed yield increase under field conditions (Smith et al., 2002). In today's soybean production, a foliar-applied, commercially available product containing LCOs (Ratchet™; Monsanto BioAg, St. Louis, MO) is being marketed for reasons listed above.

Lipo-chitooligosaccharides are also similar in structure to chitooligosaccharides (COs) which are often derived from fungal and insect cell walls. Chitooligosaccharides are an example of microbe-associated molecular pattern (MAMP), and these are known to activate plant defense responses including pattern-triggered immunity (Gough and Cullimore 2011). The presence of LCOs has also been known to indirectly elicit isoflavonoid phytoalexins (i.e., antimicrobial compounds known to accumulate rapidly at areas of pathogen infection) (Gough and Cullimore 2011). Some research has also examined the interaction between presence of LCOs and disease development. A study by Duzan et al. (2005) showed the application of the Nod factor Bj-V ($C_{18:1}$, MeFuc) to soybean induced resistance to powdery mildew, caused by the fungus *Microsphaera diffusa*. Detection of bacterial flagellin (i.e. another example of MAMP) by a plant activates plant defense responses, including the production of reactive oxygen species (ROS). Liang et al. (2013) found adding purified Nod factor from *B. japonicum* to soybean leaves reduced ROS production by 25%. Also, the same treatment to *Arabidopsis thaliana* leaves resulted in decreased ROS production, but the suppressive effect by the Nod factor was slower and weaker compared to soybean (Liang et al. 2013). These results counter those by Duzan et al.

(2005), suggesting the presence of Nod factors may lead to increased infection by bacteria on soybean.

Soybean is affected by many pathogens, including *Fusarium virguliforme* O'Donnell & T. Aoki and *Sclerotinia sclerotiorum* (Lib.) de Bary. *Fusarium virguliforme* is the causal agent of soybean sudden death syndrome (SDS). Since its discovery in 1971, SDS has spread to much of the soybean growing region of the U.S. (Hartman et al. 2015). The fungus infects soybean roots early in the growing season, as early as 14 days after planting (Leandro et al. 2012), but artificial inoculation studies have suggested infection can occur on even younger seedlings (Navi and Yang 2008). Foliar symptoms develop later in the growing season (i.e. mid-reproductive growth stages) because of phytotoxins secreted by the fungus and translocated through the xylem in the roots to the leaves.

Soybean is also among more than 400 host species impacted by *S. sclerotiorum*, the causal agent of Sclerotinia stem rot (SSR) (Boland and Hall 1994). *S. sclerotiorum* overwinters in the soil as melanized sclerotia. During extended periods of cool, moist conditions, apothecia develop and produce infectious ascospores which infect soybean flowers (Grau and Hartman 2015; Peltier et al. 2012). Due to its broad host range and persistence in the soil, management of this disease remains of importance in many soybean growing regions. At the molecular level, responses to *S. sclerotiorum* and rhizobia both regulate the production of ROS (Ranjan et al., 2017). In a separate study, silencing the expression of an NADPH oxidase (GmRBOH-VI) in soybean lead to an enhanced resistance to *S. sclerotiorum*, an increased drought tolerance but a decreased nodulation rate (Ranjan et al. 2017).

Both SDS and SSR consistently rank in the top ten soybean diseases impacting U.S. soybean yields. Sudden death syndrome ranked among the top ten of soybean yield-suppressing diseases in the U.S. in 11 of 12 years from 1996 to 2007, and it often ranked second to fifth in those years (Wrather and Koenning 2009). Further work by Koenning and Wrather (2010) showed yield loss attributed to SDS totaled 1.5 million metric tons from 2008 to 2009, making it the fifth most yield-suppressing soybean disease across those two years. From 1996 to 2009, it was estimated that SSR contributed more than 6.8 million metric tons in U.S. soybean yield loss, resulting in $1.9 billion in lost revenue for producers (Koenning and Wrather 2010; Wrather and Koenning 2009). Another 2.2 million metric tons in yield loss were attributed to SSR from 2010 to 2014 (Bradley et al. 2017). In 2014, SDS ranked second and SSR ranked fourth in overall soybean yield reductions due to disease (Bradley et al. 2017).

To our knowledge, controlled research studies examining interactions between LCOs and *F. virguliforme* and *S. sclerotiorum,* and their effect on disease development and soybean growth have not yet been performed. Therefore, the objectives of this study were to i.) characterize interactions between foliar-applied LCOs and *F. virguliforme* on early soybean root disease symptoms and early soybean growth characteristics and to ii.) characterize interactions between *S. sclerotiorum* and foliar-applied LCOs on early soybean stem lesion development. Our null hypotheses are as follows: 1) foliar application of LCOs will not affect early soybean root disease symptom development caused by *F. virguliforme,* and 2) foliar application of LCOs will not increase early soybean stem symptoms caused by *S. sclerotiorum.*

Materials and Methods

Experimental design for trials examining *F. virguliforme*

Single-spore cultures from three *F. virguliforme* isolates (00-11-183, NRRL22823, and Soy-1) were grown on potato dextrose agar [Potato Dextrose Agar (Dehydrated); Fisher Scientific, Pittsburg, PA] for 14 d at 23 ± 2°C with 12 hours diurnal light. Only one *F. virguliforme* isolate (Soy-1) originated in Wisconsin. The Soy-1 isolate was recovered from soybean, and PCR was performed on extracted DNA using ITS4 (TCCTCCGCTTATTGATATGC) and ITS5 (GGAAGTAAAAGTCGTAACAAGG) primers targeting the internal transcribed spacer region of the ribosomal DNA (White et al. 1990). The PCR program included initial denaturation at 95°C for 2 min followed by 30 cycles of 95°C for 20 sec, 55°C for 25 sec, and 72°C for 50 sec; final extension was performed at 72°C for 10 minutes (White et al. 1990). Resulting products were then sequenced, and sequences had 98% homology with *F. virguliforme* sequences in GenBank. The remaining two *F. virguliforme* isolates originated in Indiana and were recovered from soybean plants as well. Polymerase chain reaction was performed on extracted DNA from the isolates using the F6-3 forward primer (GTAAGTGAGATTTAGTCTAGGGTAGGTGAC) and R9 reverse primer (CCATCCGTCTGGGAATTTTAACTA) developed by Wang et al. (2015). The PCR cycling conditions were set at one cycle at 94°C for 3 min, followed by 35 cycles of 30 sec at 94°C, 30 sec at 65°C, and 30 sec at 72°C, and a final extension for 5 min at 72°C (Wang et al. 2015). The resulting products were sequenced and compared with sequences in GenBank to confirm the identity as *F. virguliforme*. A modified version of the cornmeal-sand medium described by Mclean and Lawrence (1993) was used as the carrier and was prepared 30 d before the establishment of the greenhouse experiment. Sand (950 g), yellow cornmeal (50

g), and distilled water (150 mL) were added to an autoclavable bag and mixed. This step was repeated two times for each isolate and six times for a non-inoculated control to achieve the desired amount of carrier. All media was autoclaved on two consecutive days for 60 min at 121 °C. The sterilized cornmeal-sand media was infested adding 25, 1 cm^2 blocks cut from infested agar on a standard-sized Petri plate, to one autoclavable bag containing 950 g sand and 50 g cornmeal. Infesting the cornmeal-sand media was performed individually for each isolate. All infested and non-infested media were incubated at 22°C ± 1°C with 12 hours diurnal light for 30 d. Bags were shaken every three to four days to provide more uniform fungal growth. Immediately before use in the greenhouse experiment, the infested cornmeal-sand media from all three *F. virguliforme* isolates was mixed.

A greenhouse experiment was conducted at the University of Wisconsin-Madison from March to June in 2015. Two separate runs (i.e. repetitions) of this experiment were performed. For each run, there were six replications of treatments organized in a split-split-plot arrangement with the whole plot factor arranged as a completely randomized design. The whole plot factor consisted of two inoculation treatments: a control and inoculation with *F. virguliforme*. Subplots consisted of two LCO treatments: one control and one application of LCOs. Sub-subplots (i.e. the experimental unit) consisted of two cultivars: Sloan (public cultivar) and CH2105R2 (Channel brand; Monsanto Co., St. Louis, MO). The cultivar Sloan was chosen due to its susceptibility to *F. virguliforme* (Tande et al. 2014; Ziems et al. 2006); whereas, cultivar CH2105R2 was chosen because of its popularity due to high-yield potential and adaptability to Wisconsin (personal observation). This cultivar is described as partially resistant to *F. virguliforme* according to Channel brand SDS rating information (Anonymous,

2014). The CH2105R2 cultivar is reported as a 2 on a 1 to 9 scale with 1 indicating most resistant.

At the time of the run establishment, both infestation treatments were prepared by combining their respective cornmeal-sand media with Metro Mix™ potting soil (Sun Gro Horticulture, Agawam, MA) in a 1 part cornmeal-sand medium to 3 parts potting soil. The resulting cornmeal-sand-potting soil mixture was used to fill individual Cone-tainers™ (Stuewe and Sons, Inc., Tangent, OR). Cone-tainers™ measured 6.5 cm in diameter and 25.5 cm in depth. Two seeds were planted into each Cone-tainer™ to ensure the growth of at least one plant, and the number of seedlings was reduced to one, where appropriate, 7 d after planting. Four Cone-tainers™, representing the four combinations of the two subplot and two sub-subplot factors within each inoculation treatment, were placed in a 15-cm diameter pot on a greenhouse bench. Each pot was placed in an aluminum tray, and the 24 pots with aluminum trays (i.e. the four combinations of the two subplot and two sub-subplot factors × six replications) were randomly assigned to positions on a greenhouse bench. The aluminum trays were rotated every seven days to mitigate potential greenhouse effects.

For each run, plants were grown for 45 d after the time of potting. During that time, greenhouse air temperature was maintained at 24 ± 5°C. Natural light was supplemented with grow lights (1,000 watts) set for a photoperiod of 16 h light day^{-1}. Plants were watered every day for the first 7 d after potting by adding approximately 200 mL of tap water to each Cone-tainer™, as well as filling the aluminum trays with tap water. After that, plants were watered every other day by filling each aluminum tray with tap water. The LCO application treatments were made at the V2 growth stage (Fehr et al. 1971) using a CO_2 backpack

sprayer calibrated to deliver 187 L ha^{-1} of spray solution. The LCO solution was applied at the earliest growth stage allowed by the label to represent the most realistic management situation, i.e. the LCO could be added to an early herbicide application. The LCO application consisted of using Rachet™ (4×10^{-7} M lipo-chitooligosaccharide concentration) at a labeled rate of 290 mL ha^{-1}, and the control consisted of water only. At 7 d after the LCO application, plants were supplemented once a week for the remainder of the experiment with nutrients using Hoagland's No. 2 basal salt mixture without ammonium phosphate at a rate of 1.51 g L^{-1} tap water. One-half liter of the nutrient solution was applied to each aluminum tray. At the end of the 45 d, plants were mostly at the beginning flowering growth stage (R1) and measured for height. After that, plants were removed from each Cone-tainer™, and the shoots and roots were separated. Roots were washed to remove particulate matter. The roots of each plant were visually rated for the percentage of disease severity (i.e. the percentage of the root system with visual disease symptoms). Root disease symptoms appeared as dark brown to black lesions. The root system from each plant was individually immersed in water in a clear plastic tray, and scanned using a flatbed scanner (Epson Perfection V700 Photo Scanner) at 400 dpi with a pixel size of 0.063 mm. The resulting images were analyzed using WinRhizo 2013 software (Regent Instruments, Inc., Quebec, Canada). For the image analysis, color classes were manually designated for the root system and the background. The data measurements collected using the image analysis included total root length, root surface area, and root volume. The software calculated these measurements based on Tennant's (Tennant 1975) statistical line intersect method (Ortiz-Ribbing and Eastburn 2003).

After the plants had been scanned from each run of the experiment, two randomly chosen plants from each inoculation treatment were used to re-isolate *F. virguliforme*. Isolations were also performed on 'healthy' and 'diseased' root tissue. Root sections, approximately 0.5 cm long, were surface disinfested with 95% ethanol and grown on potato dextrose agar for 14 days at 23 ± 2°C with 12 hours diurnal light. Morphological characteristics were then used to identify *F. virguliforme* (Leslie et al. 2006), which was recovered from 'diseased' root tissue and not from the 'healthy' root tissue (data not shown). Dry root and shoot mass data were then collected after air drying the plant parts at 60 °C for seven days.

At the start of each run of the experiment, two separate 10 g subsamples were collected from the combined cornmeal-sand medium prepared for each inoculation treatment. The same procedure was performed for each inoculation treatment after the cornmeal-sand medium was combined with the Metro Mix™ potting soil. From each subsample collected, 0.5 g was used to estimate the amount of inoculum present (Table 1). This estimation was done using the quantitative polymerase chain reaction (qPCR) methods outlined by Marburger et al. (2015). The forward primer (GCAGGCCATGTTGGTTCTGTA), reverse primer (GCACGTAAAGTGAGTCGTCTCATC), and TaqMan probe (6-FAM-ACTCAGCGCCCAGGA- MGBNFQ) sequences targeted a 244 base pair region of the *FvTox1* gene of *F. virguliforme*. The qPCR program included initial denaturation at 95°C for 2 min followed by 40 cycles of 95°C for 10 sec, 60°C for 20 sec, and 68°C for 30 sec.

****Experimental design for trials examining *S. sclerotiorum***

Sclerotia from a Wisconsin soybean isolate of *S. sclerotiorum*, collected in 2012 and designated isolate #20, were increased on carrot discs, harvested, and stored as dry sclerotia. Isolate #20 was characterized as *S. sclerotiorum* in molecular characterization and mycelial compatibility studies (Baturo-Ciesniewska et al. 2017; Willbur et al. 2017). Before inoculation, sclerotia were surface disinfested in 10% (v/v) bleach for 1 min followed by 95% ethanol for 1 min. Sclerotia were then rinsed in sterile ultrapure Milli-Q® water (EMD Millipore, Billerica, Massachusetts), blotted dry on sterile filter paper (Fisher Scientific, Qualitative P8, porosity coarse), and plated onto potato dextrose agar [Potato Dextrose Agar (Dehydrated); Fisher Scientific, Pittsburg, PA]. The inoculum was prepared by transferring a 5-mm agar plug from an actively growing PDA culture to a deep Petri plate (100 mm by 25 mm; Lab-Tek® Nunc®, Sigma-Aldrich) of PDA. The inoculum was incubated for three to four days, or until sufficient leading-edge growth of active mycelium was obtained, at room temperature (21 – 24 °C) before inoculation.

This experiment was conducted at the University of Wisconsin-Madison in a controlled environment chamber from September to December in 2015. Two separate runs (i.e. repetitions) of this experiment were performed. For each run, the experimental design was a randomized complete block design with five replications of treatments arranged as a 2 × 2 factorial. Treatment factors consisted of two experimental soybean lines (91-38 and 91-44) and two LCO applications (water control and application of LCO solution) with a single *S. sclerotiorum* inoculation (isolate #20). A putative moderately-resistant soybean experimental line, 91-38, and one susceptible experimental line, 91-44, were used based on preliminary *S. sclerotiorum* resistance screening (McCaghey and Willbur et al. 2017). The

soybean cyst nematode resistant line LN89-5717 (Nickell et al. 1994) and the partially SSR-resistant line W04-1002 (Peltier and Grau 2008) were crossed to generate these experimental lines. Seed from these experimental lines were of the F8:12 generation and were highly inbred.

Soybean seeds were planted approximately 4 cm deep in 15.25-cm diameter pots filled with moist potting mix (Sun Gro® Horticulture, Agawam, MA). In the first repetition, ten seeds of each line were planted one per pot, and 10 plants of each line were maintained for the water and LCO applications. In the second repetition, 16 seeds of each line were planted one per pot and 10 were maintained for the foliar applications. The air temperature was maintained at 22°C during the day and 18°C at night in a 14-hour photoperiod growth room. Plants were watered daily and fertilized once a week with 3.9 mL Miracle-Gro® in 1 L of water (Miracle-Gro®, Scotts Miracle-Gro Products, Marysville, OH). At the V2 growth stage, Rachet™ (4×10^{-7} lipo-chitooligosaccharide concentration) was applied. Calibrated 16 oz spray bottles (Arrow Plastic Manufacturing Co., Elk Grove, IL) and a 150-mm polypropylene powder funnel (Thermo Scientific, Nalge Nunc International, Penfield, NY) were used to evenly deliver 4.0 mL of spray solution of 1.56 mL L^{-1} Rachet™ solution in deionized water to each plant. Deionized water was applied using the same method and rate to represent the control. Plants were then allowed to grow until the V4 growth stage before inoculation.

Inoculations were conducted using the cut petiole technique described by Peltier and Grau (2008). A 1.5 cm thick agar core of actively growing mycelia was collected using 1,000 µl pipet tips (Fisher Scientific). The second trifoliate petiole on each plant was excised to a

length of 2.5 cm. Pipet tips containing the inoculum were jabbed onto the cut petiole such that mycelia and cut tissue were in direct contact. Daily stem lesion measurements were collected using a digital caliper (Thermo Fisher Scientific, Waltham, MA) for 12 days post-inoculation. The area under the disease progress curve (AUDPC) was used to assess disease severity over the 12-day epidemic (Madden et al. 2007).

Statistical analysis

Experiments with Fusarium virguliforme. Mixed-model analysis of variance (ANOVA) was conducted using PROC GLIMMIX within SAS Version 9.3 (SAS Institute, Cary, NC). Initial analyses revealed statistical differences between runs of the experiment for most growth measurements; however, further examination revealed these results were due to differences in magnitude between the two runs for those growth characteristics. Therefore, the data from both runs of the experiment were combined for analysis. Models were constructed and analyzed individually for each growth characteristic measured. Percent disease severity values were transformed for analysis using the equation $\log_{10}$('severity'+1), and root volume values were transformed using the square root transformation. For all analyses, inoculation, LCO application, soybean cultivar, and all their interactions were considered fixed effects. Run, replication × inoculation(run), replication × inoculation × LCO(run), and the overall error term were considered random effects. For all analyses, fixed effects were tested for significance at $\alpha = 0.05$, and means comparisons of significant effects were calculated based on Fisher's protected LSD. The SLICE option in SAS was used to compare means of significant interactions (Littell et al. 2006).

Experiments with Sclerotinia sclerotiorum. Mixed-model analysis of variance (ANOVA) was also conducted using PROC GLIMMIX within SAS Version 9.4. Data from both runs of the experiment were combined for analysis. The gamma distribution was used with the standard LINK function to normalize AUDPC data, and the ILINK function was used to return back-transformed means, which are presented here. LCO application, experimental soybean line, and their interaction were considered fixed effects. A nested effect of replication and run and the overall error term were used as random effects. The Kenward-Roger method was used to calculate denominator degrees of freedom (Littell et al. 2006), and fixed effect differences were evaluated at $\alpha = 0.05$.

Results and Discussion

Characterizing LCO and *F. virguliforme* interactions

The LCO application and its interactions with the other treatment factors did not influence the plant height or above-ground characteristics (Table 2). The only significant effect on the above-ground measurements was related to shoot weight between the soybean cultivars (Table 2). The shoot weight for the cultivar Sloan was 3.62 g compared to 2.67 g for CH2105R2. While the objective of this experiment was to evaluate SDS root disease symptoms, plants were also monitored for foliar SDS symptoms. During both runs of the experiment, respectively, only one and two of the inoculated plants for the cultivar Sloan exhibited some interveinal necrosis (data not shown). The remaining plants did not exhibit any foliar SDS symptoms.

Like the above-ground characteristics, the LCO application and its interactions with the other treatment factors did not affect any of the below-ground characteristics (Table 2).

For percent root disease severity, inoculation was the only significant effect (Table 2). Back-transformed values showed that inoculating with *F. virguliforme* resulted in 16.1% severity compared to 0.4% severity for the non-inoculated control.

For root weight, root length, root surface area, and root volume, there was evidence of an inoculation × cultivar interaction (Table 2). The cultivar Sloan showed greater root weight, root length, root surface area, and root volume compared to CH2105R2 within the non-inoculated control (Table 3). However, no difference between the two cultivars was observed for each characteristic within the *F. virguliforme* inoculated treatment. Inoculating with *F. virguliforme* resulted in decreased root length compared to the non-inoculated control for the cultivar Sloan, but no difference was observed for CH2105R2. Additionally, no significant decrease in root weight, root surface area, or root volume was observed for each cultivar when inoculated with *F. virguliforme* (Table 3).

These results suggested foliar-applied LCOs did not significantly impact soybean root rot caused by *F. virguliforme*. Application of LCOs in this experiment did not have an effect on above- and below-ground early-season soybean growth measurements. Furthermore, the LCO application did not interact with any of the other treatment factors to influence any of these measurements. Because a significant effect was not found, the results of this study do not support results from previous studies suggesting the presence of Nod factors can induce soybean resistance (Duzan et al. 2005) or potentially lead to increased plant infection by the pathogen (Liang et al. 2013).

Lipo-chitooligosaccharides are commercially available in soybean inoculants which contain *B. japonicum*; however, LCO-only seed treatments are not commercially available to

soybean producers. Because *F. virguliforme* infects soybean roots quickly after planting, LCOs applied as a seed treatment in combination with *B. japonicum* may provide different results. Some research has examined the role of rhizobia in controlling plant pathogens (Dakora 2003). Greenhouse experiments by Tu (1978) found root rot on soybean caused by *Phytophthora megasperma* was reduced when *B. japonicum* was applied to the potted soil immediately after planting. Follow-up experiments revealed *B. japonicum* reduced the sporulation of *P. megasperma*, *Pythium ultimum*, *Ascochyta imperfecta*, and *Fusarium oxysporum* by 75, 65, 35, and 47%, respectively (Tu 1979). Buonassissi et al. (1986) reported a reduction in root rot on snap bean caused by *Fusarium solani* f. sp. *phaseoli* when seeds were inoculated with *Rhizobium* and grown in pasteurized soil artificially infected with the pathogen. In field trials, Ehteshamul-Haque and Ghaffar (1993) found *Sinorhizobium meliloti*, *R. leguminosarum* and *B. japonicum* reduced infection of *Macrophomina phaseolina*, *Rhizoctonia solani*, and *Fusarium* spp. in both leguminous {soybean and mungbean [(*Vigna radiate* (L.) R. Wilczek.]} and non-leguminous {sunflower (*Helianthus annus* L.) and okra [*Abelmoschus esculentus* (L.) Moench]} plants. While there is evidence for reducing disease symptom development in the presence of rhizobia, the mechanisms for control are still not well understood. Tu (1979) suggested that decreased root rot was due to rhizobia parasitizing the hyphal tips of the fungus, and therefore, contact with host plant cells was reduced. Dakora (2003) suggested other mechanisms may exist. The LCOs secreted by the rhizobia might have contributed to these results.

Even though there was no evidence that the LCO application affected soybean growth or root disease development, it is possible a response to the LCOs occurred immediately after

the application (i.e. within the first 14 days or so after application). However, this may have been negated given the amount of time until the plant sampling which occurred at approximately R1. Nevertheless, the product containing LCOs used in this study (Ratchet™) is recommended for application between V2 and R1. Studying the effect of LCOs has primarily focused on early plant growth and crop establishment, but under ideal plant growth conditions (e.g., greenhouse conditions), improving early growth using LCOs may not be advantageous. Additionally, the probability of observing a response to LCO applications may be greater when early crop establishment is difficult or limiting.

Inoculating with *F. virguliforme* can result in foliar symptoms on young, susceptible plants (Tande et al. 2014). The estimated population (i.e. spores g^{-1} media) for *F. virguliforme* using qPCR methods (Table 1) was significantly higher than the estimated populations of 10^2 to 10^3 colony-forming units (CFU) g^{-1} of soil isolated from dilution plating methods that have been reported from symptomatic soybean plants in other studies (Mbofung et al. 2011; Rupe et al. 1997; Scherm et al. 1998). Even with the population estimates in this study, foliar SDS symptoms were not expected to be observed by the plant sampling time which occurred 45 days after planting. However, a few plants for the cultivar Sloan did express foliar symptoms during this experiment. The qPCR methods described by Marburger et al. (2015) and used to quantify the amount of inoculum in this study have not been correlated to root and foliar SDS disease symptoms though. Despite this, the percent root disease severity did not differ between the Sloan and CH2105R2 cultivars. While the root measurements for the cultivar Sloan were greater than CH2105R2 within the non-inoculated treatment, there was no difference in the root measurement characteristics when

each was inoculated with *F. virguliforme*. It is hypothesized that CH2105R2 would exhibit less SDS foliar symptoms than Sloan if the experiment was carried out until the mid to late reproductive stages (i.e. R4 to R7). In a field study conducted in Wisconsin, the CH2105R2 cultivar was among only two of ten cultivars examined which consistently exhibited the least amount of SDS foliar symptom development at the R5 to R7 growth stages.

****Characterizing LCO and *S. sclerotiorum* interactions**

Characteristic SSR lesions were observed on both the moderately resistant and susceptible soybean lines. Line 91-38 (moderately resistant) exhibited a mean lesion length of 49.8 mm, and line 91-44 (susceptible) exhibited a mean lesion length of 83.7 mm. The interaction between LCO application and soybean experimental line on SSR severity was not significant ($P = 0.33$). Soybean line ($P = 0.01$) and LCO application ($P = 0.02$), however, significantly affected AUDPC. The interaction term, therefore, was removed from the analysis, and fixed effects of application and line were re-evaluated. The moderately resistant line 91-38 exhibited significantly fewer symptoms than the susceptible line 91-44 ($P = 0.01$) (Figure 1). Furthermore, the LCO application resulted in significantly higher AUDPC values than the water control application ($P = 0.03$) (Figure 2). As indicated by the insignificant interaction, disease levels by LCO application were not dependent on putative SSR resistance within the lines.

To our knowledge, this is the first report characterizing the effects of foliar LCO application on SSR development in soybean. While the LCO application resulted in a significantly higher AUDPC value, it is recognized that the application rate was ten times the amount specified on the product label. As the product contains naturally occurring LCOs

formulated for corn and soybean, the label rate may not accurately reflect the concentrations which could be present in the soil post-application. Therefore, the potentially adverse effects of these LCO applications on field-grown soybeans should be considered despite the higher rate used. LCO application effects on soybean gene expression have been previously studied (Lindsay 2007; Wang et al. 2012); however, the effects of LCO applications on soybean pathogens and subsequent disease development have not been well studied. Wang et al. (2012) identified defense-related gene products, including chitinases, which are up-regulated 48 h after a foliar LCO application on stressed soybeans. Chitinases are known to both enhance host disease resistance and inhibit host defense responses in rhizobial interactions. In other studies, foliar LCO applications on soybean under optimal conditions did not affect chitinase or β-1,3-glucanase activity but did lead to an increase in salicylate levels (Lindsay 2007). Additionally, an LCO-activated gene in *Medicago truncatula*, *rip1*, was found to stimulate the localized and rapid production of ROS (Ramu et al. 2002). Surprisingly, other studies have reported a decrease of ROS production in response to Nod factors (Lohar et al. 2007; Shaw and Long 2003). This paradox may be due to a very dynamic ROS response to Nod factors with a rapid increase followed by a decrease of ROS production as showed in *P. vulgaris* by Cardenas et al. (2008). These LCO application effects could potentially reduce plant infection by the pathogen and disease development through increased host immunity. However, these interactions have not been studied in soybean.

In another study, the structurally related chitosan oligosaccharides (COS) were shown to inhibit infection of *Brassica napus* plants by *S. sclerotiorum* (Yin et al. 2013). These COS increased cytosolic Ca^{2+}, nitric oxide, and hydrogen peroxide levels which led to the

reduction of symptoms *in planta*. In soybean, however, LCO application does not seem to inhibit plant infection by *S. sclerotiorum* and results in increased SSR lesion development. Oxalic acid, which is a key pathogenicity factor of *S. sclerotiorum*, is known to induce ROS production which promotes host programmed cell death and disease (Kim et al. 2008; Ranjan et al. 2017; Williams et al. 2011). While ROS is typically a host defense response, the complex necrotrophic nature of *S. sclerotiorum* may enable this pathogen to thrive in an ROS-elevated environment. Further studies characterizing the mechanism of localized LCO activity on *S. sclerotiorum* and SSR development, however, must be conducted to understand this interaction better. More comprehensive *in vivo* and *in planta* investigations should consider LCO effects on fungal growth and development as well as the long-term changes in soybean after foliar application. *S. sclerotiorum* inoculations were conducted nearly two weeks after LCO application, and it is difficult to determine what changes may persist long enough to affect plant infection by *S. sclerotiorum*. In the field, infection occurs near soybean flowering (the R1 growth stage), and the LCO applications are recommended between the V2 and R1 growth stages. Additional studies of application timing and subsequent infection could identify which timings most strongly affect plant infection by *S. sclerotiorum*, and may help reduce unintended SSR symptom development.

Conclusions

This study was the first attempt at characterizing LCO interactions on early disease symptom development of soybean sudden death syndrome, caused by *F. virguliforme*, and Sclerotinia stem rot, caused by *S. sclerotiorum*. Our null hypotheses were 1) foliar application of LCOs will not affect early soybean root disease symptom development caused by *F. virguliforme*, and 2) foliar application of LCOs will not increase early soybean stem

symptoms caused by *S. sclerotiorum.* Considering the evidence presented here, we accept null hypothesis one and reject null hypothesis two. Foliar-applied LCOs did not significantly impact soybean root disease development or early-season above- and below-ground growth characteristics in the *F. virguliforme* experiment. However, foliar-applied LCOs significantly affected soybean stem lesion development by *S. sclerotiorum*. These results indicate that foliar-applied LCOs as a soybean management practice would not increase or decrease early disease symptom development from *F. virguliforme*, but foliar LCOs may stimulate changes in soybean which affect SSR symptom development up to two weeks following application. More studies are required to elucidate the mechanisms of these LCO-host-pathogen interactions in soybean. Because *F. virguliforme* infects soybean early in the growing season after planting, examining seed-applied rhizobia inoculants which contain LCOs may provide further insight into LCOs as promoters or inhibitors of SDS root symptom development. Foliar LCOs applied at the beginning flowering growth stage would also provide further insight into stem lesion development caused by *S. sclerotiorum*.

Literature Cited

Anonymous. 2014. Channel soybean seed guide. Monsanto Co., St. Louis, MO. Online: https://www.channel.com/about/products/Documents/2014ChannelSeedGuideSoybean.pdf.

Baturo-Ciesniewska, A., Groves, C. L., Albrecht, K. A., Grau, C. R., Willis, D. K., and Smith, D. L. 2017. Molecular identification of *Sclerotinia trifoliorum* and *Sclerotinia sclerotiorum* isolates from the United States and Poland. Plant Dis. 101:192–199.

Boland, G. J., and Hall, R. 1994. Index of plant hosts *of Sclerotinia sclerotiorum*. Can. J. Plant Pathol. 16:93-108

Bradley, C. A., Allen, T., and Esker, P. D. 2017. Estimates of soybean yield reductions caused by diseases in the United States. Univ. Illinois - Dep. Crop Sci. Ext. Outreach. Online. http://extension.cropsciences.illinois.edu/fieldcrops/diseases/yield_reductions.php.

Buonassissi, A. J., Copeman, R. J., Pepin, H. S., and Eaton, G. W. 1986. Effect of *Rhizobium* spp. on Fusarium solani f. sp. phaseoli. Can. J. of Plant Pathol. 8:140–146.

Cárdenas, L., Martínez, A., Sánchez, F., and Quinto, C. 2008. Fast, transient and specific intracellular ROS changes in living root hair cells responding to Nod factors (NFs). Plant J. 56:802-813.

Cesco, S., Neumann, G., Tomasi, N, Pinton, R., and Weisskopf, L. 2010. Release of plant borne flavonoids into the rhizosphere and their role in plant nutrition. Plant Soil 329:1-25.

Dakora, F. D. 2003. Defining new roles for plant and rhizobial molecules in sole and mixed plant cultures involving symbiotic legumes. New Phytologist 158:39-49.

Duzan, H. M., Mabood, F., Zhou, X., Souleimanov, A., and Smith, D. L. 2005. Nod factor induces soybean resistance to powdery mildew. Plant Physiol. Biochem. 43:1022-1030.

Ehteshamul-Haque, S., and Ghaffar, A. 1993. Use of rhizobia in the control of root rot diseases of sunflower, okra, soybean and mungbean. Journal of Phytopathol. 138:157–163.

Fehr, W. R., Caviness, C. E., Burmood, D. T., and Pennington, J. S. 1971. Stage of development descriptions for soybeans (*Glycine max* (L.) Merrill). Crop Sci. 11:929-931.

Gough, C., and Cullimore, J. 2011. Lipo-chitooligosaccharide signaling in endosymbiotic plant-microbe interactions. Mol. Plant-Microbe Interact. 24:867-878.

Hartman, G. L., Leandro, L. F. S., and Rupe, J. C. 2015. Sudden death syndrome. Pages 88-90 in: Compendium of Soybean Diseases and Pests. G. L. Hartman, J. C. Rupe, E. F. Sikora, L. L. Domier, J. A. David, and K. L. Steffey, eds. American Phytopathological Society, St. Paul, MN.

Kim, K. S., Min, J.-Y., and Dickman, M. B. 2008. Oxalic acid is an elicitor of plant programmed cell death during *Sclerotinia sclerotiorum* disease development. Mol. Plant. Microbe. Interact. 21:605–12.

Koenning, S. R., and Wrather, J. A. 2010. Suppression of soybean yield potential in the continental United States by plant diseases from 2006 to 2009. Plant Health Prog. Online publication. doi:10.1094/PHP-2010-1122-01-RS.

Leandro, L. F., Tatalovic, N., and Luckew, A. 2012. Soybean sudden death syndrome - advances in knowledge and disease management. CAB Rev. 7:1-14.

Leslie, JF, Summerell BA. 2006. The *Fusarium* Laboratory Manual. 1st ed. Blackwell Publishing: Ames, IA.

Liang, Y., Cao, Y., Tanaka, K., Thibivilliers, S., Wan, J., Choi, J., Kang, C.H., Qui, J., and Stacey, G. 2013. Nonlegumes respond to rhizobial nod factors by suppressing the innate immune response. Science 341:1384-1387.

Lindsay, J. K. 2007. The effect of lipo-chitooligosaccharide from *Bradyrhizobium japonicum*, on soybean salicylic acid, pathogenesis-related protein activity and gene expression. M.S. Thesis, McGill University.

Littell, R. C., Milliken, C. A., Stroup, W. W., Wolfinger, R. D., and Schabenberger, O. 2006. SAS for Mixed Models, 2nd ed. SAS Publishing, Cary, NC.

Lohar, D. P., Haridas, S., Gantt, J. S., and Vandenbosch, K. A. 2007. A transient decrease in reactive oxygen species in roots leads to root hair deformation in the legume-rhizobia symbiosis. New Phytol.173:39-49.

Madden, L. V., Hughes, G., and van den Bosch, F. 2007. The Study of Plant Disease Epidemics. The American Phytopathological Society, APS Press St. Paul, Minnesota.

Maillet, F., Poinsot, V., André, O., Puech-Pagès, V., Haouy, A., Gueunier, M., Cromer, L., Giraudet, D., Formey, D., Niebel, A., Martinez, E. A., Driguez, H., Bécard, G., and Dénarié, J. 2011. Fungal lipochitooligosaccharide symbiotic signals in arbuscular mycorrhiza. Nature 469:58-63.

Mandal, S. M., Chakraborty, D. and Dey, S. 2010. Phenolic acids act as signaling molecules in plant-microbe symbioses. Plant Signal. Behav. 5(4): 359-368.

Marburger, D. A., Venkateshwaran, M., Conley, S. P., Esker, P. D., Lauer, J. G., and Ané, J. 2015. Crop rotation and management effect on *Fusarium* spp. populations. Crop Sci. 55:365-376.

Mbofung, G. C. Y., Fessehaie, A., Bhattacharyya, M. K., and Leandro, L. F. S. 2011. A new TaqMan real-time polymerase chain reaction assay for quantification of *Fusarium virguliforme* in soil. Plant Dis. 95:1420–1426.

McCaghey, M., Willbur, J., Ranjan, A., Grau, C. R., Chapman, S., Diers, B., Groves, C., Kabbage, M., and Smith, D. L. 2017. Development and evaluation of *Glycine max* germplasm lines with quantitative resistance to *Sclerotinia sclerotiorum*. Front. Plant Sci. 8:1-13.

McLean, K. S., and Lawrence, G. W. 1993. Interrelationship of *Heterodera glycines* and *Fusarium solani* in sudden death syndrome of soybean. J. Nematol. 25:434-439.

Navi, S. S., and Yang, X. B. 2008. Foliar symptom expression in association with early infection and xylem colonization by *Fusarium virguliforme* (formerly *F. solani* f. sp. *glycines*), the causal agent of soybean sudden death syndrome. Plant Health Prog. Online publication. doi:10.1094/PHP-2008-0222-01-RS.

Navi, S. S., and Yang, X. B. 2014. Sudden death syndrome. Soybean Research & Information Initiative. North Central Soybean Research Program. Online. http://soybeanresearchinfo.com/diseases/suddendeathsyndrome.html.

Nickell, C. D., Noel, G. R., Bernard, R. L., Thomas, D. J., and Frey, K. 1994. Registration of soybean germplasm line LN89-5717, resistant to soybean cyst nematode. Crop Sci. 34:34–1133.

Ortiz-Ribbing, L. M., and Eastburn, D. M. 2003. Evaluation of digital image acquisition methods for determining soybean root characteristics. Crop Management. Online publication. doi:10.1094/CM-2003-0702-01-RS.

Ortiz-Ribbing, L. M., and Eastburn, D. M. 2004. Soybean root systems and sudden death syndrome severity: taproot and lateral root infection. Plant Dis. 88:1011-1016.

Peltier, A. J., and Grau, C. R. 2008. The influence of light on relationships between Sclerotinia stem rot of soybean in field and controlled environments. Plant Dis. 92:1510–1514.

Ramu, S. K., Peng, H. M., and Cook, D. R. 2002. Nod factor induction of reactive oxygen species production is correlated with expression of the early nodulin gene *rip1* in *Medicago truncatula*. Mol. Plant-Microbe Interact. 15:522–528.

Ranjan, A., Jayaraman, D., Grau, C., Hill, J.H., Whitham, S.A., Ane, J., Smith, D.L., and Kabbage, M. 2017. The pathogenic development of *Sclerotinia sclerotiorum* in soybean requires host specific NADPH oxidases. Mol. Plant. Pathol. *Accepted 30 March 2017*.

Roy, K. W., Rupe, J. C., Hershman, D. E., and Abney, T. S. 1997. Sudden death syndrome of soybean. Plant Dis. 81:1100-1111.

Rupe, J. C., Robbins, R. T., and Gbur, E. E. 1997. Effect of crop rotation on soil population densities of *Fusarium solani* and *Heterodera glycines* and on the development of sudden death syndrome of soybean. Crop Prot. 16:575–580.

Scherm, H., Yang X. B., and Lundeen, P. 1998. Soil variables associated with sudden death syndrome in soybean fields in Iowa. Plant Dis. 82:1152–1157.

Shaw, S. L., and Long, S. R. 2003. Nod factor inhibition of reactive oxygen efflux in a host legume. Plant Physiol. 132:2196-2204.

Smith, D. L., Prithiviraj, B., and Zhang, F. 2002. Rhizobial signals and control of plant growth. Pages 327-330 in: Nitrogen Fixation: Global Perspectives. T.M. Finan, M.R. O'Brian, D.B Layzell, K. Vessey, and W.E. Newton, eds. CABI Publishing, Wallingford, UK.

Spaink, H. P. 1996. Regulation of plant morphogenesis by lipo-chitin-oligosaccharide. Critical Reviews in Plant Sciences 15:559–582.

Sun, J., Miller, J. B., Granqvist, E., Wiley-Kalil, A., Gobbato, E., Maillet, F., Cottaz, S., Samain, E., Venkateshwaran, M., Fort, S., Morris, R. J., Ané, J. M., Dénarié, J., and Oldroyd, G. E. D. 2015. Activation of symbiosis signalling by arbuscular mycorrhizal fungi in legumes and rice. The Plant Cell 27:823-838.

Tande, C., Hadi , B., Chowdhury, R., Subramanian, S., and Byamukama, E. 2014. First report of sudden death syndrome of soybean caused by *Fusarium virguliforme* in South Dakota. Plant Dis. 98:1012.

Tennant, D. 1975. A test of the modified line intersect method for estimating root length. J. Ecol. 63:995-1001.

Tu, J. C. 1978. Protection of soybean from severe *Phytophthora* root rot by *Rhizobium*. Physiol. Plant Pathol. 12:233-240.

Tu, J. C. 1979. Evidence of differential tolerance among some root rot fungi to rhizobial parasitism *in vitro*. Physiol. Plant Pathol. 14:171-177.

Venkateshwaran, M., Volkening, J. D., Sussman, M. R., and Ané, J. M. 2013. Symbiosis and the social network of higher plants. Curr. Opin. Plant Biol. 16:118-127.

Wang, J., Jacobs, J. L., Byrne, J. M., and Chilvers, M. 2015. Improved diagnoses and quantification of *Fusarium virguliforme*, causal agent of soybean sudden death syndrome. Phytopathol. 105:378-387.

Wang, N., Khan, W., and Smith, D. L. 2012. Changes in soybean global gene expression after application of lipo-chitooligosaccharide from *Bradyrhizobium japonicum* under sub-optimal temperature. PLoS One. 7(2): e31571.

White, T. J., Bruns, T., Lee, S., and Taylor, J. W. 1990. Amplification and direct sequencing of fungal ribosomal RNA genes for phylogenetics. Pages 315-322 in: PCR Protocols: A Guide to Methods and Applications. M. A. Innis, D. H. Gelfand, J. J. Sninsky, and T. J. White, eds. Academic Press, Inc., New York.

Wilcox, J. R. 2004. World distribution and trade of soybean. Pages 1-14 in: Soybeans: Improvement, Production and Uses. H.R. Boerma and J.E. Specht, eds. American Society of Agronomy, Soil Science Society of America, Crop Science Society of America, Inc., Madison, WI.

Willbur, J. F., Ding, S., Marks, M. E., Lucas, H., Grau, C. R., Groves, C. L., Kabbage, M., and Smith, D.L. 2017. Comprehensive Sclerotinia stem rot screening of soybean germplasm requires multiple isolates of *Sclerotinia sclerotiorum*. Plant Dis. 101:344–353.

Williams, B., Kabbage, M., Kim, H.-J., Britt, R., and Dickman, M. B. 2011. Tipping the balance: *Sclerotinia sclerotiorum* secreted oxalic acid suppresses host defenses by manipulating the host redox environment. PLoS Pathog. 7:e1002107.

Wrather, J. A., and Koenning, S. R. 2009. Effects of diseases on soybean yields in the United States 1996 to 2007. Plant Health Prog. Online publication. doi:10.1094/PHP-2009-0401-01-RS.

Xie, Z. P., Staehelin, C., Vierheilig, H., Wiemken, A., Jabbouri, S., Broughton, W. J., Vogeli-Lange, R., and Boller, T. 1995. Rhizobial nodulation factors stimulate mycorrhizal colonization of nodulating and nonnodulating soybeans. Plant Physiol. 108:1519–1525.

Yin, H., Li, Y., Zhang, H.-Y., Wang, W.-X., Lu, H., Grevsen, K., et al. 2013. Chitosan oligosaccharides–triggered innate immunity contributes to oilseed rape resistance against *Sclerotinia sclerotiorum*. Int. J. Plant Sci. 174:722–732.

Ziems, A. D., Giesler, L. J., and Yuen, G. Y. 2006. First report sudden death syndrome of soybean caused by *Fusarium solani* f. sp. *glycines* in Nebraska. Plant Dis. 90:109.

Zhang, F., and Smith, D. L. 2001. Interorganismal signalling in suboptimum environments: the legume–rhizobia symbiosis. Adv. Agron. 76:125–161.

Tables and Figures

Table 7.1. Population estimates for *Fusarium virguliforme* in each inoculation treatment within each run (i.e. replication) of the experiment using quantitative polymerase chain reaction (qPCR) (Marburger et al. 2015).

Run	Inoculation treatment[a]	Media[b]	Cq[c]	Cq std. dev.[d]	Estimated population[e]
					--spores g^{-1} --
Positive control[f]	-	-	21.57	1.54	26,296,760
Negative control[g]	-	-	N/A[h]	N/A	0
1	NTC	Sand	N/A	N/A	0
1	NTC	MM	N/A	N/A	0
1	FV	Sand	22.99	0.95	9,998,160
1	FV	MM	23.78	1.02	5,839,830
2	NIC	Sand	N/A	N/A	0
2	NIC	MM	N/A	N/A	0
2	FV	Sand	25.19	1.19	2,246,600
2	FV	MM	28.46	0.79	244,220

[a]NIC: non-inoculated control; FV: inoculated with a mixture of three isolates of *F. virguliforme*.

[b]Sand: a mixture of the cornmeal-sand growth media used to grow each isolate; MM: a combination of the cornmeal-sand medium prepared for each inoculation treatment with Metro Mix™ potting soil (Sun Gro Horticulture, Agawam, MA) in a 1 part cornmeal-sand medium to 3 parts potting soil ratio.

[c]Cq: quantification cycle (i.e. the number of polymerase chain reaction cycles at which the target amplicon was quantified on based on the parameters outlined by Marburger et al. [2015]). The average represents two replications from each inoculation treatment and three technical replications used for the qPCR (n = 6).

[d]Cq std. dev.: quantification cycle standard deviation.

[e]Population estimate given in spores per g of media[b]. Equations used to estimate are outlined by Marburger et al. (2015).

[f]Positive control: DNA template used in the qPCR reaction was extracted from the *F. virguliforme* isolates used in this study.

[g]Negative control: autoclaved Milli-Q purified water used in place of DNA template.

[h]N/A: not detected and quantified by the qPCR methods used.

Table 7.2. Analysis of variance (ANOVA) results for soybean above- and below-ground growth characteristics as influenced by two inoculation treatments (non-inoculated control and inoculated with *Fusarium virguliforme*), two lipo-chitooligosaccharide (LCO) applications (water control and application of LCOs), and two soybean cultivars (Sloan and CH2105R2).

	Above-ground		Below-ground				
Source of variation	Plant height	Shoot weight	Disease severity[a]	Root weight	Root length	Root surface area	Root volume[b]
Inoculation (I)	0.0983	0.9585	<0.0001	0.7014	0.8005	0.4436	0.4797
LCO application	0.8846	0.7256	0.6338	0.6968	0.6225	0.7569	0.7877
I × LCO	0.8296	0.4302	0.4706	0.5416	0.5586	0.6072	0.8459
Cultivar (C)	0.0912	<0.0001	0.4883	0.0014	0.1488	0.1165	0.1523
I × C	0.2717	0.2086	0.8576	0.0431	0.0059	0.0152	0.0270
LCO × C	0.0936	0.1372	0.4455	0.1566	0.2083	0.4338	0.4149
I × LCO × C	0.4844	0.3121	0.3932	0.4243	0.3252	0.2865	0.3943

[a]Disease severity values were transformed for analysis using the equation $\log_{10}$('severity'+1).

[b]Root volume values were transformed for analysis using the square root transformation.

Table 7.3. Inoculation × cultivar interaction results for soybean root weight, root length, root surface area, and root volume from the *Fusarium virguliforme* experiment. All values presented are the average on a per plant basis.

		Cultivar[b]	
Variable	Inoculation[a]	Sloan	CH2105R2
		——— g ———	
Root weight	NIC	1.49 aA[c]	1.05 bA
	FV	1.36 aA	1.26 aA
		——— cm ———	
Root length[d]	NIC	3370 aA[c]	2500 bA
	FV	2740 aB	3020 aA
		——— cm^2 ———	
Root surface area[d]	NIC	538 aA[c]	386 bB
	FV	477 aA	514 aA
		——— cm^3 ———	
Root volume[de]	NIC	6.39 aA[c]	4.51 bA
	FV	5.66 aA	6.16 aA

[a]NIC, non-inoculated control; FV, inoculated with *Fusarium virguliforme*.

[b]CH2105R2, Channel Brand (Monsanto Co., St. Louis, MO); Sloan, public cultivar.

[c]Means comparisons were calculated based on Fisher's protected LSD. The SLICE option in SAS (v. 9.3) was used to compare means of this significant interaction (Littell et al., 2006). Values followed by the same lowercase letter within a row (i.e. the inoculation treatment) or by the same uppercase letter within a column (i.e. cultivar) are not significantly different at $P \leq 0.05$.

[d]Root surface area and root volume values were obtained from digital image analysis using a WinRhizo 2013 root scanner system (Regent Instruments, Inc., Quebec, Canada).

[e]Root volume values were transformed for analysis using the square root transformation. Back-transformed values are presented in this table.

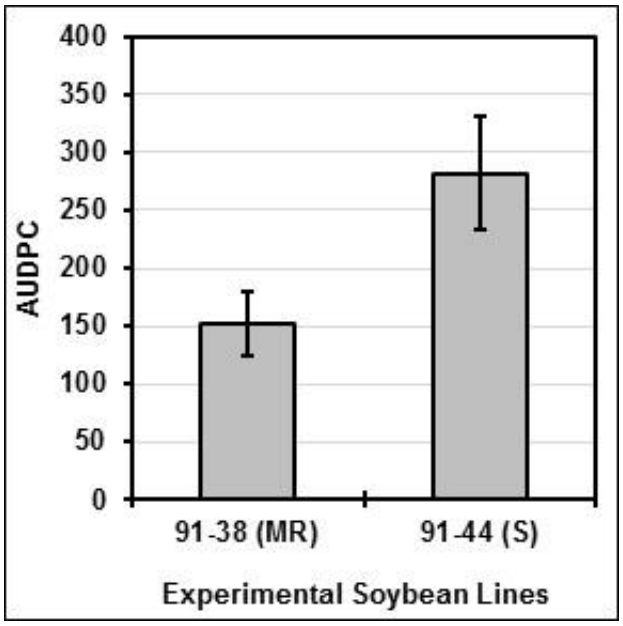

****Figure 7.1.** Soybean experimental cultivars 91-38 (MR, moderately resistant) and 91-44 (S, susceptible) response to *Sclerotinia sclerotiorum* inoculation determined by the area under the disease progress curve (AUDPC). Daily stem lesion (mm) measurements were collected for 12 days post-inoculation. Bars represent the mean values of five replications and two runs (i.e. repetitions) of the experiment. Error bars represent the standard error of the mean. Line 91-44 exhibited significantly more symptom development than line 91-38 (P = 0.01).

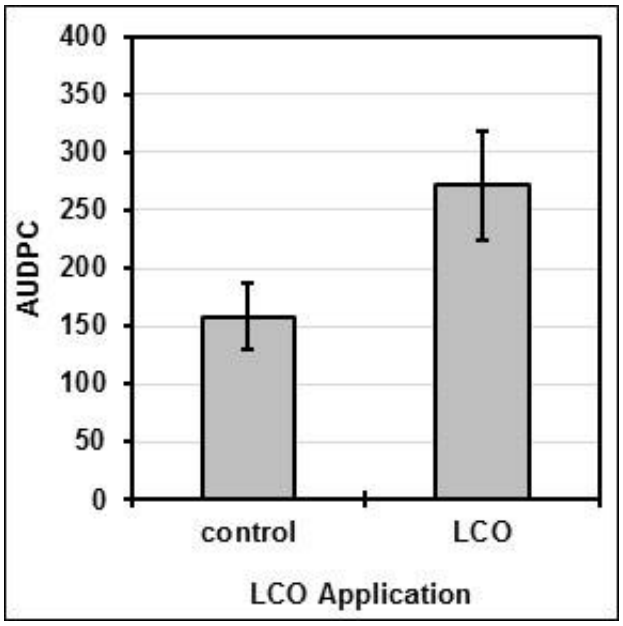

****Figure 7.2.** Soybean lipo-chitooligosaccharide (LCO) application effect on *Sclerotinia sclerotiorum* inoculation determined by the area under the disease progress curve. Daily stem lesion (mm) measurements were collected for 12 days post-inoculation. Bars represent the mean values of five replications and two runs (i.e. repetitions) of the experiment. Error bars represent the standard error of the mean. LCO applications resulted in significantly more symptom development than water control applications ($P = 0.03$).

Appendix I: Determination of mycelial compatibility grouping within a collection of *Sclerotinia sclerotiorum* isolates

Maria Weber, Hannah Lucas, and Jaime Willbur

Summary

Genetic diversity within the collection may explain variable isolate behavior; therefore, mycelial compatibility assays were conducted to investigate the genetic profile of our collection (Kohn et al. 1990). All isolate interactions were evaluated in three-way isolate challenges and compared to self-self interactions to determine mycelial compatibility (see Protocol AI.1-5). Three mycelial compatibility groupings (MCG) were observed in our collection, accounting for 25 isolates. The remaining 19 isolates were not compatible with any other isolate (Table AI.1).

The effect of MCG on isolate aggressiveness, standardized area under the disease progress curves (STAUDPC), from Fig. 2.1C was examined. A generalized linear mixed model (GLIMMIX) procedure was used to perform an analysis of variance (ANOVA) in SAS v. 9.4 (SAS Institute, Cary, NC). There were no significant differences between the aggressiveness of different MCG ($P = 0.7616$). These results are consistent with other findings (Kull et al. 2004; Lehner et al. 2016).

In our collection, MCG 1 contains 19 isolates, while MCG 2 contains four isolates, and MCG 3 contains only two isolates. More equal representation of each MCG could perhaps reveal differences between isolates of different MCG. This collection could also be further characterized using PCR-based DNA fingerprinting techniques, such as amplified fragment length polymorphisms (AFLP) analyses. This would substantiate the findings in

previous characterization assays to better understand the diversity within our isolate collection

Literature Cited

Kohn, L. M., Carbone, I., and Anderson, J. B. 1990. Mycelial interactions in *Sclerotinia sclerotiorum*. Exp. Mycol. 14:255–267.

Kull, L. S., Pedersen, W. L., Palmquist, D., and Hartman, G. L. 2004. Mycelial compatibility grouping and aggressiveness of *Sclerotinia sclerotiorum*. Plant Dis. 88:325–332 Available at: http://dx.doi.org/10.1094/PDIS.2004.88.4.325.

Lehner, M. S., Lima, R. C., Carneiro, J. E. S., Paula Junior, T. J., Vieira, R. F., and Mizubuti, E. S. G. 2016. Similar aggressiveness of phenotypically and genotypically distinct isolates of *Sclerotinia sclerotiorum*. Plant Dis. 100:360–366.

Tables and Figures

Table AI.1. Mycelial compatibility groups within a collection of 44 *S. sclerotiorum* isolates

MCG	Isolate #	Location	Host	Common Name
1	1	WI	*Glycine max*	Soybean
1	2	WI	*G. max*	Soybean
1	3	WI	*G. max*	Soybean
--[a]	5	IL	*G. max*	Soybean
3	6	IL	*Abutilon theophrasti*	Velvetleaf
3	7	IL	*A. theophrasti*	Velvetleaf
--	8	MI	*G. max*	Soybean
2	9	MI	*G. max*	Soybean
1	10	MI	*G. max*	Soybean
--	15	WI	*G. max*	Soybean
1	16	WI	*G. max*	Soybean
--	17	WI	*G. max*	Soybean
1	18	WI	*G. max*	Soybean
--	19	-[b]	*G. max*	Soybean
1	20	-	*G. max*	Soybean
--	21	-	*G. max*	Soybean
1	22	WI	*G. max*	Soybean
1	23	WI	*G. max*	Soybean
1	24	WI	*G. max*	Soybean
1	25	WI	*G. max*	Soybean
1	26	WI	*G. max*	Soybean
2	27	WI	*G. max*	Soybean
2	28	WI	*G. max*	Soybean
--	29	-	*G. max*	Soybean
1	30	WI	*G. max*	Soybean
1	31	WI	*G. max*	Soybean
1	32	WI	*G. max*	Soybean
2	33	WI	*G. max*	Soybean
--	34	-	*G. max*	Soybean
--	43	NE	*Phaseolus vulgaris*	Green bean
1	44	WI	*P. vulgaris*	Green bean
1	45	MN	*Petunia* sp.	Petunia
1	46	MN	*G. max*	Soybean
--	47	MN	*G. max*	Soybean
--	57	Poland	*Brassica napus*	Canola
--	58	Poland	*Helichrysum arenarium*	Dwarf everlast
--	59	Poland	*H. arenarium*	Dwarf everlast
--	60	Poland	*H. arenarium*	Dwarf everlast
--	61	Poland	*Daucus carota*	Carrot
--	62	Poland	*B. napus*	Canola

--	63	Poland	*D. carota*	Carrot
--	64	Poland	*Apium graveolens*	Celery
1	65	Poland	*Petroselinum crispum*	Parsley
--	66	Poland	*Lactuca sativa*	Lettuce

[a]Incompatible (--); isolate was not compatible with any other isolate.

[b]Information unknown (-); highly likely that unknown isolates are from Wisconsin soybeans.

Protocols

AI.1. Preparing Media: Potato Dextrose Agar (PDA) and Modified PDA

1. Obtain clean 1000 ml Erlenmeyer flasks. Flasks will be autoclaved and should only contain a maximum volume of half the total capacity, i.e. an autoclaved 1000 ml container should contain no more than 500 ml of solution. NOTE: 500ml of media will make approximately 25 fresh plates.

2. Place a clean, medium-sized stir bar in each flask. Weigh out 19.5 g of PDA and transfer to each flask.

3. Using a clean graduated cylinder, add 500 ml of deionized water (diH_2O) to each flask. Final concentration should be 39 g L^{-1} PDA in diH_2O.

4. Stir briefly but thoroughly using electric stir plate. Cover using double layered aluminum foil.

    - To make **modified PDA** (Kohn et al. 1990)**,** simply add 75 µl (concentration of 150 µl L^{-1}) of McCormick's red food coloring to each desired flask while stirring, prior to autoclaving.

5. Autoclave in an autoclavable tray for 30 minutes, slow exhaust.

6. Allow media to cool by either *gentle* stirring (avoid creating bubbles in the media as they will promote contamination) or by placing flasks in a water bath.

7. Before fully cooled, turn on laminar flow hood. Spray down bench surface and tools with 70% ethanol. Wipe surface using paper towel.

8. Pour media into standard-sized sterile Petri plates.

9. Once agar has solidified, store plates in 4°C refrigerator in plastic bins.

AI.2. Surface Sterilize *S. sclerotiorum* Sclerotia

1. Turn on laminar flow hood. Spray down bench surface and tools with 70% ethanol. Wipe surface using paper towel.

2. Select *S. sclerotiorum* isolates from the collection stored in the 4°C refrigerator.

3. Label the bottom of Petri dishes (not lid) with isolate number and date using a permanent marker.

4. In laminar flow hood, prepare 4 standard-sized sterile petri dishes for surface sterilization. Label and fill 3 dishes (1 each) with approximately 25 ml of 10% Clorox, 95% ethanol (EtOH), and sterile ultrapure Milli-Q® water (H_2O).

5. Turn the last petri dish lid-side down and, using flame sterilized tweezers (forceps), place 2 sterile filter papers in the lid.

   For flame sterilization of tools:
   a) Dip tool in 95% EtOH
   b) Holding tool pointed downward, place tip of tool in flame and remove to allow the ethanol to burn off (flame will dissipate)
   c) Allow to cool briefly before use (to avoid contamination, do not set cooling tools on the bench surface, place on aluminum foil or petri dish)

6. Select and surface sterilize 2 sclerotia for each isolate.

   Surface sterilization:
   a) Submerge in 10% Clorox for 1 min.
   b) Transfer to 95% EtOH for 1 min
   c) Transfer and rinse 1x in sterile Milli-Q H_2O
   d) Transfer to filter paper until dry

7. Once sclerotia are dry, transfer to clean PDA plate. Parafilm and store at 12°C.

AI.3. Transferring Isolates to Fresh PDA

1. Prepare sterile area. Obtain isolate cultures, any age, and fresh PDA plates.

2. Flame sterilize a 5-mm cork-borer. Allow to cool completely, either setting to air cool or gently pressing in clean agar.

3. Completely depress cork-borer in the leading edge of mycelium or the edge of the old plate (avoid sclerotia).

4. Using a flame sterilized spatula, gently lift circular agar sections and flip, mycelial-side down, onto a clean PDA plate.

5. Parafilm plate and store right-side up (so the agar plug stays in contact with the fresh media for 1-2 days).

AI.4. Transferring Isolates to Modified PDA: Self-Self

1. Prepare sterile area. Obtain isolate cultures, 2-3 days old (from section III), and modified PDA plates.

    - On the bottom of each plate, mark 2 dots 3.5 cm apart equidistant from the center of the plate. Use filter paper template to assist in consistently marking all plates.

2. Obtain 5-mm mycelial plugs from 1 cm **behind** the leading edge of 2-3 day old colonies (for most consistent results).

3. Transfer 2 plugs from each culture onto the same plate over each of the previously marked dots (self-self interaction).

4. Do not parafilm, store in a dark area at room temperature.

5. Score interactions after 4-7 days.

AI.5. Transferring Isolates to Modified PDA: 3-way

1. Prepare sterile area. Obtain isolate cultures, 2-3 days old (from section III), and modified PDA plates.

    - On the bottom of each plate, mark 3 dots 3.5 cm apart equidistant from the center of the plate. Use filter paper template to assist in consistently marking all plates.

2. Obtain 5-mm mycelial plugs from 1 cm **behind** the leading edge of 2-3 day old colonies (for most consistent results).

3. Transfer 1 plug from each of 3 different cultures onto the same plate over the previously marked dots (3-way interaction).

4. Do not parafilm, store in a dark area at room temperature.

5. Score interactions after 4-7 days.

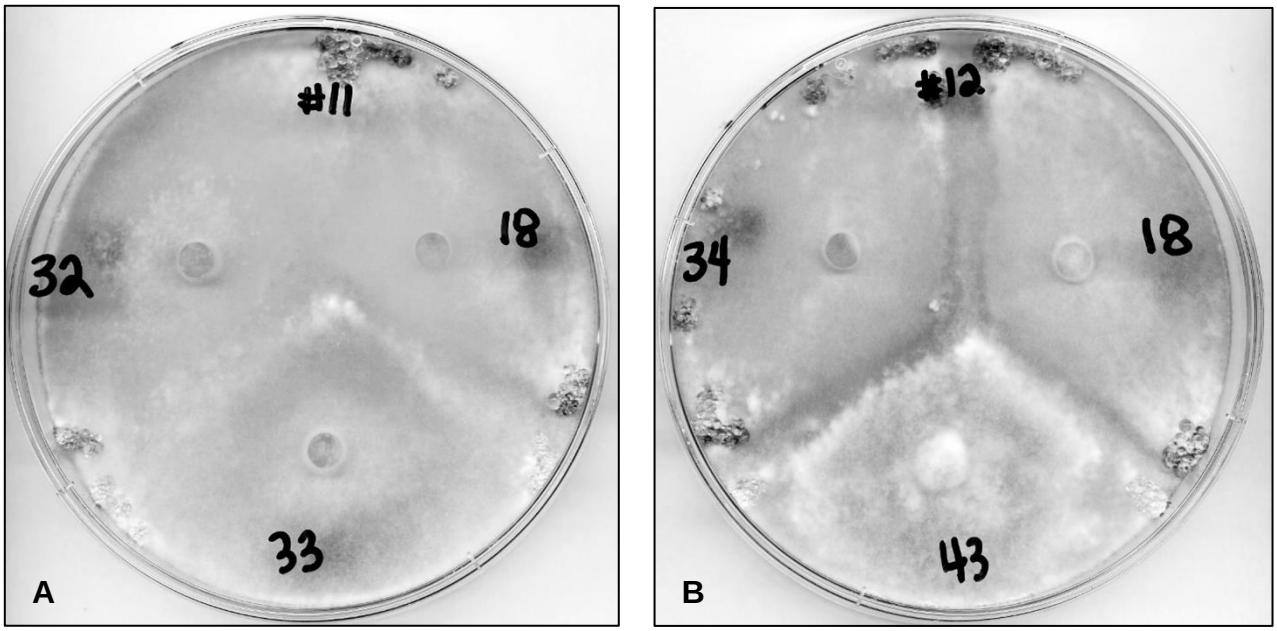

Figure AI.1. Examples of mycelial interactions 4 days post-plating. Mycelial compatibility can be observed between isolates 32 and 18 on plate #11 (A). Mycelial incompatibility can be observed between all isolates on plate #12 (B).

Appendix II: Monitoring *Sclerotinia sclerotiorum* infection in resistant and susceptible soybean stems through stem isolations

Theresa Blackwell and Jaime Willbur

Summary

Susceptible (91-44), resistant (91-145), and moderately resistant (91-38) experimental soybean lines were used to monitor stem infection of *Sclerotinia sclerotiorum*. Soybean plants were planted one per pot, and grown until the V4 (fourth trifoliate) or V5 (fifth trifoliate) growth stages. At this time, the second trifoliate leaf was cut and, the plants were either inoculated with a fluorescent isolate of *S. sclerotiorum* (1980 GFP-Nou^{R}) or mock-inoculated with a potato dextrose agar (PDA) control. Each treatment was replicated three times (rep) and repeated twice (run). After 15 days, final lesion lengths (mm) were measured, plants were harvested, and sections were taken in increments of 0.5-cm along the stem at, above, and below the node of inoculation. Sections were surface sterilized by soaking in 10% Clorox for 1 min followed by rinsing in sterile Milli-Q® (EMD Millipore) and blotting dry on sterile filter paper. Surface sterilized sections were plated onto potato dextrose agar plates, parafilmed, and stored in plastic bins at room temperature.

Binary presence (1) or absence (0) data were collected for each 0.5-cm stem section including: external necrotic lesion (L), internal vascular browning or necrosis (V), mycelial growth (G), sclerotial formation (S), and pathogen presence (P) (Table AII.1). Growth was monitored daily beginning 24 hr after plating stem sections, sclerotial formation was noted approximately 5-7 days after plating, and pathogen presence was summarized these two results. Statistical analyses were conducted in SAS v. 9.4 (SAS Institute, Cary, NC). Sums of binomial data were generated for each replicate of each treatment using the UNIVARIATE

procedure. Generalized linear mixed model (GLIMMIX) procedures were used to conduct an analysis of variance (ANOVA) where soybean line was considered a fixed effect and replication was nested within repetition [rep(run)] as a random effect.

Line was found to significantly impact both final lesion length ($P = 0.0135$) and the mean sum of sections with vascular necrosis ($P = 0.0213$) (Table AII.2). The resistant line resulted in a mean lesion length of 5.37 mm whereas the susceptible line had a mean lesion length of 35.71 mm (Table AII.2). While line did not significantly affect the sum of pathogen isolated ($P = 0.0971$), a trend was observed as the number of infected sections was 1.67 for the resistant line and 5.08 for the susceptible line (Table AII.2).

Overall, resistant soybean line 91-145 and moderately resistant line 91-38 were found to exhibit reduced final lesion length, total vascular necrosis, and *S. sclerotiorum* infection (based on isolations) than the susceptible line 91-44. Of note, in 91-145 and 91-38 the total number of sections from which *S. sclerotiorum* was successfully isolated was slightly higher than either the number of sections exhibiting external or interal necrosis (Table II.2). In 91-44, the number of infected sections was less than the number of sections exhibiting either lesion or vascular necrosis (Table II.2).

These results suggest that lesion length and vascular discoloration are representative of actual pathogen presence in more resistant soybean lines. However, in this susceptible line, the external and internal symtoms are greater than the area where *S. sclerotiorum* is isolated. In the susceptible line, symptoms may develop beyond the leading edge of active *S. sclerotiorum* mycelial growth. Resistant lines may not only limit the growth of *S.*

sclerotiorum within stem tissues, but also potentially the diffusion of pathogenicity factors into the uncolonized soybean tissues.

Tables

Table AII.1. Two repetitions (runs) of soybean stem isolations of *S. sclerotiorum* from susceptible (91-44), resistant (91-145), and moderately resistant (91-38) experimental soybean lines, each from three replications (rep). Plants were either inoculated with 1980 GFP-Nou^{R} isolate of *S. sclerotiorum* (GFP) or mock-inoculated with potato dextrose agar (PDA). Showing final lesion length and binary data for presence (1) or absence (0) of: external necrotic lesion (L), internal vascular browning or necrosis (V), mycelial growth (G), sclerotial formation (S), and pathogen presence (P) for each of the 0.5-cm sections.

Run	Rep	Line	Trt[a]	Lesion length (mm)	Section[b]	Binary[c]				
						L	V	G	S	P
1	1	91-44	GFP	145.14	-2.0	0	1	0	0	0
1	1	91-44	GFP	145.14	-1.5	0	1	0	0	0
1	1	91-44	GFP	145.14	-1.0	1	1	1	1	1
1	1	91-44	GFP	145.14	-0.5	1	1	1	1	1
1	1	91-44	GFP	145.14	0.0	1	1	0	1	1
1	1	91-44	GFP	145.14	0.5	1	1	0	0	0
1	1	91-44	GFP	145.14	1.0	1	1	0	0	0
1	1	91-44	GFP	145.14	1.5	1	1	0	0	0
1	1	91-44	GFP	145.14	2.0	1	1	0	0	0
1	1	91-44	GFP	145.14	2.5	1	1	0	0	0
1	1	91-44	GFP	145.14	3.0	1	1	0	0	0
1	1	91-44	GFP	145.14	3.5	1	1	0	0	0
1	1	91-44	GFP	145.14	4.0	1	1	0	0	0
1	1	91-44	GFP	145.14	4.5	1	1	0	1	1
1	1	91-44	GFP	145.14	5.0	1	1	1	1	1
1	1	91-44	GFP	145.14	5.5	1	1	1	1	1
1	1	91-44	GFP	145.14	6.0	1	1	1	1	1
1	1	91-44	GFP	145.14	6.5	1	1	0	1	1

1	1	91-44	GFP	145.14	7.0	1	1	0	0	0
1	1	91-44	PDA	0.00	-2.0	0	0	0	0	0
1	1	91-44	PDA	0.00	-1.5	0	0	0	0	0
1	1	91-44	PDA	0.00	-1.0	0	0	0	0	0
1	1	91-44	PDA	0.00	-0.5	0	0	0	0	0
1	1	91-44	PDA	0.00	0.0	0	0	0	0	0
1	1	91-44	PDA	0.00	0.5	0	0	0	0	0
1	1	91-44	PDA	0.00	1.0	0	0	0	0	0
1	1	91-44	PDA	0.00	1.5	0	0	0	0	0
1	1	91-44	PDA	0.00	2.0	0	0	0	0	0
1	1	91-44	PDA	0.00	2.5	0	0	0	0	0
1	1	91-44	PDA	0.00	3.0	0	0	0	0	0
1	1	91-44	PDA	0.00	3.5	0	0	0	0	0
1	1	91-44	PDA	0.00	4.0	0	0	0	0	0
1	1	91-44	PDA	0.00	4.5	0	0	0	0	0
1	1	91-44	PDA	0.00	5.0	0	0	0	0	0
1	1	91-44	PDA	0.00	5.5	0	0	0	0	0
1	1	91-44	PDA	0.00	6.0	0	0	0	0	0
1	1	91-44	PDA	0.00	6.5	0	0	0	0	0
1	1	91-44	PDA	0.00	7.0	0	0	0	0	0
1	1	91-145	GFP	5.88	1.5	0	0	0	0	0
1	1	91-145	GFP	5.88	1.0	0	0	0	0	0
1	1	91-145	GFP	5.88	0.5	0	0	0	0	0
1	1	91-145	GFP	5.88	0.0	1	0	0	1	1
1	1	91-145	GFP	5.88	-0.5	0	0	0	1	1
1	1	91-145	GFP	5.88	-1.0	0	0	0	0	0
1	1	91-145	GFP	5.88	-1.5	0	0	0	0	0
1	1	91-145	PDA	0.00	1.5	0	0	0	0	0
1	1	91-145	PDA	0.00	1.0	0	0	0	0	0
1	1	91-145	PDA	0.00	0.5	0	0	0	0	0
1	1	91-145	PDA	0.00	0.0	0	0	1	0	1
1	1	91-145	PDA	0.00	-0.5	0	0	0	0	0
1	1	91-145	PDA	0.00	-1.0	0	0	0	0	0
1	1	91-145	PDA	0.00	-1.5	0	0	0	0	0
1	1	91-38	GFP	7.39	1.5	0	0	0	0	0
1	1	91-38	GFP	7.39	1.0	0	0	0	0	0
1	1	91-38	GFP	7.39	0.5	0	0	0	0	0
1	1	91-38	GFP	7.39	0.0	1	0	0	0	0
1	1	91-38	GFP	7.39	-0.5	0	0	0	0	0

1	1	91-38	GFP	7.39	-1.0	0	0	1	0	1
1	1	91-38	GFP	7.39	-1.5	0	0	0	0	0
1	1	91-38	PDA	0.00	1.5	0	0	0	0	0
1	1	91-38	PDA	0.00	1.0	0	0	0	0	0
1	1	91-38	PDA	0.00	0.5	0	0	0	0	0
1	1	91-38	PDA	0.00	0.0	1	0	0	0	0
1	1	91-38	PDA	0.00	-0.5	0	0	0	0	0
1	1	91-38	PDA	0.00	-1.0	0	0	0	0	0
1	1	91-38	PDA	0.00	-1.5	0	0	0	0	0
1	2	91-44	GFP	11.31	3.0	0	0	0	0	0
1	2	91-44	GFP	11.31	2.5	0	1	0	0	0
1	2	91-44	GFP	11.31	2.0	0	1	0	0	0
1	2	91-44	GFP	11.31	1.5	0	1	0	0	0
1	2	91-44	GFP	11.31	1.0	1	1	1	0	1
1	2	91-44	GFP	11.31	0.5	1	1	0	1	1
1	2	91-44	GFP	11.31	0.0	1	1	0	1	1
1	2	91-44	GFP	11.31	-0.5	0	1	0	0	0
1	2	91-44	GFP	11.31	-1.0	0	1	0	1	1
1	2	91-44	PDA	0.00	3.0	0	0	0	0	0
1	2	91-44	PDA	0.00	2.5	0	0	0	0	0
1	2	91-44	PDA	0.00	2.0	0	0	0	0	0
1	2	91-44	PDA	0.00	1.5	0	0	0	0	0
1	2	91-44	PDA	0.00	1.0	0	0	0	0	0
1	2	91-44	PDA	0.00	0.5	0	0	0	0	0
1	2	91-44	PDA	0.00	0.0	0	0	0	0	0
1	2	91-44	PDA	0.00	-0.5	0	0	0	0	0
1	2	91-44	PDA	0.00	-1.0	0	0	0	0	0
1	2	91-145	GFP	7.14	1.5	0	0	0	0	0
1	2	91-145	GFP	7.14	1.0	0	0	0	0	0
1	2	91-145	GFP	7.14	0.5	0	0	0	1	1
1	2	91-145	GFP	7.14	0.0	1	0	0	1	1
1	2	91-145	GFP	7.14	-0.5	0	0	0	1	1
1	2	91-145	GFP	7.14	-1.0	0	0	0	0	0
1	2	91-145	GFP	7.14	-1.5	0	0	0	0	0
1	2	91-145	PDA	0.00	1.5	0	0	0	0	0
1	2	91-145	PDA	0.00	1.0	0	0	0	0	0
1	2	91-145	PDA	0.00	0.5	0	0	0	0	0
1	2	91-145	PDA	0.00	0.0	0	0	0	0	0
1	2	91-145	PDA	0.00	-0.5	0	0	0	0	0

1	2	91-145	PDA	0.00	-1.0	0	0	0	0	0
1	2	91-145	PDA	0.00	-1.5	0	0	0	0	0
1	2	91-38	GFP	5.55	1.0	0	0	0	0	0
1	2	91-38	GFP	5.55	0.5	1	0	0	0	0
1	2	91-38	GFP	5.55	0.0	1	1	0	1	1
1	2	91-38	GFP	5.55	-0.5	1	1	0	1	1
1	2	91-38	GFP	5.55	-1.0	0	1	0	0	0
1	2	91-38	GFP	5.55	-1.5	0	1	0	0	0
1	2	91-38	GFP	5.55	-2.0	0	0	0	0	0
1	2	91-38	PDA	0.00	1.0	0	0	0	0	0
1	2	91-38	PDA	0.00	0.5	0	0	0	0	0
1	2	91-38	PDA	0.00	0.0	0	0	0	0	0
1	2	91-38	PDA	0.00	-0.5	0	0	0	0	0
1	2	91-38	PDA	0.00	-1.0	0	0	0	0	0
1	2	91-38	PDA	0.00	-1.5	0	0	0	0	0
1	2	91-38	PDA	0.00	-2.0	0	0	0	0	0
1	3	91-44	GFP	35.03	6.5	0	0	0	0	0
1	3	91-44	GFP	35.03	6.0	0	1	0	1	1
1	3	91-44	GFP	35.03	5.5	0	1	0	1	1
1	3	91-44	GFP	35.03	5.0	0	1	0	1	1
1	3	91-44	GFP	35.03	4.5	0	1	1	1	1
1	3	91-44	GFP	35.03	4.0	0	1	0	1	1
1	3	91-44	GFP	35.03	3.5	0	1	0	1	1
1	3	91-44	GFP	35.03	3.0	0	1	0	1	1
1	3	91-44	GFP	35.03	2.5	1	1	1	1	1
1	3	91-44	GFP	35.03	2.0	1	1	1	1	1
1	3	91-44	GFP	35.03	1.5	1	1	1	1	1
1	3	91-44	GFP	35.03	1.0	1	1	1	1	1
1	3	91-44	GFP	35.03	0.5	1	1	1	1	1
1	3	91-44	GFP	35.03	0.0	1	1	1	1	1
1	3	91-44	GFP	35.03	-0.5	1	1	1	1	1
1	3	91-44	GFP	35.03	-1.0	1	1	1	1	1
1	3	91-44	GFP	35.03	-1.5	0	1	0	0	0
1	3	91-44	GFP	35.03	-2.0	0	1	0	0	0
1	3	91-44	PDA	0.00	6.5	0	0	0	0	0
1	3	91-44	PDA	0.00	6.0	0	0	0	0	0
1	3	91-44	PDA	0.00	5.5	0	0	0	0	0
1	3	91-44	PDA	0.00	5.0	0	0	0	0	0
1	3	91-44	PDA	0.00	4.5	0	0	0	0	0

1	3	91-44	PDA	0.00	4.0	0	0	0	0	0
1	3	91-44	PDA	0.00	3.5	0	0	0	0	0
1	3	91-44	PDA	0.00	3.0	0	0	0	0	0
1	3	91-44	PDA	0.00	2.5	0	0	0	0	0
1	3	91-44	PDA	0.00	2.0	0	0	0	0	0
1	3	91-44	PDA	0.00	1.5	0	0	0	0	0
1	3	91-44	PDA	0.00	1.0	0	0	0	0	0
1	3	91-44	PDA	0.00	0.5	0	0	0	0	0
1	3	91-44	PDA	0.00	0.0	0	0	0	0	0
1	3	91-44	PDA	0.00	-0.5	0	0	0	0	0
1	3	91-44	PDA	0.00	-1.0	0	0	0	0	0
1	3	91-44	PDA	0.00	-1.5	0	0	0	0	0
1	3	91-44	PDA	0.00	-2.0	0	0	0	0	0
1	3	91-145	GFP	5.45	1.0	0	0	1	0	1
1	3	91-145	GFP	5.45	0.5	0	0	1	0	1
1	3	91-145	GFP	5.45	0.0	1	0	1	1	1
1	3	91-145	GFP	5.45	-0.5	0	0	0	0	0
1	3	91-145	GFP	5.45	-1.0	0	0	1	0	1
1	3	91-145	PDA	0.00	1.0	0	0	0	0	0
1	3	91-145	PDA	0.00	0.5	0	0	0	0	0
1	3	91-145	PDA	0.00	0.0	0	0	0	0	0
1	3	91-145	PDA	0.00	-0.5	0	0	0	0	0
1	3	91-145	PDA	0.00	-1.0	0	0	0	0	0
1	3	91-38	GFP	5.34	1.0	0	0	0	0	0
1	3	91-38	GFP	5.34	0.5	0	0	0	0	0
1	3	91-38	GFP	5.34	0.0	1	0	0	1	1
1	3	91-38	GFP	5.34	-0.5	0	0	0	0	0
1	3	91-38	GFP	5.34	-1.0	0	0	0	0	0
1	3	91-38	PDA	0.00	1.0	0	0	0	0	0
1	3	91-38	PDA	0.00	0.5	0	0	0	0	0
1	3	91-38	PDA	0.00	0.0	0	0	0	0	0
1	3	91-38	PDA	0.00	-0.5	0	0	0	0	0
1	3	91-38	PDA	0.00	-1.0	0	0	0	0	0
2	1	91-44	GFP	6.04	13.5	0	1	0	0	0
2	1	91-44	GFP	6.04	13.0	0	1	0	0	0
2	1	91-44	GFP	6.04	12.5	0	1	0	0	0
2	1	91-44	GFP	6.04	12.0	0	1	0	0	0
2	1	91-44	GFP	6.04	11.5	0	1	0	0	0
2	1	91-44	GFP	6.04	11.0	0	1	0	0	0

2	1	91-44	GFP	6.04	10.5	0	1	0	0	0
2	1	91-44	GFP	6.04	10.0	0	1	0	0	0
2	1	91-44	GFP	6.04	9.5	0	1	0	0	0
2	1	91-44	GFP	6.04	9.0	0	1	0	0	0
2	1	91-44	GFP	6.04	8.5	0	1	0	0	0
2	1	91-44	GFP	6.04	8.0	0	1	0	0	0
2	1	91-44	GFP	6.04	7.5	0	1	0	0	0
2	1	91-44	GFP	6.04	7.0	1	1	0	0	0
2	1	91-44	GFP	6.04	6.5	1	1	0	0	0
2	1	91-44	GFP	6.04	6.0	1	1	0	0	0
2	1	91-44	GFP	6.04	5.5	1	1	0	0	0
2	1	91-44	GFP	6.04	5.0	1	1	1	1	1
2	1	91-44	GFP	6.04	4.5	1	1	1	1	1
2	1	91-44	GFP	6.04	4.0	1	1	0	0	0
2	1	91-44	GFP	6.04	3.5	1	1	0	0	0
2	1	91-44	GFP	6.04	3.0	1	1	0	0	0
2	1	91-44	GFP	6.04	2.5	1	1	0	0	0
2	1	91-44	GFP	6.04	2.0	1	1	1	1	1
2	1	91-44	GFP	6.04	1.5	1	1	1	1	1
2	1	91-44	GFP	6.04	1.0	1	1	1	1	1
2	1	91-44	GFP	6.04	0.5	1	1	1	1	1
2	1	91-44	GFP	6.04	0.0	1	1	1	1	1
2	1	91-44	GFP	6.04	-0.5	1	1	1	1	1
2	1	91-44	GFP	6.04	-1.0	1	1	1	1	1
2	1	91-44	GFP	6.04	-1.5	1	1	1	1	1
2	1	91-44	GFP	6.04	-2.0	1	1	1	1	1
2	1	91-44	GFP	6.04	-2.5	1	1	1	1	1
2	1	91-44	GFP	6.04	-3.0	1	1	1	1	1
2	1	91-44	GFP	6.04	-3.5	1	1	0	0	0
2	1	91-44	GFP	6.04	-4.0	1	1	0	0	0
2	1	91-44	PDA	0.00	13.5	0	0	0	0	0
2	1	91-44	PDA	0.00	13.0	0	0	0	0	0
2	1	91-44	PDA	0.00	12.5	0	0	0	0	0
2	1	91-44	PDA	0.00	12.0	0	0	0	0	0
2	1	91-44	PDA	0.00	11.5	0	0	0	0	0
2	1	91-44	PDA	0.00	11.0	0	0	0	0	0
2	1	91-44	PDA	0.00	10.5	0	0	0	0	0
2	1	91-44	PDA	0.00	10.0	0	0	0	0	0
2	1	91-44	PDA	0.00	9.5	0	0	0	0	0

2	1	91-44	PDA	0.00	9.0	0	0	0	0	0
2	1	91-44	PDA	0.00	8.5	0	0	0	0	0
2	1	91-44	PDA	0.00	8.0	0	0	0	0	0
2	1	91-44	PDA	0.00	7.5	0	0	0	0	0
2	1	91-44	PDA	0.00	7.0	0	0	0	0	0
2	1	91-44	PDA	0.00	6.5	0	0	0	0	0
2	1	91-44	PDA	0.00	6.0	0	0	0	0	0
2	1	91-44	PDA	0.00	5.5	0	0	0	0	0
2	1	91-44	PDA	0.00	5.0	0	0	0	0	0
2	1	91-44	PDA	0.00	4.5	0	0	0	0	0
2	1	91-44	PDA	0.00	4.0	0	0	0	0	0
2	1	91-44	PDA	0.00	3.5	0	0	0	0	0
2	1	91-44	PDA	0.00	3.0	0	0	0	0	0
2	1	91-44	PDA	0.00	2.5	0	0	0	0	0
2	1	91-44	PDA	0.00	2.0	0	0	0	0	0
2	1	91-44	PDA	0.00	1.5	0	0	0	0	0
2	1	91-44	PDA	0.00	1.0	0	0	0	0	0
2	1	91-44	PDA	0.00	0.5	0	0	0	0	0
2	1	91-44	PDA	0.00	0.0	0	0	0	0	0
2	1	91-44	PDA	0.00	-0.5	0	0	0	0	0
2	1	91-44	PDA	0.00	-1.0	0	0	0	0	0
2	1	91-44	PDA	0.00	-1.5	0	0	0	0	0
2	1	91-44	PDA	0.00	-2.0	0	0	0	0	0
2	1	91-44	PDA	0.00	-2.5	0	0	0	0	0
2	1	91-44	PDA	0.00	-3.0	0	0	0	0	0
2	1	91-38	GFP	5.81	2.0	0	0	0	0	0
2	1	91-38	GFP	5.81	1.5	0	0	0	0	0
2	1	91-38	GFP	5.81	1.0	0	0	0	0	0
2	1	91-38	GFP	5.81	0.5	1	0	1	1	1
2	1	91-38	GFP	5.81	0.0	1	0	1	1	1
2	1	91-38	GFP	5.81	-0.5	1	0	0	0	0
2	1	91-38	GFP	5.81	-1.0	0	0	0	0	0
2	1	91-38	GFP	5.81	-1.5	0	0	0	0	0
2	1	91-38	PDA	0.00	2.0	0	0	0	0	0
2	1	91-38	PDA	0.00	1.5	0	0	0	0	0
2	1	91-38	PDA	0.00	1.0	0	0	0	0	0
2	1	91-38	PDA	0.00	0.5	0	0	0	0	0
2	1	91-38	PDA	0.00	0.0	0	0	0	0	0
2	1	91-38	PDA	0.00	-0.5	0	0	0	0	0

2	1	91-38	PDA	0.00	-1.0	0	0	0	0	0
2	1	91-38	PDA	0.00	-1.5	0	0	0	0	0
2	2	91-44	GFP	62.43	1.5	0	0	0	0	0
2	2	91-44	GFP	62.43	1.0	0	0	0	0	0
2	2	91-44	GFP	62.43	0.5	0	0	1	1	1
2	2	91-44	GFP	62.43	0.0	1	0	1	1	1
2	2	91-44	GFP	62.43	-0.5	1	0	0	0	0
2	2	91-44	GFP	62.43	-1.0	0	0	0	0	0
2	2	91-44	GFP	62.43	-1.5	0	0	0	0	0
2	2	91-44	PDA	62.43	1.5	0	0	0	0	0
2	2	91-44	PDA	62.43	1.0	0	0	0	0	0
2	2	91-44	PDA	62.43	0.5	0	0	0	0	0
2	2	91-44	PDA	62.43	0.0	0	0	0	0	0
2	2	91-44	PDA	62.43	-0.5	0	0	0	0	0
2	2	91-44	PDA	62.43	-1.0	0	0	0	0	0
2	2	91-44	PDA	62.43	-1.5	0	0	0	0	0
2	2	91-145	GFP	11.94	2.0	0	0	0	0	0
2	2	91-145	GFP	11.94	1.5	0	0	0	0	0
2	2	91-145	GFP	11.94	1.0	1	0	1	1	1
2	2	91-145	GFP	11.94	0.5	1	0	1	1	1
2	2	91-145	GFP	11.94	0.0	1	0	1	1	1
2	2	91-145	GFP	11.94	-0.5	1	0	1	1	1
2	2	91-145	GFP	11.94	-1.0	0	0	0	0	0
2	2	91-145	GFP	11.94	-1.5	0	0	0	0	0
2	2	91-145	PDA	0.00	2.0	0	0	0	0	0
2	2	91-145	PDA	0.00	1.5	0	0	0	0	0
2	2	91-145	PDA	0.00	1.0	0	0	0	0	0
2	2	91-145	PDA	0.00	0.5	0	0	0	0	0
2	2	91-145	PDA	0.00	0.0	0	0	0	0	0
2	2	91-145	PDA	0.00	-0.5	0	0	0	0	0
2	2	91-145	PDA	0.00	-1.0	0	0	0	0	0
2	2	91-145	PDA	0.00	-1.5	0	0	0	0	0
2	2	91-38	GFP	10.29	2.0	0	0	1	1	1
2	2	91-38	GFP	10.29	1.5	0	1	1	1	1
2	2	91-38	GFP	10.29	1.0	0	1	1	1	1
2	2	91-38	GFP	10.29	0.5	1	1	1	1	1
2	2	91-38	GFP	10.29	0.0	1	1	1	1	1
2	2	91-38	GFP	10.29	-0.5	1	1	1	1	1
2	2	91-38	GFP	10.29	-1.0	1	1	1	1	1

2	2	91-38	GFP	10.29	-1.5	0	1	1	1	1
2	2	91-38	GFP	10.29	-2.0	0	0	0	0	0
2	2	91-38	PDA	0.00	2.0	0	0	0	0	0
2	2	91-38	PDA	0.00	1.5	0	0	0	0	0
2	2	91-38	PDA	0.00	1.0	0	0	0	0	0
2	2	91-38	PDA	0.00	0.5	0	0	0	0	0
2	2	91-38	PDA	0.00	0.0	0	0	0	0	0
2	2	91-38	PDA	0.00	-0.5	0	0	0	0	0
2	2	91-38	PDA	0.00	-1.0	0	0	0	0	0
2	2	91-38	PDA	0.00	-1.5	0	0	0	0	0
2	2	91-38	PDA	0.00	-2.0	0	0	0	0	0
2	3	91-44	GFP	106.19	20.0	0	0	0	0	0
2	3	91-44	GFP	106.19	19.5	0	1	0	0	0
2	3	91-44	GFP	106.19	19.0	1	1	0	0	0
2	3	91-44	GFP	106.19	18.5	1	1	0	0	0
2	3	91-44	GFP	106.19	18.0	1	1	0	0	0
2	3	91-44	GFP	106.19	17.5	1	1	0	0	0
2	3	91-44	GFP	106.19	17.0	1	1	0	0	0
2	3	91-44	GFP	106.19	16.5	1	1	0	0	0
2	3	91-44	GFP	106.19	16.0	1	1	0	0	0
2	3	91-44	GFP	106.19	15.5	1	1	0	0	0
2	3	91-44	GFP	106.19	15.0	1	1	0	0	0
2	3	91-44	GFP	106.19	14.5	1	1	0	0	0
2	3	91-44	GFP	106.19	14.0	1	1	0	0	0
2	3	91-44	GFP	106.19	13.5	1	1	0	0	0
2	3	91-44	GFP	106.19	13.0	1	1	1	1	1
2	3	91-44	GFP	106.19	12.5	1	1	0	0	0
2	3	91-44	GFP	106.19	12.0	1	1	1	1	1
2	3	91-44	GFP	106.19	11.5	1	1	1	1	1
2	3	91-44	GFP	106.19	11.0	1	1	1	1	1
2	3	91-44	GFP	106.19	10.5	1	1	1	1	1
2	3	91-44	GFP	106.19	10.0	1	1	1	1	1
2	3	91-44	GFP	106.19	9.5	1	1	1	1	1
2	3	91-44	GFP	106.19	9.0	1	1	1	1	1
2	3	91-44	GFP	106.19	8.5	1	1	1	1	1
2	3	91-44	GFP	106.19	8.0	1	1	1	1	1
2	3	91-44	GFP	106.19	7.5	1	1	1	1	1
2	3	91-44	GFP	106.19	7.0	1	1	1	1	1
2	3	91-44	GFP	106.19	6.5	1	1	0	0	0

2	3	91-44	GFP	106.19	6.0	1	1	0	0	0
2	3	91-44	GFP	106.19	5.5	1	1	1	1	1
2	3	91-44	GFP	106.19	5.0	1	1	0	0	0
2	3	91-44	GFP	106.19	4.5	1	1	0	0	0
2	3	91-44	GFP	106.19	4.0	1	1	1	1	1
2	3	91-44	GFP	106.19	3.5	1	1	0	0	0
2	3	91-44	GFP	106.19	3.0	1	1	0	0	0
2	3	91-44	GFP	106.19	2.5	1	1	0	0	0
2	3	91-44	GFP	106.19	2.0	1	1	0	0	0
2	3	91-44	GFP	106.19	1.5	1	1	0	0	0
2	3	91-44	GFP	106.19	1.0	1	1	1	1	1
2	3	91-44	GFP	106.19	0.5	1	1	0	0	0
2	3	91-44	GFP	106.19	0.0	1	1	0	0	0
2	3	91-44	GFP	106.19	-0.5	1	1	1	1	1
2	3	91-44	GFP	106.19	-1.0	1	1	1	1	1
2	3	91-44	GFP	106.19	-1.5	1	1	1	1	1
2	3	91-44	GFP	106.19	-2.0	0	1	1	1	1
2	3	91-44	PDA	0.00	20.0	0	0	0	0	0
2	3	91-44	PDA	0.00	19.5	0	0	0	0	0
2	3	91-44	PDA	0.00	19.0	0	0	0	0	0
2	3	91-44	PDA	0.00	18.5	0	0	0	0	0
2	3	91-44	PDA	0.00	18.0	0	0	0	0	0
2	3	91-44	PDA	0.00	17.5	0	0	0	0	0
2	3	91-44	PDA	0.00	17.0	0	0	0	0	0
2	3	91-44	PDA	0.00	16.5	0	0	0	0	0
2	3	91-44	PDA	0.00	16.0	0	0	0	0	0
2	3	91-44	PDA	0.00	15.5	0	0	0	0	0
2	3	91-44	PDA	0.00	15.0	0	0	0	0	0
2	3	91-44	PDA	0.00	14.5	0	0	0	0	0
2	3	91-44	PDA	0.00	14.0	0	0	0	0	0
2	3	91-44	PDA	0.00	13.5	0	0	0	0	0
2	3	91-44	PDA	0.00	13.0	0	0	0	0	0
2	3	91-44	PDA	0.00	12.5	0	0	0	0	0
2	3	91-44	PDA	0.00	12.0	0	0	0	0	0
2	3	91-44	PDA	0.00	11.5	0	0	0	0	0
2	3	91-44	PDA	0.00	11.0	0	0	0	0	0
2	3	91-44	PDA	0.00	10.5	0	0	0	0	0
2	3	91-44	PDA	0.00	10.0	0	0	0	0	0
2	3	91-44	PDA	0.00	9.5	0	0	0	0	0

2	3	91-44	PDA	0.00	9.0	0	0	0	0	0
2	3	91-44	PDA	0.00	8.5	0	0	0	0	0
2	3	91-44	PDA	0.00	8.0	0	0	0	0	0
2	3	91-44	PDA	0.00	7.5	0	0	0	0	0
2	3	91-44	PDA	0.00	7.0	0	0	0	0	0
2	3	91-44	PDA	0.00	6.5	0	0	0	0	0
2	3	91-44	PDA	0.00	6.0	0	0	0	0	0
2	3	91-44	PDA	0.00	5.5	0	0	0	0	0
2	3	91-44	PDA	0.00	5.0	0	0	0	0	0
2	3	91-44	PDA	0.00	4.5	0	0	0	0	0
2	3	91-44	PDA	0.00	4.0	0	0	0	0	0
2	3	91-44	PDA	0.00	3.5	0	0	0	0	0
2	3	91-44	PDA	0.00	3.0	0	0	0	0	0
2	3	91-44	PDA	0.00	2.5	0	0	0	0	0
2	3	91-44	PDA	0.00	2.0	0	0	0	0	0
2	3	91-44	PDA	0.00	1.5	0	0	0	0	0
2	3	91-44	PDA	0.00	1.0	0	0	0	0	0
2	3	91-44	PDA	0.00	0.5	0	0	0	0	0
2	3	91-44	PDA	0.00	0.0	0	0	0	0	0
2	3	91-44	PDA	0.00	-0.5	0	0	0	0	0
2	3	91-44	PDA	0.00	-1.0	0	0	0	0	0
2	3	91-44	PDA	0.00	-1.5	0	0	0	0	0
2	3	91-44	PDA	0.00	-2.0	0	0	0	0	0
2	3	91-145	GFP	12.62	1.5	0	0	0	0	0
2	3	91-145	GFP	12.62	1.0	0	0	0	0	0
2	3	91-145	GFP	12.62	0.5	0	0	1	1	1
2	3	91-145	GFP	12.62	0.0	1	0	1	1	1
2	3	91-145	GFP	12.62	-0.5	1	0	1	1	1
2	3	91-145	GFP	12.62	-1.0	1	0	0	0	0
2	3	91-145	GFP	12.62	-1.5	0	0	0	0	0
2	3	91-145	GFP	12.62	-2.0	0	0	0	0	0
2	3	91-145	GFP	12.62	-2.5	0	0	0	0	0
2	3	91-145	PDA	12.62	1.5	0	0	0	0	0
2	3	91-145	PDA	12.62	1.0	0	0	0	0	0
2	3	91-145	PDA	12.62	0.5	0		0	0	0
2	3	91-145	PDA	12.62	0.0	1	0	0	0	0
2	3	91-145	PDA	12.62	-0.5	1	1	0	0	0
2	3	91-145	PDA	12.62	-1.0	1	0	0	0	0
2	3	91-145	PDA	12.62	-1.5	0	0	0	0	0

2	3	91-145	PDA	12.62	-2.0	0	0	0	0	0
2	3	91-145	PDA	12.62	-2.5	0	0	0	0	0
2	3	91-38	GFP	0.00	1.5	0	0	0	0	0
2	3	91-38	GFP	6.50	1.0	0	0	0	0	0
2	3	91-38	GFP	6.50	0.5	1	0	1	1	1
2	3	91-38	GFP	6.50	0.0	1	0	1	1	1
2	3	91-38	GFP	6.50	-0.5	1	0	0	0	0
2	3	91-38	GFP	6.50	-1.0	1	0	0	0	0
2	3	91-38	GFP	6.50	-1.5	0	0	0	0	0
2	3	91-38	GFP	6.50	-2.0	0	0	0	0	0
2	3	91-38	PDA	0.00	1.5	0	0	0	0	0
2	3	91-38	PDA	0.00	1.0	0	0	0	0	0
2	3	91-38	PDA	0.00	0.5	0	0	0	0	0
2	3	91-38	PDA	0.00	0.0	0	0	0	0	0
2	3	91-38	PDA	0.00	-0.5	0	0	0	0	0
2	3	91-38	PDA	0.00	-1.0	0	0	0	0	0
2	3	91-38	PDA	0.00	-1.5	0	0	0	0	0
2	3	91-38	PDA	0.00	-2.0	0	0	0	0	0
2	1	91-145	GFP	8.80	1.5	0	0	0	0	0
2	1	91-145	GFP	8.80	1.0	0	0	0	0	0
2	1	91-145	GFP	8.80	0.5	0	0	0	0	0
2	1	91-145	GFP	8.80	0.0	1	0	0	0	0
2	1	91-145	GFP	8.80	-0.5	1	0	1	1	1
2	1	91-145	GFP	8.80	-1.0	0	0	0	0	0
2	1	91-145	GFP	8.80	-1.5	0	0	0	0	0
2	1	91-145	GFP	8.80	-2.0	0	0	0	0	0
2	1	91-145	PDA	0.00	1.5	0	0	0	0	0
2	1	91-145	PDA	0.00	1.0	0	0	0	0	0
2	1	91-145	PDA	0.00	0.5	0	0	0	0	0
2	1	91-145	PDA	0.00	0.0	0	0	0	0	0
2	1	91-145	PDA	0.00	-0.5	0	0	0	0	0
2	1	91-145	PDA	0.00	-1.0	0	0	0	0	0
2	1	91-145	PDA	0.00	-1.5	0	0	0	0	0
2	1	91-145	PDA	0.00	-2.0	0	0	0	0	0

Table AII.2. Mean final lesion length (mm) and sums of external necrotic lesion (Sum Lesion), internal vascular browning or necrosis (Sum Vascular), and pathogen presence (Sum Pathogen) for experimental soybean lines, 91-145 (resistant), 91-38 (moderately resistant), and 91-44 (susceptible). Sums represent the mean number of 0.5-cm sections from which lesion was observed, vascular necrosis was detected, or *S. sclerotiorum* was isolated.

Line	Final Lesion Length (mm)		Sum Lesion		Sum Vascular		Sum Pathogen	
	Mean	SE	Mean	SE	Mean	SE	Mean	SE
91-145	5.37	7.98	1.17	2.14	0.08333	2.4326	1.6667	1.1367
91-38	3.25	7.64	1.43	2.04	1.2368	2.2937	1.5037	1.0611
91-44	35.71	7.98	7.92	2.14	10.3333	2.4326	5.0833	1.1367
F	5.01		2.97		4.41		2.53	
p-value	0.0135		0.0670		0.0213		0.0971	

Appendix III: Quantification of *Sclerotinia sclerotiorum* ergosterol content in soybean stem tissue

Hannah Lucas and Jaime Willbur

Introduction

Sclerotinia stem rot (SSR), or white mold, is a fungal disease of many host plants, particularly soybean. This pathogen develops in moist, cool climates, and can be characterized by wilting, bleaching of the stem, and eventual plant death[5]. The SSR disease cycle involves overwintering structures called sclerotia, which germinate to form apothecia: a fruiting body that produces spores. These spores land on soybean flowers, where they germinate to form mycelia, and travel down the plant causing the aforementioned symptoms[5]. With 11,000 soybean farmers in Wisconsin[4], pathogens of this crop are of serious economic priority. In Wisconsin, SSR ranks third in the most economically concerning diseases of soybean. This creates a need for complete understanding of how *S. sclerotiorum* is virulent on soybean. Confocal and fluorescent microscopic imaging of stem colonization by *S. sclerotiorum* will give insight into differences in colonization between resistant verses susceptible soybean varieties. Knowledge of the exact location of active mycelia growth surrounding the necrotic stem lesion will lead to more precise and efficient microscopic imaging. Ergosterol is the unique sterol found in fungal cell walls. Quantification of this compound in sections of inoculated soybean stem will indicate actively growing mycelia, and thus give clues into the appropriate stem area to select for microscopy.

Objectives

1. Use methods established to quantify ergosterol in fungal mycelia[1,2,3] to develop a repeatable method of quantifying ergosterol content from soybean stems infected with *S. sclerotiorum* (Protocol AIII.1-2).
2. Determine if actively growing mycelia exists outside of the stem lesion.
3. Determine the approximate distance from the stem lesion that contains fungal tissue in order to more closely target stem sections for microscopic imaging of stem colonization by *S. sclerotiorum.*

Results and Conclusions

Negative percent ergosterol values, and miniscule positive values for results in the preliminary replication indicated that ergosterol was being lost at some point in the methods process (Table AIII.1). After adding additional vortexing steps, all ergosterol values were positive in replicate 2 (Table AIII.1). All three negative controls, containing uninfected plant stem tissue, were of the lowest value (Fig. AIII.1). The positive control, containing pure mycelia, showed the highest ergosterol content (Fig. AIII.1).

This value was still significantly lower than those calculated in the study done by Arthington-Skaggs et al[1]. Ergosterol content measured between one and two percent in 1g of *Candida albicans* cells in this study – nearly four degrees of magnitude higher. In the study done by Yarden et al.[2], ergosterol content for wild type *S. sclerotiorum* was 0.42% per gram of wet mycelia, highlighting that it is possible this method to be applied to the organism. However, spectrophotometer readings of lesion sample A (A_L) and the positive control from replicate 2, showed absorption patterns that are characteristic of ergosterol (*data not shown*). This peak pattern was not observed in any other samples.

Low ergosterol values may be a result of poor lesion development in replicate 2: only variety A had a significate lesion develop on one out of three plant stems after 14 days post-inoculation. Varieties B and C displayed incompatible reactions at the petiole node, and did not develop lesions. It is possible that the isolate used in this experiment, 1980 GFP-Nou^{R}, is losing aggressiveness, and needs to be re-isolated from an infected plant to re-gain aggressiveness.

The amount of mycelia in three 2-cm sections of stem may also be too small for sufficient detection. More than three 2-cm sections from separate plants should be combined in order to increase the chance of ergosterol detection, without decreasing the sensitivity of the location of detection on the stem.

These possibilities, however, still do not explain the low ergosterol value for the positive control in replicate 2 when compared to past studies. Further optimization of these methods is necessary to achieve an ergosterol value closer to 0.5% per gram for the positive control. Until then, presence of ergosterol could be determined qualitatively based on observance of the characteristic four peaks via a spectrophotometer reading.

Literature Cited

[1]Arthington-Skaggs, B. A. et al. (1999). Quantitation of ergosterol content: Novel method for determination of fluconazole susceptibility of *Candida albicans*. *Journal of Clinical Microbiology*. 37(10) 3332-3337.

[2]Yarden, O. et al. (2014). *Sclerotinia sclerotiorum* catalase SCAT1 affects oxidative stress tolerance, regulates ergosterol levels and controls pathogenic development. *Physiological and Molecular Plant Pathology*. 85: 34-41.

[3]Morey, K. (2014) Measuring Ergosterol from *S. sclerotiorum*. Unpublished protocol.

[4]U.S. and Wisconsin Soybean Facts. *The Wisconsin Soybean Association.* Retrieved May 16, 2016 from http://www.wisoybean.org/news/soybean_facts.php

[5]Smith, D. White Mold in Wisconsin. *Wisconsin Field Crops Pathology.* Retrieved May 16, 2016, from http://fyi.uwex.edu/fieldcroppathology/soybean_pests_diseases/white_mold/

[6]Heffer Link, V., and K. B. Johnson. 2007. White Mold. The Plant Health Instructor. DOI: 10.1094/PHI-I-2007-0809-01.

Tables and Figures

Table AIII.1. Ergosterol content (per gram of tissue) in susceptible (91-44), resistant (91-145), and moderately resistant (91-38) experimental soybean lines

Line	Tissue Type[a]	A230	A281.5	Ergosterol (%)	Weight (g)	% Ergosterol (per g)
Replicate 1						
91-44	(-) control	0.324	0.288	0.00037	2.5	0.00015
91-145	(-) control	0.276	0.226	0.00025	2.0	0.00012
91-38	(-) control	0.203	0.216	0.00035	2.0	0.00018
91-44	necrotic lesion	0.178	0.126	0.00009	1.5	0.00006
91-44	necrotic vascular, 2-cm above lesion	0.084	0.145	0.00034	1.3	0.00026
91-44	asymptomatic	0.147	0.054	-0.00010	1.3	-0.00008
91-145	necrotic lesion	0.280	0.152	-0.00002	0.8	-0.00002
91-145	necrotic vascular, 2-cm above lesion	0.203	0.102	-0.00004	1.4	-0.00003
91-145	necrotic vascular, 4- to 6-cm above lesion	0.319	0.136	-0.00015	0.6	-0.00024
91-145	necrotic vascular, 6- to 8-cm above lesion	0.409	0.186	-0.00015	0.1	-0.00122
91-145	necrotic vascular, 8- to 10-cm above lesion	0.808	0.270	-0.00063	0.1	-0.00967
91-145	asymptomatic	0.256	0.104	-0.00014	0.7	-0.00019
91-38	necrotic lesion	0.238	0.146	0.00004	0.9	0.00005
91-38	necrotic vascular, 2-cm above lesion	.	.	.	1.9	.
91-38	necrotic vascular, 4- to 6-cm above lesion	0.269	0.095	-0.00019	0.6	-0.00032
91-38	necrotic vascular, 6- to 8-cm above lesion	0.185	0.089	-0.00005	0.4	-0.00013
91-38	asymptomatic	0.222	0.123	0.00000	1.5	0.00000
Replicate 2						
91-44	(-) control	0.243	0.147	0.00004	1.3	0.00003
91-145	(-) control	0.032	0.030	0.00004	1.4	0.00003
91-38	(-) control	0.411	0.294	0.00022	1.9	0.00012
.	(+) control, mycelia	0.413	0.886	0.00226	3.5	0.00065
91-44	necrotic lesion	0.344	0.223	0.00010	0.6	0.00017
91-44	necrotic vascular, 2-cm above lesion	0.262	0.181	0.00012	0.8	0.00015
91-44	necrotic vascular, 4- to 6-cm above lesion	0.354	0.227	0.00010	0.3	0.00033
91-44	asymptomatic	0.257	0.180	0.00012	0.5	0.00025
91-145	necrotic lesion	0.294	0.201	0.00013	0.5	0.00025
91-145	necrotic vascular, 2-cm above lesion	0.311	0.237	0.00022	1.2	0.00018
91-145	asymptomatic	0.331	0.255	0.00024	1.0	0.00024
91-38	necrotic lesion	0.314	0.221	0.00016	0.9	0.00017
91-38	necrotic vascular, 2-cm above lesion	0.351	0.267	0.00024	1.8	0.00014
91-38	asymptomatic	0.327	0.227	0.00015	1.2	0.00013

[a]Sections (2 cm) of each tissue type, from all three replicates, were combined for extraction.

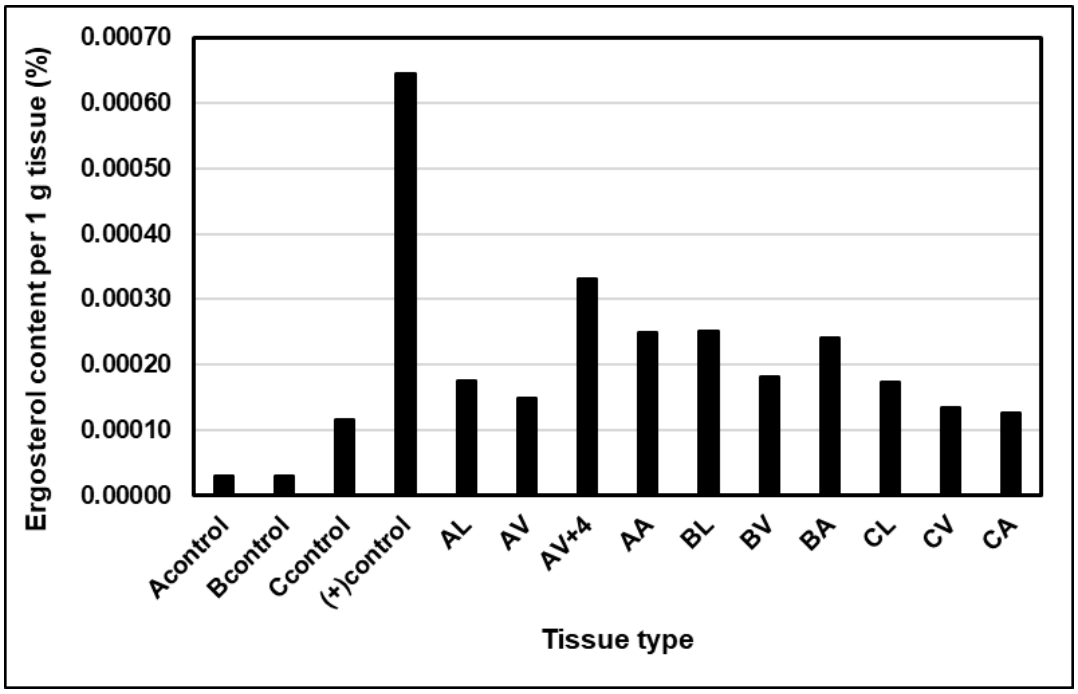

Figure AIII.1. Ergosterol content per 1 g of tissue in from *S. sclerotiorum* inoculated or mock-inoculated experimental soybean lines 91-44 (A), 91-145 (B), and 91-38 (C), showing results for only the second replicate of spectrometer data. Inoculated soybeans were inoculated with the 1980 GFP-Nou^{R} isolate of *S. sclerotiorum*. Tissue types shown include non-inoculated control (control), positive mycelia control [(+) control], lesion (L), necrotic vascular (V), additional necrotic vascular (V+4), and asymptomatic (A). Each line x inoculation treatment was replicated 3 times. At 14 days post-inoculation, 2-cm sections of each tissue type were taken from each replicate and pooled for the ergosterol extraction.

Protocols

AIII.1. Preliminary Protocol: Ergosterol Extraction from Plant Tissue

Preliminary methods, used in replicate 1, were based off of a protocol for measuring ergosterol content in *S. sclerotiorum*[3], optimized from Yarden et al. (2013)[4].

1. Six plants each of soybean lines 91-44 (A), 91-145 (B), and 91-38 (C), were planted in a controlled growth chamber.

2. At the V3 growth stage, three of each line was inoculated with thick PDA inoculated with *S. sclerotiorum* isolate 1980 GFP-Nou^R at the 2nd trifoliate petiole. The remaining three plants were inoculated at the 2nd trifoliate petiole with thick PDA containing no inoculum to serve as negative controls. Inoculated plants were arranged in a randomized block fashion until harvest at 14 DPI. Lesion measurements were noted.

3. A 2-cm section of the stem lesion (L), the necrotic tissue (directly above lesion, V), and asymptomatic tissue (A) were taken from each plant. Three sections from the same variety were combined into one sample. Sample weights were noted.

4. A positive control of 1980 GFP-Nou^R mycelia was prepared by inoculating 100 mL PDB with 10 plugs of inoculum, on a rotary shaker at 100 rpm for 24 hours. Mycelia was filtered and partially dried.

5. Samples were ground with liquid nitrogen and stored at 80°C in a 15-mL falcon tube until ready to proceed.

6. 3 mL 25% alcoholic KOH was added to each sample and vortexed vigorously. A piece of parafilm was placed under the cap to better seal the conical tube.

7. Samples were incubated in an 85°C water bath for 1 hour.

8. The top liquid layer of each sample was transferred to a glass test tube. Three milliliters n-heptane and 1 mL water were added to each sample.

9. The top aqueous layer of each sample was measured with a spectrophotometer from 230-300 nm.

10. Percent ergosterol was measured by the equation:

$$\%\ \text{Ergosterol} + \%24(28)\text{DHE} = \left[\left(\frac{\text{A281.5}}{290}\right) \times \text{F}\right]$$

$$\%24(28)\text{DHE} = \left[\left(\frac{\text{A230}}{518}\right) \times \text{F}\right]$$

where A designates the absorbance at wavelengths 281.5 and 230 and F indicates the dilution factor in ethanol before taking a spectrometer reading.

AIII.2. Ergosterol Extraction from Plant Tissue (Modifications)

After consulting the original journal article[1] cited in Yarden et al.[2], the following method modifications were made and used in replicate 2:

1. In step 6 of protocol AIII.1, samples were vortexed for at least one minute.

2. Thirty minutes into incubation at 85°C, all samples were vortexed for 15-20 seconds.

3. After incubation, samples were allowed to cool to room temperature.

4. Upon addition of 3 mL n-heptane and 1 mL water, samples were vortexed for 1.5 minutes.

5. Pictures were taken of all spectrometer readings to verify the presence of the characteristic 4 ergosterol peaks.

Appendix IV: Transformation of *Sclerotinia sclerotiorum* with red fluorescent protein

Hannah Lucas and Jaime Willbur

Summary

The objective of this project was to create a tool to assist in monitoring *Sclerotinia sclerotiorum* infection in resistant and susceptible soybean stems. The current fluorescent isolate is 1980 GFP-Nou^{R} (from J. Rollins, University of Florida), however, green fluorescence is difficult to distinguish in necrotic infected soybean tissues. The isolate is also only weakly aggressive and not necessarily representative of the populations of isolates infecting soybeans in the North Central region. Through this research, we aimed to generate a mutants of an aggressive *S. sclerotiorum* isolate, which expresses red fluorescent protein (RFP) or green fluorescent protein (GFP).

Polyethylene glycol-mediated transformations were used to transform *S. sclerotiorum* protoplasts with the mcherry vector (pNDH-OCT) or the GFP vector (pNDH-OGG) (Schumacher 2012). These vectors contained an ampicillin resistance cassette for prokaryotic selection and a hygromycin resistance cassette for post-transformation selection. A double restriction digest was performed at the NotI and NcoI sites to confirm the identities of these vectors (*data not shown*).

The protoplasting and transformation protocols were adapted from Rollins (2003) with the following modifications:

- First mycelial growth incubation in broth was increased from 24 hr to 48 hr
- Protoplasting incubation time was increased from 2 hr to 3 hr

- Hygromycin selection was conducted on amended PDA (rather than an amended RM media overlay) using a modified concentration of 50 mg ml^{-1} (originally 100 mg ml^{-1})
- The amount of DNA used in transformations of protoplasts was increased from 5 mg to 10 mg
- The protoplasting incubation temperature was increased from room temperature to 29°C

Overall, these modifications resulted in the generation of healthy protoplasts, much larger in size and more numerous than the protoplasts generated using the original protocol. Protoplast size increased from 10-20 μm to 20-25 μm and concentration increased from ~$1x10^7$ protoplasts ml^{-1} to ~$1x10^8$ protoplasts ml^{-1} (Fig. AIV.1). Furthermore, the improvements to the protoplasts resulted in successful transformation of isolate #20 (see Table 2.1) with RFP (Fig. AIV.2). Unfortunately, this transformation was not stable and fluorescence was not sustained on hygromycin media.

Literature Cited

Schumacher, Julia (2012). Tools for *Botrytis cinerea*: New expression vectors make the grey mold fungus more accessible to cell biology approaches. *Fungal Genetics and Biology*. 49: 483-497.

Rollins, Jeffery A (2003). The *Sclerotinia sclerotiorum* pac1 gene is required for sclerotial development and virulence. *Molecular Plant Microbe Interactions*. 9: 785-795.

Figures

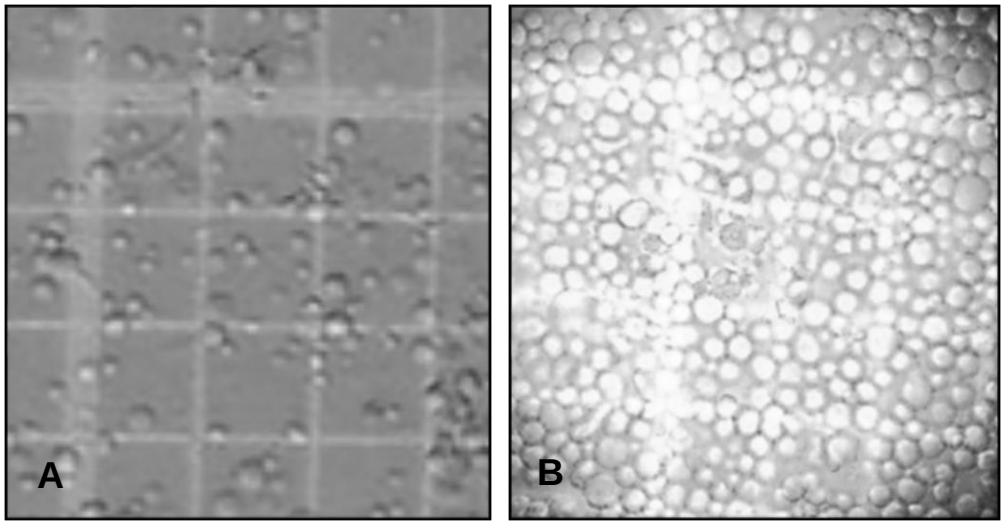

Figure AIV.1. *S. sclerotiorum* protoplasts before (A) and after (B) protocol modifications described in the Appendix IV summary. Protoplast size increased from 10-20 μm to 20-25 μm and concentration increased from ~$1x10^7$ protoplasts ml^{-1} to ~$1x10^8$ protoplasts ml^{-1}.

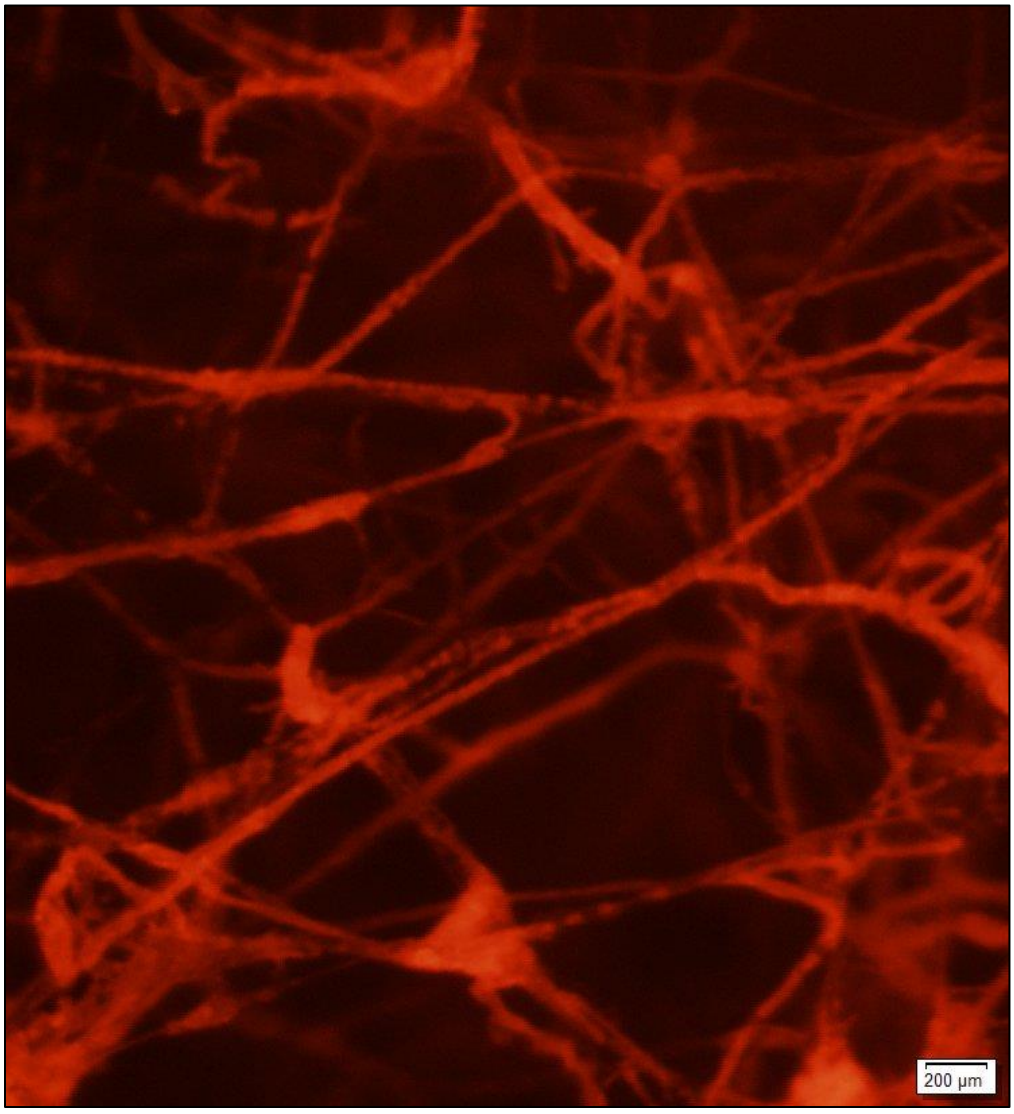

Figure AIV.2. Successful transformation of aggressive *S. sclerotiorum* isolate #20 using an mcherry vector to express the red fluorescent protein. Imaged on an epifluorescent microscope.

Protocols

AIV.1. Protoplasting and Transformation of *S. sclerotiorum*

Adapted from Rollins (2003). Modifications in bold.

Reagents & Media

- Media: Potato dextrose broth (PDB) or **potato dextrose agar (PDA)** (autoclaved to sterilize)
- 1M Sorbitol: (FW 182.2) need at least 250 ml for 2 isolates
- RM media: Sucrose 239.6 g L^{-1}; Yeast Extract 0.5 g L^{-1}; Agar 15 g L^{-1} (bottom agar); Agar 8 g L^{-1} (top agar)
- STC: 1M Sorbitol; 50 mM Tris-HCl; 50 mM Calcium chloride ($CaCl_2$, FW 147.02); pH 8.0
- PTC: 40% polyethylene glycol (PEG 3350) in STC
- PEG solution: 2 parts 60% PEG 3350 in STC: 1 part sterile KTC
- KTC: 1.8 M Potassium chloride (KCl, FW 74.56); 150 mM Tris, pH 8; 150 mM $CaCl_2$
- All solutions vacuum filter sterilized (unless otherwise specified) and stored at room temperature.

Protoplast Preparation

1. Inoculate 100 ml of PDB in 250 ml flask with 10 plugs of mycelia from the leading edge of PDA plates. Incubate flasks at room temperature for **48 hr** at ~150 rpm.

2. Transfer mycelia to sterile Waring blender (autoclaved), blend mycelia in 5 sec pulses. Harvest hyphae by filtering through a sterile filter paper and funnel.

3. Suspend 30-50 µl in 100 ml of PDB in 250 ml flask. Incubate at room temperature overnight at ~150 rpm.

4. Collect mycelia by filtration through sterile Miracloth (or sterile filter paper). Wash 1x with 10 ml of 1M Sorbitol.

5. Resuspend washed mycelia in 20 ml of 1M Sorbitol containing 10 mg/ml Sigma Lysing Enzyme (200 mg enzyme in 20 ml of 1M Sorbitol) – filter sterilize lysing solution using 0.2 µm syringe filter.

6. Incubate at **29°C** for **~3 hr** at ~70 rpm. Check for release of protoplasts under light microscope and proceed when most hyphae have digested.

7. Collect protoplasts in 50 ml conical tubes by filtering out mycelial debris through sterile Miracloth (or sterile filter paper). [Add 20 ml of 0.6 M KCl over.] Spin down protoplasts at 2500 rpm for 10 min. Wash and pellet protoplasts 1x with 10ml STC. Resuspend in 1 ml STC (transfer to sterile 2.0 ml centrifuge tubes).

8. Count protoplasts and resuspend in STC at a concentration of $1x10^8$ protoplasts/ml. Keep on ice in 1.5 ml centrifuge tubes during transformation steps.

9. Store at -80 C: add 12.5 µl DMSO to 1 ml protoplasts. Or add 7% DMSO.

Transformation

1. Mix **10 µg** of GFP or RFP DNA with $1x10^7$ protoplasts (100 µl protoplast solution in STC). Add deionized water for negative controls. Incubate on ice for 30 min.

   Example reactions:
   - 100 µl protoplasts + GFP in STC (15 µl of GFP-2 in 85 µl STC) = 200 µl
   - 100 µl protoplasts + RFP in STC (20 µl of mCh-2 in 80 µl STC) = 200 µl
   - 100 µl protoplasts + sterile ddH2O in STC = 200 µl

2. Add 1 ml PTC or 1 ml of PEG soln (in 2 additions of 500 µl gently mixing in between) to protoplast-DNA mixture and incubate at room temperature for 20 min. (=1200 µl)

3. Evenly spread 500 µl protoplast-DNA mixture (using a flame sterilized, cooled glass spreader) over a plate of potato dextrose agar (amended with **50 µg ml^{-1}** hygromycin).

4. Transformants will appear in 5-7 days on top agar. Transfer a single hyphal tip of transformant onto 100 µg/ml hygromycin amended PDA plates.

Appendix V: Monitoring *Sclerotinia sclerotiorum* colonization in resistant and susceptible soybean stem tissue

Kelsey Azzolino and Jaime Willbur

Abstract

There are no commercially-available resistant varieties of soybean tocombat Sclerotinia stem rot (SSR), and little information is available to explain resistance mechanisms. The objectives were to examine any notable differences in the stem-colonization patterns of resistant and susceptible soybean, and use this information to help explain SSR resistance. Experimental lines 91-44 (susceptible) and 91-145 (resistant) were inoculated with the #43 *S. sclerotiorum* isolate or mock-inoculated with PDA replicated four times. Cross-sections were taken at the margin between the symptomatic and asymptomatic area at five days post-inoculation (DPI). Lactophenol aniline blue stain was used to distinguish the hyphal elements from soybean tissue. Light microscopy was used to obtain vessel counts, perform color analyses, and explore stem tissues, in order to measure differences in infection of resistant and susceptible lines. There were no significant differences between the vessel counts of either the resistant and susceptible lines, and the hyphal elements were mostly found near or around xylem elements. There were no significant differences internally between resistant and susceptible lines in the exploratory imaging; the susceptible line, however, tended to have more infected cells and hyphal elements. This suggests, as the epidemic progresses, there will be a higher level of infection in the susceptible line. At 5 days post-inoculation (DPI), stem lesion measurements were not significant between both the susceptible and resistant lines. In summary, the data evaluated

indicated that there were limited observable trends between the 91-44 (susceptible) and 91-145 (resistant) lines 5 DPI.

Introduction

Sclerotinia stem rot (SSR), also called white mold of soybean caused by *Sclerotinia sclerotiorum*, is a significant soil borne disease that has dramatically affected Northern and Central areas throughout the U.S (Kurle et al. 2001). Yield loss due to SSR in 1997, 2004, and 2009 range from 35, 60, and 59 million bushels (Peltier et al. 2012). Manufacturer's losses during these time periods range from $227, 334 and 560 million USD (Peltier et al. 2012). Due to the considerable levels of disease incidence throughout soybean growing regions, SSR was ranked second in estimated yield and dollar loss compared to the twenty-three other soybean diseases in the U.S. from 1996-2009 (Peltier et al. 2012). In 2014, SSR was ranked fourth in plant diseases in the U.S., and second in Wisconsin, with a yield loss of 37.2 million bushels (Koenning and Wrather 2006; Koenning and Wrather 2010; Wrather et al. 2003; Wrather et al. 2001). In order for SSR to develop, there needs to be a conducive environment, which involves saturated, moist soil, and temperatures that range from 40-60 °F (Peltier et al. 2012). *Sclerotinia sclerotiorum* overwinters in the soil, and germinates to produce apothecia. The apothecia generate ascospores, which colonize senescing flowers and spread to stem tissue (Mueller et al. 2011).

No completely resistant varieties are available commercially for SSR management, and many resistance mechanisms are not well understood. The partially resistant varieties that are available have significantly less disease incidence than susceptible varieties, however, disease will still occur under optimal conditions and with adequate levels of

inoculum. Therefore, it is imperative to commercialize a fully resistant variety. Based on previous studies, results have shown that there are lower levels of infection in resistant varieties (Grau et al. 1982). Breeding for resistance, however, is difficult because resistance mechanisms are not well understood. It is important, therefore, to examine the colonization patterns of susceptible and resistant soybeans in order to help explain potential resistance mechanisms.

A study was conducted at the Department of Plant Pathology at the University of Minnesota in order to examine the pathogenic response of soybean (*Glycine max* L. Merr.) and two types of the pathogen *Phialophora gretata* (Impullitti and Malvick 2014). Soybean stems were inoculated with a wildtype (WT) or GFP and RFP-labeled strain of types A or B *P. gregata* (Impullitt and Malvick 2014). Cross-sections of stem tissues were taken, stained with lactophenol aniline blue solution (Remel, Lenexa, KS), and imaged using light microscopy to examine notable differences between varieties (Impullitti and Malvick 2014). Microscopic observations were similar in susceptible and resistant varieties, although symptoms were more severe in susceptible plants (Impullitti and Malvick 2014). The fungus colonized the xylem vessels in both susceptible and resistant varieties (Impullitti and Malvick 2014). Additionally, these studies concluded that resistant varieties had a higher number of vessel counts compared to susceptible varieties, which led to increased resistance to colonization by *P. gregata* (Impullitti and Malvick 2014). Colonization of *S. sclerotiorum* in resistant and susceptible soybean, therefore, may be characterized using fungal staining, fluorescent isolates, and vessel quantification.

Another study examined the colonization patterns in flower parts of *S. sclerotiorum* in

sunflower head rot disease. Any differences in flower parts at different times of susceptible (HA 89) and tolerant (HA 302) varieties were observed using histopathological techniques (Rodriguez et al. 2004). In both varieties, at 24 h post-inoculation, there were no significant differences in symptoms between the HA 89 and HA 302 variety (Rodriguez et al. 2004). However, at 12 days post-inoculation there were notable levels of significance in the tissues infected, in which the susceptible variety was more colonized (Rodriguez et al. 2004). This shows that as the epidemic progresses, mycelial colonization increases in the susceptible as compared to the tolerant variety. However, both varieties were colonized with mycelial growth on the surface and interior tissues (Rodriguez et al. 2004).

Since soybean flowers are the main infection court for *S. sclerotiorum,* floral tissue may also be of interest in monitoring colonization. Another study investigated the infection of *S. sclerotiorum* in resistant (plants expressing oxalate oxidase) and susceptible (wild type) soybean flowers (Davidson et al. 2016). While less total plant disease was observed in the resistant variety, no differences were detected in initial floral colonization of the two varieties (Davidson et al. 2016). In soybean, therefore, explanations for resistance to *S. sclerotiorum* may be better identified in stem, rather than floral, tissue. As mentioned above, Impullitti and Malvick were able to characterize soybean resistance responses to another necrotrophic fungal pathogen in stem tissue (2014), which provides further evidence for studying colonization in stem tissue.

Based on previous studies, results have shown that resistant varieties have shown to be more effective at resisting fungal infection. The objectives of our studies were to examine the colonization patterns between susceptible and resistant soybean lines, to if see we could detect any notable differences in the colonization of the resistant and susceptible soybean

stem tissues, and if those differences reveal something about soybean resistance mechanisms to *S. sclerotiorum.* Our hypothesis was: less colonization by *S. sclerotiorum* would be present in a resistant soybean line.

Materials and Methods

Sample preparation. Experimental soybean lines 91-44 (susceptible) and 91-145 (resistant) were planted into six-inch pots containing Sungro Horticulture Propagation Mix, and grown in a growth chamber with a 14-h photoperiod, set to 22°C during the day and 18°C at night. At growth stages V4 (fourth trifoliate) to V5 (fifth trifoliate), plants were inoculated with isolate #43, which is the well-characterized isolate 1980, a GFP-1980 nourseothricin resistant (NOU^R) isolate, or mock-inoculated with potato dextrose agar (PDA). A petiole inoculation at the second trifoliate was performed using actively growing mycelial cultures. Plants were harvested for analysis five days post-inoculation (DPI). Trials that compared the colonization between the resistant and susceptible lines were replicated four times.

Prior to sectioning, final stem lesions (in mm) were measured, at 5 DPI, with an electronic digital caliber (Fisher Scientific). Stem segments were then taken from the margin of the asymptomatic and symptomatic area of the 91-44 (S) and 91-145 (S) inoculated and mock-inoculated treatments. Six small cross-sections were hand-cut using a razor blade dipped in 95% ethanol under an Olympus dissecting microscope. Each cross-section was soaked in deionized water in a petri dish until further processing.

Cross-sections were heat-cleared using Visikol solution. Visikol clearing solution has been used as a replacement to chloral hydrate, and has been proven to be an effective alternative when used for light microscopy (Villani et al. 2013). Its ability to clear whole

tissues in a short period of time allows for the optimization of staining techniques (Villani et al. 2013). On a slide, Visikol solution was dropped over cross-sections, which were then covered with a cover slip and heated over a Bunsen burner for one minute. Cross-sections were then rinsed in deionized water for three minutes to remove the chlorophyll.

For light microscopy, cross-sections, of #43-inoculated or mock-inoculated control treatments, were dipped in a petri plate containing Remel^{TM} lactophenol aniline blue stain (ThermoFisher Scientific) for one minute. During the first 30 seconds, the cross-sections were submerged in the solution and then removed for the following 30 seconds, which allowed for the sections to drain. Afterward, sections were blotted on a paper towel, mounted on a slide with 1-2 drops of polyvinyl glycerol (or "glycerin glue") mounting solution (Zander 2014), covered with cover slip, and allowed to dry.

For fluorescent microscopy, cross-sections of 1980 GFP NOU^{R} treatments were hand-cut using a razor blade dipped in 95% ethanol and sectioned under an Olympus dissecting microscope. Each cross-section was then soaked in deionized water in a petri plate for further processing. Cross-sections were placed onto a slide containing Visikol clearing solution, covered with a cover slip, and heated over a Bunsen burner for one minute. Cross-sections were then rinsed in deionized water for three minutes to remove the chlorophyll, blotted on paper towel, and then mounted as previously described.

Microscopic imaging. For light microscopy, the Cellsens standard program was used to collect images of all cross sections. Continuous imaging was performed on an Olympus BX60 microscope, connected to an Olympus DP73 camera, at a magnification of 100x. An exposure between 3.0-3.5 ms was used to examine each cross- section. A fine focus brought the vessels to the finest focal point, and the International Standards Organization (ISO), light

sensitivity was set at 200 in order to assess the stained hyphal elements. A vivid contrast was used at a high image quality, and snapshots were taken at a resolution of 2400x1800 pixels.

Additionally, exploratory images were collected using the previously mentioned Olympus microscope, camera, and software. In all sections, ≥ 10 images were taken at 400x magnification in representative areas, concentrating on infected tissues (in inoculated sections), but also in areas with no disease.

For fluorescent imaging, a Zeiss 510 Meta confocal laser scanning microscope (CLSM) located in the Newcomb imaging center (University of Wisconsin – Madison) was used to collect fluorescent images of the sections inoculated with the GFP isolate, #43 isolate, and mock-inoculated controls.

Image analysis. ImageJ (National Institutes of Health) software was used to assemble continuous, overlapping images taken of each section with light microscopy. These images were stitched together, using the MosaicJ plug-in, and the resulting mosaic images were used to measure the surface area and the number of vessels colonized within each whole section of each line x inoculation treatment in all four replicates. Using ImageJ, the number of vessels and area surrounding each cross-section were recorded in each mosaic created using a multimedia tool and a polygon tool.

WINRHIZO root scanning software, at a resolution of 96 dpi, was used to calculate the total diseased area within each cross-section in replicates 1 and 2. A color analysis measured the surface area of different sections of stem, and categorized the diseased and healthy tissue according to established color classes. Color classes were identified in WINRHIZO using images with obvious infected areas to distinguish stained “diseased” areas from non-stained healthy tissue or background area.

Light microscopy was used to take composite exploratory images, ≥ 10 per section, in 3 sections per stem. These sections comprised an outer location 1, the epidermis, a middle location 2, the xylem vascular tissue, and an inner location 3, the pith. The number of infected cells, hyphae per cell, location in section, and distance from vessel elements were recorded.

Statistical analyses. All analyses were conducted in SAS v. 9.4 (SAS Institute). The GLIMMIX procedure was used to evaluate fixed and random effects in generalized linear mixed models using an analysis of variance (ANOVA). Experimental soybean line, 91-44 (S) and 91-145 (R), and inoculation method, isolate #43 and mock-inoculated control, as well as the interaction between line and inoculation were treated as fixed effects in all models. Replicate was treated as a random effect in all models. All effects were evaluated at the α=0.05 significance level.

For vessel count analyses, the UNIVARIATE procedure was used to generate means for number of vessels, the area of sections (pixels^2), and area-corrected vessel number (#vessels / area of section) across all three-stem sections. Four replicates of area-corrected vessel numbers were evaluated using the previously mentioned fixed effects.

For color analyses, the UNIVARIATE procedure was used to generate means for the areas (cm^2) of the total section, background color, healthy color, and diseased color across all sections. These means were used to generate area-corrected diseased areas (diseased area inoculated / total section area). These area-corrected means were then used to correct for background stain in the control sections (diseased area inoculated – diseased area mock-inoculated control). These area- and control-corrected diseased values were used to evaluate the previously described fixed effects for the first two replicates of data.

For exploratory image analyses, the UNIVARIATE procedure was used to generate means, of number of hyphal elements, location within the stem, and distance from vascular elements, and sums, of number of infected cells and number of hyphal elements, within each section. A subsequent UNIVARIATE procedure was used to generate means across all three sections for each line by inoculation combination in all four replicates. Final means across sections were used to evaluate the described fixed effects on number of infected cells, number of hyphal elements, location within the stem, and distance from vascular elements.

Results

Confocal microscopy. The GFP infected soybean stem tissues sections autofluoresced red and green. Therefore, confocal microscopy using the green fluorescent isolate was problematic, and could not be used (*results not shown*).

Vessel counts. There was no significant difference between the numbers of vessels in either the resistant or susceptible lines ($P = 0.389$) or the inoculated and mock-inoculated treatments ($P = 0.8391$) (Fig. AV.1).

Color analyses. Using the area- and background-corrected means, there was a larger stained ("diseased") area in the 91-44 (S) line ($P = 0.0502$) (Fig. AV.2).

Exploratory imaging analyses: Using the mean data generated for each section and treatment, no significant differences were found between lines 91-44 (S) and 91-145 (R) (Table AV.1). The mean number of hyphal elements per cell showed no significant differences between the experimental lines, ($P = 0.6815$) with estimated means of 1.14 and 1.20, respectively (Table AV.1). No significant differences were detected in the mean numbers of hyphal elements per section ($P = 0.4208$), but number of hyphal elements in the 91-44 (S) sections were slightly higher than those in the 91-145 (R) sections, with estimated

means of 268.25 and 220.08, respectively (Table AV.1) (Fig. AV.3). The mean number of infected cells per section in the experimental lines showed no significant differences (P = 0.5772), but were slightly higher in the 91-44 (S) line, with an estimated mean of 197.67 (Table 1) (Fig. AV.5). The mean location of infected cells within each section showed no significant differences in either line or inoculated sections. Most hyphal elements, however, were mainly located in location two, in the xylem vascular tissue. The 91-44 (S) and 91-145 (R) lines had estimated mean locations of 1.85 and 1.74. The inoculated isolate, and background stain in the mock-inoculated treatments had mean locations of 2.93 and 2.46 (Table AV.1). Infected cells in location two ranged from one to fifteen cells from a vascular element. The mean numbers of hyphal elements across all treatments were roughly three cells from a vessel element. The 91-44 (S) and 91-145 (R) lines had estimated mean distances of 2.68 and 2.71. The inoculated isolate and mock-inoculated control had estimated values of 2.93 and 2.46 (Table AV.1).

There were significantly higher numbers of hyphal elements in the inoculated sections, (P = 0.0022) than in the non-inoculated sections, with estimated means of 365.42 and 122.92, respectively (Table AV.1) (Fig. AV.4). Similar results were observed in the mean number of infected cells per section, (P = 0.003), with estimated means of 271.46 for line 91-44 and 99.042 for line 91-145 (Table AV.1) (Fig. AV.6).

Lesion length. There were no significant differences in final lesion length between 91-44 (S) and 91-145 (R) lines (P = 0.9357), with estimated means of 8.09 and 8.25 (Table AV.1) (Fig. AV.7). There were significant differences in lesion lengths of the inoculated and the mock-inoculated control (P < 0.0001), with estimated means of 16.18 and 0.16 (~ 0.00) (Table AV.1) (Fig. AV.8).

Discussion

Successful infection was obtained using the isolate #43, which was not observed in the mock-inoculated controls. There were few notable differences between the 91-44 (S) and 91-145 (R) line. Colonization patterns of the 91-44 (S) line tended to have a higher level of infection, which suggests that as the epidemic progresses, there will be a higher infection rate, and higher numbers of hyphal elements within the infected cells.

The GFP isolates were not strongly fluorescent. Also, the infected soybean tissues auto fluoresced red and green. Confocal microcopy was not possible, therefore, staining and clearing methods were optimized for light microscopy. Further development of imaging techniques and analyses helped to determine vessel counts. Exploratory images helped to quantify the amount of infection, number of infected cells, and the distance of infection from the vessel elements.

In order to observe fresh tissue for sectioning at the initial interaction, lesion measurements were taken at 5 DPI; at which there were no observable differences in external symptoms. It is likely that at 10 DPI, as the epidemic progresses, trends both internally and externally will become significant. Rodriguez et al. (2004), identified different colonization patterns of *S. sclerotiorum* on susceptible and resistant varieties of sunflower in floral tissues, that at the t3 stage (12 day DPI).

Based on previous studies, as well as the trends observed in the results between lines, this suggests that at 10 DPI, as the infection spreads, both internal and external symptoms will likely become significant in the 91-44 (S) line. Since there were slightly higher levels of infection in the susceptible line at 5 DPI, it is important to continue to examine the colonization patterns of susceptible and resistant soybean stem tissues. This trend will likely

continue as the epidemic progresses, widening the gap between the susceptible and resistant lines, which helps to explain resistance mechanisms, and suggests that the resistant line will be effective against SSR.

Literature Cited

Peltier, A.J., Bradley, C.A., Chilvers, M.I., Malvick, D.K., Mueller, D.S., Wise, K.A., and Esker, P.D. 2012. Biology, yield loss, and control of Sclerotinia stem rot of soybean. J Integr Pest Manag. 3(2):B1-B7.

Davidson, A. L., Blahut-Beatty, L., Itaya, A., Zhang, Y., Zheng, S., and Simmonds, D.2016. Histopathology of *Sclerotinia sclerotiorum* infection and oxalic acid function in susceptible and resistant soybean. Plant Pathol. 65:878–887.

Grau, C., Radke, V., and Gillespie, F. 1982. Resistance of soybean cultivars to *Sclerotinia sclerotiorum*. Plant Dis. 66:506–508.

Impullitti, A. E., & Malvick, D. K. 2014. Anatomical response and infection of soybean during latent and pathogenic infection by type A and B of *Phialophora gregata*. PloS one. 9(5), e98311.

Kurle, J. E., C. R., Grau, E. S., Oplinger, and Mengistu, A. 2001. Tillage, Crop Sequence, and Cultivar Effects on Sclerotinia stem rot incidence and Yield in Soybean. Agron. J. 93:973-982. doi:10.2134/agronj2001.935973x.

Koenning, S. R., and Wrather, J. A. 2010. Suppression of soybean yield potential in the continental United States by plant diseases from 2006 to 2009. Online. Plant Health Progress doi:10.1094/PHP-2010-122-01-RS.

Mueller, D., Bradley, C., Chilvers, M., Michigan E. P., Malvick, D., Peltier, A., Sisson, A. and Wise, A. 2011. Management of white mold in soybean. North Central Soybean Research Program.

Rodriguez, M. A., Venedikian, N., Bazzalo, M. E., & Godeas, A. 2004. Histopathology of *Sclerotinia sclerotiorum* attack on flower parts of *Helianthus annuus* heads in tolerant and susceptible varieties. Mycopathologia. 157(3), 291-302.

Wrather, J. A., Koenning, S. R., and Anderson, T. R. 2003. Effect of diseases on soybean yields in the United States and Ontario (1999 to 2002). Online. Plant Health Progress doi:10.1094/PHP-2003-0325-01-RV.

Wrather, J. A., and Koenning, S. R. 2006. Estimates of disease effects on soybean yields in the United States 2003 to 2005. Journal of Nematology. 38:173-180.

Villani, T. S., Adolfina R. K., and Simon, A. 2013. An improved clearing and mounting solution to replace chloral hydrate in microscopic applications. Applications in Plant Sciences 1.5): 1300016.

Wrather, J. A., Stienstra, W. C., and Koenning, S. R. 2001. Soybean disease loss estimates for the United States from 1996 to 1998. Canadian Journal of Plant Pathology 23:122-131.

Zander, R. H. (Missouri B. G. 2014. Four water-soluble mounting media for microslides. Phytoneuron. 32:1–4.

Tables and Figures.

Table AV.1. Table summary of exploratory image results of 91-44 (S) and 91-145(R) line with *P* values, and inoculated and mock-inoculated controls and *P* values at 5 DPI.

Results	**Line**			**Inoculation**		
	91-44	91-145	*P*-value	43	Control	*P*-value
Mean sum infected cells	197.67	172.83	0.58	271.46	99.04	0.0030
Mean sum hyphal elements	268.25	220.08	0.42	365.42	122.92	0.0022
Mean hyphal elements (per cell)	1.14	1.20	0.68	1.32	1.017	0.0783
Mean location within section	1.85	1.74	0.26	1.77	1.83	0.4317
Mean distance from vascular elements	2.68	2.71	0.94	2.93	2.46	0.2999
Mean lesion results	8.09	8.25	0.94	16.18	0.16	<0.0001

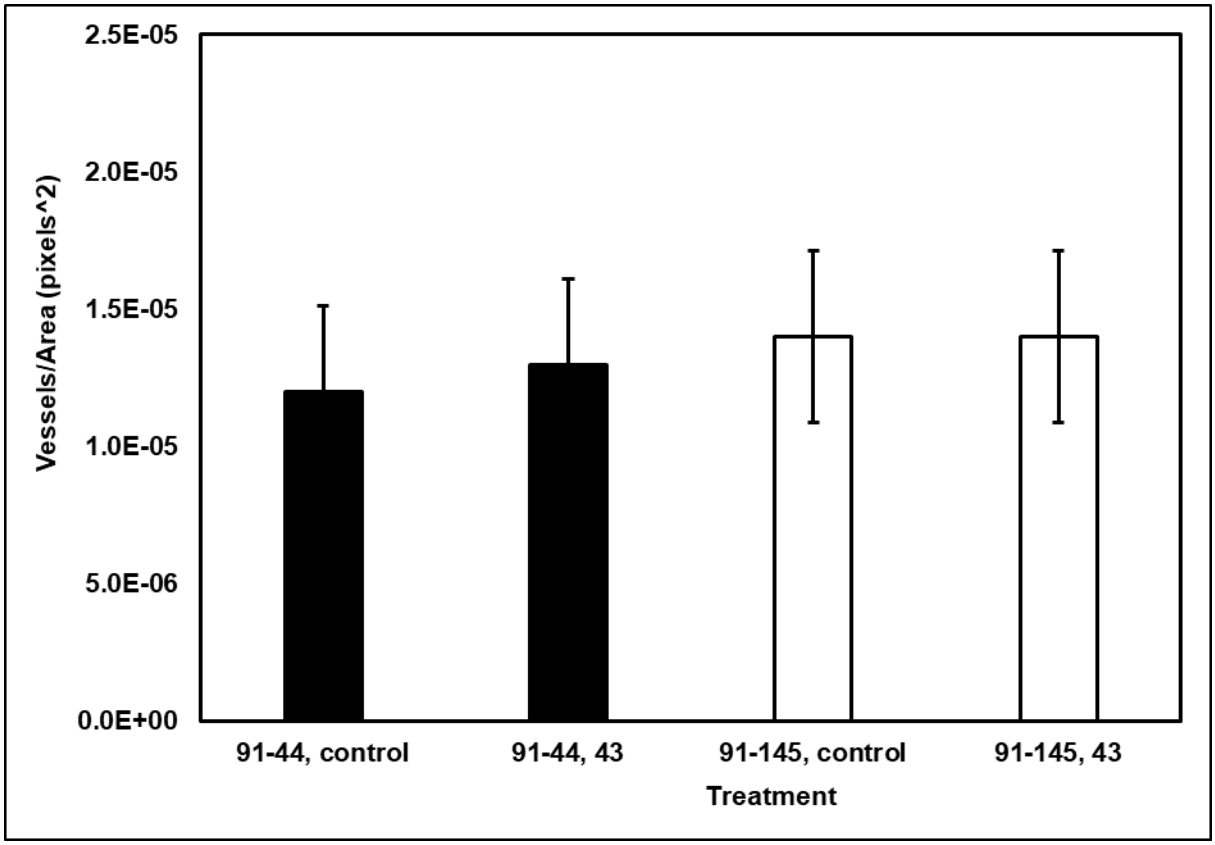

Figure AV.1. Mean number of vessels per area (pixels^2) of 91-44 (S), 91-145 (R) line, and #43 isolate, mock-inoculated PDA inoculum. There were no significant differences between susceptible and resistant line, and inoculated isolate and mock-inoculated control ($P > 0.05$).

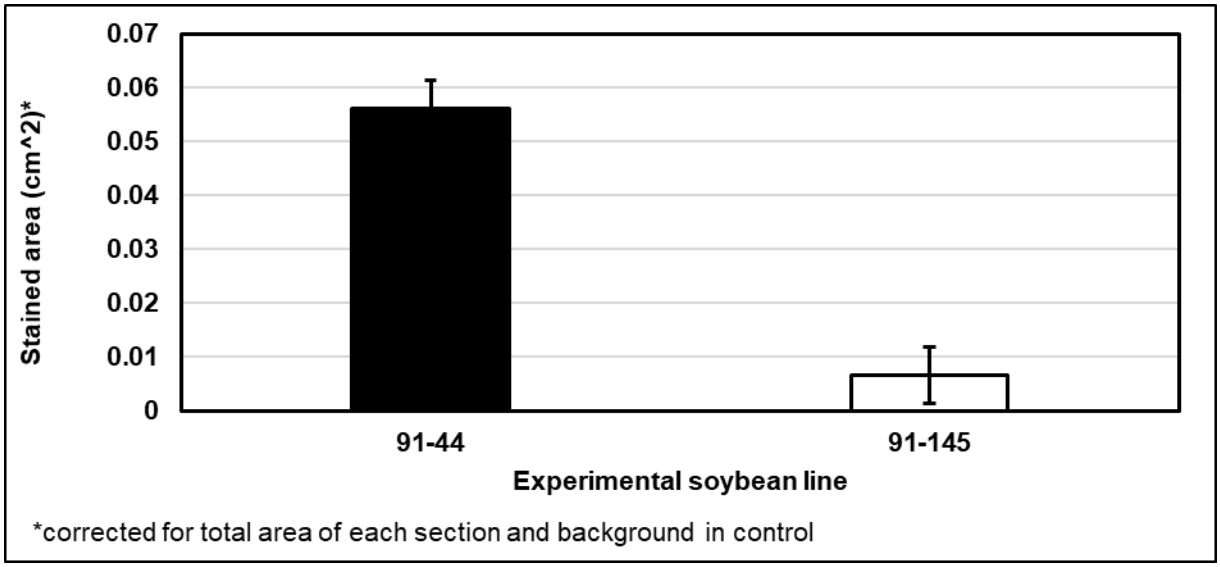

Figure AV.2. Total background and surface area corrected stained area (cm^2) in sections from 91-44 (S) and 91-145 (R) lines. There was a significant difference between the stained ("diseased"), area in the 91-44 (S) and 91-145 (R) lines ($P < 0.05$).

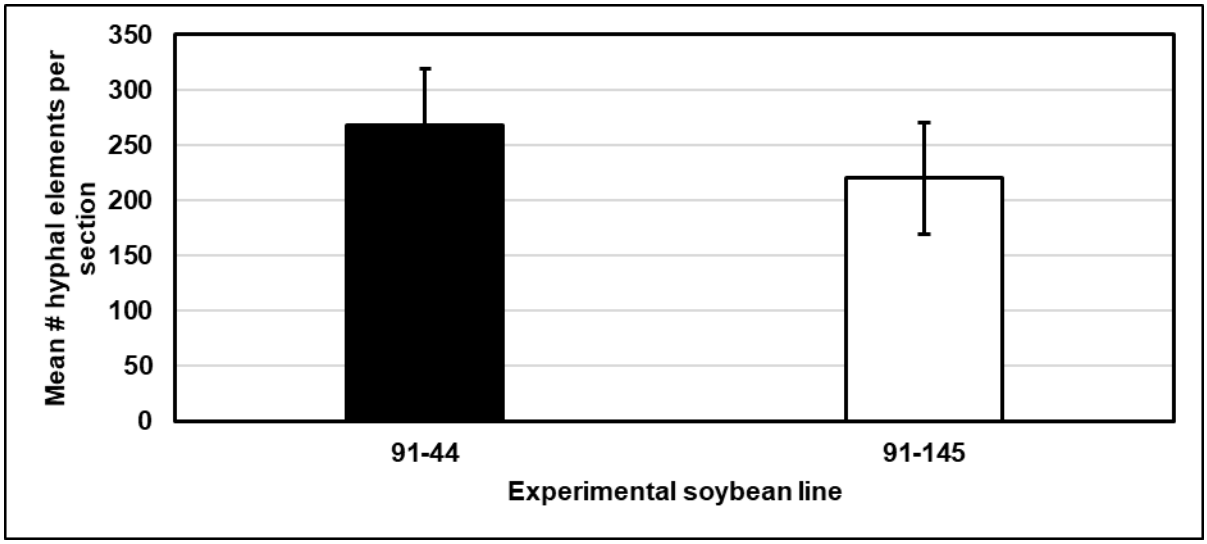

Figure AV.3. Mean number of hyphal elements per section of 91-44 (S) line and 91-145 (R) line. There was not a significant difference between the resistant and susceptible lines ($P > 0.05$) with estimated means of 268.25 and 220.08.

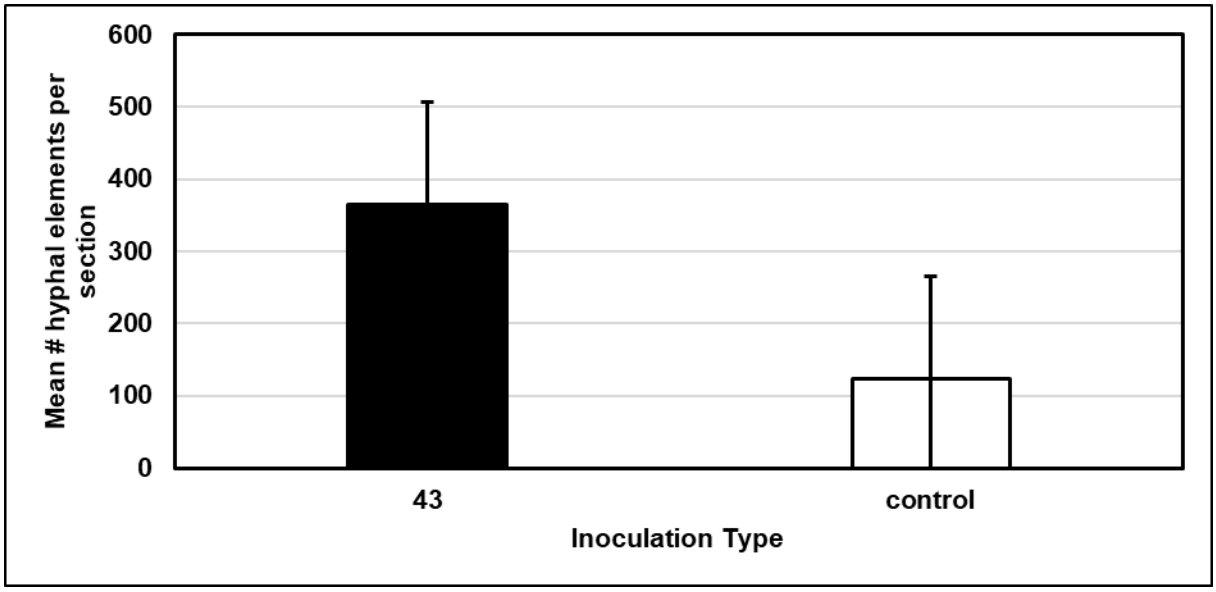

Figure AV.4. Mean number of hyphal elements per section of #43 isolate and mock-inoculated control. There was a significant difference between the inoculated and mock-inoculated sections ($P < 0.01$) with estimated means of 365.42 and 122.92.

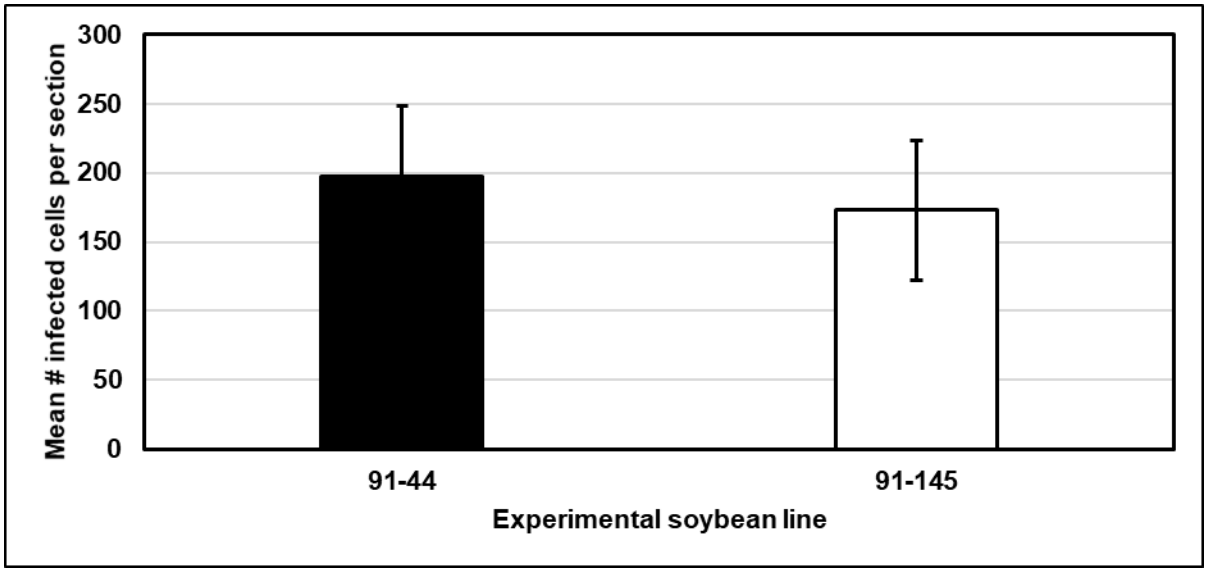

Figure AV.5. Mean number of infected cells per section of 91-44(S) susceptible line and 91-145(R) resistant line. There were no significant differences between the 91-44 (S) and 91-145 (R) ($P > 0.05$), with estimated means of 197.67 and 172.83.

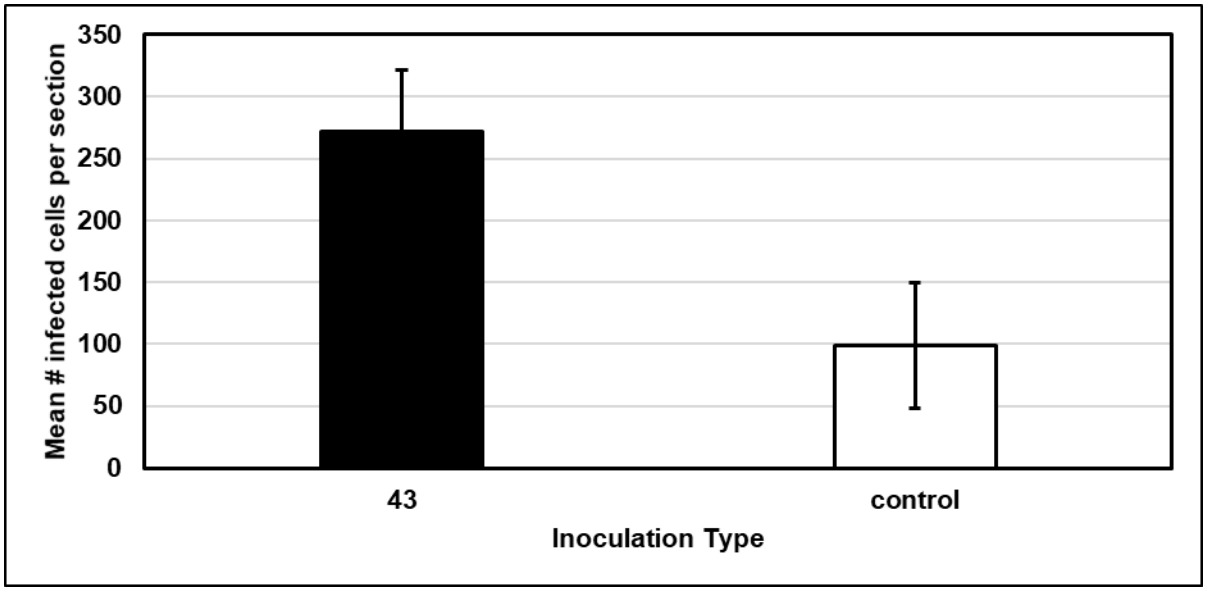

Figure AV.6. Mean number of infected cells per section of #43 isolates and mock inoculated control. There is a significant difference between the number of infected cells in the #43 inoculated and mock inoculated control sections ($P<0.01$), with estimated means of 271.46 and 99.0417.

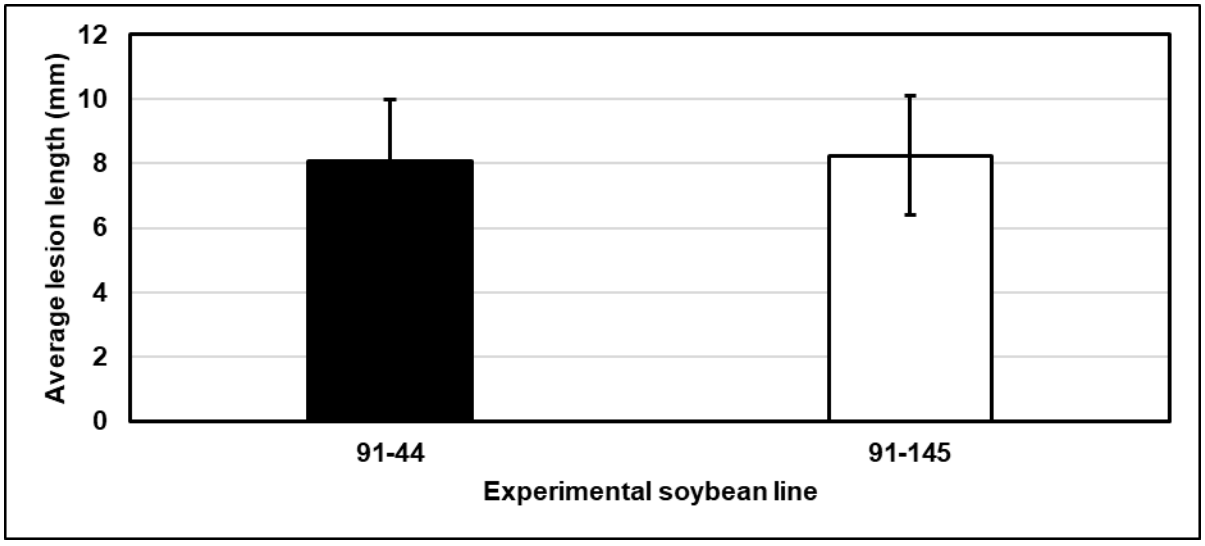

Figure AV.7. Average lesion length of the 91-44 susceptible line and the 91-145-resistant line 5 days post-inoculation (DPI). The 91-44 susceptible line has an estimated mean of 8.0925, and the 91-145 has an estimated value of 8.2486. There is no significant difference between lesion lengths of the resistant or susceptible line ($P > 0.05$).

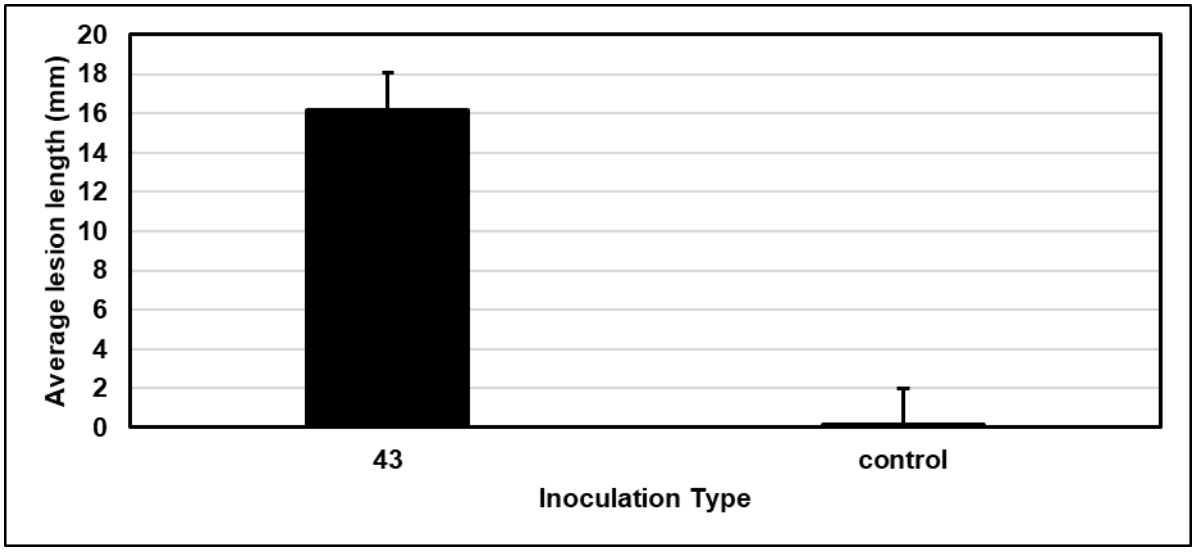

Figure AV.8. Average lesion length of the #43 isolate and the mock-inculcated PDA at 5 days post-inoculation (DPI). There were significant differences between the inoculated and the mock-inoculated control ($P < 0.0001$), with estimated means of 16.18 and 0.16 (~ 0.00).

Appendix VI. Light effects on *Sclerotinia sclerotiorum* apothecial production in field and controlled environment studies

Hannah Lucas, Maria Weber, Theresa Blackwell, Kelsey Azzolino, and Jaime Willbur

Introduction

Sclerotinia sclerotiorum apothecial development is influenced by different light intensities (Sun and Yang 2000) and requires ultraviolet wavelengths of light between 276 and 319 nm (Thaning and Nilsson 2000). Light has also been identified to play a role in *Botrytis cinerea* growth and sporulation (Tan and Epton 1973) and in Stemphylium leaf spot, caused by *S. botryosum*, development in alfalfa (Cowling and Gilchrist 1982). Near-ultraviolet wavelengths of light have even been shown to influence conidial development in *Alternaria tomato* (Kumagai and Oda 1969). Field and controlled environment studies were conducted to determine the effects of the soybean canopy and various light profiles on *S. sclerotiorum* apothecial production and subsequent Sclerotinia stem rot (SSR) development.

Furthermore, in Wisconsin agronomic studies have determined that soybeans planted on either a 0.19- or 0.38-m row spacing will consistently yield 7-10% more than soybeans planted at a wider 0.76-m row spacing (Bertram and Pedersen 2004). Additionally, this study reports that, at a narrow 0.38-m row spacing, optimal yields may be achieved at population densities of 432,500 – 680,000 seeds ha^{-1}. Optimal population densities for 0.76-m rows, however, range from 310,000 – 555,000 seeds ha^{-1}. The development of *S. sclerotiorum*, and subsequent soybean infection, is known to be dependent on canopy closure and favored by cool, moist conditions (Boland 1988). High-yielding soybean row spacing and seeding rates, therefore, inherently increase the risk of SSR development by reducing the time to full canopy closure and by reducing canopy ventilation.

Studies in Brazil have shown that narrow row spacing and high population density increases SSR disease severity and incidence (Jaccoud-Filho et al., 2016). The seeding rates used in this research, however, are not representative of the optimal populations recommended for soybeans grown in the North Central region. In Michigan, population was also found to be positively correlated with disease severity and negatively correlated with yield (Lee et al. 2005); this research, however, only considered a narrow range of high density seeding rates in 0.19- or 0.76-m row spacings. As a result, it is difficult to give regionally appropriate white mold management recommendations to Wisconsin soybean growers. Effective integrated management systems require evaluation of regional standards in irrigation, row spacing, seeding rate, and fungicide treatment and their effects on white mold incidence and severity. Moreover, it is important to investigate how manipulation of these practices directly affects the biology surrounding fungal development.

The objectives of these studies were to: 1) determine qualities and quantities of light necessary in apothecial development, 2) use narrow bandpass interference filters to monitor apothecial development, 3) evaluate total solar and ultraviolet radiation above and below soybean canopies, and 4) investigate current, standard soybean management practices, including irrigation, row spacing, population density, and fungicide treatment, for use in integrated SSR management.

Materials and Methods

Controlled environment studies of apothecial development. Protocols AVI.1.1-1.2 were used to prepare sclerotia of the *S. sclerotiorum* isolate #30 and saturated sand environments for apothecial development assays. Of note, wide-mouth, straight-sided, round sampling glass jars (Qorpak®, VWR Scientific, 6 oz) were filled with 50 cc of dry, extra fine,

washed white play sand (KolorScape®, Home Depot), saturated with 19 ml of deionized water, and autoclaved twice prior to placement of surface disinfested sclerotia on the sand. Once sclerotia were placed, the jars were fitted with small, clear Petri dish lids (ThermoFisher Scientific, deep dishes with lids, 60 x 20 mm) and sealed with parafilm. The sample jars were placed in a dark 4°C incubator for 30 days, then moved to a dark 12°C for 40 days, and finally subjected to the light treatment chambers.

Light chambers consisted of opaque PVC tubes fitted with opaque lids with an inset to hold narrow (10 nm) bandpass filters (Edmund Optics, Barrington, NJ). After the dark conditioning periods, the jars and lenses were randomized prior to light treatments. Only one set of lens chambers were available, so the experiment was replicated three times; each replicate was conducted separately over time. The treatments included lens which allowed 10-nm ranges of light to pass through (at 270, 280, 300, 310, 320, 450, 589, and 720 nm), a negative control which blocked all wavelengths of ultraviolet (UV), and a positive control (plain glass) which allowed all light to pass through (CONTROL). After 25-65 days under the light treatments, the number of apothecia and stipes were recorded for each sclerotia (Table AVI.1).

Apothecia and stipe counts collected at either 64 or 65 days under light treatments were analyzed using statistical procedures in SAS v. 9.4 (SAS Institute, Cary, NC). A UNIVARIATE procedure was used to generate the mean number of apothecia produced (per sclerotia) under each lens for each replicate. These means were then used in a generalized linear mixed model (GLIMMIX) procedure to test the effect of lens on the number of apothecia and stipes in an analysis of variance (ANOVA). Replicate was considered a random effect.

Field studies of light effects on apothecial development. Research trials were conducted at University of Wisconsin-Madison agricultural research stations in West Madison, Arlington, and Hancock, Wisconsin (see Table 4.1 and 5.1) and used to monitor light effects on *S. sclerotiorum* apothecial development in soybean fields. Plots were intensively monitored for apothecial development; scouting was done in three 0.76-m x 0.76-m squares in the center two rows of each 3.0 x 6.1 m plot as described in Willbur et al. (2017).

In all locations, on-site light and weather variables were monitored with a variety of sensors connected to a Campbell Scientific datalogger (Model CR1000). Air temperature, relative humidity, rain fall, wind speed, leaf wetness, soil temperature, and soil moisture data were collected as described in Willbur et al. (2017). Quantities of light were also monitored using pyranometers (Campbell Scientific, Apogee SP-100, Model CS300-L25) to collect hourly total and mean solar radiation (SR) quantities; ultraviolet (UV) sensors (Campbell Scientific, Apogee SU-100) were used to collect hourly and total UV light quantities. Sensors were attached to a levelled base (with the cable pointing north as specified in the product manual) and fixed above or below the canopy.

In 2015-2016, one solar and one UV sensor were placed in each of the following locations: a) 1.1 m above the ground (above the canopy), b) 10 cm above the ground between two soybean rows at a 0.76 m spacing, and c) 10 cm above the ground in a soybean row at a 0.76 m spacing. In 2017, sensors were purchased for two additional locations: d) 10 cm above the ground between two soybean rows at a 0.38 m spacing, and c) 10 cm above the ground in a soybean row at a 0.38 m spacing (the light data from different row spacings was not analyzed in this project).

All sensors were connected to the datalogger, which was attached to a 10-ft tripod (Campbell Scientific, Model CM106B) constructed where apothecia presence was monitored. Measurements were taken every 5 min and averaged to calculate hourly conditions. In all locations, weather data collection began prior to first detection of apothecia and continued from approximately the V1 (first trifoliate) to the R8 (full maturity) growth stage.

Preliminary data (collected from West Madison in 2015 and Arlington in 2016) were used to test the light effects on apothecial presence. In SAS v. 9.4 (SAS Institute, Cary, NC), means of hourly average SR (W m^{-2}), hourly total SR (MJ m^{-2}), hourly average UV (µmol m^{-2} s^{-1}), and total UV (µmol m^{-2} s^{-1}) were generated using a UNIVARIATE procedure. Additionally, ratios of UV:SR quantities were generated for hourly total and average observations above the canopy, below the canopy in the row, and below the canopy between the rows. The daily means of these ratios were then generated in the previously described UNIVARIATE procedure. Means of the solar and UV readings, as well as the means of the ratios in each environment were correlated with daily mean apothecial observations from each treatment in a CORR procedure. Correlation coefficients were evaluated at the $\alpha = 0.05$ significance level. Highly correlated variables were used in generalized linear mixed model (GLIMMIX) regression analyses, using the solution option.

Evaluation of soybean management practices to suppress apothecial and SSR development. In 2017, trials in Hancock and Arlington were also used to evaluate the performance of an industry standard susceptible soybean variety under 0.38- or 0.76-m row spacing planted at population densities of 275,000, 350,000, 425,000, and 500,000 seeds ha^{-1}. Additionally, the efficacy of industry standard control applications of Aproach (9 fl oz $acre^{-1}$

applied at R1 and R3) and Endura (8 fl oz acre^{-1} applied at R1) were evaluated against a non-treated control for each of the row spacing and seeding rate combinations. Each combination of treatments was randomized in a split-split plot design and replicated four times in each field trial location.

SSR incidence (DI), severity (DS), severity index (DIX) data were collected at R6 or R7 (beginning maturity). Severity data was collected according to the protocols in Willbur et al. (2017). The true DI was collected by counting the total number of symptomatic plants in the center two rows and converting to a percentage of the total stand count. The DIX was calculated as by multiplying the true DI by the average DS of symptomatic plants. Yield was collected in the center two rows of each plot, adjusted to 13% moisture, and converted to kg ha^{-1}. DIX and yield were used to evaluate the various fungicide treatments and the mean DI of the non-treated plots was used in full season model validations.

Statistical analyses were conducted in SAS v. 9.4. For each location a GLIMMIX procedure was used to conduct an ANOVA using the DIX data as the response variable. The split-split plot design was analyzed using the following SAS code:

```
*split-split plot, normal dist, all interactions
considered;
proc glimmix data=integrated_ nobound plots=studentpanel;
class rep row pop fung;
model newdix = row pop row*pop fung row*fung pop*fung
row*pop*fung/dist=n ddfm=kr;
random rep rep*row rep*row*pop;
lsmeans row*pop*fung/diff cl plots=mean(sliceby=row cl
connect);
run;


*split-split plot, lognormal dist, all interactions
considered;
proc glimmix data=integrated_ nobound plots=studentpanel;
```

```
class rep row pop fung;
model newdix = row pop row*pop fung row*fung pop*fung
row*pop*fung/dist=lognormal ddfm=kr;
random rep rep*row rep*row*pop;
lsmeans row*pop*fung/diff cl plots=mean(sliceby=row cl
connect);
run;
```

where the fixed effects of row, population (pop), fungicide (fung), and all interactions were considered. Random effects of rep rep*row and rep*row*pop were included to represent the constraints placed on the randomization of the replicates within the whole plot (row) and split-plot (population) levels. A lognormal distribution was used to normalize Arlington data (low levels of disease). A Kenward Roger degrees of freedom adjustment was used to correct for bias. Means were generated for any significant effects using the lsmeans statement.

Results and Conclusions

Narrow bands of ultraviolet light are required for apothecial production. Light filters were found to significantly impact the number of apothecia produced per sclerotia (P = 0.0080), but not stipe production (P = 0.7335) (Table AVI.2). Apothecial production only occurred under lens filters of 300, 310, and 320 nm, which are marketed to allow > 5% light transmission in the 295-310, 305-320, and 315-330 nm ranges, respectively (Edmund Optics) (Fig. AVI.1). The 300 nm spectra indicates < 5% transmission occurs from 290-295 nm and from 310-315 nm. Low light transmission (< 5%) also occurs in the 310 nm filter from 300-305 and 320-325 nm, and in the 320 nm filter from 310-315 and 330-335 nm. As apothecia formed in all three light environments, apothecia either require more than one wavelength of light in this range or extremely small amounts of these wavelengths (< 5% transmission). Further studies verifying the transmission of light through these lenses should be conducted using a spectrophotoradiometer which detects light in the UV range.

Overall, apothecia formation appears to require light between 295 and 330 nm. This is a narrower range of light than what was previously found to be required for *S. sclerotiorum* apothecial development (Thaning and Nilsson 2000). In particular, the 300-nm treatment was the only bandpass filter to produce numbers of apothecia comparable to the control (more than one per sclerotia). Additionally, jars placed under the UV cut-off filter (which blocks all wavelengths of light below 350 nm) did not produce any apothecia. These results suggest soybean SSR could be managed through the manipulation of the canopy or soil environment to block or prevent these wavelengths from reaching developing apothecia.

Effects of solar and ultraviolet radiation on apothecial development in soybean fields. Preliminary data from 2015 and 2016 identified further evidence that ultraviolet light is important for *S. sclerotiorum* apothecial development. As the soybean canopy closed there was a noticeable shift in light quantity, it was further noted that as the canopy closed, the UV:SR ratio became larger (despite SR continuing to be most prevalent). Congruently, Pearson correlation coefficients were highest for the daily mean of the hourly mean UV:SR quantities collected between the rows (r = 0.31, P = 0.0001). Regressions of this mean ratio and the corresponding daily mean quantities of mean UV and SR data collected between the rows were investigated. The lognormal distribution was used to normalize the data. The mean ratio of UV:SR were found to significantly explain apothecial numbers in the following regression model:

$$Mean\ apothecia = 4.23\ \left[Mean\left(\frac{Mean\ UV}{Mean\ SR}\right)\right]_{BB} + 0.22 \qquad \text{(AVI.1)}$$

where the mean of the ratio of mean UV:SR quantities is collected below the canopy and between the rows (BB). These studies indicate that the ratio of UV to SR light penetrating the

canopy between the rows significantly affects apothecial development. This ratio appears to become larger as the canopy closes (i.e. both UV and SR quantities are reduced, but UV is less affected, so the ratio becomes larger) which triggers apothecial production.

Effects of row spacing and population density on apothecial and SSR development. In 2017, the integrated management trial conducted in Arlington, Wisconsin experienced very low disease pressure, only a single apothecia was detected between early R1 and R4, and resulting levels of disease were also extremely low, 0.99% DIX in non-treated plots. As a result, no effects or interactions of effects were found to significantly impact DIX ($P > 0.05$).

In the trial conducted in Hancock, high numbers of apothecia and correspondingly high levels of disease pressure, 26.9% in non-treated plots, were observed. A significant three-way interaction between row, population, and fungicide treatment was detected ($P = 0.0476$) (Table AVI.4). Of these main effects, when considered separately, row was found to be most influential with 33% DIX at the narrower row spacing compared to only 21% in the wider row spacing. Population density also contributed to some of these differences; lower populations (275,000 and 350,000 seeds ha^{-1}) resulted in overall means of 26 and 23% DIX whereas higher populations (425,000, and 500,000 seeds ha^{-1}) resulted in 29 and 30% DIX.

Furthermore, while no significant effects of row, population, or fungicide treatment were detected for mean apothecial numbers collected at R4 ($P > 0.05$), the numbers of apothecia were consistently lower under wider row spacing and population densities at Hancock, WI (Table AVI.6). Additionally, yield was only found to be significantly impacted by population density ($P = 0.0048$). The lower populations of 275,000 and 350,000 seeds ha^{-1}

resulted in the lowest yields with 3,585 and 3,698.8 kg ha^{-1}, respectively. Wider row spacings resulted in a yield increase of between 309.4 and 431.8 kg ha^{-1} (or 4.6-6.4 bu a^{-1}).

Unfortunately, no significant fungicide effects were observed with these picoxystrobin (Aproach, 9 fl oz a^{-1}) treatments. Potential explanations for the low efficacy of this product are described further in Chapter 5. Likely, the longevity of this product when applied at R3 was not adequate to offer sustained protection from SSR infection during the later epidemic of apothecia (occurring around R4). Potential adjustments to systems using this product and the apothecial model for SSR management are discussed in further detail in Chapter 5.

Overall, the irrigated environment of the Hancock trial was more conducive for apothecial and disease development. In this location, there was a significant interaction of row*population*fungicide. Soybeans planted at a wider row spacing (0.76 m) were found to develop 10% less disease, and lower populations (275,000 and 350,000 seeds ha^{-1}) were found to be responsible for a further 5% disease reduction. This decrease in disease is likely due to the reduced amounts of apothecia observed under these row spacings and populations. Furthermore, yield was impacted only by population and not by row spacing, suggesting that potential yield benefits resulting from this practice are, unfortunately, easily circumvented under elevated levels of disease in narrow row spacing environments. Areas experiencing persistent SSR prevalence would benefit from using wider row spacing and lower population densities to assist in SSR management.

Literature Cited

Bertram, M. G., and Pedersen, P. 2004. Adjusting management practices using glyphosate-resistant soybean cultivars. Agron. J. 96:462–468.

Boland, G. J. 1988. Epidemiology of Sclerotinia stem rot of soybean in Ontario. Phytopathology. 78:1241.

Cowling, W. A., and Gilchrist, D. G. 1982. Effect of light and moisture on severity of Stemphylium leaf spot of alfalfa. Plant Dis. 66:291–294.

Jaccoud-Filho, D., Fadel Sartori, F., Manosso-Neto, M., Maurício Vrisman, C., da Cunha Pierre, M. L., Berger-Neto, A., et al. 2016. Influence of row spacing and plant population density on management of " white mould " in soybean in southern Brazil. Aust. J. Crop Sci. 10:161–168.

Koenning, S. R., and Wrather, J. A. 2010. Suppression of soybean yield potential in the continental United States by plant diseases from 2006 to 2009. Plant Heal. Prog.

Kumagai, T., and Oda, Y. 1969. Blue and near ultraviolet reversible photoreaction in conidial development of the fungus, *Alternaria tomato*. Dev Growth Differ. 11:130–142 Available at: http://www.ncbi.nlm.nih.gov/pubmed/5392521.

Lee, C. D., Renner, K. A., Penner, D., Hammerschmidt, R., and Kelly, J. D. 2005. Glyphosate-resistant soybean management system effect on Sclerotinia stem rot. Weed Technol. 19:580–588.

Peltier, A. J., Bradley, C. A., Chilvers, M. I., Malvick, D. K., Mueller, D. S., Wise, K. A., et al. 2012. Biology, yield loss and control of Sclerotinia stem rot of soybean. J. Integr. Pest Manag. 3:1–7.

De Souza Jaccoud-Filho, D., Fadel Sartori, F., Manosso-Neto, M., Maurício Vrisman, C., da Cunha Pierre, M. L., Berger-Neto, A., et al. 2016. Influence of row spacing and plant population density on management of " white mould " in soybean in southern Brazil. 10:161–168.

Sun, P., and Yang, X. B. 2000. Light, temperature, and moisture effects on apothecium production of Sclerotinia sclerotiorum. Plant Dis. 84:1287–1293.

Tan, K. K., and Epton, H. A. S. 1973. Effect of light on the growth and sporulation of *Botrytis cinerea*. Trans. Br. Mycol. Soc. 61:145–157 Available at: http://linkinghub.elsevier.com/retrieve/pii/S0007153673800968.

Thaning, C., and Nilsson, H.-E. 2000. A narrow range of wavelengths active in regulating apothecial development in *Sclerotinia sclerotiorum*. J. Phytopathol. 631:627–631.

United States Department of Agriculture - National Agricultural Statistics Service (USDA-NASS). 2015. United States soybean prices. USDA-NASS:Washington, DC.

Wrather, A., Shannon, G., Balardin, R., Carregal, L., Escobar, R., Gupta, G., et al. 2010. Effect of diseases on soybean yield in the top eight producing countries in 2006. Plant Heal. Prog.

Tables and Figures

Table AVI.1. Record of apothecia and stipe formation in three replicates of development assays. In each opaque (light blocking) tube, a glass jar containing 5 sclerotia was subjected to treatments of various wavelengths (nm). The treatments included lens which allowed narrow (10 nm) ranges of light to pass through (270, 280, 300, 310, 320, 450, 589, 720), a negative control which blocked all wavelengths of ultraviolet (UV), and a positive control which allowed all light to pass through (CONTROL). After a number of days under the light treatments (Days), the number of apothecia (Apo) and stipes (Sti) were recorded for each sclerotia (Scl).

Rep	Date	Days	Tube#	Lens (nm)	Iso	Jar	Scl	Apo	Sti
1	11/7/2016	25	1	589	30	8	1	0	0
1	11/7/2016	25	1	589	30	8	2	0	0
1	11/7/2016	25	1	589	30	8	3	0	0
1	11/7/2016	25	1	589	30	8	4	0	0
1	11/7/2016	25	1	589	30	8	5	0	0
1	11/7/2016	25	2	300	30	6	1	0	2
1	11/7/2016	25	2	300	30	6	2	1	2
1	11/7/2016	25	2	300	30	6	3	0	0
1	11/7/2016	25	2	300	30	6	4	0	0
1	11/7/2016	25	2	300	30	6	5	0	0
1	11/7/2016	25	3	310	30	7	1	0	0
1	11/7/2016	25	3	310	30	7	2	1	0
1	11/7/2016	25	3	310	30	7	3	0	1
1	11/7/2016	25	3	310	30	7	4	0	0
1	11/7/2016	25	3	310	30	7	5	0	0
1	11/7/2016	25	4	450	30	4	1	0	0
1	11/7/2016	25	4	450	30	4	2	0	0
1	11/7/2016	25	4	450	30	4	3	0	0
1	11/7/2016	25	4	450	30	4	4	0	0
1	11/7/2016	25	4	450	30	4	5	0	0
1	11/7/2016	25	5	720	30	3	1	0	4
1	11/7/2016	25	5	720	30	3	2	0	0
1	11/7/2016	25	5	720	30	3	3	0	0

1	11/7/2016	25	5	720	30	3	4	0	1
1	11/7/2016	25	5	720	30	3	5	0	0
1	11/7/2016	25	6	UV	30	9	1	0	0
1	11/7/2016	25	6	UV	30	9	2	0	0
1	11/7/2016	25	6	UV	30	9	3	0	0
1	11/7/2016	25	6	UV	30	9	4	0	0
1	11/7/2016	25	6	UV	30	9	5	0	0
1	11/7/2016	25	7	270	30	5	1	0	0
1	11/7/2016	25	7	270	30	5	2	0	0
1	11/7/2016	25	7	270	30	5	3	0	0
1	11/7/2016	25	7	270	30	5	4	0	0
1	11/7/2016	25	7	270	30	5	5	0	0
1	11/7/2016	25	8	280	30	10	1	0	0
1	11/7/2016	25	8	280	30	10	2	0	1
1	11/7/2016	25	8	280	30	10	3	0	1
1	11/7/2016	25	8	280	30	10	4	0	0
1	11/7/2016	25	8	280	30	10	5	0	1
1	11/7/2016	25	9	320	30	2	1	0	0
1	11/7/2016	25	9	320	30	2	2	0	0
1	11/7/2016	25	9	320	30	2	3	0	0
1	11/7/2016	25	9	320	30	2	4	1	0
1	11/7/2016	25	9	320	30	2	5	0	0
1	11/7/2016	25	10	CONTROL	30	1	1	0	0
1	11/7/2016	25	10	CONTROL	30	1	2	0	0
1	11/7/2016	25	10	CONTROL	30	1	3	1	0
1	11/7/2016	25	10	CONTROL	30	1	4	0	0
1	11/7/2016	25	10	CONTROL	30	1	5	0	0
1	11/15/2016	33	1	589	30	8	1	0	0
1	11/15/2016	33	1	589	30	8	2	0	0
1	11/15/2016	33	1	589	30	8	3	0	0
1	11/15/2016	33	1	589	30	8	4	0	1
1	11/15/2016	33	1	589	30	8	5	0	0
1	11/15/2016	33	2	300	30	6	1	0	2
1	11/15/2016	33	2	300	30	6	2	3	0
1	11/15/2016	33	2	300	30	6	3	0	0
1	11/15/2016	33	2	300	30	6	4	0	0
1	11/15/2016	33	2	300	30	6	5	0	1
1	11/15/2016	33	3	310	30	7	1	0	0
1	11/15/2016	33	3	310	30	7	2	1	0
1	11/15/2016	33	3	310	30	7	3	0	3

1	11/15/2016	33	3	310	30	7	4	0	0
1	11/15/2016	33	3	310	30	7	5	0	0
1	11/15/2016	33	4	450	30	4	1	0	0
1	11/15/2016	33	4	450	30	4	2	0	0
1	11/15/2016	33	4	450	30	4	3	0	0
1	11/15/2016	33	4	450	30	4	4	0	0
1	11/15/2016	33	4	450	30	4	5	0	0
1	11/15/2016	33	5	720	30	3	1	6	0
1	11/15/2016	33	5	720	30	3	2	0	0
1	11/15/2016	33	5	720	30	3	3	0	0
1	11/15/2016	33	5	720	30	3	4	0	2
1	11/15/2016	33	5	720	30	3	5	0	0
1	11/15/2016	33	6	UV	30	9	1	0	0
1	11/15/2016	33	6	UV	30	9	2	0	0
1	11/15/2016	33	6	UV	30	9	3	0	0
1	11/15/2016	33	6	UV	30	9	4	0	0
1	11/15/2016	33	6	UV	30	9	5	0	0
1	11/15/2016	33	7	270	30	5	1	0	0
1	11/15/2016	33	7	270	30	5	2	0	0
1	11/15/2016	33	7	270	30	5	3	0	0
1	11/15/2016	33	7	270	30	5	4	0	0
1	11/15/2016	33	7	270	30	5	5	0	0
1	11/15/2016	33	8	280	30	10	1	0	0
1	11/15/2016	33	8	280	30	10	2	0	6
1	11/15/2016	33	8	280	30	10	3	0	1
1	11/15/2016	33	8	280	30	10	4	0	1
1	11/15/2016	33	8	280	30	10	5	0	2
1	11/15/2016	33	9	320	30	2	1	0	0
1	11/15/2016	33	9	320	30	2	2	0	0
1	11/15/2016	33	9	320	30	2	3	0	0
1	11/15/2016	33	9	320	30	2	4	1	1
1	11/15/2016	33	9	320	30	2	5	1	0
1	11/15/2016	33	10	CONTROL	30	1	1	0	0
1	11/15/2016	33	10	CONTROL	30	1	2	0	0
1	11/15/2016	33	10	CONTROL	30	1	3	1	0
1	11/15/2016	33	10	CONTROL	30	1	4	0	0
1	11/15/2016	33	10	CONTROL	30	1	5	0	0
1	11/22/2016	40	1	589	30	8	1	0	0
1	11/22/2016	40	1	589	30	8	2	0	0
1	11/22/2016	40	1	589	30	8	3	0	1

1	11/22/2016	40	1	589	30	8	4	0	1
1	11/22/2016	40	1	589	30	8	5	0	0
1	11/22/2016	40	2	300	30	6	1	1	1
1	11/22/2016	40	2	300	30	6	2	3	0
1	11/22/2016	40	2	300	30	6	3	0	0
1	11/22/2016	40	2	300	30	6	4	0	0
1	11/22/2016	40	2	300	30	6	5	1	0
1	11/22/2016	40	3	310	30	7	1	0	0
1	11/22/2016	40	3	310	30	7	2	1	0
1	11/22/2016	40	3	310	30	7	3	2	2
1	11/22/2016	40	3	310	30	7	4	0	0
1	11/22/2016	40	3	310	30	7	5	0	0
1	11/22/2016	40	4	450	30	4	1	0	0
1	11/22/2016	40	4	450	30	4	2	0	0
1	11/22/2016	40	4	450	30	4	3	0	0
1	11/22/2016	40	4	450	30	4	4	0	0
1	11/22/2016	40	4	450	30	4	5	0	0
1	11/22/2016	40	5	720	30	3	1	0	6
1	11/22/2016	40	5	720	30	3	2	0	1
1	11/22/2016	40	5	720	30	3	3	0	0
1	11/22/2016	40	5	720	30	3	4	0	4
1	11/22/2016	40	5	720	30	3	5	0	0
1	11/22/2016	40	6	UV	30	9	1	0	0
1	11/22/2016	40	6	UV	30	9	2	0	1
1	11/22/2016	40	6	UV	30	9	3	0	0
1	11/22/2016	40	6	UV	30	9	4	0	0
1	11/22/2016	40	6	UV	30	9	5	0	0
1	11/22/2016	40	7	270	30	5	1	0	0
1	11/22/2016	40	7	270	30	5	2	0	0
1	11/22/2016	40	7	270	30	5	3	0	0
1	11/22/2016	40	7	270	30	5	4	0	0
1	11/22/2016	40	7	270	30	5	5	0	0
1	11/22/2016	40	8	280	30	10	1	0	1
1	11/22/2016	40	8	280	30	10	2	0	6
1	11/22/2016	40	8	280	30	10	3	0	1
1	11/22/2016	40	8	280	30	10	4	0	1
1	11/22/2016	40	8	280	30	10	5	0	2
1	11/22/2016	40	9	320	30	2	1	0	0
1	11/22/2016	40	9	320	30	2	2	0	2
1	11/22/2016	40	9	320	30	2	3	0	1

1	11/22/2016	40	9	320	30	2	4	2	0
1	11/22/2016	40	9	320	30	2	5	1	0
1	11/22/2016	40	10	CONTROL	30	1	1	0	0
1	11/22/2016	40	10	CONTROL	30	1	2	0	0
1	11/22/2016	40	10	CONTROL	30	1	3	1	0
1	11/22/2016	40	10	CONTROL	30	1	4	0	2
1	11/22/2016	40	10	CONTROL	30	1	5	0	0
1	12/16/2016	64	1	589	30	8	1	0	0
1	12/16/2016	64	1	589	30	8	2	0	0
1	12/16/2016	64	1	589	30	8	3	0	1
1	12/16/2016	64	1	589	30	8	4	0	1
1	12/16/2016	64	1	589	30	8	5	0	0
1	12/16/2016	64	2	300	30	6	1	1	2
1	12/16/2016	64	2	300	30	6	2	3	0
1	12/16/2016	64	2	300	30	6	3	0	0
1	12/16/2016	64	2	300	30	6	4	0	0
1	12/16/2016	64	2	300	30	6	5	1	0
1	12/16/2016	64	3	310	30	7	1	0	0
1	12/16/2016	64	3	310	30	7	2	1	0
1	12/16/2016	64	3	310	30	7	3	3	1
1	12/16/2016	64	3	310	30	7	4	0	0
1	12/16/2016	64	3	310	30	7	5	0	1
1	12/16/2016	64	4	450	30	4	1	0	0
1	12/16/2016	64	4	450	30	4	2	0	0
1	12/16/2016	64	4	450	30	4	3	0	0
1	12/16/2016	64	4	450	30	4	4	0	0
1	12/16/2016	64	4	450	30	4	5	0	0
1	12/16/2016	64	5	720	30	3	1	0	5
1	12/16/2016	64	5	720	30	3	2	0	1
1	12/16/2016	64	5	720	30	3	3	0	0
1	12/16/2016	64	5	720	30	3	4	0	4
1	12/16/2016	64	5	720	30	3	5	0	1
1	12/16/2016	64	6	UV	30	9	1	0	0
1	12/16/2016	64	6	UV	30	9	2	0	0
1	12/16/2016	64	6	UV	30	9	3	0	0
1	12/16/2016	64	6	UV	30	9	4	0	0
1	12/16/2016	64	6	UV	30	9	5	0	0
1	12/16/2016	64	7	270	30	5	1	0	0
1	12/16/2016	64	7	270	30	5	2	0	0
1	12/16/2016	64	7	270	30	5	3	0	0

1	12/16/2016	64	7	270	30	5	4	0	0
1	12/16/2016	64	7	270	30	5	5	0	0
1	12/16/2016	64	8	280	30	10	1	0	1
1	12/16/2016	64	8	280	30	10	2	0	6
1	12/16/2016	64	8	280	30	10	3	0	1
1	12/16/2016	64	8	280	30	10	4	0	1
1	12/16/2016	64	8	280	30	10	5	0	2
1	12/16/2016	64	9	320	30	2	1	0	0
1	12/16/2016	64	9	320	30	2	2	3	0
1	12/16/2016	64	9	320	30	2	3	1	0
1	12/16/2016	64	9	320	30	2	4	2	0
1	12/16/2016	64	9	320	30	2	5	1	0
1	12/16/2016	64	10	CONTROL	30	1	1	0	0
1	12/16/2016	64	10	CONTROL	30	1	2	0	0
1	12/16/2016	64	10	CONTROL	30	1	3	1	0
1	12/16/2016	64	10	CONTROL	30	1	4	0	4
1	12/16/2016	64	10	CONTROL	30	1	5	0	0
2	1/17/2017	34	1	310	30	6	1	0	0
2	1/17/2017	34	1	310	30	6	2	0	0
2	1/17/2017	34	1	310	30	6	3	0	0
2	1/17/2017	34	1	310	30	6	4	0	0
2	1/17/2017	34	1	310	30	6	5	0	0
2	1/17/2017	34	2	270	30	1	1	0	1
2	1/17/2017	34	2	270	30	1	2	0	0
2	1/17/2017	34	2	270	30	1	3	0	0
2	1/17/2017	34	2	270	30	1	4	0	4
2	1/17/2017	34	2	270	30	1	5	0	2
2	1/17/2017	34	3	CONTROL	30	11	1	0	0
2	1/17/2017	34	3	CONTROL	30	11	2	1	1
2	1/17/2017	34	3	CONTROL	30	11	3	1	2
2	1/17/2017	34	3	CONTROL	30	11	4	0	0
2	1/17/2017	34	3	CONTROL	30	11	5	0	2
2	1/17/2017	34	4	UV	30	8	1	0	0
2	1/17/2017	34	4	UV	30	8	2	0	3
2	1/17/2017	34	4	UV	30	8	3	0	0
2	1/17/2017	34	4	UV	30	8	4	0	0
2	1/17/2017	34	4	UV	30	8	5	0	0
2	1/17/2017	34	5	320	30	2	1	0	0
2	1/17/2017	34	5	320	30	2	2	0	0
2	1/17/2017	34	5	320	30	2	3	0	0

2	1/17/2017	34	5	320	30	2	4	0	0
2	1/17/2017	34	5	320	30	2	5	0	0
2	1/17/2017	34	6	280	30	10	1	0	2
2	1/17/2017	34	6	280	30	10	2	0	1
2	1/17/2017	34	6	280	30	10	3	0	1
2	1/17/2017	34	6	280	30	10	4	0	3
2	1/17/2017	34	6	280	30	10	5	0	3
2	1/17/2017	34	7	300	30	4	1	0	5
2	1/17/2017	34	7	300	30	4	2	0	0
2	1/17/2017	34	7	300	30	4	3	0	0
2	1/17/2017	34	7	300	30	4	4	0	0
2	1/17/2017	34	7	300	30	4	5	0	3
2	1/17/2017	34	8	720	30	12	1	0	2
2	1/17/2017	34	8	720	30	12	2	0	1
2	1/17/2017	34	8	720	30	12	3	0	3
2	1/17/2017	34	8	720	30	12	4	0	1
2	1/17/2017	34	8	720	30	12	5	0	2
2	1/17/2017	34	9	589	30	5	1	0	0
2	1/17/2017	34	9	589	30	5	2	0	1
2	1/17/2017	34	9	589	30	5	3	0	1
2	1/17/2017	34	9	589	30	5	4	0	1
2	1/17/2017	34	9	589	30	5	5	0	0
2	1/17/2017	34	10	450	30	7	1	0	0
2	1/17/2017	34	10	450	30	7	2	0	0
2	1/17/2017	34	10	450	30	7	3	0	4
2	1/17/2017	34	10	450	30	7	4	2	3
2	1/17/2017	34	10	450	30	7	5	0	4
2	1/24/2017	41	1	310	30	6	1	0	0
2	1/24/2017	41	1	310	30	6	2	0	0
2	1/24/2017	41	1	310	30	6	3	0	1
2	1/24/2017	41	1	310	30	6	4	0	0
2	1/24/2017	41	1	310	30	6	5	0	0
2	1/24/2017	41	2	270	30	1	1	0	1
2	1/24/2017	41	2	270	30	1	2	0	0
2	1/24/2017	41	2	270	30	1	3	0	0
2	1/24/2017	41	2	270	30	1	4	0	4
2	1/24/2017	41	2	270	30	1	5	0	2
2	1/24/2017	41	3	CONTROL	30	11	1	0	0
2	1/24/2017	41	3	CONTROL	30	11	2	1	1
2	1/24/2017	41	3	CONTROL	30	11	3	1	2

2	1/24/2017	41	3	CONTROL	30	11	4	3	1
2	1/24/2017	41	3	CONTROL	30	11	5	1	4
2	1/24/2017	41	4	UV	30	8	1	0	0
2	1/24/2017	41	4	UV	30	8	2	0	4
2	1/24/2017	41	4	UV	30	8	3	0	0
2	1/24/2017	41	4	UV	30	8	4	0	0
2	1/24/2017	41	4	UV	30	8	5	0	0
2	1/24/2017	41	5	320	30	2	1	0	0
2	1/24/2017	41	5	320	30	2	2	0	0
2	1/24/2017	41	5	320	30	2	3	0	0
2	1/24/2017	41	5	320	30	2	4	0	0
2	1/24/2017	41	5	320	30	2	5	0	1
2	1/24/2017	41	6	280	30	10	1	0	3
2	1/24/2017	41	6	280	30	10	2	0	1
2	1/24/2017	41	6	280	30	10	3	0	1
2	1/24/2017	41	6	280	30	10	4	0	4
2	1/24/2017	41	6	280	30	10	5	0	6
2	1/24/2017	41	7	300	30	4	1	0	5
2	1/24/2017	41	7	300	30	4	2	0	0
2	1/24/2017	41	7	300	30	4	3	0	0
2	1/24/2017	41	7	300	30	4	4	0	0
2	1/24/2017	41	7	300	30	4	5	0	3
2	1/24/2017	41	8	720	30	12	1	0	25
2	1/24/2017	41	8	720	30	12	2	0	2
2	1/24/2017	41	8	720	30	12	3	0	3
2	1/24/2017	41	8	720	30	12	4	0	1
2	1/24/2017	41	8	720	30	12	5	0	2
2	1/24/2017	41	9	589	30	5	1	0	0
2	1/24/2017	41	9	589	30	5	2	0	1
2	1/24/2017	41	9	589	30	5	3	0	2
2	1/24/2017	41	9	589	30	5	4	0	1
2	1/24/2017	41	9	589	30	5	5	0	0
2	1/24/2017	41	10	450	30	7	1	0	1
2	1/24/2017	41	10	450	30	7	2	0	0
2	1/24/2017	41	10	450	30	7	3	0	4
2	1/24/2017	41	10	450	30	7	4	1	4
2	1/24/2017	41	10	450	30	7	5	0	4
2	1/31/2017	48	1	310	30	6	1	0	0
2	1/31/2017	48	1	310	30	6	2	0	0
2	1/31/2017	48	1	310	30	6	3	1	3

2	1/31/2017	48	1	310	30	6	4	0	0
2	1/31/2017	48	1	310	30	6	5	0	0
2	1/31/2017	48	2	270	30	1	1	0	1
2	1/31/2017	48	2	270	30	1	2	1	1
2	1/31/2017	48	2	270	30	1	3	0	0
2	1/31/2017	48	2	270	30	1	4	0	4
2	1/31/2017	48	2	270	30	1	5	0	3
2	1/31/2017	48	3	CONTROL	30	11	1	0	0
2	1/31/2017	48	3	CONTROL	30	11	2	1	1
2	1/31/2017	48	3	CONTROL	30	11	3	1	3
2	1/31/2017	48	3	CONTROL	30	11	4	4	1
2	1/31/2017	48	3	CONTROL	30	11	5	5	1
2	1/31/2017	48	4	UV	30	8	1	0	0
2	1/31/2017	48	4	UV	30	8	2	0	3
2	1/31/2017	48	4	UV	30	8	3	0	0
2	1/31/2017	48	4	UV	30	8	4	0	0
2	1/31/2017	48	4	UV	30	8	5	0	0
2	1/31/2017	48	5	320	30	2	1	0	1
2	1/31/2017	48	5	320	30	2	2	0	0
2	1/31/2017	48	5	320	30	2	3	0	0
2	1/31/2017	48	5	320	30	2	4	0	2
2	1/31/2017	48	5	320	30	2	5	0	1
2	1/31/2017	48	6	280	30	10	1	0	4
2	1/31/2017	48	6	280	30	10	2	0	2
2	1/31/2017	48	6	280	30	10	3	0	2
2	1/31/2017	48	6	280	30	10	4	0	6
2	1/31/2017	48	6	280	30	10	5	0	11
2	1/31/2017	48	7	300	30	4	1	3	3
2	1/31/2017	48	7	300	30	4	2	0	0
2	1/31/2017	48	7	300	30	4	3	0	0
2	1/31/2017	48	7	300	30	4	4	0	2
2	1/31/2017	48	7	300	30	4	5	0	3
2	1/31/2017	48	8	720	30	12	1	0	3
2	1/31/2017	48	8	720	30	12	2	0	3
2	1/31/2017	48	8	720	30	12	3	0	3
2	1/31/2017	48	8	720	30	12	4	0	1
2	1/31/2017	48	8	720	30	12	5	0	2
2	1/31/2017	48	9	589	30	5	1	0	2
2	1/31/2017	48	9	589	30	5	2	0	2
2	1/31/2017	48	9	589	30	5	3	0	2

2	1/31/2017	48	9	589	30	5	4	0	1
2	1/31/2017	48	9	589	30	5	5	0	0
2	1/31/2017	48	10	450	30	7	1	0	2
2	1/31/2017	48	10	450	30	7	2	0	0
2	1/31/2017	48	10	450	30	7	3	0	6
2	1/31/2017	48	10	450	30	7	4	0	6
2	1/31/2017	48	10	450	30	7	5	0	4
2	2/9/2017	57	1	310	30	6	1	0	2
2	2/9/2017	57	1	310	30	6	2	0	0
2	2/9/2017	57	1	310	30	6	3	3	2
2	2/9/2017	57	1	310	30	6	4	0	1
2	2/9/2017	57	1	310	30	6	5	0	0
2	2/9/2017	57	2	270	30	1	1	0	1
2	2/9/2017	57	2	270	30	1	2	0	1
2	2/9/2017	57	2	270	30	1	3	0	0
2	2/9/2017	57	2	270	30	1	4	0	5
2	2/9/2017	57	2	270	30	1	5	0	3
2	2/9/2017	57	3	CONTROL	30	11	1	0	1
2	2/9/2017	57	3	CONTROL	30	11	2	1	2
2	2/9/2017	57	3	CONTROL	30	11	3	1	4
2	2/9/2017	57	3	CONTROL	30	11	4	5	1
2	2/9/2017	57	3	CONTROL	30	11	5	3	2
2	2/9/2017	57	4	UV	30	8	1	0	0
2	2/9/2017	57	4	UV	30	8	2	0	3
2	2/9/2017	57	4	UV	30	8	3	0	0
2	2/9/2017	57	4	UV	30	8	4	0	1
2	2/9/2017	57	4	UV	30	8	5	0	0
2	2/9/2017	57	5	320	30	2	1	0	1
2	2/9/2017	57	5	320	30	2	2	0	0
2	2/9/2017	57	5	320	30	2	3	0	1
2	2/9/2017	57	5	320	30	2	4	0	5
2	2/9/2017	57	5	320	30	2	5	1	0
2	2/9/2017	57	6	280	30	10	1	0	4
2	2/9/2017	57	6	280	30	10	2	0	3
2	2/9/2017	57	6	280	30	10	3	0	2
2	2/9/2017	57	6	280	30	10	4	0	6
2	2/9/2017	57	6	280	30	10	5	0	15
2	2/9/2017	57	7	300	30	4	1	3	2
2	2/9/2017	57	7	300	30	4	2	0	0
2	2/9/2017	57	7	300	30	4	3	0	0

2	2/9/2017	57	7	300	30	4	4	1	2
2	2/9/2017	57	7	300	30	4	5	0	5
2	2/9/2017	57	8	720	30	12	1	0	3
2	2/9/2017	57	8	720	30	12	2	0	5
2	2/9/2017	57	8	720	30	12	3	0	3
2	2/9/2017	57	8	720	30	12	4	0	1
2	2/9/2017	57	8	720	30	12	5	0	3
2	2/9/2017	57	9	589	30	5	1	0	1
2	2/9/2017	57	9	589	30	5	2	0	3
2	2/9/2017	57	9	589	30	5	3	0	2
2	2/9/2017	57	9	589	30	5	4	0	2
2	2/9/2017	57	9	589	30	5	5	0	0
2	2/9/2017	57	10	450	30	7	1	0	4
2	2/9/2017	57	10	450	30	7	2	0	0
2	2/9/2017	57	10	450	30	7	3	0	7
2	2/9/2017	57	10	450	30	7	4	0	6
2	2/9/2017	57	10	450	30	7	5	0	4
2	2/16/2017	64	1	310	30	6	1	0	2
2	2/16/2017	64	1	310	30	6	2	0	0
2	2/16/2017	64	1	310	30	6	3	5	0
2	2/16/2017	64	1	310	30	6	4	1	0
2	2/16/2017	64	1	310	30	6	5	1	0
2	2/16/2017	64	2	270	30	1	1	0	1
2	2/16/2017	64	2	270	30	1	2	0	1
2	2/16/2017	64	2	270	30	1	3	0	0
2	2/16/2017	64	2	270	30	1	4	0	3
2	2/16/2017	64	2	270	30	1	5	0	3
2	2/16/2017	64	3	CONTROL	30	11	1	0	0
2	2/16/2017	64	3	CONTROL	30	11	2	2	2
2	2/16/2017	64	3	CONTROL	30	11	3	1	3
2	2/16/2017	64	3	CONTROL	30	11	4	6	1
2	2/16/2017	64	3	CONTROL	30	11	5	3	2
2	2/16/2017	64	4	UV	30	8	1	0	0
2	2/16/2017	64	4	UV	30	8	2	0	3
2	2/16/2017	64	4	UV	30	8	3	0	0
2	2/16/2017	64	4	UV	30	8	4	0	1
2	2/16/2017	64	4	UV	30	8	5	0	0
2	2/16/2017	64	5	320	30	2	1	0	1
2	2/16/2017	64	5	320	30	2	2	0	0
2	2/16/2017	64	5	320	30	2	3	0	2

2	2/16/2017	64	5	320	30	2	4	0	9
2	2/16/2017	64	5	320	30	2	5	1	0
2	2/16/2017	64	6	280	30	10	1	0	4
2	2/16/2017	64	6	280	30	10	2	0	4
2	2/16/2017	64	6	280	30	10	3	0	2
2	2/16/2017	64	6	280	30	10	4	0	7
2	2/16/2017	64	6	280	30	10	5	0	16
2	2/16/2017	64	7	300	30	4	1	4	0
2	2/16/2017	64	7	300	30	4	2	0	0
2	2/16/2017	64	7	300	30	4	3	0	0
2	2/16/2017	64	7	300	30	4	4	2	1
2	2/16/2017	64	7	300	30	4	5	0	6
2	2/16/2017	64	8	720	30	12	1	0	3
2	2/16/2017	64	8	720	30	12	2	0	5
2	2/16/2017	64	8	720	30	12	3	0	4
2	2/16/2017	64	8	720	30	12	4	0	1
2	2/16/2017	64	8	720	30	12	5	0	4
2	2/16/2017	64	9	589	30	5	1	0	3
2	2/16/2017	64	9	589	30	5	2	0	3
2	2/16/2017	64	9	589	30	5	3	0	2
2	2/16/2017	64	9	589	30	5	4	0	2
2	2/16/2017	64	9	589	30	5	5	0	0
2	2/16/2017	64	10	450	30	7	1	0	4
2	2/16/2017	64	10	450	30	7	2	0	0
2	2/16/2017	64	10	450	30	7	3	0	7
2	2/16/2017	64	10	450	30	7	4	0	5
2	2/16/2017	64	10	450	30	7	5	0	4
3	6/1/2017	28	1	280	30	6	1	0	0
3	6/1/2017	28	1	280	30	6	2	0	0
3	6/1/2017	28	1	280	30	6	3	0	0
3	6/1/2017	28	1	280	30	6	4	0	0
3	6/1/2017	28	1	280	30	6	5	0	0
3	6/1/2017	28	2	320	30	3	1	0	0
3	6/1/2017	28	2	320	30	3	2	0	0
3	6/1/2017	28	2	320	30	3	3	0	0
3	6/1/2017	28	2	320	30	3	4	0	0
3	6/1/2017	28	2	320	30	3	5	0	0
3	6/1/2017	28	3	589	30	8	1	0	0
3	6/1/2017	28	3	589	30	8	2	0	0
3	6/1/2017	28	3	589	30	8	3	0	0

3	6/1/2017	28	3	589	30	8	4	0	0
3	6/1/2017	28	3	589	30	8	5	0	0
3	6/1/2017	28	4	720	30	5	1	0	0
3	6/1/2017	28	4	720	30	5	2	0	0
3	6/1/2017	28	4	720	30	5	3	0	0
3	6/1/2017	28	4	720	30	5	4	0	0
3	6/1/2017	28	4	720	30	5	5	0	0
3	6/1/2017	28	5	310	30	10	1	0	0
3	6/1/2017	28	5	310	30	10	2	0	0
3	6/1/2017	28	5	310	30	10	3	0	0
3	6/1/2017	28	5	310	30	10	4	0	0
3	6/1/2017	28	5	310	30	10	5	0	0
3	6/1/2017	28	6	CONTROL	30	4	1	0	1
3	6/1/2017	28	6	CONTROL	30	4	2	0	4
3	6/1/2017	28	6	CONTROL	30	4	3	5	1
3	6/1/2017	28	6	CONTROL	30	4	4	0	0
3	6/1/2017	28	6	CONTROL	30	4	5	0	0
3	6/1/2017	28	7	UV	30	7	1	0	0
3	6/1/2017	28	7	UV	30	7	2	0	0
3	6/1/2017	28	7	UV	30	7	3	0	0
3	6/1/2017	28	7	UV	30	7	4	0	3
3	6/1/2017	28	7	UV	30	7	5	0	0
3	6/1/2017	28	8	300	30	11	1	0	0
3	6/1/2017	28	8	300	30	11	2	0	0
3	6/1/2017	28	8	300	30	11	3	0	0
3	6/1/2017	28	8	300	30	11	4	0	0
3	6/1/2017	28	8	300	30	11	5	0	0
3	6/1/2017	28	9	270	30	12	1	0	0
3	6/1/2017	28	9	270	30	12	2	0	0
3	6/1/2017	28	9	270	30	12	3	0	0
3	6/1/2017	28	9	270	30	12	4	0	0
3	6/1/2017	28	9	270	30	12	5	0	0
3	6/1/2017	28	10	450	30	1	1	0	0
3	6/1/2017	28	10	450	30	1	2	0	0
3	6/1/2017	28	10	450	30	1	3	0	0
3	6/1/2017	28	10	450	30	1	4	0	0
3	6/1/2017	28	10	450	30	1	5	0	0
3	6/9/2017	36	1	280	30	6	1	0	0
3	6/9/2017	36	1	280	30	6	2	0	0
3	6/9/2017	36	1	280	30	6	3	0	0

3	6/9/2017	36	1	280	30	6	4	0	0
3	6/9/2017	36	1	280	30	6	5	0	0
3	6/9/2017	36	2	320	30	3	1	0	0
3	6/9/2017	36	2	320	30	3	2	0	0
3	6/9/2017	36	2	320	30	3	3	0	0
3	6/9/2017	36	2	320	30	3	4	0	0
3	6/9/2017	36	2	320	30	3	5	0	0
3	6/9/2017	36	3	589	30	8	1	0	0
3	6/9/2017	36	3	589	30	8	2	0	0
3	6/9/2017	36	3	589	30	8	3	0	0
3	6/9/2017	36	3	589	30	8	4	0	0
3	6/9/2017	36	3	589	30	8	5	0	0
3	6/9/2017	36	4	720	30	5	1	0	0
3	6/9/2017	36	4	720	30	5	2	0	0
3	6/9/2017	36	4	720	30	5	3	0	0
3	6/9/2017	36	4	720	30	5	4	0	0
3	6/9/2017	36	4	720	30	5	5	0	0
3	6/9/2017	36	5	310	30	10	1	0	0
3	6/9/2017	36	5	310	30	10	2	0	0
3	6/9/2017	36	5	310	30	10	3	0	0
3	6/9/2017	36	5	310	30	10	4	0	0
3	6/9/2017	36	5	310	30	10	5	0	0
3	6/9/2017	36	6	CONTROL	30	4	1	4	0
3	6/9/2017	36	6	CONTROL	30	4	2	3	0
3	6/9/2017	36	6	CONTROL	30	4	3	5	1
3	6/9/2017	36	6	CONTROL	30	4	4	0	5
3	6/9/2017	36	6	CONTROL	30	4	5	0	0
3	6/9/2017	36	7	UV	30	7	1	0	1
3	6/9/2017	36	7	UV	30	7	2	0	1
3	6/9/2017	36	7	UV	30	7	3	0	4
3	6/9/2017	36	7	UV	30	7	4	0	4
3	6/9/2017	36	7	UV	30	7	5	0	0
3	6/9/2017	36	8	300	30	11	1	0	0
3	6/9/2017	36	8	300	30	11	2	0	5
3	6/9/2017	36	8	300	30	11	3	0	0
3	6/9/2017	36	8	300	30	11	4	0	0
3	6/9/2017	36	8	300	30	11	5	0	0
3	6/9/2017	36	9	270	30	12	1	0	0
3	6/9/2017	36	9	270	30	12	2	0	0
3	6/9/2017	36	9	270	30	12	3	0	0

3	6/9/2017	36	9	270	30	12	4	0	0
3	6/9/2017	36	9	270	30	12	5	0	0
3	6/9/2017	36	10	450	30	1	1	0	0
3	6/9/2017	36	10	450	30	1	2	0	0
3	6/9/2017	36	10	450	30	1	3	0	0
3	6/9/2017	36	10	450	30	1	4	0	0
3	6/9/2017	36	10	450	30	1	5	0	0
3	6/15/2017	42	1	280	30	6	1	0	0
3	6/15/2017	42	1	280	30	6	2	0	0
3	6/15/2017	42	1	280	30	6	3	0	0
3	6/15/2017	42	1	280	30	6	4	0	0
3	6/15/2017	42	1	280	30	6	5	0	0
3	6/15/2017	42	2	320	30	3	1	0	0
3	6/15/2017	42	2	320	30	3	2	0	0
3	6/15/2017	42	2	320	30	3	3	0	0
3	6/15/2017	42	2	320	30	3	4	0	0
3	6/15/2017	42	2	320	30	3	5	0	0
3	6/15/2017	42	3	589	30	8	1	0	0
3	6/15/2017	42	3	589	30	8	2	0	0
3	6/15/2017	42	3	589	30	8	3	0	0
3	6/15/2017	42	3	589	30	8	4	0	0
3	6/15/2017	42	3	589	30	8	5	0	0
3	6/15/2017	42	4	720	30	5	1	0	0
3	6/15/2017	42	4	720	30	5	2	0	0
3	6/15/2017	42	4	720	30	5	3	0	0
3	6/15/2017	42	4	720	30	5	4	0	0
3	6/15/2017	42	4	720	30	5	5	0	0
3	6/15/2017	42	5	310	30	10	1	0	0
3	6/15/2017	42	5	310	30	10	2	0	0
3	6/15/2017	42	5	310	30	10	3	0	0
3	6/15/2017	42	5	310	30	10	4	0	0
3	6/15/2017	42	5	310	30	10	5	0	0
3	6/15/2017	42	6	CONTROL	30	4	1	4	0
3	6/15/2017	42	6	CONTROL	30	4	2	3	1
3	6/15/2017	42	6	CONTROL	30	4	3	5	1
3	6/15/2017	42	6	CONTROL	30	4	4	0	8
3	6/15/2017	42	6	CONTROL	30	4	5	0	0
3	6/15/2017	42	7	UV	30	7	1	0	1
3	6/15/2017	42	7	UV	30	7	2	0	1
3	6/15/2017	42	7	UV	30	7	3	0	4

3	6/15/2017	42	7	UV	30	7	4	0	5
3	6/15/2017	42	7	UV	30	7	5	0	0
3	6/15/2017	42	8	300	30	11	1	0	0
3	6/15/2017	42	8	300	30	11	2	3	5
3	6/15/2017	42	8	300	30	11	3	0	1
3	6/15/2017	42	8	300	30	11	4	0	1
3	6/15/2017	42	8	300	30	11	5	0	0
3	6/15/2017	42	9	270	30	12	1	0	0
3	6/15/2017	42	9	270	30	12	2	0	0
3	6/15/2017	42	9	270	30	12	3	0	0
3	6/15/2017	42	9	270	30	12	4	0	0
3	6/15/2017	42	9	270	30	12	5	0	0
3	6/15/2017	42	10	450	30	1	1	0	0
3	6/15/2017	42	10	450	30	1	2	0	0
3	6/15/2017	42	10	450	30	1	3	0	0
3	6/15/2017	42	10	450	30	1	4	0	0
3	6/15/2017	42	10	450	30	1	5	0	0
3	6/23/2017	50	1	280	30	6	1	0	0
3	6/23/2017	50	1	280	30	6	2	0	0
3	6/23/2017	50	1	280	30	6	3	0	0
3	6/23/2017	50	1	280	30	6	4	0	0
3	6/23/2017	50	1	280	30	6	5	0	0
3	6/23/2017	50	2	320	30	3	1	0	0
3	6/23/2017	50	2	320	30	3	2	0	0
3	6/23/2017	50	2	320	30	3	3	0	0
3	6/23/2017	50	2	320	30	3	4	0	0
3	6/23/2017	50	2	320	30	3	5	0	0
3	6/23/2017	50	3	589	30	8	1	0	0
3	6/23/2017	50	3	589	30	8	2	0	0
3	6/23/2017	50	3	589	30	8	3	0	0
3	6/23/2017	50	3	589	30	8	4	0	0
3	6/23/2017	50	3	589	30	8	5	0	0
3	6/23/2017	50	4	720	30	5	1	0	0
3	6/23/2017	50	4	720	30	5	2	0	0
3	6/23/2017	50	4	720	30	5	3	0	0
3	6/23/2017	50	4	720	30	5	4	0	0
3	6/23/2017	50	4	720	30	5	5	0	0
3	6/23/2017	50	5	310	30	10	1	0	0
3	6/23/2017	50	5	310	30	10	2	0	0
3	6/23/2017	50	5	310	30	10	3	0	0

3	6/23/2017	50	5	310	30	10	4	0	0
3	6/23/2017	50	5	310	30	10	5	0	0
3	6/23/2017	50	6	CONTROL	30	4	1	4	0
3	6/23/2017	50	6	CONTROL	30	4	2	4	2
3	6/23/2017	50	6	CONTROL	30	4	3	5	1
3	6/23/2017	50	6	CONTROL	30	4	4	3	6
3	6/23/2017	50	6	CONTROL	30	4	5	0	1
3	6/23/2017	50	7	UV	30	7	1	0	1
3	6/23/2017	50	7	UV	30	7	2	0	1
3	6/23/2017	50	7	UV	30	7	3	0	5
3	6/23/2017	50	7	UV	30	7	4	0	7
3	6/23/2017	50	7	UV	30	7	5	0	0
3	6/23/2017	50	8	300	30	11	1	0	0
3	6/23/2017	50	8	300	30	11	2	6	2
3	6/23/2017	50	8	300	30	11	3	1	1
3	6/23/2017	50	8	300	30	11	4	1	2
3	6/23/2017	50	8	300	30	11	5	0	0
3	6/23/2017	50	9	270	30	12	1	0	0
3	6/23/2017	50	9	270	30	12	2	0	0
3	6/23/2017	50	9	270	30	12	3	0	0
3	6/23/2017	50	9	270	30	12	4	0	0
3	6/23/2017	50	9	270	30	12	5	0	0
3	6/23/2017	50	10	450	30	1	1	0	0
3	6/23/2017	50	10	450	30	1	2	0	0
3	6/23/2017	50	10	450	30	1	3	0	0
3	6/23/2017	50	10	450	30	1	4	0	0
3	6/23/2017	50	10	450	30	1	5	0	0
3	7/8/2017	65	1	280	30	6	1	0	0
3	7/8/2017	65	1	280	30	6	2	0	0
3	7/8/2017	65	1	280	30	6	3	0	0
3	7/8/2017	65	1	280	30	6	4	0	0
3	7/8/2017	65	1	280	30	6	5	0	0
3	7/8/2017	65	2	320	30	3	1	0	0
3	7/8/2017	65	2	320	30	3	2	0	0
3	7/8/2017	65	2	320	30	3	3	0	0
3	7/8/2017	65	2	320	30	3	4	0	0
3	7/8/2017	65	2	320	30	3	5	0	0
3	7/8/2017	65	3	589	30	8	1	0	0
3	7/8/2017	65	3	589	30	8	2	0	0
3	7/8/2017	65	3	589	30	8	3	0	0

3	7/8/2017	65	3	589	30	8	4	0	0
3	7/8/2017	65	3	589	30	8	5	0	0
3	7/8/2017	65	4	720	30	5	1	0	0
3	7/8/2017	65	4	720	30	5	2	0	0
3	7/8/2017	65	4	720	30	5	3	0	0
3	7/8/2017	65	4	720	30	5	4	0	0
3	7/8/2017	65	4	720	30	5	5	0	0
3	7/8/2017	65	5	310	30	10	1	0	0
3	7/8/2017	65	5	310	30	10	2	0	0
3	7/8/2017	65	5	310	30	10	3	0	0
3	7/8/2017	65	5	310	30	10	4	0	0
3	7/8/2017	65	5	310	30	10	5	0	0
3	7/8/2017	65	6	CONTROL	30	4	1	5	0
3	7/8/2017	65	6	CONTROL	30	4	2	5	1
3	7/8/2017	65	6	CONTROL	30	4	3	5	1
3	7/8/2017	65	6	CONTROL	30	4	4	3	6
3	7/8/2017	65	6	CONTROL	30	4	5	1	2
3	7/8/2017	65	7	UV	30	7	1	0	1
3	7/8/2017	65	7	UV	30	7	2	0	1
3	7/8/2017	65	7	UV	30	7	3	0	5
3	7/8/2017	65	7	UV	30	7	4	0	9
3	7/8/2017	65	7	UV	30	7	5	0	0
3	7/8/2017	65	8	300	30	11	1	0	0
3	7/8/2017	65	8	300	30	11	2	6	2
3	7/8/2017	65	8	300	30	11	3	2	0
3	7/8/2017	65	8	300	30	11	4	2	1
3	7/8/2017	65	8	300	30	11	5	0	0
3	7/8/2017	65	9	270	30	12	1	0	0
3	7/8/2017	65	9	270	30	12	2	0	0
3	7/8/2017	65	9	270	30	12	3	0	0
3	7/8/2017	65	9	270	30	12	4	0	0
3	7/8/2017	65	9	270	30	12	5	0	0
3	7/8/2017	65	10	450	30	1	1	0	0
3	7/8/2017	65	10	450	30	1	2	0	0
3	7/8/2017	65	10	450	30	1	3	0	0
3	7/8/2017	65	10	450	30	1	4	0	0
3	7/8/2017	65	10	450	30	1	5	0	0

Table VI.2. Means and standard deviations (SD) of the number of apothecia and stipes (per sclerotia) formed under each lens treatment after 64 or 65 days collected from three replicates

Lens Trt	Apothecia		Stipes	
	Mean	SD	Mean	SD
270	0.00 c[z]	0.39	0.53	0.95
280	0.00 c	0.39	2.93	0.95
300	1.40 ab	0.39	0.80	0.95
310	0.73 bc	0.39	0.27	0.95
320	0.53 bc	0.39	0.80	0.95
450	0.00 c	0.39	1.33	0.95
589	0.00 c	0.39	0.80	0.95
720	0.00 c	0.39	1.87	0.95
CONTROL	2.13 a	0.39	1.47	0.95
UV	0.00 c	0.39	1.33	0.95
LSD	1.16		ns	
F	3.61		0.66	
P-value	0.0080		0.7335	

[z]Means followed by the same letter are not different based on Fisher's least significant difference (LSD) evaluated at the $\alpha = 0.05$ significance level.

Table VI.3. Coefficients and corresponding *p*-values of Pearson correlations between means of various light quantities, above and below the canopy, and mean apothecial numbers collected from West Madison in 2015 and Arlington in 2016

Variable	Mean of	Location	Pearson Correlation Coefficient	p-value
MeanMSR_A	hourly mean SR	above canopy	-0.0654	0.4187
MeanTSR_A	hourly total SR	above canopy	-0.0372	0.6460
MeanMSR_BB	hourly mean SR	below canopy, between rows	0.0108	0.8943
MeanTSR_BB	hourly total SR	below canopy, between rows	0.0179	0.8248
MeanMSR_BI	hourly mean SR	below canopy, in the row	-0.1522	0.0586
MeanTSR_BI	hourly total SR	below canopy, in the row	-0.1760	0.0285
MeanMUV_A	hourly mean UV	above canopy	-0.1012	0.2101
MeanTUV_A	hourly total UV	above canopy	0.1001	0.2152
MeanMUV_BB	hourly mean UV	below canopy, between rows	-0.0087	0.9148
MeanTUV_BB	hourly total UV	below canopy, between rows	0.2208	0.0058
MeanMUV_BI	hourly mean UV	below canopy, in the row	-0.2076	0.0096
MeanTUV_BI	hourly total UV	below canopy, in the row	-0.2192	0.0062
MeanMUVSR_A	ratio mean UV:SR	above canopy	-0.1777	0.0270
MeanTUVSR_A	ratio total UV:SR	above canopy	-0.1065	0.1873
MeanMUVSR_BB	ratio mean UV:SR	below canopy, between rows	0.3066	0.0001
MeanTUVSR_BB	ratio total UV:SR	below canopy, between rows	0.2794	0.0004
MeanMUVSR_BI	ratio mean UV:SR	below canopy, in the row	-0.2082	0.0093
MeanTUVSR_BI	ratio total UV:SR	below canopy, in the row	-0.2332	0.0035

Table AVI.4. Means and standard errors (SE) of disease severity index (DIX) values for each combination of row spacing, population density, and fungicide treatment, significant three-way interaction (P = 0.0476), Hancock, WI 2017

Row (m)	Population (1,000 seeds ha^{-1})	Fungicide	DIX (%)	SE
0.38	275	Non-treated	35.5	7.3
0.38	275	Aproach 9oz/a (R1+R3)	22.3	7.3
0.38	275	Aproach 9oz/a (Model)	42.8	7.3
0.38	350	Non-treated	30.3	7.3
0.38	350	Aproach 9oz/a (R1+R3)	34.9	7.3
0.38	350	Aproach 9oz/a (Model)	28.9	7.3
0.38	425	Non-treated	31.0	7.3
0.38	425	Aproach 9oz/a (R1+R3)	37.3	7.3
0.38	425	Aproach 9oz/a (Model)	35.9	7.3
0.38	500	Non-treated	32.6	7.3
0.38	500	Aproach 9oz/a (R1+R3)	35.2	7.3
0.38	500	Aproach 9oz/a (Model)	33.2	7.3
0.76	275	Non-treated	11.9	7.3
0.76	275	Aproach 9oz/a (R1+R3)	23.2	7.3
0.76	275	Aproach 9oz/a (Model)	19.3	7.3
0.76	350	Non-treated	22.3	7.3
0.76	350	Aproach 9oz/a (R1+R3)	12.4	7.3
0.76	350	Aproach 9oz/a (Model)	11.4	7.3
0.76	425	Non-treated	21.7	7.3
0.76	425	Aproach 9oz/a (R1+R3)	20.1	7.3
0.76	425	Aproach 9oz/a (Model)	28.9	7.3
0.76	500	Non-treated	29.9	7.3
0.76	500	Aproach 9oz/a (R1+R3)	22.6	7.3
0.76	500	Aproach 9oz/a (Model)	28.6	7.3

Table AVI.5. Means and standard errors (SE) of yield for each population density, only significant effect (P = 0.0048), Hancock, WI 2017

Population (1,000 seed/ha)	Mean Yield (kg/ha)	SE
275	3585.8	101.1
350	3698.8	96.3
425	4008.1	96.3
500	4017.6	96.3

Table AVI.6. Means and standard errors (SE) of mean apothecia for each row by population combination, no significant effect ($P = 0.8591$), however, number of apothecia consistently lower under wider row spacing and population densities, Hancock, WI 2017

Row (m)	Population (1,000 seed/ha)	Mean Apothecia	SE
0.38	275	2.6	1.6
0.38	350	2.1	1.3
0.38	425	2.2	1.3
0.38	500	3.2	1.9
0.76	275	0.9	0.6
0.76	350	1.8	1.1
0.76	425	1.6	1.0
0.76	500	3.0	1.8

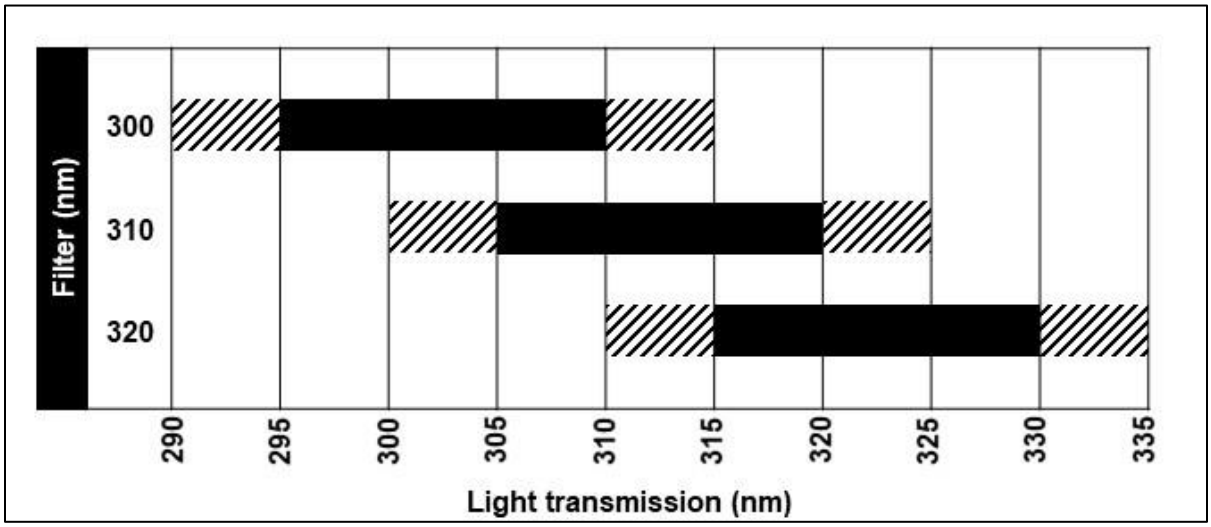

Figure AVI.1. Wavelengths of light transmission for three lens filters which resulted in apothecial production, shown in 5 nm increments. Dark bars (▬) indicate >5% transmission and diagonal lines (▨) indicates <5% transmission between those wavelengths, according to manufacturer coating curves (Edmund Optics Inc.).

Protocols

VI.1 Apothecial Production in Jars

Purpose: Artificially produce apothecia, from sclerotia under controlled temperatures and light regimes, to determine narrow ranges of wavelengths which are required for apothecial development.

VI.1.1 Preparation of Sclerotia:

Prepare carrot cultures:

1. Cut slices (discs) of unpeeled carrots approximately ¼ in. thick.
2. Place ~150 ml of carrot slices in a 250 erlenmeyer flask.
3. Using an automatic pipette, pipet 5 ml of deionized water (dispensed using the yellow handle and tube over the sink in rm 491) into each flask.
4. Cover flasks with aluminum foil (double layer).
5. Autoclave flasks for 30 minutes, slow exhaust.
6. Remove from autoclave and allow to cool to room temperature.

Inoculate carrot cultures:

7. Transfer isolates to PDA. Allow to grow at room temperature in the dark for 2-3 days.
8. Using a #2 cork-borer (5-mm diameter), cut 5 agar plugs from the leading edge of the mycelial growth.
9. Recover flask with double layer of aluminum foil. Wrap ½ strip of parafilm around foil at neck of the flask so that aluminum foil is secure.
10. Place flasks in dark drawer at room temperature for 10-14 days. NOTE: Wait for carrots to break down, and most white sclerotial initials to disappear; need mostly dark, black sclerotia.

Sieve carrot cultures:

NOTE: Wear disposable latex or nitrile gloves.

11. Nest a No. 10 (2.00 mm) sieve in a No. 18 (1.00 mm) sieve and place in a soil sink.
12. To harvest sclerotia from carrot culture, remove foil and add water to ~250 ml. Shake and swirl to dislodge carrots and mycelia.

13. Pour water and carrot mass onto nested sieves. Using gloved hands and sprayer, work/wash carrot and mycelial tissue through the sieve and collect sclerotia.

14. Transfer only mature black sclerotia (initials are white/gray/green) to 3 layered paper towels on metal counter next to sink. Allow sclerotia to dry for 48 hr.

15. Dispose of mycelial and carrot waste caught on 1.00 mm sieve by transferring into the autoclave waste bin!

16. Clean sieves by soaking in a bleach solution for only 2-3 minutes (metal will oxidize in bleach!!), followed by scrubbing with soap and water. Spray down with water to remove carrot debris and allow to dry.

17. After 48 hr, transfer sclerotia for each isolate to a labelled, clean 15 ml conical tube.

VI.1.2 Preparation of Sand Jars:

Prepare jars:

1. Using a 50-ml plastic beaker, measure 50 cc (=50 ml) of dry fine, washed play sand (KolorScape®), previously sieved through a No. 18 or 1.00 mm sieve and transfer to clean glass jars. NOTE: Inspect jars for cracks at or around the base, discard imperfect jars.

2. Using an automatic pipet, pipet 19 ml of deionized water over sand in each jar. Amount of water may vary depending on type of sand used. NOTE: Sand should be saturated, but there should be no standing water present on the surface of the sand. Excess water should be removed using a pipette or dropper.

3. Seal jars with a single layer of aluminum foil.

4. Place jars in an autoclave-able metal pan and fill with water to level of sand in jars.

5. Autoclave jars for 45 minutes, slow exhaust.

6. Autoclave jars again for 45 minutes, slow exhaust the next day. Allow to cool to room temperature.

Set up apothecial jars:

7. Surface sterilize sclerotia, which have dried for 48 hr, in a labelled 15 ml conical tube:

    1) Fill tube with 10% Clorox solution until all sclerotia are covered. Shake and allow sclerotia to soak for 2 minutes. Carefully pour off solution into waste beaker leaving sclerotia in beaker.

2) Fill tube with 95% ethanol until all sclerotia are covered. Shake and allow to soak for 1 minute. Pour off ethanol into waste beaker.

3) Fill tubes with sterile deionized water until all sclerotia are covered. Briefly shake to rinse sclerotia. Pour off water into waste beaker.

4) Transfer sclerotia to a petri dish lined with a double layer of filter paper. Allow to dry at back of hood until dry (~5-10 minutes).

5) Using sterilized forceps (dipped in 95% ethanol and flamed), place 5 similarly sized sclerotia in "pentagon" shape on the surface of sand in each jar. NOTE: Do not bury sclerotia, but slightly press to anchor into place.

8. Replace aluminum foil with the lid of a small plastic petri dish (from box on shelf below petri dishes in closet of main lab). Toss bottom of petri dish.

9. Parafilm the lid onto the jar to create an airtight seal.

10. Arrange jars evenly on a plastic lab tray and move to the dark 4°C refrigerator for 30 days. **Check sclerotia weekly.** NOTE: Press door firmly at edges to ensure a tight seal and constant temperature!

11. After 30 days, move jars to dark 12 C incubator on the 3rd floor.

12. After 40 days (or when stipes are 5 mm long), move jars to 16-18°C 12 hr light/12 hr dark light treatments.

13. After 1-2 weeks, record the number of stipes per sclerotia.

14. After 4-9 weeks, count and record the number of apothecia per sclerotia.